UNIVERSITÀ DEGLI STUDI DI NAPOLI FEDERICO II

DOTTORATO DI RICERCA IN
BIOLOGIA
(XXXII CICLO)

Biomarkers of environmental stress in different plants
Marcatori molecolari di inquinamento ambientale in diverse piante

TUTOR
PROF. ADRIANA BASILE

DOTTORANDA
MARESCA VIVIANA

2017-2020

INDEX

SUMMARY

Chapter 1: To evaluate the responses to heavy metal stress, the effects of As and Cd toxicity in *Coriandrum sativum* and *Brassica napus* L. and the possible treatments to mitigate these effects were studied. Therefore, it has been used a Triacontanol (TRIA) growth regulator, is reported to stimulate plant growth at a very low concentration when exogenously applied to various plant species. The effects of heavy metals on two bryophytes *Leptodictyum riparium* (exposed *in vitro* and in field) and *Lunularia cruciata* (gathered in field) were studied thereafter. Because of their ancientness and their peculiar phylogenetic position bryophytes are fundamental for the elucidation of important aspects of the plant evolutionary history, including traits of metal detoxification and homeostasis.

Chapter 2: We have been studied the changes in the chemical profile of essential oils and antioxidant enzymes activity in *Mentha x piperita* L. (Mitcham variety) and *Mentha arvensis* L. (var. piperascens), in response to heat stress. In addition, it has been used salicylic acid (SA) and melatonin (M), two brassinosteroids that play an important role in regulating physiological processes, to assess their potential to mitigate heat stress.

Chapter 2: The effects of nitrogen (N) deposition, tropospheric ozone (O_3) and their interaction were investigated in two Mediterranean tree species, *Fraxinus ornus* L. (deciduous) and *Quercus ilex* L. (evergreen), having different leaf habits and resource use strategies. An experiment was conducted under controlled condition to analyse how nitrogen deposition affects the ecophysiological and biochemical traits, and to explore how the nitrogen-induced changes influence the response to O_3.

Introduction

Plants live in constantly changing environments that are often unfavorable or stressful for growth and development. These adverse environmental conditions include biotic stress, such as pathogen infection and herbivore attack, and abiotic stress, such as drought, heat, cold, nutrient deficiency, and excess of salt or heavy metals.

How plants sense stress signals and adapt to adverse environments are fundamental biological questions.

Plants cannot escape adverse environmental conditions (Manik et al., 2015). Due to the constantly changing environment, abiotic stress is the main factor affecting crop growth and productivity, as plants are sessile organisms.

Identifying the mechanisms through which plants counteract abiotic stress and maintain their growth and survival holds significance for plants in coping with global climate change.

Plants and animals share some response mechanisms to unfavorable environmental conditions; however, plants, being sessile organisms, have developed, in the course of their evolution, highly sophisticated and efficient strategies of response to cope with and adapt to different types of abiotic and biotic stress imposed by the frequently adverse environment.

Stress can be understood as a stimulus or influence that is outside the normal range of homeostatic control in a given organism: if a stress tolerance is exceeded, mechanisms are activated at molecular, biochemical, physiological, and morphological levels; once stress is controlled, a new physiological state is established, and homeostasis is reestablished. When the stress is retired, the plant may return to the original state or to a new physiological situation (Fraire-Velázquez et al., 2011).

In the last years, and because of the great interest for both basic and applied research, there has been an important progress in the understanding of the mechanisms and processes underlying abiotic stress adaptation and defense in different plant species (Hirayama and Shinozaki, 2010, Fraire-Velázquez et al., 2011).

Biomarkers may be used as an early warning system of specific or general stress at each biological level, from molecules to ecosystems. The sensitivity of a species and, thus, the

efficiency of a biomarker will depend on the degree of already present adaptation to environmental stress and on the homogeneity of the investigated population.

Biomarkers for specific environmental stresses are scarce; better known are biomarkers for environmental stress complexes such as heavy metals, physiological drought and extreme temperature or biomarkers as a reaction on a full scale of environmental stresses. It is argued that a battery of biomarkers is necessary to evaluate chemical hazards to species.

More recently, the concept of ‘‘biomarker’’ has gained popularity among environmental managers. The term biomarker has been defined by the National Academy of Sciences in the USA as follows: ‘‘A biomarker is a xenobiotically induced variation in cellular or biochemical components or processes, structures, or functions that is measurable in a biological system or sample’’ (NRC 1987). In practical terms, biomarkers are endpoints of ecotoxicological tests that register an effect on a living organism. There is, however, some confusion surrounding the use of the term biomarker. Many scientists view biomarkers merely as responses at the molecular, biochemical or physiological levels, while others take a wider perspective and include the accumulation of chemicals in the tissues of living organisms and even responses at the whole organism, population, community or ecosystem levels. One of the key functions of biomarkers is to provide an early warning signal of significant biological effects (Lam et al., 2001) and it is generally believed that sub-organismic (molecular, biochemical and physiological) responses precede those that occur at higher levels of biological organization (Connell et al., 2009).

It is often argued that since biomarker effects are measured in living organisms, the information generated is particularly useful for the protection of biological species, and ultimately the management and conservation of natural ecosystems. Notwithstanding, there is a need to examine the overall advantages (benefits) and disadvantages (limitations) of biomarker-based monitoring programs with a particular emphasis on a cost-effective use of limited resources.

Biomarkers can respond to stress with differing degrees of specificity. Some biomarkers are highly specific. Other, perhaps most, biomarkers, are less specific and respond to environmental stress in general.

Plants have evolved regulated, complex mechanisms that confer protection and hence aid survival under critical conditions. The sensing of biotic or abiotic stress conditions induces signaling cascades that activate ion channels, kinase cascades, production of reactive oxygen species (ROS), accumulation of hormones such as salicylic acid, ethylene, jasmonic acid, and abscisic acid. These signals ultimately induce expression of specific subsets of defense genes that lead to the assembly of the overall defense reaction (Jaspers and Kangasjärvi, 2010). In order to activate or upregulate these complex signaling cascades, it is essential for the plant system to successfully sense the stress factors and trigger an appropriate response. Reactive oxygen species (ROS) are universally considered as the common focal points (the common factor in almost all abiotic stresses that triggers downstream responses) in abiotic stress signaling (Mittler et al., 2011; Noctor et al., 2014; S. Singh et al., 2015, 2017; Xia et al., 2015; R. Singh et al., 2016). Control conditions favoring the usual growth and development of plants also constitutively induce the production of ROS. However, this induction is at a basal level and the ROS produced are scavenged via various antioxidant mechanisms without causing any major physiological damage (Foyer and Noctor, 2005).

The ROS cause deleterious and lethal damage to proteins, DNA, and lipids (Foyer and Noctor, 2005). Antioxidants involved in scavenging of ROS can be enzymes like superoxide dismutase (SOD), ascorbate peroxidase (APX), guaiacol peroxidase (GPX), glutathione S-transferase (GST), and catalase (CAT) or low molecular weight compounds like ascorbic acid (AsA), reduced glutathione (GSH), α-tocopherol, carotenoids, phenolics, flavonoids, and proline (Gill et al., 2011).

Toxic metal ions at cellular level, evoke oxidative stress and promote DNA damage and/or impair DNA repair mechanisms, impede membrane functional integrity, nutrient homeostasis and perturb protein function and activity (Tamás et al., 2014). On the other hand, plant cells have evolved a myriad of adaptive mechanisms to manage excess metal ions and utilize detoxification mechanisms to prevent their participations in unwanted toxic reactions. In the first line of defense, plants utilize strategies that prevent or reduce uptake by restricting metal ions to the apoplast through binding them to the cell wall or to cellular exudates, or by inhibiting long distance transport (Manara, 2012; Hasan et al., 2015). In contrast, when present

at elevated concentrations, cells activate a complex network of storage and detoxification strategies, such as chelation of metal ions with phytochelatins and metallothioneins in the cytosol, trafficking, and sequestration into the vacuole by vacuolar transporters.

O_3 impacts plants by increasing the oxidation load, thereby triggering the production of reactive oxygen species (ROS) that lead to alterations of functional processes at different levels (Bytnerowicz et al., 2007, Vries et al., 2014). The production of ROS activates the detoxifying barrier in the apoplast and enzymatic activity at the symplastic level that have high metabolic cost (Vainonen et al., 2015, Das et al., 2015), and the capacity to increase antioxidant defences is recognized as a key factor in determining O_3 tolerance (Cotrozzi et al., 2016; Guidi et al., 2010; Nali et al., 2004; Scalet et al., 1995).

Heat stress affects the plants by altering various pathways, namely the rate of primary and secondary metabolism. Impaired functions of primary and secondary metabolites trigger plants to stimulate defense mechanisms.

In my research, has focused on studying the effects of three types of environmental alterations: heavy metal stress, heat stress, ozone stress using a wide range of biomarkers in order to be able create biomarker-based monitoring programs. In particular, the biomarkers tested were: the activity of antioxidant enzymes in relation to heavy metal stress, heat stress and ozone stress. Ultrastructural damage, thiol peptide content, expression levels of protein and DNA damage in relation to heavy metal stress. All these biological responses have been studied in relation to other analyzes to improve understanding of the effects of different stresses on plants.

Reference

Bytnerowicz A, Omasa K, Paoletti E. Integrated effects of air pollution and climate change on forests: A northern hemisphere perspective. Environ Pollut. 2007;147: 438–445. doi:10.1016/j.envpol.2006.08.028

Connell, D. W., Lam, P., Richardson, B., & Wu, R. (2009). *Introduction to ecotoxicology*. John Wiley & Sons.

Cotrozzi L, Remorini D, Pellegrini E, Landi M, Massai R, Nali C, et al. Variations in physiological and biochemical traits of oak seedlings grown under drought and ozone stress. Physiol Plant. 2016;157: 69–84. doi:10.1111/ppl.12402

Das P, Nutan KK, Singla-Pareek SL, Pareek A. Oxidative environment and redox homeostasis in plants: dissecting out significant contribution of major cellular organelles. Front Environ Sci. 2015;2. doi:10.3389/fenvs.2014.00070

Foyer, C.H., Noctor, G. 2005. Redox homeostasis and antioxidant signaling: a metabolic interface between stress perception and physiological responses. Plant Cell 17:1866–1875. http://dx.doi.org/10. 1105/tpc.105.033589.

Fraire-Velázquez, S., Rodríguez-Guerra, R., & Sánchez-Calderón, L. (2011). Abiotic and biotic stress response crosstalk in plants. *Abiotic Stress Response in Plants—Physiological, Biochemical and Genetic Perspectives*, 3-26.

Gill, S. S., Khan, N. A., Anjum, N. A., and Tuteja, N. (2011). "Amelioration of cadmium stress in crop plants by nutrients management: morphological, physiological and biochemical aspects," in *Plant Nutrition and Abiotic Stress Tolerance III, Plant Stress 5 (Special Issue 1)*, eds N. A. Anjum and F. Lopez-Lauri, (Ikenobe: Global Science Books Ltd., UK), 1–23.

Guidi L, Degl'Innocenti E, Giordano C, Biricolti S, Tattini M. Ozone tolerance in Phaseolus vulgaris depends on more than one mechanism. Environ Pollut. 2010;158: 3164–3171. doi:10.1016/j.envpol.2010.06.037

Hasan, M., Ahammed, G. J., Yin, L., Shi, K., Xia, X., Zhou, Y., ... & Zhou, J. (2015). Melatonin mitigates cadmium phytotoxicity through modulation of phytochelatins biosynthesis, vacuolar sequestration, and antioxidant potential in Solanum lycopersicum L. *Frontiers in Plant Science*, *6*, 601.

Hirayama, T., & Shinozaki, K. (2010). Research on plant abiotic stress responses in the post-genome era: Past, present and future. *The Plant Journal*, *61*(6), 1041-1052.

Jaspers P, Kangasjärvi J (2010) Reactive oxygen species in abiotic stress signaling. Physiol Plantarum 138:405–413

Lam, P. K., & Gray, J. S. (2001). Predicting effects of toxic chemicals in the marine environment. *Marine Pollution Bulletin*, *42*(3), 169-173.

Manara, A. (2012). Plant responses to heavy metal toxicity. In *Plants and heavy metals* (pp. 27-53). Springer, Dordrecht.

Manik, S.M.; Shi, S.; Mao, J.; Dong, L.; Su, Y.; Wang, Q.; Liu, H. The calcium sensor CBL-CIPK is involved in plant's response to abiotic stresses. Int. J. Genom. 2015, 2015, 493191.

Mittler, R., Vanderauwera, S., Suzuki, N., Miller, G. A. D., Tognetti, V. B., Vandepoele, K., ... & Van Breusegem, F. (2011). ROS signaling: the new wave?. Trends in plant science, 16(6), 300-309.

Nali C, Paoletti E, Marabottini R, Della Rocca G, Lorenzini G, Paolacci AR, et al. Ecophysiological and biochemical strategies of response to ozone in Mediterranean evergreen broadleaf species. Atmos Environ. 2004;38: 2247–2257. doi:10.1016/j.atmosenv.2003.11.043

Noctor, G., Mhamdi, A., & Foyer, C. H. (2014). The roles of reactive oxygen metabolism in drought: not so cut and dried. Plant physiology, 164(4), 1636-1648.

NRC (National Research Council) (1987) Biological markers in environmental health research. Environ Health Perspect 74:3–9

Scalet M, Federico R, Guido MC, Manes F. Peroxidase activity and polyamine changes in response to ozone and simulated acid rain in Aleppo pine needles. Environ Exp Bot. 1995;35: 417–425. doi:10.1016/0098-8472(95)00001-3

Singh, R., Singh, S., Parihar, P., Mishra, R. K., Tripathi, D. K., Singh, V. P., ... & Prasad, S. M. (2016). Reactive oxygen species (ROS): beneficial companions of plants' developmental processes. *Frontiers in plant science*, *7*, 1299.

Singh, S., Tripathi, D. K., Singh, S., Sharma, S., Dubey, N. K., Chauhan, D. K., & Vaculík, M. (2017). Toxicity of aluminium on various levels of plant cells and organism: a review. Environmental and Experimental Botany, 137, 177-193.

Tamás, M. J., Sharma, S. K., Ibstedt, S., Jacobson, T., & Christen, P. (2014). Heavy metals and metalloids as a cause for protein misfolding and aggregation. *Biomolecules*, *4*(1), 252-267.

Vainonen JP, Kangasjärvi J. Plant signalling in acute ozone exposure. Plant Cell Environ. 2015;38: 240–252. doi:10.1111/pce.12273

Vries W de, Dobbertin MH, Solberg S, Dobben HF van, Schaub M. Impacts of acid deposition, ozone exposure and weather conditions on forest ecosystems in Europe: an overview. Plant Soil. 2014;380: 1–45. doi:10.1007/s11104-014-2056-2

Xia, X. J., Zhou, Y. H., Shi, K., Zhou, J., Foyer, C. H., & Yu, J. Q. (2015). Interplay between reactive oxygen species and hormones in the control of plant development and stress tolerance. *Journal of experimental botany*, *66*(10), 2839-2856.

CHAPTER 1

Heavy metal stress

Ecotoxicology and Environmental Safety 144 (2017) 268–274

Contents lists available at ScienceDirect

Ecotoxicology and Environmental Safety

journal homepage: www.elsevier.com/locate/ecoenv

Effects of triacontanol on ascorbate-glutathione cycle in *Brassica napus* L. exposed to cadmium-induced oxidative stress

Elham Asadi karam[a], Viviana Maresca[b], Sergio Sorbo[c], Batool Keramat[a], Adriana Basile*[b]

[a] Biology Department, Shahid Bahonar University of Kerman, Kerman, Iran

[b] Biology Department, University of Naples "Federico II", via Cinthia, 80126, Naples, Italy

[c] Ce.S.M.A, Microscopy Section, University of Naples Federico II, via Cinthia, 80126 Naples, Italy

*Corresponding author. Email: *adbasile@unina.it*

Abstract

The ability of exogenous triacontanol (TRIA), a plant growth regulator, to reduce Cd toxicity was studied in canola (*Brassica napus* L.) plants. The following biological parameters were examined in canola seedlings to investigate TRIA-induced tolerance to Cd toxicity: seedling growth, chlorophyll damage and antioxidant response. In particular, TRIA application reduced Cd-induced oxidative damage, as shown by reduction of ROS content, lipoxygenase (LOX) activity and lipid peroxidation level. TRIA pretreatment increased non-enzymatic antioxidant contents (ascorbate, AsA, glutathione and GSH), phytochelatins content (PCs) and activities of antioxidant enzymes such as superoxide dismutase (SOD), catalase (CAT), ascorbate peroxidase (APX), guaiacol peroxidase (GPX), monodehydroascorbate reductase (MDHAR), dehydro ascorbate reductase (DHAR), and glutathione reductase (GR), so reducing the oxidative stress. These results clearly indicate the protective ability of TRIA to modulate the redox status through the antioxidant pathway AGC and GSH, so reducing Cd-induced oxidative stress.

Keywords: Cadmium, Glutathione-Ascorbate cycle, Triacontanol.

1. Introduction

Cadmium toxicity leads to health impairment in living organisms, so it represents an ecologically hazardous toxic metal. As Cd enters the trophic chain through plants, it is noteworthy to know how the plants respond to Cd. Plants growing in a Cd-added growth media show biochemical and physiological disorders: chlorosis, necrosis, leaf rolling, growth inhibition, damage of membrane functions, alteration of ion homeostasis, decreased water and nutrient transportation, photosynthesis inhibition, altered metabolism, altered activities of several key enzymes, and even cell death (Ehsan *et al.*, 2014). A common consequence of heavy metal (HM) toxicity is the excessive accumulation of reactive oxygen species (ROS) and methylglyoxal (MG), both of which can cause peroxidation of lipids, oxidation of protein, inactivation of enzymes, DNA damage and/or interact with other vital constituents of plant cells (Hossain *et al.*, 2012). An antioxidant system is well equipped with different antioxidant components to scavenge over-produced ROS and then protects plants from oxidative injury (Hasanuzzaman *et al.*, 2013). Furthermore, chelation, binding, exclusion, active excretion, and compartmentalization of Cd are some adaptive mechanisms by which plants avoid toxic effects of Cd (Basile *et al.*, 2009, 2012a, 2012b, 2013, 2015; Carginale *et al.*, 2004; Nahar *et al.*, 2016; Zagorchev *et al.*, 2013).

Plant hormones increase stress tolerance in plants by regulating various physiological and biochemical processes (Shahbaz *et al.*, 2011). Their crucial roles encourage the seeking for new plant growth regulators and elucidation of their roles in regulating different plant processes (Perveen *et al.*, 2014). One of relatively new PGRs, the Triacontanol (TRIA), is reported to stimulate plant growth even at a very low concentration, when exogenously applied to various plant species (Verma *et al.*, 2011). TRIA has been reported to enhance photosynthesis (Eriksen *et al.*, 1981) and water and mineral nutrients uptake (Chen *et al.*, 2003), to regulate activities of various enzymes (Naeem *et al*., 2012), and to increase various organic compounds in leaf tissues (Kumaravelu *et al.*, 2000; Chen *et al.*, 2003). So TRIA has received much attention in recent years as a plant growth regulator. It may play an important role in resistance of some plants to abiotic stresses, such as salinity (Shahbaz *et al.*, 2013;

Perveen *et al.*, 2014), chilling (Borowski and Blamowski, 2009) and arsenic toxicity (Asadi karam *et al.*, 2016).

This study focuses on the response to oxidative stress in canola seedlings under Cd stress and investigates the ability of exogenous TRIA as a regulator of the glutathione-ascorbate cycle and the antioxidant metabolism, and as enhancer of tolerance to oxidative stress.

2. Material and methods

2.1. Plant growth and treatments

Seeds of canola (*Brassica napus* L.) were sterilized using 0.1 % sodium hypochlorite solution, washed with distilled water and planted in pots filled with perlite. Pots were transferred in growth chamber with day/night temperature of 25/20°C and a 16 h light/8 h dark photoperiod, with 70% relative humidity. During the first week from the sowing, seedlings were irrigated with distilled water; then half strength Hoagland's nutrient solution (pH 5.7 ± 0.1) was used to irrigate plants every other day. The 21-day-old seedlings, at the three leaf stage, were exposed to TRIA (Sigma Aldrich) and Cd treatments. Two concentrations of TRIA in ethanol solutions, at10 and 20 µM, were applied as foliar spray at the three leaf stage for 7 days. After pretreatment, plants were irrigated with Hoagland's solution containing 1.5 mM $CdCl_2$ for 7 days. At the end of experiment, leaves of both the treated and the untreated samples (control) were collected, immediately frozen in liquid nitrogen and then stored at -80°C for the analyses.

2.2. Plant growth evaluation

At the end of the experiment, the weights of 10 randomly selected fresh seedlings from each treatment were measured and expressed as fresh weight (FW) grams.

2.3. Physiological and biochemical parameter evaluation

The level of lipid peroxidation in plant tissues was evaluated by measuring the malondialdehyde (MDA) content by using thiobarbituric acid (Heath and Packer, 1968).

The H_2O_2 content in the plants was measured by reaction with potassium iodide (KI), according to Velikova *et al*. (2000). The amount of H_2O_2 was extrapolated from the standard curve.

A fluorescent technique using 2', 7'-dichlorofluorescin diacetate (DCFH-DA) has been used for quantitative measurement of ROS production. DCFH-DA is de-esterified intracellularly and turns to nonfluorescent 2', 7'-dichlorofluorescin (DCFH). DCFH is then oxidized by ROS to highly fluorescent 2′, 7′-dichlorofluorescein (DCF) (LeBel et al 1990). Briefly, leaf samples were immediately frozen in liquid nitrogen and ground thoroughly with prechilled mortar and pestle. The resulting powder (150 mg) was then resuspended in TrisHCl 40 mM pH 7.4, sonicated, and centrifuged at 12,000g for 30 min. The supernatant (500 µL) was collected and protein content determined. An aliquot (10 µL) of each sample was incubated with 5 µM DCFH-DA for 30 min at 37°C followed by recording of the final fluorescence value, which was detected at excitation (488 nm) and emission (525 nm) wavelength. DCF formation was quantified from a standard curve (0.05-1.0 µM).

The ASC and dehydroascorbate (DHA) contents were measured as described by De Pinto *et al.* (1999). Briefly, total ASC was determined after reduction of DHA to ASC with dithiotreitol (DTT), and the content of DHA was estimated by the difference between the total ASC pool (ASC plus DHA) and ASC.

The GSH content was determined by the spectrophotometric method of Ellman (1959), where GSH was oxidized in 2.6 ml of a sodium phosphate buffer (pH 7.0) containing 0.2 ml of a sample extract and 0.2 ml of 6 mM 5,5'-dithiobis-(2 nitrobenzoic) acid (DTNB). The absorbance was monitored at 412 nm. The GSH content was calculated from a standard curve constructed using GSH over the range 0-100 µM.

Measurement of non-protein thiol content was measured according to Sedlak and Lindsay (1968). Samples were homogenized in 0.02 M EDTA in an ice bath. Aliquots of 5 ml of the homogenates were mixed with 4 ml distilled water and 1 ml of 50% TCA. The contents were mixed and after 15 min the tubes were centrifuged for 15 min. 2 ml of the supernatant was mixed with 4 ml of 0.4 M Tris buffer (pH 8.9), 0.1 ml of DTNB and absorbance was read within 5 min at 412 nm against a reagent blank. Total phytochelatins concentrations were

calculated by subtracting the amount of GSH from the total amount of NPT according to De Vos et al. (1992).

2.4. Enzyme extraction and activity evaluation

For protein extraction and analysis, the extracts of frozen samples prepared in a 50 mM potassium phosphate buffer (pH 7) containing 1mM phenylmethane sulfonyl fluoride (PMSF), 1 mM sodium ethylene diaminetetraacetic acid (Na_2EDTA), and 1% (m/v) polyvinylpyrrolidone (PVP) were centrifuged at 15,000 *g* at 4 °C for 15 min and the supernatants were used for the estimation of protein content and enzyme activities. The total protein content was measured according to the method of Bradford (1976) using bovine serum albumin as standard. All spectrophotometric analyses were conducted in a final volume of 3 ml by using a *Cary 50* UV/visible spectrophotometer.

Superoxide dismutase (SOD, EC 1.15.1.1) activity was assayed by measuring its ability to inhibit the photochemical reduction of nitro blue tetrazolium chloride (NBT) (Giannopolitis and Ries, 1977). One unit of SOD activity was defined as the amount of enzyme required to cause 50% inhibition of NBT reduction at 560 nm. Catalase activity (CAT, EC 1.11.1.6) was assayed by monitoring the decrease in the absorbance of H_2O_2 within 30s at 240 nm. Unit of activity was taken as the amount of enzyme that decomposes 1 µmol of H_2O_2 in 1 minute (Dhindsa *et al.*, 1981). The decrease in hydrogen peroxide was inferred from the decline in absorbance at 240 nm.

Ascorbate peroxidase (EC 1.11.1.11) was assayed by monitoring the decrease in absorbance at 290 nm due to ASC oxidation (Nakano and Asada, 1987). One unit of APX activity was defined as the amount of enzyme that decomposed 1 mmol of ascorbate per minute. Guaiacol peroxidase (GPX; EC 1.11.1.7) activity was determined by a method derived from Plewa *et al.* (1991). One unit of GPX activity was defined as the amount of enzyme that produced 1 mmol of tetraguaiacol per minute. For the measurement of the LOX (EC 1.13.11.12) activity, we used the Minguez-Mosquera *et al.* (1993) method. The enzyme unit was defined as 1 µmol of the product formed per min. Glutathione reductase (GR; EC1.6.4.2) activity was determined following the decrease in absorbance at 340 nm associated with the oxidation of NADPH

(Foyer and Halliwell, 1976). One unit of GR was defined as the amount of enzyme that oxidized 1 μmol of NADPH per minute.

Monodehydroascorbate reductase (MDHAR, EC 1.6.5.4) activity was assayed at 340 nm with microplate assay kit (Mybiosource) according to the manufacturer's instructions. One unit of MDHAR activity was defined as the amount of enzyme that oxidizes 1 μmol NADH per minute. A molar coefficient of 6.2 mM^{-1} cm^{-1} was used for the calculation of enzyme activity.

Dehydroascorbate reductase (DHAR, EC 2.5.1.18) activity was measured at 265 nm with microplate assay kit (Mybiosource) according to the manufacturer's instructions. One unit of DHAR activity was defined as the amount of enzyme that produces 1 μmol of AsA per minute.

2.5. Element Analysis by ICP-OES

Samples of shoot were oven dried at 70°C for 72 h and after determination of dry biomass, 0.5g samples dissolved in 10 ml 65% (w/v) nitric acid (supra pure, Merck). After digestion, the volume of each sample was adjusted to 50 mL using double deionized water. Total concentration of Cd was determined by inductively coupled plasma atomic emission spectroscopy (ICP, OES, Varian CO). The stability of the device was evaluated after determination of every ten samples by examining the internal standard. Reagent blanks were also prepared to detect potential contamination during the digestion and analytical procedure. The samples were analyzed in triplicates. Also, we used standards solutions with a final Cd concentration in range of plants in the analyzed solution (As standard solution, MERCK) for quality control (Sagner, 1998).

2.6. Statistical data analysis

Data were analyzed by using two-way analysis of variance (ANOVA). Differences between means were considered significant at a confidence level of $P \leq 0.05$. All statistical analyses were done using the software SPSS package, version 18.0. The Duncan test analysis was done to determine the significant difference between treatments.

3. Results

3.1. Cd accumulation, Plant growth evaluation and chlorophyll content in shoot

Canola plants exposed to $CdCl_2$ accumulated substantial amounts of Cd in the leaves (Table 1). There was a positive correlation between Cd concentration in nutrient solutions and Cd content in leaves. After 7-d exposure to 1.5 mM $CdCl_2$, the young leaves contained 0.119 mg g^{-1}DW. Application of 10 and 20 μM TRIA decreased shoot Cd content in canola plants by 28 and 24%, respectively, compared to cd treatment. Application of 1.5 mM $CdCl_2$ decreased shoot fresh weight of seedlings by 27%, compared to control. The exogenous TRIA mitigated the negative effects of Cd and increased the growth (Table 1). The reduction of total chl (a + b) in Cd concentration indicates destructive nature of Cd. Exogenous TRIA pretreatment increased chl content under Cd stress. Total chl increased after TRIA addition by 23 and 11% at 1.5 mM $CdCl_2$ (Table 1).

3.2. Oxidative stress evaluation

Oxidative stress of Cd-treated canola seedlings was shown by increased ROS content, H_2O_2 generation and lipid peroxidation. Cd stress increased lipid peroxidation or MDA level, H_2O_2 content and ROS amount by 59, 48 and 188%, respectively, compared to control seedlings. The activity of LOX increased under Cd stress, which partly contributed to the oxidative stress. TRIA pretreatment decreased ROS, H_2O_2 contents, LOX activity, and subsequently the lipid peroxidation or MDA level, in comparison to Cd-treated samples with no TRIA pretreatment (Table 1).

3.3. Ascorbate and glutathione pool, content of phytochelatins

Under Cd stress, in comparison to control samples, ascorbate content decreased by 38% and DHA increased by 25%, which resulted into a decrease of the AsA/DHA ratio (Fig. 1A–D). Cadmium also induced increase of the endogenous GSH level, in comparison to control. TRIA pretreatment on the Cd-treated samples increased AsA content, GSH level and ASA/DHA ratio, in comparison to TRIA-untreated, Cd-exposed samples (Fig. 1A–D). In the leaves, treatment with 1.5 mM Cd caused an increase in PCs content (Fig. 1E). PCs content increased

from 15 μmol g^{-1}(protein), in the leaves of control plants, to 22 μmol g^{-1}(protein), in 1.5 mM Cd treated. The PCs synthesis was associated with GSH increase. During the time course of experiment, the GSH content increased and a high PCs contents have been detected in leaves of TRIA-untreated plants (Fig. 1C-E). Addition of 10 and 20 μM TRIA led to an immediate and significant increase in the GSH content. At the same time, there was a marked increase in PCs contents.

3.3. Antioxidant enzyme evaluation

Superoxide dismutase activity increased under Cd stress and in TRIA-added Cd treatments. Under Cd stress, CAT activity decreased by 37%, compared to control; TRIA pretreatment restored CAT activity (Table. 2).

The activity of GPX increased by 129%, under Cd stress, compared to control. When seedlings were supplied with exogenous TRIA 10 and 20μM and Cd, GPX activity increased by 112 and 113%, respectively, compared to control (Table. 2).

The activity of APX decreased under Cd stress, compared to control. Exogenous TRIA pretreatment increased its activity under Cd stress (Table. 2).

Activity of MDHAR and DHAR decreased under Cd stress, compared to control seedlings. MDHAR and DHAR activity increased by 39.11 and 273%, respectively, when the seedlings were pretreated with 10μM TRIA before Cd treatments.

Activity of GR increased under severe Cd stress, compared to control. Under Cd stress, exogenous TRIA pretreatment increased GR activity, compared to Cd-only treatment (Table. 2).

4. Discussion

Cadmium toxicity is responsible for reduction of nutrient uptake, inhibition of cell division and elongation, damaging photosynthetic pigments and net photosynthesis, which ultimately results in strong inhibition of plant growth (Dias *et al.*, 2013; Ehsan *et al.*, 2014). In our study on canola seedlings, shoot fresh weight decreased in Cd-treated samples; TRIA pretreatment reduced Cd-induced growth inhibition. The decrease in plant growth was proportional to the

uptake of Cd. The data showed that Cd treatment increased Cd accumulation of shoot in the canola significantly in comparison to the control. It is concluded that the Cd accumulation had a distinct correlation with the reduction in the growth of canola. The results are in accordance with other studies with *Lepidium sativum, Brassica juncea*, and *Lycopersicon esculentum* (Gill *et al*. 2011, 2012, Gratão *et al*. 2012). Reduction in cell growth appears to be due to Cd mediated cell damage, inhibition of mitosis, restricted cell wall synthesis and deposition of lignin in the cell wall (Kumari *et al*. 2015). On the other hand, TRIA has effect on alleviating Cd accumulation of canola plants under Cd stress. Furthermore, TRIA application reversed growth inhibition and increased growth in Cd-affected seedlings (compared to Cd stress alone). The ability of TRIA to modulate plant physiology and biochemistry so as to improve growth under metal stress was reported in an our previous work (Asadi karam *et al.*, 2016). The growth promoting ability of TRIA in crop plants has been especially focused on its synergistic interaction with phytohormones and induction of 9-b-L (+) adenosine, which has a structure similar to cytokinin (Naeem *et al.*, 2012). The induction of 9-b-L (+) adenosine by TRIA is thought to be one of the reasons for the increase in dry matter and other growth parameters, as it turns on a rapid cascade of metabolic events throughout the plant within 1 min (Naeem *et al.*, 2012).

Chlorophyll content in canola leaf declined with increasing Cd as also reported in Dias *et al.* (2013). Cadmium-induced reduction in chlorophyll content and chlorosis might be due to the reduction of Fe in leaves and to the negative effects of Cd on chlorophyll metabolism (Chaffei *et al.*, 2004). Cadmium-induced degradation of chlorophyll, due to the high activity of chlorophyll-degrading enzyme and/or the inhibition of its biosynthesis, was proposed to reduce both photosynthesis and growth in other studies (Dias *et al.*, 2013). Oxidative damage of photosynthetic pigments is also a common deleterious effect of cadmium (Nahar *et al.*, 2016). Similar reasons are supposed to be involved in decrease of the chlorophyll content in canola leaf exposed to Cd stress. However, chlorophyll content increased after TRIA pretreatment, compared to Cd stress only. TRIA is reported to affect various plant characteristics, increasing CO_2 assimilation rate (Haugstad *et al.*, 1983), size and number of chloroplasts (Chen *et al.*, 2002), and chloroplast membrane viscosity (Ivanov and Angelov,

1997). Among these, regulation of photosynthesis is a complex process, which is known to be modulated by TRIA; that can be explained by different mechanisms such as increased Hill reaction activity (Verma *et al.*, 2011), specific activity of Rubisco, activity of photosystem (PS) I and II complexes (Moorthy and Kathiresan, 1993), up-regulation of genes (*rbc*S isogene profile) related to photosynthesis and suppression of stress-related genes in rice (Chen *et al.*, 2002). In our previous experiment, the reduction in biomass and induction of lipid peroxidation under toxicity condition were partially alleviated by applying TRIA (Asadi karam *et al.*, 2016). Our data suggested that TRIA might have played a key role in protecting the structure and function of cell membranes and pigments under Cd toxicity.

Impairing the antioxidant system (Nahar *et al.*, 2016), the electron transport chain, and the metabolism of essential elements (Dong *et al.*, 2006), Cd causes oxidative stress. Cadmium slows down or holds or blocks the photoactivation of PSII by inhibiting electron transfer, leading to the generation of ROS (Sigfridsson *et al.*, 2004). That metal was also suggested to stimulate ROS production in the mitochondrion electron transfer chain (Heyno *et al.*, 2008). This experiment showed that cadmium increased ROS, lipid peroxidation and LOX activity, the last being reduced by exogenous TRIA application. Our finding that exogenous TRIA reduced ROS and lipid peroxidation is in agreement with our previous work (Asadi karam *et al.*, 2016). Being AsA the most abundant antioxidant, it directly quenches many ROSs (Gill and Tuteja, 2010); so, its reduction after Cd treatments is supposed to be responsible for ROS generation and oxidative stress. Decreased AsA and increased DHA levels observed in Cd-treated canola seedlings. Reduced AsA content is correlated to APX activity and reduction of MDHAR and DHAR activities which recycle AsA, but exogenous addition of TRIA with Cd decreased DHA and increased AsA level by increasing MDHAR and DHAR activities, which increased the ratio of AsA/DHA (compared to Cd stress alone). GSH has a role in ROS detoxification, conjugation of metabolites, and detoxification of xenobiotics, and signaling action, which triggers adaptive responses under stress condition (Foyer and Noctor, 2005). Plant heavy metal stress response is often associated with increased GSH level (Gill and Tuteja, 2010; Kanwar *et al.,* 2015). In our experiment the contents of GSH increased under Cd stress, compared to control. During ROS scavenging GSH is oxidized to GSSG and then GR recycles

GSH. In our Cd-treated seedlings, exogenous TRIA increased both the activity of GR and GSH level, in comparison to Cd-only treated seedlings. In our canola samples TRIA pretreatment increased GSH level and decreased H_2O_2 content. TRIA might have a role in GSH biosynthesis or regeneration, which increased the GSH level. In the present study exogenous TRIA also enhanced other components of AsA-GSH cycle. TRIA might have signaling roles in enhancing biosynthesis of APX, MDHAR, DHAR, and GR. Otherwise, TRIA might have other roles leading to the increase of their activities. There are no data on the effect of TRIA on the activity of these enzymes, so the mechanism leading to the increase of these enzymes is not yet clear. This work is an important progress to better understand the matter.

Moreover, Glutathione as a sulfur-containing tripeptide thiol is involved in the plant protections against heavy metals as a precursor in the synthesis of phytochelatins (PCs) and in the scavenging of ROS by the ascorbate–glutathione cycle (Xiong *et al*., 2010). PCs bind a metal and transport it to a vacuole, and among the metals, PC is most effective in chelating Cd (Zagorchev *et al.,* 2013). In this study, increasing PC content in canola may be caused by increase content of GSH in the response of Cd toxicity. Recently, Gupta *et al.,* (2009) demonstrated that PC synthesis is stimulated by heavy metal supply in *Brassica juncea* due to the overexpression of PCs gene. The PC–metal complex is often sequestered in the vacuoles (Sharma *et al.,* 2010). Increase of GSH content and PC content in Cd-affected canola plant (compared to control) is corroborating with the findings of previous studies (Najmanova *et al.,* 2012; Nahar *et al.,* 2016). After TRIA application with Cd stress, the contents of GSH and PC increased which probably indicates upregulation of Cd chelation and sequestration capacity by TRIA.

SOD provides the first line of defense against ROS (Gill *et al.,* 2015). In Cd-treated samples the SOD reduced activity was not enough to counteract the occurring oxidative load. When exogenous TRIA was applied, the activity of SOD increased significantly, which reduced H_2O_2 generation. Exogenous TRIA application was reported to increase SOD activity in salinity-affected *Triticum aestivum* (Perveen *et al*., 2014). These findings support the results of the present study. The activity of CAT is involved in converting H_2O_2 to H_2O and O_2.

Cadmium, replacing Fe from the active center of CAT, inhibits the enzyme functioning (Nazar *et al.*, 2012). In Cd-treated samples, the Cd-induced reduction of the CAT activity was probably one of the reasons accounting for the increase of H_2O_2. As our results showed, exogenous TRIA significantly increased CAT activity, in comparison to Cd treatment alone. Furthermore, TRIA application increased CAT activity also in salinity-affected *Triticum aestivum* (Perveen *et al.*, 2014).That finding supports the results of the present study. Glutathione dependent conjugation of lipid hydroperoxides and endobiotic substrates by GPX and GST contributes in defending plant from metal toxicity effects. Scavenging of peroxides and other electrophiles, GPX and GST protect cell components from oxidative damage (Gill and Tuteja, 2010). In our experiment, under Cd stress, the activity of GPX increased in comparison to control. GPX activity was also significantly improved by TRIA in Cd-stressed *Zea mays,* which supports the roles of TRIA at improving GPX activity (Ahmad *et al.*, 2012).

5. Conclusion

In conclusion, the tolerance of canola to the Cd-induced oxidative stress seems to be dependent upon the efficiency of the antioxidant system, which maintains the redox homeostasis and integrity of cellular components. Then, the ASC-GSH cycle enzymes might play major roles in preserving the Cd-stressed canola plants. On the whole, our findings support the hypothesis that the higher efficiency of the antioxidants after TRIA application could be responsible for the increased tolerance to Cd. Exogenous application of TRIA improved the non-enzymatic antioxidant level, phytochelatins content and increased the activities of antioxidant enzymes and reduced oxidative damage. Exogenous TRIA alleviated growth inhibition and improved chlorophyll content. Finally, the ASC-GSH cycle enzymes under the Cd stress and TRIA applications may have a significant role in canola heavy metal tolerance.

Figure and Table

Treatments		Shoot Cd content (mg g^{-1} DW)	Shoot fresh weight (g $seedling^{-1}$)	Total Chl (a + b) (mg g^{-1} FW)	MDA content (µmol g^{-1} FW)	H_2O_2 content (µmol g^{-1} FW)	ROS content (Flourescence intensity)	LOX activity (U/mg protein)
Cd (mM)	TRIA (µM)							
0	0	0.0002±0.00001d	4.39±0.22a	3.73±0.03a	0.61±0.08d	4.6±0.22c	2231±345.12c	15.11±2.08c
1.5	0	0.119±0.027a	3.18±0.14d	2.14±0.06e	0.97±0.15a	6.85±0.30a	6436±594.07 a	25.64±3.77a
0	10	0.001±0.0004d	4.29±0.92a	3.65±0.05a	0.63±0.07d	5.03±0.24c	1884±215.20d	16.35±1.91c
1.5	10	0.085±0.012bc	3.45±0.38c	2.64±0.11c	0.86±0.04b	5.35±0.31b	3796±443.89b	23.70±2.68b
0	20	0.0004±0.00002d	3.57±0.13b	2.81±0.03b	0.75±0.09c	4.29±0.26d	2728±362.71c	18.49±1.46c
1.5	20	0.090±0.003ab	3.53±0.32c	2.38±0.02d	0.92±0.14a	5.15±0.19c	3433±221.32b	24.85±3.47ab

Table1. Effects of cadmium and triacontanol on the growth and the biochemical parameters in canola leaves. Note: values are expressed as mean ± SE (n = 3). The different letters indicate significant differences among treatments at $p \leq 0.05$ according to Duncan's multiple range tests

Treatments		**CAT activity (U/mg protein)**	**SOD activity (U/mg protein)**	**APX activity (U/mg protein)**	**GPX activity (U/mg protein)**	**GR activity (U/mg protein)**	**MDHAR activity (U/mg protein)**	**DHAR activity (U/mg protein)**
Cd (mM)	**TRIA (µM)**							
0	**0**	31.31±1.62cd	19.96±0.14e	1.53±0.13a	6.38±0.89d	0.8±0.08c	6.05±0.21d	24.93±3.10d
1.5	**0**	19.48±0.84f	33.03±0.13b	0.94±0.11c	14.67±1.65a	1.05±0.15b	11.48±0.68c	15.18±2.26ef
0	**10**	35.24±2.02c	21.95±0.24d	1.07±0.15b	9.33±0.47d	1.12±0.10b	13.06±1.2b	19.61±1.02e
1.5	**10**	42.68±2.81b	35.62±0.1ab	1.54±0.11a	13.56±1.36b	1.8±0.35a	15.97±1.70ab	56.74±4.37a
0	**20**	29.98±1.43e	24.79±0.12c	0.91±0.09c	10.45±0.78c	0.93±0.20c	17.39±2.60a	42.07±2.65b
1.5	**20**	49.60±2.07a	38.58±0.25a	1.45±0.22ab	13.62±2.6b	1.91±0.18ab	12.65±1.35c	36.16±3.47c

Table 2. Effects of cadmium and triacontanol application on Catalase, Superoxide dismutase, Ascorbate peroxidase, Guaiacol peroxidase, Glutathione reductase, Monodehydroascorbate reductase and Dehydroascorbate reductase activies in *Brassica napus* leaves.

Note: Values are means ± SE (n = 3). The different letters indicate significant differences among treatments at $p \leq 0.05$ according to Duncan's multiple range tests

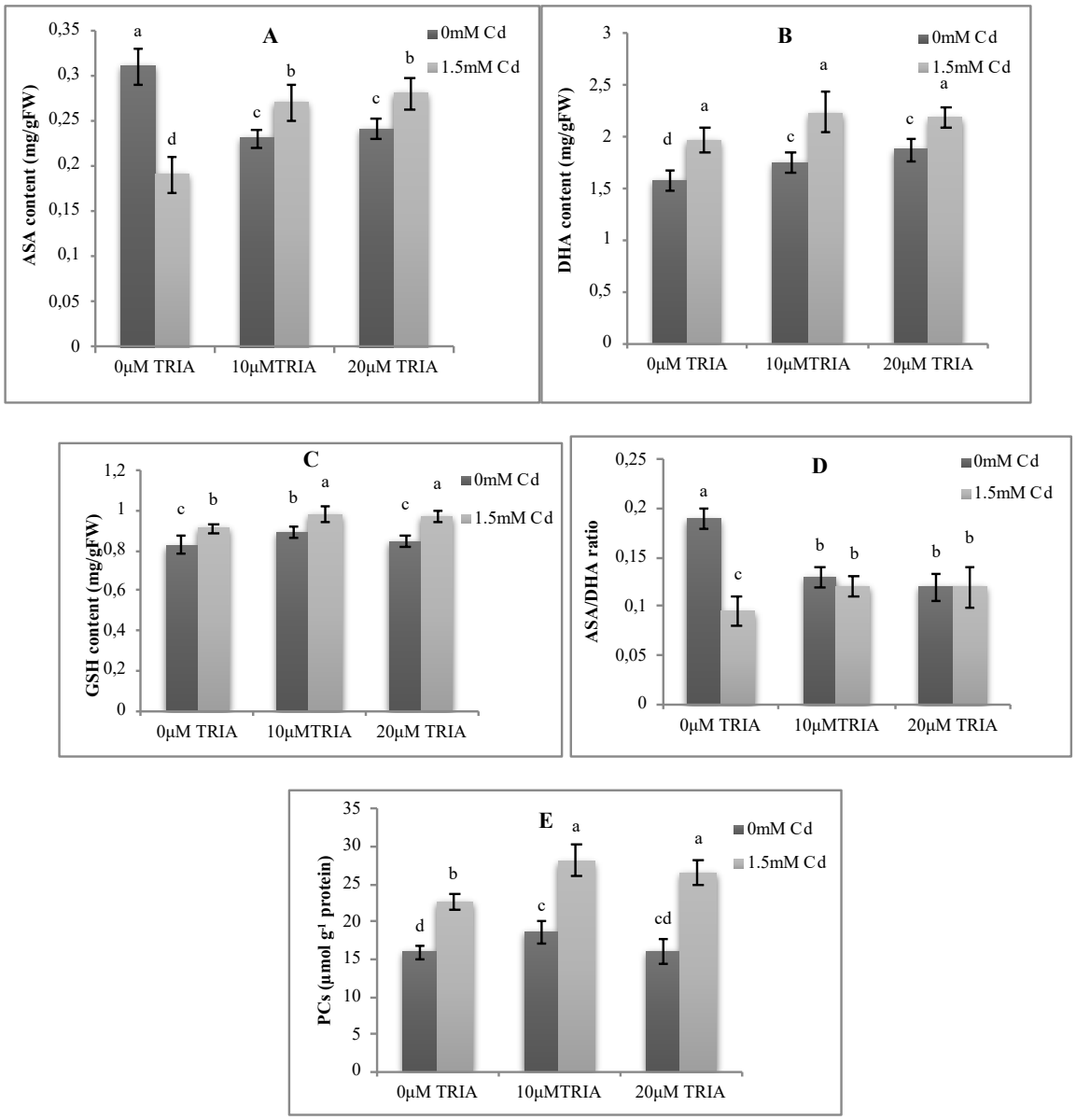

Figure.1. Effects of cadmium and triacontanol on (A) Ascorbate, (B) Dehydroascorbate, (C) Reducted glutathione content, (D) ASA/DHA ratio and (E) Phytochelatins content in *Brassica napus* leaves. Values are means ± SE (n = 3). In the individual column, bars with different letters are statistically different ($P < 0.05$) according to Duncan's multiple range tests.

References

Ahmed, H.F.S., Metwally, H. H. El- Shafey, A.S. 2012. Effect of cadmium on growth, flowering and fruiting of Zea mays L. and possible roles of triacontanol in alleviating cadmium toxicity. Int. J. Acad. Res. https://doi.org/10.7813/2075-4124.2012/4-5/A.1.

Asadi karam, E., Keramat, B., Asrar, Z and Mozafari, H. 2016. Triacontanol-induced changes in growth, oxidative defense system in Coriander (*Coriandrum sativum*) under arsenic toxicity. Ind J. Plant Physiol. https://doi.org/10.1007/s40502-016-0213-8.

Basile, A., Sorbo, S., Aprile, G., Conte, B., Castaldo Cobianchi, R., Pisani, T., Loppi, S. 2009. Heavy metal deposition in the italian "Triangle of death" determined with the moss *Scorpiurium circinatum*. Environ. Pollut. 157: 2255-2260. http://dx.doi.org/10.1016/j.envpol.2009.04.001.

Basile, A., Sorbo, S., Cardi, M., Lentini, M., Castiglia, D., Cianciullo, P., Conte, B., Loppi, S., Esposito, S. 2015. Effects of heavy metals on ultrastructure and Hsp70 induction in *Lemna minor* L. exposed to water along the Sarno River, Italy. Ecotox. Environ. Safe. 114 : 93–101. http://dx.doi.org/10.1016/j.ecoenv.2015.01.009.

Basile, A., Sorbo, S., Conte, B., Cardi, M., Esposito, S. 2013. Ultrastructural changes and Heat Shock Proteins 70 induced by atmospheric pollution are similar to the effects observed under in vitro heavy metals stress in *Conocephalum conicum* (Marchantiales e Bryophyta). Environ. Pollut. 182 209e216. http://dx.doi.org/10.1016/j.envpol.2013.07.014.

Basile, A., Sorbo, S., Conte, B., Cobianchi, R., Trinchella, F., Capasso, V., Carginale, V. 2012a. Toxicity, accumulation, and removal of heavy metals by three aquatic macrophytes. Int. J. Phytoremediation. 14:374–387. http://dx.doi.org/10.1080/15226514.2011.620653.

Basile, A., Sorbo, S., Pisani, T., Paoli, L., Munzi, S., Loppi, S., 2012b. Bioaccumulation and ultrastructural effects of Cd, Cu, Pb and Zn in the moss *Scorpiurum circinatum* (Brid.) Fleisch. & Loeske. Environ. Pollut. 166 208-211. http://dx.doi.org/10.1016/j.envpol.2012.03.018.

Borowski, E., Blamowski, Z.K. 2009. The effect of triacontanol 'TRIA'and Asahi-SL on the development and metabolic activity of sweet basil (Ocimum basilicum L.) plants treated with chilling. Folia Hort. 21, 39–48. https://doi.org/10.2478/fhort-2013-0124.

Bradford, M. M. 1976. A rapid and sensitive method for the quantitation of microgram quantities of protein utilizing the principle of protein-dye binding. Anal. Biochem. 72:248–254. https://doi.org/10.1016/0003-2697(76)90527-3.

Carginale, V., Trinchella, F., Capasso, C., Cafiero, G., Sorbo, S., Basile, A. 2004. Accumulation, localization and toxic effects of cadmium in the liverwort Lunularia cruciata. Protoplasma 223: 53-61. https://doi.org/10.1007/s00709-003-0028-0.

Cataldo, D.A., Garland, R., Wildung, R.E. 1983. Cadmium uptake kinetics in intact soybean plants. Plant Physiol. 73:844–848. http://dx.doi.org/10.1104/pp.73.3.844.

Chaffei, C., Pageau, K., Suzuki, A., Gouia, H., Ghorbel, H.M., Mascalaux- Daubresse, C. 2004. Cadmium toxicity induced changes in nitrogen management in Lycopersicon esculentum leading to a metabolic safeguard through an amino acid storage strategy. Plant Cell Physiol. 45:1681–1693. https://doi.org/10.1093/pcp/pch192.

Chen, X., Yuan, H., Chen, R., Zhu, L., Du, B., Weng, Q., He, G. 2002. Isolation and characterization of triacontanol regulated genes in rice (Oryza sativa L.): possible role of triacontanol as plant growth stimulator. Plant Cell Physiol. 43:869-876. https://doi.org/10.1093/pcp/pcf100.

Chen, X., Yuan, H., Chen, R., Zhu, L., He, G. 2003. Biochemical and photochemical changes in response to triacontanol in rice (Oryza sativa L.). Plant Growth Regul. 40: 249-256. https://doi.org/10.1023/A:1025039027270.

Cos, P., Rajan, P., Vedernikova, I., Calomme, M., Pieters, L., Vlietinck, A.J., Augustyns, K., Haemers, A., Berghe, D.V. 2002. In vitro antioxidant profile of phenolic acid derivatives. Free Radical Res. 36:711–716. http://dx.doi.org/10.1080/10715760290029182.

De Pinto, M.C., Francis, D., De Gara, L. 1999. The redox state of the ascorbate-dehydroascorbate pair as a specific sensor of cell division in tobacco BY-2 cells. Protoplasma 209: 90-97. http://dx.doi.org/10.1007/BF01415704.

Dhindsa, R.S., Plumb-Dhindsa, P., and Thrope, T.A. 1981. Leaf Senescence: correlated with increased levels of membrane permeability and lipid per oxidation and decreased levels of superoxide dismutase and catalase. J. Exp. Bot. 32: 43–101. https://doi.org/10.1093/jxb/32.1.93.

Dias MC, Monteiro C, Moutinho-Pereira J, Correia C, Gonçalves B, Santos C (2013). Cadmium toxicity affects photosynthesis and plant growth at different levels. Acta Physiol. Plant. 35:1281–1289.

Dong, J., Wu, F.B., Zhang, G.P. 2006. Influence of cadmium on antioxidant capacity and four microelement concentrations in tomato seedlings (Lycopersicon esculentum). Chemosphere 64:1659–1666. http://dx.doi.org/10.1016/j.chemosphere.2006.01.030.

Ehsan, S., Ali, S., Noureen, S., Mahmood, K., Farid, M., Ishaque, W., Shakoor, M.B., Rizwan, M. 2014. Citric acid assisted phytoremediation of cadmium by Brassica napus L. Ecotoxicol. Environ. Saf. 106:164– 172. http://dx.doi.org/10.1016/j.ecoenv.2014.03.007.

Ellman, G. 1959. Tissue sulfhydryl groups. Arch. Biochem. Biophys. 32: 70–77. http://dx.doi.org/10.1016/0003-9861(59)90090-6.

Eriksen, A.B., Sellden, G., Skogen, D., Nilson. S. 1981. Comparative analysis of the effect of triacontanol on photosynthesis, photorespiration and growth of tomato (C3-plants) and maize (C4-plants). Planta 152: 44-49. http://dx.doi.org/10.1007/BF00384983.

Foyer, C.H., Halliwell, B. 1976. The presence of glutathione and glutathione reductase in chloroplast: a proposed role in ascorbic acid metabolism. Planta 133:21–25. http://dx.doi.org/10.1007/BF00386001.

Foyer, C.H., Noctor, G. 2005. Redox homeostasis and antioxidant signaling: a metabolic interface between stress perception and physiological responses. Plant Cell 17:1866–1875. http://dx.doi.org/10.1105/tpc.105.033589.

Giannopolitis, C.N., Ries, S.K. 1977. Superoxide dismutases I: Occurrence in higher plants. Plant Physiol. 59: 309–314. http://dx.doi.org/10.1104/pp.59.2.309.

Gill, S.S., Anjum, N.A., Gill, R., Yadav, S., Hasanuzzaman, M., Fujita, M., Mishra, P., Sabat, S.C., Tuteja, N. 2015. Superoxide dismutase mentor of abiotic stress tolerance in crop plants. Environ. Sci. Pollut. Res. 22: 10375–10394. http://dx.doi.org/10.1007/s11356-015-4532-5.

Gill, S.S., Tuteja, N. 2010. Polyamines and abiotic stress tolerance in plants. Plant Signal. Behav. 5:26–33. http://dx.doi.org/10.4161/psb.5.1.10291.

Gill, S.S., Tuteja, N., 2010b. Reactive oxygen species and antioxidant machinery in abiotic stress tolerance in crop plants. Plant Physiol. Biochem. 48, 909–930. http://dx.doi.org/10.1016/j.plaphy.2010.08.016.

Gill, S.S., Khan, N.A., Tuteja, N., 2011. Differential cadmium stress tolerance in five indian mustard (*Brassica juncea* L.) cultivars. An evaluation of the role of antioxidant machinery. Plant Signal. Behav. 6, 293–300. http://dx.doi.org/10.4161/psb.6.2.15049.

Gill, S.S., Anjum, N.A., Gill, R., Yadav, S., Hasanuzzaman, M., Fujita, M., Mishra, P., Sabat, S.C., Tuteja, N., 2015. Superoxide dismutase mentor of abiotic stress tolerance in crop plants. Environ. Sci. Pollut. Res. 22, 10375–10394. http://dx.doi.org/10.1007/s11356-015-4532-5.

Gratão, P.L., Monteiro, C.C., Carvalho, R.F., Tezotto, T., Piotto, F.A., Peres, L.E.P., Azevedo, R.A., 2012. Biochemical dissection of diageotropica and never ripe tomato mutants to Cd-stressful conditions. Plant Physiol. Biochem. 56, 79–96. http://dx.doi.org/10.1016/j.plaphy.2012.04.009.

Gupta, M., Sharma, P., Sarin, N.B., Sinha, A.K., 2009. Differential response of arsenic stress in two varieties of Brassica juncea L. Chemosensory 74, 1201–1208. http://dx.doi.org/10.1016/j.chemosphere.2008.11.023.

Hasanuzzaman, M., Hossain, M.A., Fujita, M. 2011. Nitric oxide modulates antioxidant defense and the methylglyoxal detoxification system and reduces salinity-induced damage of wheat seedlings. Plant Biotechnol. Rep. 5:353–365. http://dx.doi.org/10.1007/s11816-011-0189-9.

Hasanuzzaman, M., Nahar, K., Alam, M.M., Roychowdhury, R., Fujita, M. 2013. Physiological, biochemical, and molecular mechanisms of heat stress tolerance in plants. Int. J. Mol. Sci. 14:9643–9684. http://dx.doi.org/10.3390/ijms14059643.

Haugstad, M., Ulsaker, L.K., Ruppel, A., Nilsen, S. 1983. The effect of triacontanol on growth, photosynthesis and photorespiration in Chlamydomonas reinhardtii and Anacystis nidulans. Physiol. Plant 58:451-456. http://dx.doi.org/10.1111/j.1399-3054.1983.tb05726.x.

Heath, R.L., Packer, L. 1968. Photoperoxidation in isolated chloroplast. I. Kinetics and stoichiometry of fatty acid peroxidation. Arch. Biochem. Biophys. 125:189–198. http://dx.doi.org/10.1016/0003-9861(68)90654-1.

Heyno, E., Klose, C., Krieger-Liszkay, A. 2008. Origin of cadmium-induced reactive oxygen species production: mitochondrial electron transfer versus plasma membrane NADPH oxidase. New Phytol. 179:687–699. http://dx.doi.org/10.1111/j.1469-8137.2008.02512.x.

Hossain, M.A., Piyatida, P., Teixeira da Silva, J.A., Fujita, M. 2012. Molecular Mechanism of Heavy Metal Toxicity and Tolerance in Plants: Central Role of Glutathione in Detoxification of Reactive Oxygen Species and Methylglyoxal and in Heavy Metal Chelation. J. Bot. http://dx.doi.org/10.1155/2012/872875.

Ivanov, A.G., Angelov, M.N. 1997. Photosynthesis response to triacontanol correlates with increased dynamics of mesophyll protoplast and chloroplast membranes. Plant Growth Regul. 21:145-152. http://dx.doi.org/10.1023/A:1005790121111.

Kanwar, M. K., Poonam, & Bhardwaj, R. (2015). Arsenic induced modulation of antioxidative defense system and brassinosteroids in *Brassica juncea* L. Ecotoxicology and Environmental Safety, 115, 119–125. http://dx.doi.org/10.1016/j.ecoenv.2015.02.016.

Kumaravelu, G., Livingstone, V.D., Ramanujam, M.P. 2000. Triacontanol-induced changes in the growth, photosynthetic pigments, cell metabolites, flowering and yield of green gram. Biol. Plantarum 43, 287–290. http://dx.doi.org/10.1023/A:1002724831619.

Kumari, N, Parmar, P. and Sharma, V. 2015. Differential gene expression in two contrasting wheat cultivars under cadmium stress. Biologia Plantarum 59 (4): 701-707 http://dx.doi.org/10.1007/s10535-015-0550-x.

LeBel CP, Ali SF, McKee M, Bondy SC. Organometal-induced increases in oxygen reactive species: the potential of 2',7'-dichlorofluorescin diacetate as an index of neurotoxic damage. Toxicol Appl Pharmacol. 1990;104:17–24. http://dx.doi.org/10.1016/0041-008X(90)90278-3.

Lichtenthaler, H. 1987. Chlorophylls and carotenoids: pigments of photosynthetic bio membranes. Methods Enzymol. 148: 350-382. http://dx.doi.org/10.1016/0076-6879(87)48036-1.

Minguez-Mosquera, M.I., Jaren-Galen, M., Garrido-Fernandez, J. 1993. Lipoxygenase activity during pepper ripening and processing of paprika. Phytochemistry 32: 1103-1108. http://dx.doi.org/10.1016/S0031-9422(00)95073-8.

Miyake, C., Asada, K. 1992. Thylakoid-bound ascorbate peroxidase in spinach chloroplasts and photoreduction of its primary oxidation product monodehydroascorbate radicals in thylakoids. Plant Cell Physiol. 33: 541-553. https://doi.org/10.1093/oxfordjournals.pcp.a078288.

Moorthy, P., Kathiresan, K. 1993. Physiological responses of mangrove seedling to triacontanol. Biol. Plantarum 35:577–581. https://doi.org/10.1007/BF02928035.

Naeem, M., Masroor, M. A., & Moinuddin, A. 2012. Triacontanol: A potent plant growth regulator in agricultural crops. J. Plant Interact. 7, 129–142. http://dx.doi.org/10.1080/17429145.2011.619281.

Nahar, K., Hasanuzzaman, M., Alam, M.M., Rahman, A., Suzuki, T., Fujita, M. 2016. Polyamine and nitric oxide crosstalk: antagonistic effects on cadmium toxicity in mung bean plants through upregulating the metal detoxification, antioxidant defense, and methylglyoxal detoxification systems. Ecotoxicol. Environ. Saf. 126:245–255. http://dx.doi.org/10.1016/j.ecoenv.2015.12.026.

Najmanova J, Neumannova E, Leonhardt T, Zitka O, Kizek R, Macek T, Mackova M, Kotrba P (2012) Cadmium-induced production of phytochelatins and speciation of intracellular cadmium in organs of *Linum usitatissimum* seedlings. Ind Crop Prod 36:536–542 http://dx.doi.org/10.1016/j.indcrop.2011.11.008.

Nakano, V., Asada, K. 1981. Hydrogen peroxide is scavenged by ascorbate–specific peroxidase in spinach chloroplasts. Plant Cell Physiol. 22:867–880. https://doi.org/10.1093/oxfordjournals.pcp.a076232.

Nazar, R., Iqbal, N., Masood, A., Khan, M.I.R., Syeed, S., Khan, N.A. 2012. Cadmium toxicity in plants and role of mineral nutrients in its alleviation. American J. Plant Sci. 3:1476–1489. 10.4236/ajps.2012.310178.

Pal, J., Ganguly, S., Khandakar, S.T., Acharya, K. 2010. In vitro free radical scavenging activity of wild edible mushroom, *Pleurotus squarrosulus* (Mont.) Singer Indian. J. Exp. Biol. 47; 1210-1218. http://dx.doi.org/10.1155/2014/748531.

Perveen, S., Shahbaz, M., Ashraf, M. 2014. Triacontanol-induced changes in growth, yield, and leaf water relations, oxidative defense system, minerals, and some key osmoprotectants in wheat (*Triticum aestivum* L.) under saline conditions. Turk. J. Bot., 38: 1–18. http://dx.doi.org/10.3906/bot-1401-19.

Plewa, M.J., Smith S.R., Wanger, E.D. 1991. Diethyl dithiocarbamate suppresses the plant activation of aromatic amines into mutagens by inhibiting tobacco cell peroxidase. Mutat. Res. 247: 57-64. http://dx.doi.org/10.1016/0027-5107(91)90033-K.

Sagner, S., Kneer, R., Wanner, G., Cosson, J. P., Deus-Neumann, B. and Zenk, M. H. 1998. Hyperaccumulation, complexation and distribution of nickel in *Sebertia acuminata*. *Phytochemistry* 47: 339–347. http://dx.doi.org/10.1016/S0031-9422(97)00593-1.

Sedlak J, Lindsay RH (1968) Estimation of total, protein- bound, and non-protein sulfhydryl groups in tissue by Ellman's reagent. Anal Biochem 25:192–208 http://dx.doi.org/10.1016/0003-2697(68)90092-4.

Shahbaz, M., Ashraf, M., Akram, N.A., Hanif, A., Hameed, S., Joham, S., Rehman, R. 2011. Salt-induced modulation in growth, photosynthetic capacity, proline content and ion accumulation in sunflower (*Helianthus annuus* L.). Acta Physiol. Plant. 33:1113-1122. http://dx.doi.org/10.1007/s11738-010-0639-y.

Shahbaz, M., Noreen, N., Perveen, S. 2013. Triacontanol modulates photosynthesis and osmoprotectants in canola (*Brassica napus* L.) under saline stress. J. Plant Interact. 8: 250–259. http://dx.doi.org/10.1080/17429145.2013.764469.

Sharma I., Pati P. K., Bhardwaj R. (2010). Regulation of growth and antioxidant enzyme activities by 28-homobrassinolide in seedlings of *Raphanus sativus* L. under cadmium stress. *Indian J. Biochem. Biophys.* 47 172–177.

Sigfridsson, K.G.V., Bernát, G., Mamedov, F., Styring, S. 2004. Molecular interference of Cd^{2+} with photosystem II. Biochim. Biophys. Acta 1659:19–31. http://dx.doi.org/10.1016/j.bbabio.2004.07.003.

Sorbo, S., Aprile, G., Strumia, S., Castaldo Cobianchi R., Leone A., Basile A. 2008. Trace element accumulation in *Pseudevernia furfuracea* (L.) Zopf exposed in Italy's so-called Triangle of Death. Sci. Total Environ. 407: 647-654. http://dx.doi.org/10.1016/j.scitotenv.2008.07.071.

Velikova, V., Yordanov, I., Edreva, A. 2000. Oxidative stress and some antioxidant systems in acid rain-treated bean plants protective role of exogenous polyamines. Plant Sci. 151:59–66. http://dx.doi.org/10.1016/S0168-9452(99)00197-1.

Verma, A., Malik, C.P., Gupta, V.K., Bajaj, B.K. 2011. Effects of in vitro triacontanol on growth, antioxidant enzymes, and photosynthetic characteristics in *Arachis hypogaea* L. Braz. J. Plant Physiol. 23(4):271-277. http://dx.doi.org/10.1590/S1677-04202011000400004.

Xiong J, Fu G, Tao L, Zhu Ch (2010) Roles of nitric oxide in alleviating heavy metal toxicity in plants. Arch Biochem Biophys 497:13–20. http://dx.doi.org/10.1016/j.abb.2010.02.014.

Zagorchev, L., Seal, C.E., Kranner, I., Odjakova, M. 2013. A central role for thiols in plant tolerance to abiotic stress. Int. J. Mol. Sci. 14:7405–7432. http://dx.doi.org/10.3390/ijms14047405.

Environmental and Experimental Botany 141 (2017) 161–169

Contents lists available at ScienceDirect

Environmental and Experimental Botany

journal homepage: www.elsevier.com/locate/envexpbot

Interaction of triacontanol and arsenic on the ascorbate-glutathione cycle and their effects on the ultrastructure in *Coriandrum sativum* L.

Elham Asadi karam[a], Batool Keramat[a], Sergio Sorbo[b] , Viviana Maresca[c] , Zahra Asrar[a], Hossein Mozafari[d], Adriana Basile*[c]

[a]Biology Department, Shahid Bahonar University of Kerman, Kerman, Iran

[b]Ce.S.M.A, Microscopy Section, University of Naples Federico II, via Cinthia, 80126 Naples, Italy

[c]Biology Department, University of Naples "Federico II", via Cinthia, 80126, Naples, Italy

[d]Department of Ecology, Institute of Science and High Technology and Environmental Sciences, Graduate University of Advanced Technology, Mahan, Kerman, Iran.

*Corresponding author email: adbasile@unina.it

Abstract

Exogenous application of triacontanol (TRIA) has the ability to mitigate the adverse effects of abiotic stresses by modulating a number of physio-biochemical processes in different plants. However, information about how its effects may be mediated under heavy metal stress is scanty. In this study, we evaluated how TRIA exerted its role against the toxicity of sodium arsenate in coriander (*Coriandrum sativum* L.). The activities of enzymes, including ascorbate peroxidase (APX), glutathione reductase (GR), monodehydroascorbate reductase (MDHAR), dehydroascorbate reductase (DHAR) and glutathione-S-transferase (GST), were measured. In addition, the contents of ascorbate (ASC), dehydroascorbate (DHA), reduced glutathione (GSH) and some elements including both As and the nutrients Ca, Mg, Zn, K, P were determined. Results suggested that As decreased GSH, ASA and DHA contents, a clear indication of oxidative stress, but their amounts were raised by TRIA treatment. Also, As

stress decreased plant Ca, Zn, K, Mg and P contents, while TRIA improved their uptake and inhibited As accumulation. As 200 μM treatment inhibited the activities of APX, MDHAR, DHAR, and GR, enzymes of the ascorbate-glutathione cycle (AGC). TRIA supplementation restored and even enhanced the activity of all the AGC enzymes. 10 μM TRIA treatment increased GST gene expression and activity to a greater extent than under only As treatment. TRIA-alone treatments did not change the mentioned parameters.
Transmission electron microscopy (TEM) observations showed that TRIA was able to protect cells, and most of all chloroplasts, from As-induced damage.
These results clearly indicate the protective role of TRIA in modulating the redox status of the plant system through the antioxidant AGC and GSH enzymes, which could counteract arsenic-induced oxidative stress.

Keywords: Arsenic, Ascorbate-glutathione cycle, Coriander, Triacontanol, Ultrastructure.

1. Introduction

Heavy metals are important environmental pollutants and many of them are toxic even at very low concentrations. Arsenic (As), one of the most toxic metalloids, is widely distributed in the environment and is non-essential for plants (Farooq et al., 2016). The presence of As in irrigation water or soil could hamper normal growth of plants inducing biomass reduction (Finnegan and Chen 2012). Arsenic is known to induce production of reactive oxygen species (ROS), which are counteracted by plant antioxidant enzymes and compounds (Farooq et al., 2016). ROS, generated in the cell wall as well as inside the cell, affect membrane permeability, enzyme activity, metabolic pool, plant biomass, inducing leaf chlorosis and necrosis (Upadhyaya et al., 2014). To scavenge ROS, plants involve strong antioxidant defense system, comprising antioxidant molecules, such as glutathione, vitamin C, polyphenols, flavonoids, and antioxidant enzymes, such as superoxide dismutase, catalase, guaiacol peroxidases, glutathione reductase, ascorbate peroxidase, monodehydroascorbate reductase and dehydroascorbate reductase (Asadi karam et al., 2017). The non-enzymatic antioxidants include ascorbate (ASC) and GSH, two main constituents of the ASC-GSH cycle, also involved in detoxification of H_2O_2 in chloroplasts and cytosol (Sinha and Saxena, 2006). Scavenging H_2O_2 by ascorbate peroxidase (APX) is the first step of the ASC-GSH cycle, which maintains the ASC pool in its reduced form (Foyer and Halliwell, 1976). Plant dehydroascorbate reductase (DHAR) is an important reducing enzyme, involved in the ascorbate-glutathione recycling reaction. DHA must be converted to AsA by DHAR in presence of glutathione (GSH) as a reducing agent. Thus, DHAR is a key factor in maintaining a reduced AsA level in the adaptation to environmental conditions. In plants, the monodehydroascorbate reductase (MDHAR) is an enzymatic component of the glutathione-ascorbate cycle, which is one of the major antioxidant systems of plant cells for protection against ROS-induced damages (Aravind and Prasad, 2005; Pandey et al., 2009). Glutathione reductase (GR) is a key enzyme for maintaining the GSH pool (Rennenberg, 1982). Glutathione S-transferases (GST), induced by both toxic metals and oxidative stress, are ubiquitous enzymes, which perform functional roles using the tripeptide glutathione (GSH) as

a co-substrate or coenzyme (Ghelfi et al., 2011). The GSH-dependent catalytic functions include the conjugation and resulting detoxification of cytotoxic products. It has been observed that As induces the GST activity in mesquite and maize plant (Mokgalaka- Matlala et al., 2009; Mylona et al., 1998)

Plant hormones increase stress tolerance in plants by regulating various physiological and biochemical processes (Shahbaz et al., 2011). Research on their crucial roles led to the discovery of new plant growth regulators (PGRs) and the elucidation of their roles in modulating plant processes (Perveen et al., 2012). One of relatively new PGRs, Triacontanol (TRIA), is reported to stimulate plant growth at a very low concentration when exogenously applied to various plant species like groundnut (Verma et al., 2009), rice, maize, and wheat (Perveen et al., 2011). TRIA has been reported to enhance photosynthesis (Eriksen et al., 1981) and water and mineral nutrient uptake (Chen et al., 2003), to regulate activities of various enzymes (Naeem et al., 2011), and to increase the amounts of organic compounds in leaf tissues (Kumaravelu et al., 2000; Chen et al., 2003). TRIA has received much more attention in recent years as a plant growth regulator. It may play an important role in resistance of some plants to abiotic stresses, such as salinity in coriander (Asadi karam and Keramat, 2017) and *Triticum aestivum* (Perveen et al., 2014), and cadmium toxicity in *Erythrina variegata* (Muthuchelian et al., 2001). Our previous report has shown that TRIA mitigates As-induced oxidative stress in coriander plants (Asadi karam et al., 2016).

The aim of this paper is to confirm the hypothesis that TRIA is able to mitigate As-induced oxidative stress by stimulating the ASC-GSH cycle and the activity of GST enzyme. Furthermore, we aimed at evaluating the protective ability of TRIA against As-induced alterations of the cell ultrastructure.

2. Material and methods

2.1. Plant growth and treatments

Seeds of coriander (*Coriandrum sativum* L.) were sterilized using 0.1 % sodium hypochlorite solution, washed by distilled water and planted in pots filled with perlite. Fresh Hoagland's nutrient solution (pH 5.7 ± 0.1) was prepared for irrigation (Hoagland and Arnon, 1950). The plants were kept in a greenhouse with 16 h light/ 8 h dark photoperiod, 25°C day – 20°C night, and a relative atmospheric humidity of 70%. Triacontanol (TRIA, Sigma Aldrich) was dissolved in ethanol. At the three-leaved stage, seedlings were sprayed with TRIA at concentrations of 0, 5, 10, and 20 $\mu mol \cdot L^{-1}$ once a day for 72 h. Our preliminary experiment showed that these three concentrations created the most measurable effects on As-stressed coriander seedlings. After TRIA treatments, seedlings were irrigated by Hoagland's solution containing sodium arsenate salt (Na_2HASO_4) at 0, 100 and 200 µM. After a 6 day-treatment with As, shoots were uprooted, fresh weight (FW) was recorded and the plant material was immediately frozen in liquid nitrogen and stored at -80°C for the next analyses. All treatments were replicated three times.

2.2. Determination of biochemical parameters

The ascorbate (ASC) and dehydroascorbate (DHA) contents were measured as described by De Pinto et al. (1999). Briefly, total ASC was determined after reduction of DHA to ASC with dithiotreitol (DTT); DHA content was estimated by the difference between the total ASC pool (ASC plus DHA) and ASC.

The GSH content was determined by the spectrophotometric method of Ellman (1959), where GSH was oxidized in 2.6 ml of a sodium phosphate buffer (pH 7.0) containing 0.2 ml of a sample extract and 0.2 ml of 6 mM 5,5'-dithiobis-(2 nitrobenzoic) acid (DTNB). The absorbance was monitored at 412 nm. The GSH content was calculated from a standard curve constructed using GSH over the range 0-100 µM.

2.3. Element Analysis by ICP-OES

Samples of shoot were oven dried at 70°C for 72 h. After determination of the dry biomass, 0.5 g samples were dissolved in 10 ml of 65% (w/v) nitric acid (supra pure, Merck). After digestion, the volume of each sample was adjusted to 50 mL using double deionized water. Total concentration of As, Ca, P, K, Mg and Zn were determined by inductively coupled plasma atomic emission spectroscopy (ICP, OES, Varian CO). The stability of the device was evaluated after determination of every ten samples by examining the internal standard. Reagent blanks were also prepared to detect potential contamination during the digestion and analytical procedure. The samples were analyzed in triplicates. For quality control, we also used standard solutions with As, Ca, P, K, Mg and Zn known concentrations within the range of plant analyzed solutions (As standard solution, MERCK) (Sagner, 1998).

2.4. Enzyme extraction and activity determination

For protein extraction and analysis, the extracts of frozen samples prepared in a 50 mM potassium phosphate buffer (pH 7) containing 1mM phenylmethane sulfonyl fluoride (PMSF), 1 mM sodium ethylene diaminetetraacetic acid (Na_2EDTA), and 1 %(m/v) polyvinylpyrrolidone (PVP) were centrifuged at 15000 *g* at 4 °C for 15 min. The supernatants were used for the estimation of protein content and enzyme activities. The total protein content was measured according to the method of Bradford (1976), using bovine serum albumin as standard. All the spectrophotometric analyses were conducted in a final volume of 3 ml by using a *Cary 50* UV/visible spectrophotometer.

Ascorbate peroxidase (APX; EC 1.11.1.11) was assayed by monitoring the decrease in the absorbance at 290 nm due to ASC oxidation (Nakano and Asada, 1981). The reaction mixture contained 50 mM potassium phosphate (pH 7.0), 0.1 mM EDTA, 0.15 mM H_2O_2, 0.5 mM ASC, and 0.15 ml of the enzyme extract. One unit of APX activity was defined as the amount of enzyme that decomposed 1 mmole of ascorbate per minute.

The glutathione reductase (GR; EC1.6.4.2) activity was determined following the decrease in the absorbance at 340 nm associated with the oxidation of NADPH (Foyer and Halliwell,

1976). The assay contained 50 mM Tris-HCl (pH 7.8), 150 μM NADPH, 500 μM oxidized glutathione (GSSG) and 0.05 ml of the enzyme extract. One unit of GR was defined as the amount of enzyme that oxidized 1 μmole of NADPH per minute.

Monodehydroascorbate reductase (MDHAR, EC 1.6.5.4) activity was assayed at 340 nm with microplate assay kit (Mybiosource), according to the manufacturer's instructions. One unit of MDHAR activity was defined as the amount of enzyme that oxidizes 1 μmole of NADH per minute. A molar coefficient of 6.2 mM^{-1} cm^{-1} was used for the calculation of enzyme activity.

Dehydroascorbate reductase (DHAR, EC 2.5.1.18) activity was measured at 265 nm with microplate assay kit (Mybiosource), according to the manufacturer's instructions. One unit of DHAR activity was defined as the amount of enzyme that produces 1 μmole of AsA per minute

Glutathione S-transferase (GST, EC 2.5.1.18) activity was measured using a commercial kit (CS0410, Sigma). The conjugation of GSH to 1-chloro-2, 4-dinitrobenzene (CDNB) catalysed by GST was monitored at 340 nm for 4 min. The reaction mixture contained 4 μL of extract and 196 μL of reaction solution (200 mM GSH and 100 mM CDNB in Dulbecco's buffer at pH 7). The activity was calculated with $\varepsilon = 9.6$ mM^{-1} cm^{-1} (Habig and Jakoby, 1981). A GST unit is defined as the amount of enzyme that catalyses the formation of 1 μmole of the GS-DNB conjugate per minute at 25 °C and pH 7.

2.5. Transmission electron microscopy

For conventional Transmission Electron Microscopy (TEM), sections from leaflets of *Brassica napus* samples were fixed with 3% glutaraldehyde in phosphate buffer (65 mM, pH 7.2–7.4) at room temperature for 2 h, post-fixed with 1% osmium tetroxide in the aforementioned phosphate buffer for 1.5 hours at room temperature, dehydrated with ethanol up to propylene oxide and finally embedded in epoxy Spurr resin. After sectioning, the 40 nm thick slices were mounted on copper grids, stained with UAR stain (Electron Microscopy Sciences) and Reynold's lead citrate and observed under an EM 208S FEI TEM, using an accelerating voltage of 80 KV.

2.6. Gene expression

One hundred mg of leaf tissue was ground thoroughly in liquid nitrogen using a pre-chilled mortar and pestle. Total RNA was extracted with Trizol reagent, according to the manufacturer's instructions (Invitrogen). The concentration of the RNA was read using a NanoDrop ND-1000 spectrophotometer, working at 260 nm. The quality of the RNA was checked by both 1% agarose gel and NanoDrop at the 260/280 ratio. The expression of genes was analyzed using reverse transcription polymerase chain reaction (RT-PCR).

First strand cDNA synthesis was performed from preheated and snap cold treated 5µl of total RNA, using an oligo (dT) primer in a 20 µl reaction containing: 10x reverse transcription reaction buffer, HyperScript ^{TM} reverse transcriptase, ZymAll^{TM} RNase Inhibitor and dNTPs. The reaction was carried out at 55°C for 60 min, followed by a 5 min step at 85°C and then by cooling to 4°C. We performed the PCR reactions using glyceraldehyde phosphate dehydrogenase gene (GAPDH) as internal reference. The following specific primers were used and checked for dimer formation:

F-TGAPDH: CTCGCGCTATGAATGTCGCC

R-TGAPDH: TTCGCTCAGTCTGAGCAGAC

F-GST: AGCTCGTCGCCTTCAAGTTC

R-GST: ACATCCTTAAGCTCGGCAAG

Three different and independent cDNA sets were used. To determine the expression of GST, 2 µL of the cDNA was used in the real-time PCR assay, using 1µl of each forward and reverse primer in 20 µl as a final volume. PCR reaction was performed in duplicate for 35 cycles under the following conditions: denaturation at 95 °C, for 3 min; annealing at 60°C, for 1 min; extension at 72 °C, for 10 min. Each experiment was repeated at least three times in order to ensure reproducibility. A no reverse transcriptase control (No-RT) was performed for all samples to monitor DNA contamination. PCR products were detected on 1% agarose gels by ethidium bromide staining. Interpretation of differential expression was performed in an optical density of electrophoresis PCR. In particular, the RT-PCR was screened by using the

software ImageJ: the intensity of each band was escorted as an area interposed under Gaussian curve.

2.7. Statistical data analysis

Data were analyzed using one-way analysis of variance (ANOVA). Differences between means were considered as significant at a confidence level of $P \leq 0.05$. All statistical analyses were done using the software SPSS package, version 18.0. The Duncan test analysis was done to determine the significant difference between different treatments.

3. Results

3.1. Plant growth

Shoot fresh weights from As-treated plants decreased significantly with increasing As concentration. As at 200 μM had the maximum effect on shoot fresh weight, decreasing it by 157.7% in comparison to the As-untreated control seedlings. TRIA pretreatment alleviated reductions in shoot fresh weight under As-treatment (Fig 1).

3.2. Ions accumulation

The results from ICP, OES analysis showed that As ions accumulated significantly in the shoots treated with As only and with no TRIA, in comparison to As-untreated plants (Table 1), the maximum effect being at 200 μM As, increasing bioaccumulation by 339.9%. Application of TRIA decreased shoot As content at both 100 and 200μM. As-treatment at 200μM without TRIA induced the greatest decrease in the Ca and P contents in the shoots. Generally, in this condition application of TRIA increased Ca and P contents. The lowest arsenic concentration 100 μM gave not significant difference with the untreated plants as for Ca and P contents.

Table 1 show the effects of As-treatments on the concentration of some nutrients, such as Mg, K and Zn, in the shoots. In general, these data demonstrated that foliar application of TRIA considerably improved nutrient uptake and accumulation in As-stressed plants, while As treatments, at 100 and 200 μM without TRIA, decreased accumulation of these elements in comparison to the As-untreated samples.

3.3. Ascorbate, dehydroascorbate and glutathione content

The ASC, DHA and GSH contents of *C. sativum* leaves exposed to As, with or without TRIA pretreatments, are showed in Fig 2. As caused a significant decrease in ASC and GSH contents in absence of TRIA pretreatment. Differently, these effects were not observed in plants pretreated with TRIA, where the ASC content even increased. The maximum ASC content was observed under 100 μM As +10 μM TRIA (Fig. 2A).

In the only As-treated samples, the DHA content increased after 100 μM As and decreased after 200 μM As. Decrease at 200 μM As was preserved by the pretreatments with 10 and 20 μM TRIA. The highest DHA values were observed in 10 μM TRIA + As-treated samples (Fig. 2B). The results indicate that the application of TRIA improved the ASC pool under As stress.

3.4. Response of antioxidant enzymes

The activities of APX and GR after As- and TRIA-treatments are shown in Fig 3. In the As-exposed plants with no TRIA pretreatment, there was a significant decrease in the activities of APX and GR in comparison to the As-unexposed ones (control) (Fig 3). However, after As-treatments TRIA-pretreatments significantly increased the activities of these enzymes. Without As treatment, TRIA had negligible effects on these activities, but a great induction of TRIA could be observed under As supply (Fig 3).

The activities of MDHAR and DHAR were found to decrease with increasing As concentrations. Differently, the TRIA-pretreatments before As-exposure enhanced the MDHAR and DHAR activities. The maximum enhancement in their activities was observed after 5 and 10 μM TRIA- pretreatments under As-exposure (Fig. 4).

3.5. GST activity and Gene expression

With increasing As concentration from 0 to 200 μM, GST activity increased rapidly, reaching the maximum at 200 μM As. Exogenous TRIA addition along with As decreased GST activity, in comparison to the As-only treatment (Fig 5). Transcript level of GST gene was altered in response to As 200μM and TRIA 10μM and their combination (Fig 6). The value from the As-untreated control samples was comparable to that from the only TRIA-treated samples. Differently, the only As-treatment produced a band with an area two fold the As-untreated control. This gene expression increased further in the sample treated with both As and TRIA, where the intensity reached 3 fold the untreated control sample. This finding was according to the GST activity.

3.6. Ultrastructural observations

TEM observations of untreated control samples of *Coriandrum sativum* L. showed cells with a large and electron clear, central vacuole surrounded by a thin layer of cytoplasm lying beneath a thin cell wall (Fig 7.a). The cytoplasm contained numerous lenticular chloroplasts (Fig 7.a, b). The chloroplasts had a well-developed thylakoid system with grana and intergrana membranes submerged in an abundant stroma (Fig 7.b, c). Mitochondria had numerous, electron clear cristae contained in the matrix (Fig 7.d).

TRIA only-treated samples gave electron dense micrographs. Like in control samples, the whole cells had a large, electron clear, central vacuole surrounded by a thin cytoplasm arranged beneath the cell wall. The cytoplasm contained numerous large chloroplasts with well-developed thylakoid systems, nuclei and large lipid droplets (Fig 7.e). The large chloroplasts had the same arrangement as the control (Fig 7.f, g). The mitochondria contained numerous cristae in the matrix (Fig 7.h), just like in the untreated control samples.

The As-treated samples, compared to control untreated samples, appeared changed. Cells were plasmolysed; the cytoplasm was poorly electron dense and contained swollen chloroplasts (Fig 7.i). The swollen chloroplasts contained a poor thylakoid system with grana and intergrana membranes (Fig 7.j, k). Mitochondria still featured cristae, but electron clear areas were visible inside (Fig 7.l, m). Cytoplasm showed multivesicular bodies (Fig 7.m).

The samples treated with both TRIA and As had an appearance comparable to the TRIA only-treated samples (Fig 7.n). The chloroplasts appeared just like those from TRIA only-treated samples (Fig 7.o, p). Mitochondria, even though preserving cristae, showed electron clear areas inside, just like those from As only-treated samples (Fig 7.q).

4. Discussion

The present study shows that one of the most visible effects of As-treatments is a decrease of shoot fresh weights. Our data suggest that the decrease in plant growth is related to the uptake of As and nutrition elements. Some Authors reported that the excess heavy metal induce disturbance in mineral nutrition (Finnegan and Chen 2012). Arsenate is easily incorporated

into plant cells through the high-affinity phosphate transport system (Finnegan and Chen 2012). Competition between As and P physiologically results in blocking the electron transport chain and, therefore, inhibiting ATP synthesis (Pigna et al. 2009). This leads to a disruption of energy flow in cells and finally inhibits plant growth and development. As also influences the uptake of other mineral nutrients in plants. In fact, it was reported that As addition impairs the uptake of K, Ca, Mg, Mn and Zn (Pigna et al 2009). That is according with our finding showing that As highest concentration, 200μM, decreases the uptake of K, Ca and Zn. Similar changes have been observed in other plants in presence of the same metal (Pigna et al 2009). Our data show that Mg uptake decreased with increasing As (Table 1). One major role of Mg is to act as a cofactor in enzymes activating phosphorylation processes; Mg is also the central atom of the chlorophyll molecule. The found decrease in Mg uptake could probably depend on the ability of As to uncouple the oxidative phosphorylation with a consequent decrease in the chlorophyll content. In addition, a reduction in its uptake may also be a result of the toxic effect of As on plant mineral nutrition (Marschner, 1995).

TRIA is a plant growth regulator able to modulate various growth processes under normal or stress conditions (Asadi karam et al., 2016). In the present study, pretreatment with TRIA mitigates the adverse effects of As on growth plant. The growth promoting ability of TRIA in crop plants has been especially focused on its synergistic interaction with phytohormones and induction of 9-b-L (+) adenosine, which has a structure similar to cytokinin (Naeem et al., 2011). The induction of 9-b-L (+) adenosine by TRIA is thought to be one of the reasons for the increase in dry matter and other growth parameters (Naeem et al., 2011). Data in Table 1 show that TRIA application proved effective at increasing Mg, Zn, P, K and Ca contents in the shoots. Enhancement in leaf nutrients due to TRIA application could be attributed to the compositional or chemical changing in plants, leading to alterations in nitrogen concentration (Knowles and Ries, 1981). Probably, increased uptake of nutrients enhanced photosynthesis and improved translocation of photosynthates and other metabolites, which may contribute to the improved growth of TRIA-treated plants. These findings are in accordance with data on TRIA ability at improving the contents of essential nutrients, i.e. N, P, K, and Ca in plant tissues (Naeem et al., 2009, 2011; Khandaker et al., 2013). Our previous data suggested that

TRIA have played a key role in protecting the structure and function of cell membranes and improving the uptake of other mineral nutrients in plants under heavy metal toxicity (Asadi karam et al., 2017).

In this our previous experiment, induction of oxidative stress under As toxicity was partially alleviated by applying TRIA. That was evidenced by the decreased amounts of ROS, such as H_2O_2, and increased activities of superoxide dismutase and catalase enzymes in the leaves of TRIA-treated coriander (Asadi karam et al., 2016). Such a process was facilitated by the active oxygen scavenging system, which includes several antioxidant enzymes, and is able to enhance membrane stability. The ASC-GSH cycle is involved in scavenging H_2O_2 in plant cells (Wu et al., 2017). For the study of non-enzymatic antioxidant defense, we measured ASC, DHA and GSH in shoots under As stress. In the present study, reduced amounts of ASC and GSH were observed in As-treated plants. This result is according to Hasanuzzaman and Fujita (2013), who reported a decrease in ASC and GSH contents and the GSH/GSSG ratio in As-treated wheat (*Triticum aestivum*). This might be attributed to As toxicity (Sanchez-viveros, 2010). Therefore, the measured decline in the content of ASC and GSH in *C. sativum* could be partially due to its consumption, while acting as antioxidant and limiting lipid peroxidation. In this study, TRIA enhanced the content of ASA, DHA and GSH by regulating the activities of enzymes of the ASA–GSH cycle, such as APX, MDHAR, DHAR, and GR. All that is in agreement with literature data reporting a stimulating effect of TRIA (Li et al., 2006; Barrameda- Medina et al., 2014). ASC and GSH are able to detoxify ROS by a direct scavenging or by acting as substrate in the enzymatic reactions (APX and GR). So an increase or protection of their contents by TRIA pretreatment is able to enhance tolerance against As-induced oxidative stress in *C. sativum*. Tolerance of some plants to heavy metals is associated with increases in both APX and GR activities (Madhava Rao and Sresty, 2000), while we observed a decrease in the GR, APX activity under As stress (Fig 3), which was alleviated by the TRIA applications. This result is according to Zare Dehabadi et al., (2014), who reported a decrease in GR activity in sweet basil seedling under As stress. The activities of MDHAR and DHAR (Fig 4) in the coriander seedlings decreased with increasing As; differently higher activities of the same enzymes under stress conditions were found in other plants (Mittova et

al., 2002, Arora et al., 2010). Some of the enzymes are sensitive to inhibition by heavy metals, like Cu and As, which react with thiol groups at the active sites (Garg and Singla, 2011). Thus, the reduced activity of enzymes, such as GR, may be due to their inactivation by As ions. Some researchers think that this reduction could be due to different effects of heavy metals, like As and Cd, at the transcriptional and post transcriptional levels (Romero-puertas et al., 2007; Gupta et al., 2013). In addition, considerable decrease in GR, which acts in GSH regeneration in the ASC–GSH cycle, affects the decrease in GSH content under As stress (Zare Dehabadi et al., 2014). Our data provided that GSH content is increased in plants by TRIA application. This result is similar with those of Aziz and Shahbaz (2015), who reported an increase of GR activity in TRIA-treated sunflower. TRIA might have signaling roles in enhancing biosynthesis of APX, MDHAR, DHAR, and GR. Otherwise, TRIA might also have other roles leading to the increase of their activities (Asadi karam et al., 2017). On the other hand, increasing the activities of enzymes involved in the ASA–GSH cycle by TRIA treatment could be maintained by regulation of the amounts of defense hormones. For example, Waqas et al (2016) have reported that TRIA treatment enhanced jasmonic acid (JA) in mungbean under heat stress. An increase in the activities of enzymes involved in the ASA–GSH cycle was observed in JA-treated wheat seedlings (Shan et al., 2015).

Moreover, Glutathione as a sulfur-containing tripeptide thiol is involved in plant protection against heavy metals as a precursor in the synthesis of phytochelatins (PCs) (Xiong et al. 2010). In our study, decreasing GSH content may be caused by increased conversion of GSH to PC in response of As toxicity. GSH can directly bind with ROS and detoxify them through a reaction catalyzed by glutathione-S-transferases (GSTs). GST catalyzes the conjugation of various electrophiles with reduced glutathione, detoxifying both exogenously and endogenously derived toxic compounds (Dixit et al., 2011). An increase in GST activity was observed in pumpkin (*Curbita maxima*) seedlings subjected to Cd, Cr, Mn, and As stress (Fujita and Hossain, 2003; Hossain et al., 2006) and in rice (*Oryza sativa* L.) seedlings in response to Cd (Hu et al., 2009). Similarly, our results showed that As toxicity enhanced GST activity and gene expression in coriander plants; TRIA+As treatment increased the gene expression more than As only and TRIA only treatments. The present work is the first study

concerning the effect of TRIA on GST activity in plants, so the mechanism leading to the increase of this enzyme is not yet clear. This work is an important progress to better understand the matter. Increasing the capacity of ROS quenching could be maintained by over-expression of glutathione-S-transferases.

TEM observations of untreated control samples revealed the typical appearance of mature cells from the leaf photosynthetic parenchyma. Both chloroplasts and mitochondria had a typical appearance. In literature no electron microscopy data are available on the application of TRIA to plants. TEM observations of TRIA-treated plants showed a healthy appearance of cells, which micrographs are well-electron dense and show large chloroplasts, several nuclei and cytoplasmic lipid droplets. There are not any reports on the influence of TRIA on cell structure. The cytoplasmic lipid droplets could also be interpreted as an accumulation of intermediate metabolites, which might be effect of the already known stimulating activity of TRIA on metabolic pathways (Ivanov and Angelov, 1997; Masroor et al., 2014). TEM observations on As-treated plants demonstrate ultrastructural damage. Plasmolysis of the whole cell, swelling of chloroplasts with increased plastoglobules and thylakoid system depletion, mitochondrion electron clear areas, multivesicular bodies are all frequent damages reported in heavy metal-treated plants, from angiospermophyta (Dalla Vecchia et al., 2005; Basile et al., 2012a, 2015) to lichens (Sorbo et al., 2011; Paoli et al., 2013, 2014), passing through bryophytes (Basile et al., 2012a, b, 2013).

Heavy metal toxicity was suggested to be possibly related to oxidative stress on tissues (Stohs and Bagchi, 1995). Higher doses of arsenate produced oxidative damage in clover plants (Mascher et al., 2002). Hartley-Whitaker and Meharg, (2001) reported significant lipid peroxidation in As-exposed *Holcus lanatus* due to an increase in reactive oxygen species. All that could suggest that membranes, particularly in organelles involved in reactive oxygen species production, are common targets of heavy metal damage. Chloroplast is known to produce superoxide radical during electron transport and mitochondrion is the main site of oxidative metabolism. All that is consistent with our finding that chloroplasts and mitochondria are main targets of As-induced damage.

Plasmolysis and swelling of chloroplasts were also observed in As-treated *Pteris vittata* (Li et al., 2006). These phenomena can be explained by a metal-induced damage to the membrane selective permeability causing drifting of ions and the accompanying solvent across the membranes (Schwartzman and Cidlowsky, 1993). All that finally ends up causing swelling or shrinkage of organelles or the whole cell, due to the filling or depriving the cell compartments. Oxidative damage can also explain the occurrence of multivesicular bodies. That ultrastructure was already observed in heavy metal-treated plants (Basile et al., 2012b, 2013, 2015; Esposito et al., 2012) and related to autophagic and endocytic phenomena (Thompson and Vierstra, 2005; Todeschini et al., 2011). Chiarelli and Roccheri, (2012) reported As to enhance autophagy via ROS, which could account for the occurrence of multivesicular bodies in our As-treated samples. Micrographs of the whole cells from As- and TRIA-treated samples are comparable to those from the TRIA only-treated plants and quite different from the As-treated ones. The appearance is electron-dense and healthy; the chloroplasts are large and well-equipped with thylakoids; nuclei are frequently visible. Even though the overall arrangement of the cells and the chloroplasts are healthy, mitochondria are not. Just like in As-treated samples, they still exhibit electron clear areas, which may be regarded as degenerated areas with no cristae and weak matrix. So, our TEM results show that TRIA has an overall protective effect against the As damage. That is consistent with our biochemical results, showing an enhancement of antioxidant activity, and also agrees with an our previous work, reporting a protective effect of TRIA in *Coriandrum sativum* under As toxicity (Asadi karam et al., 2016). We reported that As acts most of its toxic effects also via an oxidative stress, which is counteracted by TRIA. The remaining damage in the mitochondria of the TRIA+As-treated samples could be due to the abundant ROS production in the main site of the oxidative metabolism, which summarized with As-induced oxidative chemicals.

5. Conclusions

In conclusion, the coriander tolerance to As could dependent upon the efficiency of the antioxidant system, which maintained the redox homeostasis and integrity of cellular

components. So, the ASC-GSH cycle enzymes probably played major roles in the As-stressed coriander plants. So we can conclude that our findings support the hypothesis that the higher efficiency of the antioxidant system after TRIA-treatment could explain coriander tolerance to As.

Furthermore, TRIA influence on ROS quenching could be also maintained by over-expression and/or enhancing GST activity along with stimulating ASC-GSH cycle enzymes, which may also contribute to As tolerance of coriander.

Figure and table

Treatments		As	Ca	P	K	Mg	Zn
As	TRIA						
0	0	0.0001±0.0 fg	26.84±1.54 d	4.79±0.10 ab	42.57±3.05 a	15.02±1.11a	0.13±0.004a
0	5	0.0005±0.0 fg	28.53±2.72 c	5.67±0.51 a	42.42±2.53 a	11.48±1.08 ab	0.098±0.001b
0	10	0.001±0.0 fg	28.5±2.36 c	4.43±0.26 b	40.46±2.75 ab	11.42±2.25ab	0.096±0.003b
0	20	0.001±0.0 fg	28.24±1.90 c	4.61±0.16 ab	40.47±3.44 ab	12.58±2.29 ab	0.88±0.005bc
100	0	0.17±0.02 c	27.02±2.82 cd	3.96±0.29 b	15.43±1.05 e	5.21±0.74 d	0.024±0.001e
200	0	0.34±0.012 a	6.91±0.64 g	0.44±0.04 e	6.63±0.84 g	0.42±0.08 g	0.001±0.0001i
100	5	0.077±0.004 e	40.31±3.02 b	4.58±0.25 ab	22.73±2.06 d	7.58±0.34 c	0.042±0.002e
200	5	0.26±0.02 b	15.77±1.84 f	1.46±0.13 d	13.99±0.74 ef	1.15±0.73f	0.007±0.0001hi
100	10	0.076±0.019 e	44.68±3.69 a	3.96±0.64 b	25.18±1.08 c	9.48±1.06 bc	0.061±0.001d
200	10	0.21±0.010 c	19.08±1.22 e	1.82±0.12 d	21.26±1.17 d	4.05±0.69 de	0.022±0.0003ef
100	20	0.10±0.006 d	43.03±2.59 a	4.45±0.46 b	25.83±1.45 cd	5.77±0.70 d	0.011±0.0001g
200	20	0.24±0.015 b	23.71±1.31 d	2.54±0.22 c	27.92±2.06 c	5.47±0.95 d	0.001±0.0001i

Table1. Effects of As and TRIA application on As, Ca, P, K, Mg, Zn (mg/gr DW) contents in coriander leaves. Values with different letters are statistically different.

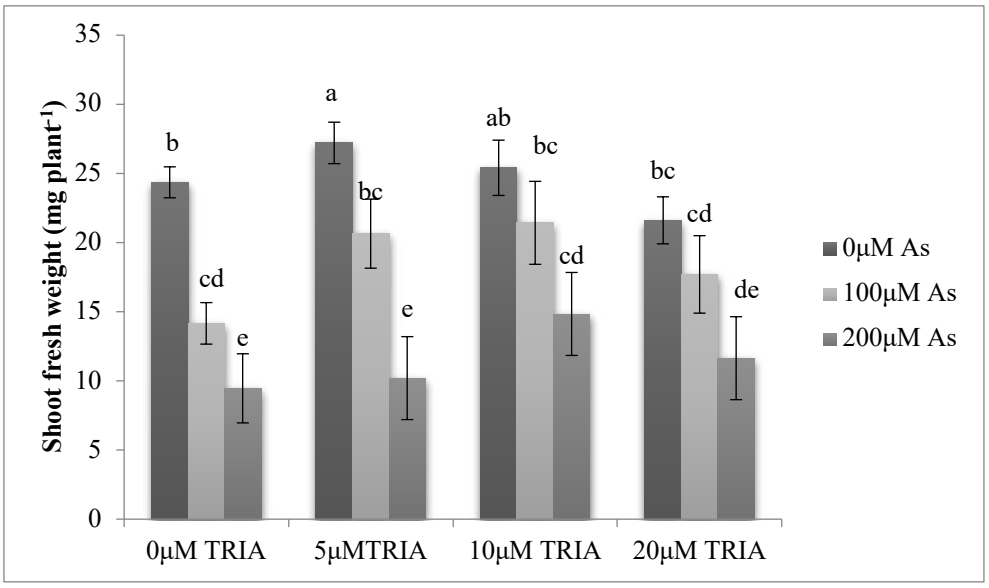

Figure 1. Effects of As and TRIA on shoot fresh weight of *Coriandrum sativum*. Values are means ± SE (n = 3). Bars with different letters are statistically different ($P < 0.05$) according to Duncan's multiple range tests.

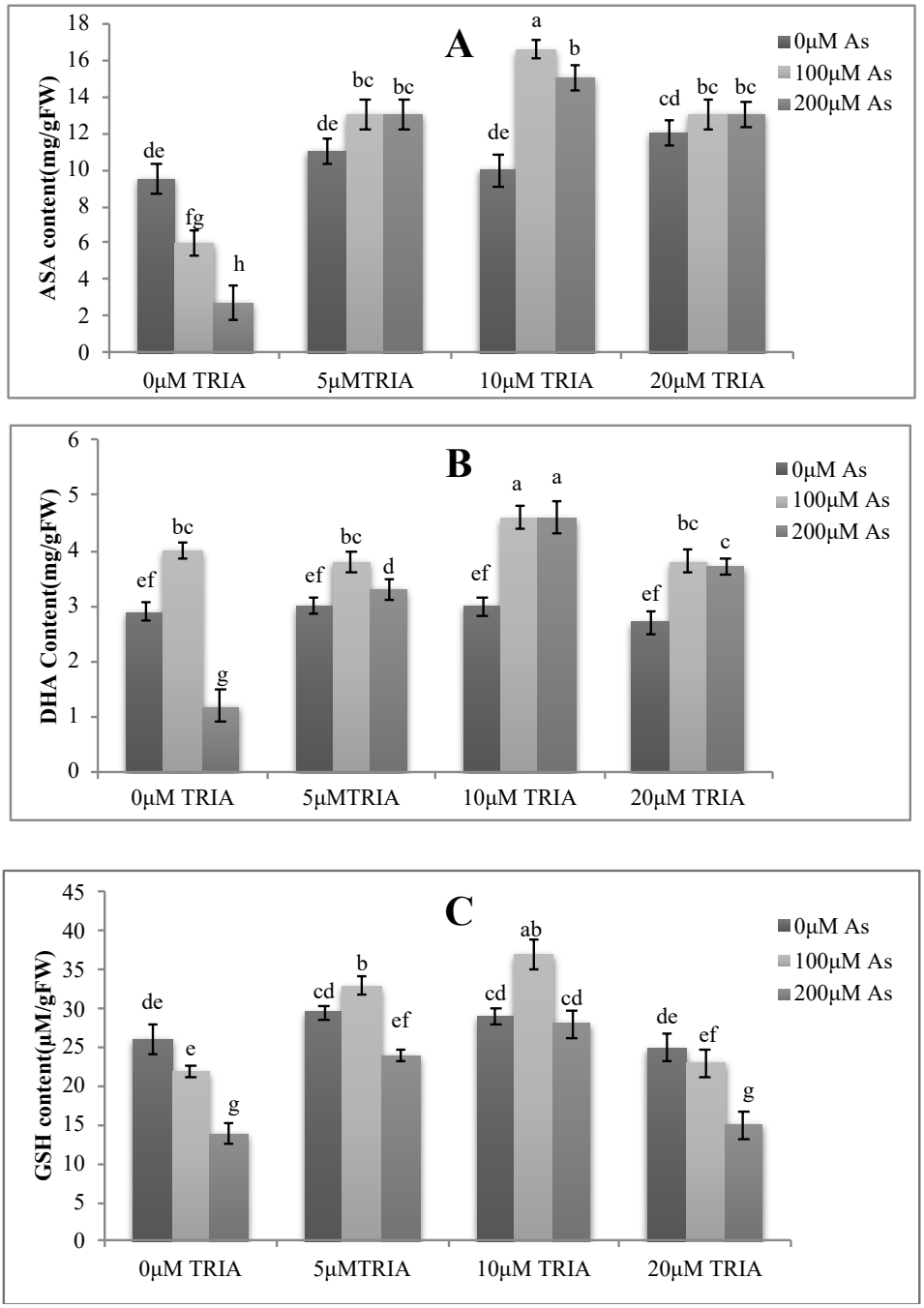

Figure 2. Effects of As and TRIA on (A) ASA, (B) DHA, and (C) GSH contents in *Coriandrum sativum*. Values are means ± SE (n = 3). Bars with different letters are statistically different ($P < 0.05$) according to Duncan's multiple range tests.

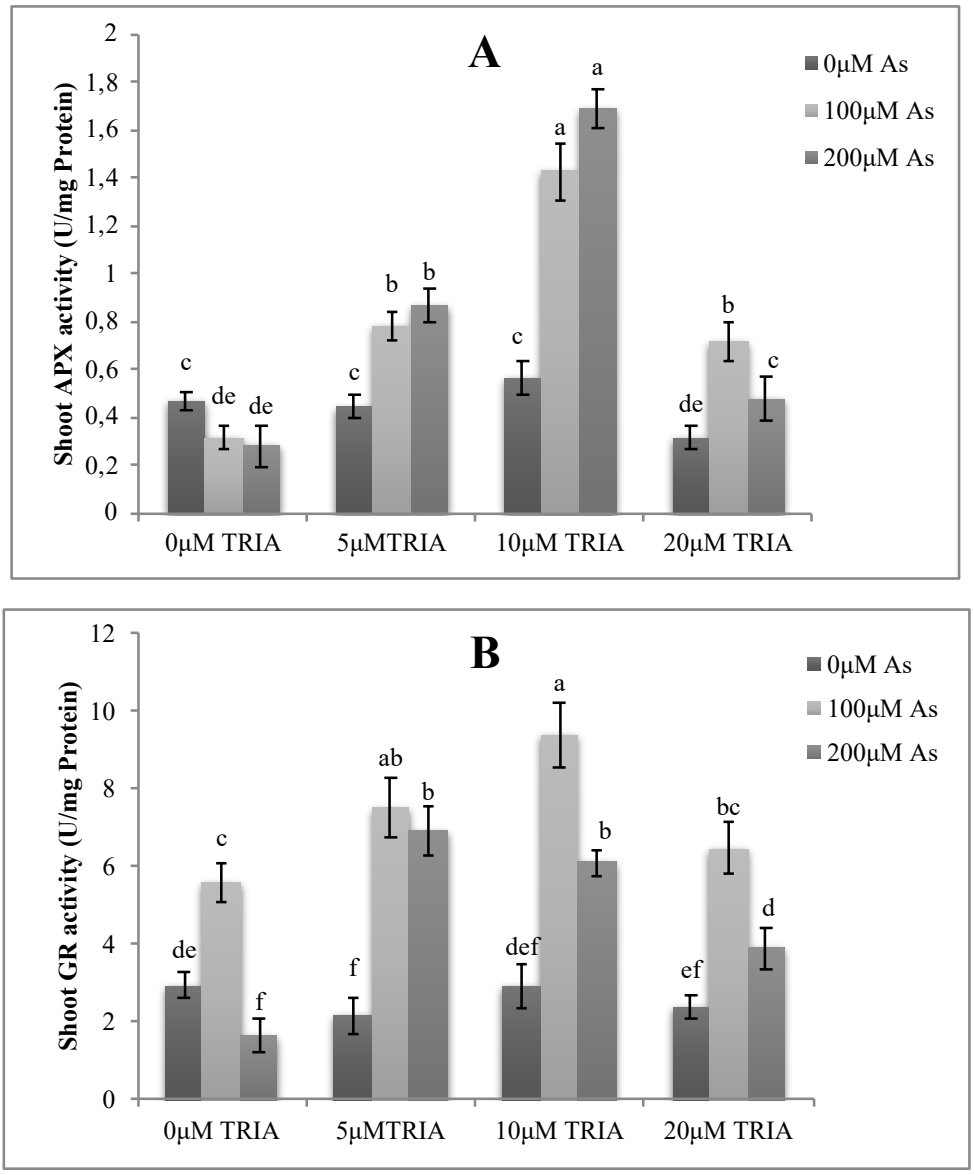

Figure 3. Effects of As and TRIA on (A) Ascorbate reductase and (B) Glutathione reductase in *Coriandrum sativum*. Values are means ± SE ($n = 3$). Bars with different letters are statistically different ($P < 0.05$) according to Duncan's multiple range tests.

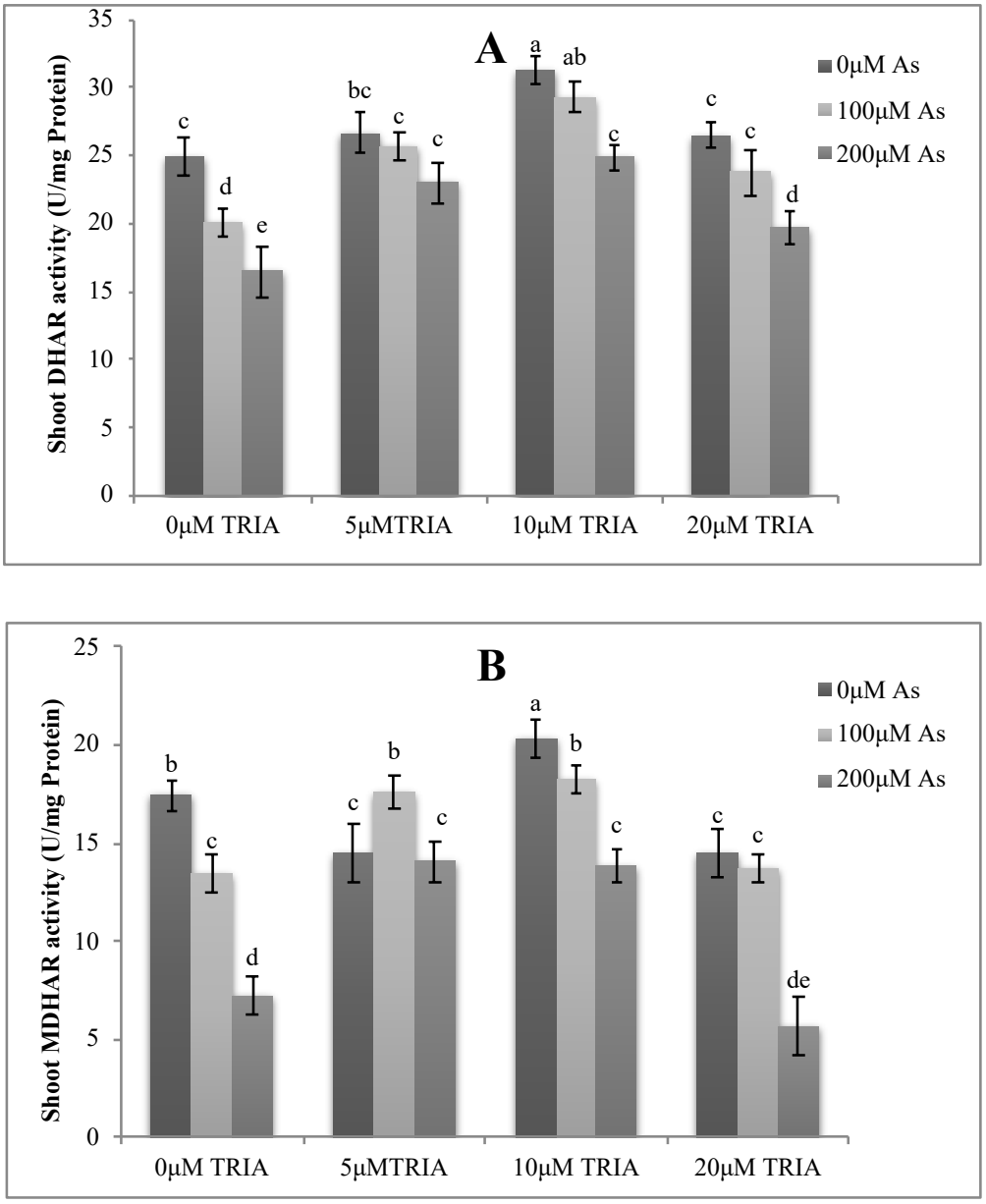

Figure 4. Effects of As and TRIA on (A) Dehydroascorbate reductase activity and (B) Monodehydroascorbate reductase activity in *Coriandrum sativum* leaves. Values are means ± SE ($n = 3$). Bars with different letters are statistically different ($P < 0.05$) according to Duncan's multiple range tests.

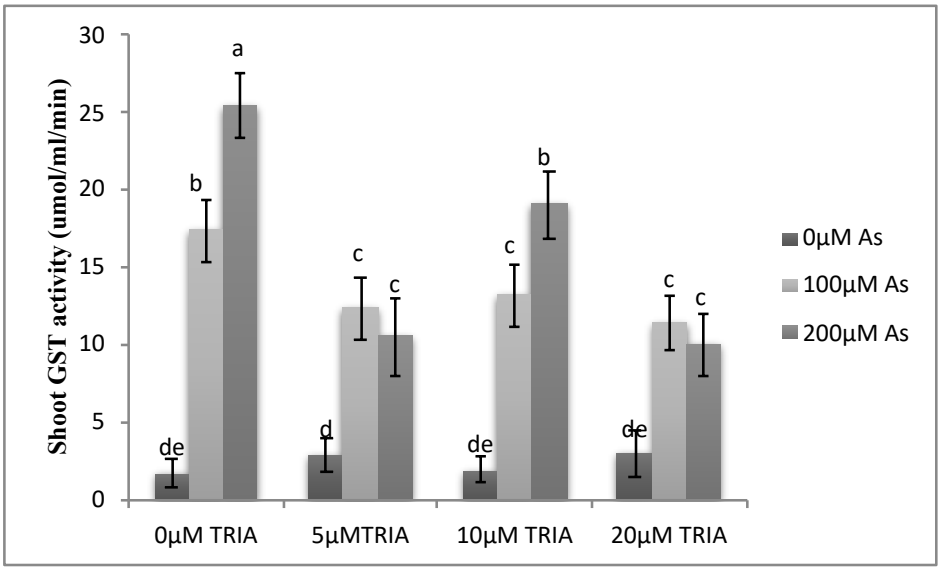

Figure 5. Effects of As and TRIA on GST activity in *Coriandrum sativum*. Values are means ± SE (n = 3). Bars with different letters are statistically different ($P < 0.05$) according to Duncan's multiple range tests.

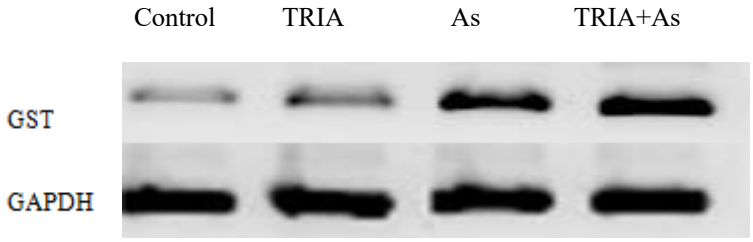

Figure 6. Analysis of mRNA expression of the GST gene by semi-quantitative RT-PCR. Effects of 10µM TRIA, As 200 µM and their combination on the gene expression in coriander. Glyceraldehyde phosphate dehydrogenase (GAPDH) gene was used as internal control to normalize different samples.

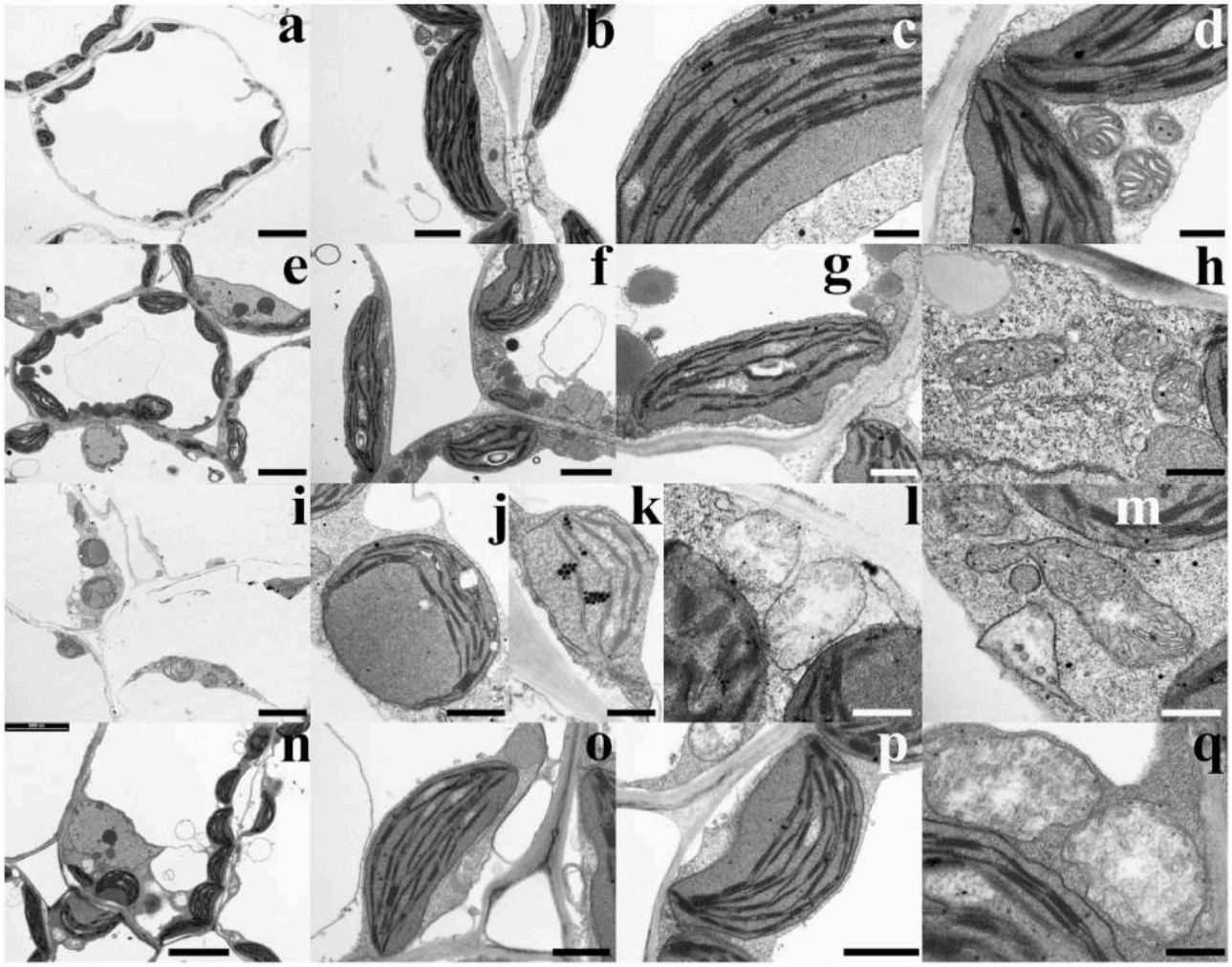

Figure 7. The table shows TEM micrographs of *Coriandrum sativum* L. samples.

(a-d) Untreated control samples. **(a)** A whole cell with a large central vacuole and chloroplasts. **(b)** Typical lenticular chloroplasts with thylakoid system and stroma. **(c)** Detail of a chloroplast with thylakoid system featuring grana and intergrana membranes. **(d)** Mitochondria with well-developed cristae next to chloroplasts. **(e-h)** Triacontanol-treated samples. **(e)** A whole cell showing a central vacuole, large chloroplasts, cytoplasmic lipid droplets and nuclei. **(f-g)** Chloroplasts with a well-developed thylakoid system. **(h)** Mitochondria with well-developed cristae. **(i-m)** As-treated samples. **(i)** The low magnificated micrograph shows plasmolysed cells with swollen chloroplasts. **(j-k)** Swollen chloroplasts with thylakoid system and plastoglobules. **(l)** Altered mitochondria with a poor cristae system and electron clear, degeneration areas. **(m)** A multivesicular body next to mitochondria. The large mitochondrion, even though preserving cristae, has an inner electron clear degenerated area. **(n-q)** Triacontanol + As-treated samples. **(n)** The whole cell exhibits an appearance comparable to the triacontanol-treated samples. **(o p)** Control-like chloroplasts with no evident alterations. **(q)** Mitochondria with few cristae and electron clear degenerated areas.

Scale bars: **5 µ** (a, e, i, n), **2 µ** (f), **1 µ** (b, g, j, o, p), **500 nm** (h, k, l, m, q), **300 nm** (c, d).

References

Aravind. P., Prasad, M.N.V., 2005. Modulation of cadmium-induced oxidative stress in *Ceratophyllum demersum* by zinc involves ascorbate–glutathione cycle and glutathione metabolism. Plant Physiol. Biochem. 43(2), 107-116. doi: http://doi.org/10.1016/j.plaphy.2005.01.002.

Arora, P., Bhardwaj, R., Kumar Kanwar, M., 2010. 24-epibrassinolide regulated diminution of Cr metal toxicity in *Brassica juncea* L. plants. Braz. J. Plant Physiol. 22(3), 159-165. doi: http://dx.doi.org/10.1590/S1677-04202010000300002.

Asadi karam, E., Keramat B., 2017. Foliar spray of triacontanol improves growth by alleviating oxidative damage in coriander under salinity. Ind. J. Plant Physiol. 22, 120. doi: http://doi.org/10.1007/s40502-017-0286-z.

Asadi karam, E., Keramat, B., Asrar, Z., Mozafari, H., 2016. Triacontanol-induced changes in growth, oxidative defense system in Coriander (*Coriandrum sativum*) under arsenic toxicity. Ind J Plant Physiol. 21, 137-142. doi: http://dx.doi.org/10.1007/s40502-016-0213-8.

Asadi karam, E., Maresca, V., Sorbo, S., Keramat B., Basile, A. 2017. Effects of triacontanol on ascorbate-glutathione cycle in *Brassica napus* L. exposed to cadmium-induced oxidative stress. Ecotoxicology and Environmental Safety, 144; 268-274. doi: http://dx.doi.org/10.1016/j.ecoenv.2017.06.035.

Aziz, R., Shahbaz, M., 2015. Triacontanol-induced Regulation in the Key Osmoprotectants and Oxidative Defense System of Sunflower Plants at Various Growth Stages under Salt Stress. Int. J. Agric. Biol. 5, 881–890. doi: http://dx.doi.org/10.17957/IJAB/15.0022.

Barrameda-Medina, Y., Montesinos-Pereira, D., Romero, L., Blasco, B., Ruiz, J.M., 2014. Role of GSH homeostasis under Zn toxicity in plants with different Zn tolerance. Plant Sci. 227, 110-121. doi: http://doi.org/10.1016/j.plantsci.2014.07.010.

Basile, A., Sorbo, S., Cardi, M., Lentini, M., Castiglia, D., Cianciullo, P., Conte, B., Loppi, S., Esposito, S., 2015. Effects of heavy metals on ultrastructure and Hsp70 induction in *Lemna minor* L. exposed to water along the Sarno River, Italy. Ecotoxicol. Environ. Saf. 114, 93–101. doi: http://dx.doi.org/10.1016/j.ecoenv.2015.01.009.

Basile, A., Sorbo, S., Conte, B., Cardi, M., Esposito, S., 2013. Ultrastructural changes and Heat Shock Proteins 70 induced by atmospheric pollution are similar to the effects observed under in vitro heavy metals stress in *Conocephalum conicum* (Marchantiales - Bryophyta). Environ. Pollut. 182, 209–216. doi: http://dx.doi.org/10.1016/j.envpol.2013.07.014.

Basile, A., Sorbo, S., Conte, B., Castaldo, Cobianchi, R., Trinchella, F., Capasso, C., Carginale, V., 2012a. Toxicity, accumulation, and removal of heavy metals by three aquatic macrophytes. Int. J. Phytoremediation 14, 374–387. doi: http://dx.doi.org/10.1007/s11356-015-4807-x.

Basile, A., Sorbo, S., Pisani, T., Paoli, L., Munzi, S., Loppi, S., 2012b. Bioaccumulation and ultrastructural effects of Cd, Cu, Pb and Zn in the moss *Scorpiurum circinatum* (Brid). Fleisch. & Loeske. Environ. Pollut. 166, 208–211. doi: http://dx.doi.org/10.1016/j.envpol.2012.03.018.

Bradford, M.M., 1976. A rapid and sensitive method for the quantitation of microgram quantities of protein utilizing the principle of protein-dye binding. Anal Chem. 72, 248–254. doi: http://dx.doi.org/10.1016/0003-2697(76)90527-3.

Chen, X., Yuan, H., Chen, R., Zhu, L., He, G., 2003. Biochemical and photochemical changes in response to triacontanol in rice (*Oryza sativa* L.). Plant Growth Regul. 40, 249-256. doi: http://dx.doi.org/10.1023/A:1025039027270.

Chiarelli, R., Roccheri, M.C., 2012. Heavy Metals and Metalloids as Autophagy Inducing Agents: Focus on Cadmium and Arsenic. Cells 1, 597-616. doi: http://dx.doi.org/10.3390/cells1030597.

Dalla Vecchia, F., La Rocca, N., Moro, I., De Faveri, S., Andreoli, C., Rascio, N., 2005. Morphogenetic, ultrastructural and physiological damages suffered by submerged leaves of *Elodea canadensis* exposed to cadmium. Plant Sci. 168(2), 329–338. doi: http://dx.doi.org/10.1016/j.plantsci.2004.07.025.

De Pinto, M.C., Francis, D., De Gara, L., 1999. The redox state of the ascorbate-dehydroascorbate pair as a specific sensor of cell division in tobacco BY-2 cells. Protoplasma. 209, 90-97. doi: http://dx.doi.org/10.1007/BF01415704.

Dixit, P., Mukherjee, P.K., Ramachandran, V., Eapen, S., 2011. Glutathione transferase from Trichoderma virens enhances cadmium tolerance without enhancing its accumulation in transgenic *Nicotiana tabacum*. PLoS One. 6(1), e16360. doi: https://doi.org/10.1371/journal.pone.0016360.

Ellman, G.L.,1959. Tissue sulfhydryl groups. Arch. Biochem. Biophys. 82, 70–77. doi: https://doi.org/10.1016/0003-9861(59)90090-6.

Eriksen, A.B., Sellden, G., Skogen, D., Nilson, S., 1981. Comparative analysis of the effect of triacontanol on photosynthesis, photorespiration and growth of tomato (C3-plants) and maize (C4-plants). Planta. 152, 44-49. doi: https://doi.org/10.1007/BF00384983.

Esposito, S., Sorbo, S., Conte, B., Basile, A., 2012. Effects of heavy metals on ultrastructure and HSP70s induction in the aquatic moss *Leptodictyum riparium* Hedw. Int. J. Phytoremediation 14, 443–455. doi: http://dx.doi.org/10.1080/ 15226514.2011.620904.

Farooq, M.A., Islam, F., Ali, B., Najeeb, U., Mao, B., Yan, G., Siddique, K.H.M., Zhou, W., 2016. Arsenic toxicity in plants: Cellular and molecular mechanisms of its transport and metabolism. Environ. Exp. Bot. 132, 42-52. doi: http://dx.doi.org/10.1016/j.envexpbot.2016.08.004.

Finnegan, P.M., Chen, W., 2012. Arsenic toxicity: the effects on plant metabolism. Front. Physiol. 3(182), 1–18. http://dx.doi.org/10.3389/fphys.2012.00182.

Foyer, C.H., Halliwell, B., 1976. The presence of glutathione and glutathione reductase in chloroplast: a proposed role in ascorbic acid metabolism. Planta 133, 21–25. doi: http://dx.doi.org/10.1007/BF00386001.

Fujita, M., Hossain, M.Z., 2003. Molecular cloning of cDNAs for three tau-type glutathione S-transferases in pumpkin (*Cucurbita maxima*) and their expression properties. Physiol Plant 117, 85-92. doi: http://doi.org/10.1034/j.1399-3054.2003.1170111.x.

Garg, N., Singla, P., 2011. Arsenic toxicity in crop plants: physiological effects and tolerance mechanisms. Environ. Chem. Lett. 9, 303–321. doi: http://dx.doi.org/10.1007/s10311-011-0313-7.

Ghelfi, A., Gaziola, S.A., Cia, M.C., Chabregas, S.M., Falco, M.C., Kuser-Falcão, P.R., Azevedo, R.A., 2011. Cloning, expression, molecular modelling and docking analysis of glutathione transferase from *Saccharum officinarum*. Ann. Appl. Biol. 159, 267-280. doi: http://dx.doi.org/10.1111/j.1744-7348.2011.00491.x.

Gupta, D.K., Inouheb, M., Rodrı´guez-Serrano, M., Romero-Puertas, M.C., Sandalio, L.M., 2013. Oxidative stress and arsenic toxicity: role of NADPH oxidases. Chemosphere 90(6), 1987–1996. doi: http://dx.doi.org/10.1016/j.chemosphere.2012.10.066.

Habig, W.H., Jakoby, W.B., 1981. Assays for differentiation of glutathione S-transferases. Methods Enzymol. 77, 398–405. doi: http://dx.doi.org/10.1016/S0076-6879(81)77053-8.

Hartley-Whitaker, J., Meharg, A.A., 2001. Copper and arsenate induced oxidative stress in *Holcus lahnatus* L. clones with differential sensitivity. Plant Cell Environ. 24, 713-722. doi: http://dx.doi.org/10.1046/j.0016-8025.2001.00721.x.

Hasanuzzaman, M., Fujita, M., 2013. Exogenous sodium nitroprusside alleviates arsenic-induced oxidative stress in wheat (*Triticum aestivum* L.) seedlings by enhancing antioxidant defense and glyoxalase system. Ecotoxicology 22(3), 584–596. doi: http://dx.doi.org/10.1007/s10646-013-1050-4.

Hoagland, D.R., Arnon, D.I., 1950. The water-culture method for growing plants without soil. *Calif Agric Exp Sta Circ.,* 347, 1–32.

Hossain, M.Z., Hossain, M.D., Fujita, M., 2006. Induction of pumpkin glutathione S-transferases by different stresses and its possible mechanisms. Biol. Plant. 50(2), 210-218. doi: http://doi.org/10.1007/s10535-006-0009-1.

Hu, Y., Ge, Y., Zhang, C., Ju, T., Cheng, W., 2009. Cadmium toxicity and translocation in rice seedlings are reduced by hydrogen peroxide pretreatment. Plant Growth Regul. 59(1), 51-61. doi: http://doi.org/10.1007/s10725-009-9387-7.

Ivanov, A.G., Angelov, M.N., 1997. Photosynthesis response to triacontanol correlates with increased dynamics of mesophyll protoplast and chloroplast membranes. Plant Growth Regul. 21, 145-152. doi: http://dx.doi.org/10.1023/A:1005790121111.

Khan, M.M.A., Hashmi, N., Moinuddin and Dar, T.A, 2014. Changes in growth, yield, photosynthetic characteristics, enzyme activities and essential oil production of fennel (*Foeniculum vulgare* Mill.) under growth regulator treatments. Journal of Essential Oil Research 26:105-113. http://dx.doi.org/10.1080/10412905.2013.860408.

Khandaker, M.M., Faruq, G., Rahman, M.M., Sofian-Azirun, M., Boyce, A.N., 2013. The influence of 1 -triacontanol on the growth, flowering, and quality of potted Bougainvillea plants (*Bougainvillea glabra* var. "Elizabeth Angus") under natural conditions. Sci. World J, 1-13. doi: https://doi.org/10.1155/2013/308651

Knowles, N.R., Ries, S.K., 1981. Rapid growth and apparent total nitrogen increases in rice and corn plants following application of triacontanol. Plant Physiol. 68, 1279-1284. doi: https://doi.org/10.1104/pp.68.6.1279

Kumaravelu, G., Livingstone, V.D., Ramanujam, M.P., 2000. Triacontanol-induced changes in the growth, photosynthetic pigments, cell metabolites, flowering and yield of green gram. Biol. Plantarum 43, 287–290. doi: http://dx.doi.org/10.1023/A:1002724831619.

Li, X.W., Chen, T.B., Huang Z.C., Lei, M., Liao, X.Y., 2006. Effect of arsenic on chloroplast ultrastructure and calcium distribution in arsenic hyperaccumulator *Pteris vittata* L. Chemosphere 62(5), 803-809. doi: http://doi.org/10.1016/j.chemosphere.2005.04.055.

Madhava Rao, K.V., Sresty, T.V., 2000. Antioxidative parameters in the seedlings of pigeon pea (*Cajanus cajan* (L.) Mill Spaugh) in response to Zn and Ni stresses. Plant Sci. 157, 113-128. doi: http://doi.org/10.1016/S0168-9452(00)00273-9.

Marschner, H., 1995. Mineral Nutrition of Higher Plants. 2nd ed. Academic Press, London.

Mascher, R., Lippmann, B., Holzinger, S., Bergmann, H., 2002. Arsenate toxicity: effects on oxidative stress response molecules and enzymes in red clover plants. Plant Sci. 163, 961–969. doi: http://doi.org/10.1016/S0168-9452(02)00245-5.

Mittova, V., Tal, M., Volokita, M., Guy, M., 2002. Salt stress induces up-regulation of an efficient chloroplast antioxidant system in the salt-tolerant wild tomato species *Lycopersicon pennellii* but not in the cultivated species. Physiol. Plant 115, 393-400. doi: http://dx.doi.org/10.1034/j.1399-3054.2002.1150309.x

Mokgalaka-Matlala, N.S., Flores-Tavizón, E., Castillo-Michel, H., Peralta-Videa, J.R., Gardea-Torresdey, J.L., 2009. Arsenic tolerance in mesquite (Prosopissp.): low molecular weight thiols synthesis and glutathione activity in response to arsenic. Plant Physiol. Biochem. 47, 822-826. doi: http://dx.doi.org/10.1016/j.plaphy.2009.05.007.

Muthuchelian, K., Bertamini, M., Nedunchezhian, N., 2001. Triacontanol can protect *Erythrina variegata* from cadmium toxicity. J. Plant Physiol. 158, 1487–1490. doi: https://doi.org/10.1078/0176-1617-00627.

Mylona, P.V., Polidoros, A.N., Scandalios, J.G., 1998. Modulation of antioxidant responses by arsenic in maize. Free Rad. Biol. Med. 25, 576-585. doi: http://doi.org/10.1016/S0891-5849(98)00090-2.

Naeem, M., Khan, M.M., Moinuddin, A., Manzer Siddiqui, H., 2009. Triacontanol stimulates nitrogen-fixation, enzyme activities, photosynthesis, crop productivity and quality of hyacinth bean (*Lablab purpureus* L.). Scientia Horticulturae 121(4), 389-396. doi: https://doi.org/10.1016/j.scienta.2009.02.030.

Naeem, M., Masroor, M. A., & Moinuddin, A., 2011. Triacontanol: A potent plant growth regulator in agricultural crops. J. Plant. Interact. 7, 129–142. doi: http://dx.doi.org/10.1080/17429145.2011.619281.

Nakano, V., Asada, K., 1981. Hydrogen peroxide is scavenged by ascorbate–specific peroxidase in spinach chloroplasts. Plant Cell Physiol. 22, 867–880. doi: https://doi.org/10.1093/oxfordjournals.pcp.a076232.

Pandey, N., Pathak, G.C., Pandey, D.K., Pandey, R., 2009. Heavy metals, Co, Ni, Cu, Zn and Cd, produce oxidative damage and evoke differential antioxidant responses in spinach. Braz. J. Plant Physiol. 21, 103-111. doi: http://dx.doi.org/10.1590/S1677-04202009000200003.

Paoli, L., Fiorini, E., Munzi, S., Sorbo, S., Basile, A., Loppi, S., 2013. Antimony toxicity in the lichen Xanthoria parietina (L.) Th.Fr. Chemosphere 93, 2269-2275. doi: https://doi.org/10.1016/j.chemosphere.2013.07.082.

Paoli, L., Fiorini, E., Munzi, S., Sorbo, S., Basile, A., Loppi, S., 2014. Uptake and acute toxicity of cerium in the lichen *Xanthoria parietina*. Ecotoxicol. Environ. Saf. 104, 379-385. doi: http://doi.org/10.1016/j.ecoenv.2014.02.028.

Perveen, S., M. Shahbaz and M. Ashraf, 2014. Triacontanol-induced changes in growth, yield, leaf water relations, oxidative defense system, minerals, and some key osmoprotectants in wheat (*Triticum aestivum* L.) under saline conditions. Turk. J. Bot. 38, 1–18.

Perveen, S., Shahbaz, M., Ashraf, M., 2011. Modulation in activities of antioxidant enzymes in salt stressed and non-stressed wheat (*Triticum aestivum* L.) plants raised from seed treated with triacontanol. Pak. J. Bot. 43(5), 2463-2468.

Perveen, S., Shahbaz, M., Ashraf, M., 2012. Changes in mineral composition, uptake and use efficiency of salt stressed wheat (*Triticum aestivum* L.) plants raised from seed treated with triacontanol. Pak. J. Bot. 44, 27-35.

Pigna, M., Cozzolino, V., Violante, A., Meharg, A.A., 2009. Influence of phosphate on the arsenic uptake by wheat (*Triticum durum* L.) irrigated with arsenic solutions at three different concentrations. Water Air Soil Pollut 197, 371–380. doi: https://doi.org/10.1007/s11270-008-9818-5.

Rennenberg, H., 1982. Glutathione metabolism and possible biological roles in higher plants. Phytochemistry. 21, 71- 81. doi: https://doi.org/10.1016/0031-9422(80)85045-X.

Romero-Puertas, M.C., Corpas, F.J., Rodrı´guez-Serrano, M., Gomez, M., Rio, L.A.D., Sandalio, L.M., 2007. Differential expression and regulation of antioxidative enzymes by cadmium in pea plants. Plant Physiol. 164, 1346-1357. doi: http://doi.org/10.1016/j.jplph.2006.06.018.

Sagner, S., Kneer, R., Wanner, G., Cosson, J.P., Deus-Neumann, B., Zenk, M.H., 1998. Hyperaccumulation, complexation and distribution of nickel in Sebertia acuminata. Phytochemistry 47, 339–347. http://dx.doi.org/10.1016/S0031-9422(97)00593-1.

Sanchez-Viveros, G., 2010. Short term effects of As-induced toxicity on growth, chlorophyll and carotenoid contents and total content of phenolic compounds of *Azolla filiculoides*. Water Air Soil Pollut. 217, 455-462 doi: http://doi.org/10.1007/s11270-010-0600-0.

Schwartzman, R.A., Cidlowsky, J.A., 1993. Apoptosis: the biochemistry and molecular biology of programmed cell death. Endocr. Rev. 14, 133–151. doi: http://dx.doi. org/10.1210/edrv-14-2-133.

Shahbaz, M., Ashraf, M., Akram, N.A., Hanif, A., Hameed, S., Joham, S., Rehman, R., 2011. Salt-induced modulation in growth, photosynthetic capacity, proline content and ion accumulation in sunflower (*Helianthus annuus* L.). Acta Physiol. Plant 33, 1113-1122. doi: http://dx.doi. org/10.1007/s11738-010-0639-y.

Shan C, Zhou Y, Liu M (2015) Nitric oxide participates in the regulation of the ascorbate-glutathione cycle by exogenous jasmonic acid in the leaves of wheat seedlings under drought stress. Protoplasma 252, 1397–1405. doi: http://dx.doi. org/10.1007/s00709-015-0756-y.

Sinha, S., Saxena, R. 2006. Effect of iron on lipid peroxidation, and enzymatic and non-enzymatic antioxidants and bacosidecontent in medicinal plant *Bacopa monnieri* L. Chemosphere 62, 1340-1350. doi: http://doi.org/10.1016/j.chemosphere.2005.07.030.

Sorbo, S., Sinkkonen, A., Aprile, G., Strumia, S., Castaldo Cobianchi, R., Leone, A., Basile, A., 2011. Ultrastructural effects of trace elements and environmental pollution in Italian "Triangle of Death" on *Pseudevernia furfuracea* (L.) Zopf. Plant Biosyst. 145, 461–471. doi: http://dx.doi.org/10.1080/11263504.2011.558722.

Stohs, S.J., Bagchi, D., 1995. Oxidative mechanisms in the toxicity of metal ions. Free Radical Biol. Med. 18, 321-326. doi: https://doi.org/10.1016/0891-5849(94)00159-H.

Thompson, A.R., Vierstra, R.D., 2005. Autophagic recycling: lessons from yeast help define the process in plants. Curr. Opin. Plant Biol. 8, 165-173. doi: http://doi.org/10.1016/j.pbi.2005.01.013.

Todeschini, V., Lingua, G., D'Agostino, G., Carniato, F., Roccotiello, E., Berta, G., 2011. Effects of high zinc concentration on poplar leaves: a morphological and biochemical study. Environ. Expt. Bot. 71, 50–56. doi: http://doi.org/10.1016/j.envexpbot.2010.10.018.

Upadhyaya, H, Shome, S., Roy, D. and Bhattacharya, M. K. 2014. Arsenic Induced Changes in Growth and Physiological Responses in *Vigna radiate* Seedling: Effect of Curcumin Interaction. American Journal of Plant Sciences 5: 3609-3618.doi: http://dx.doi.org/10.4236/ajps.2014.524377.

Verma, A., Malik, C.P., Sinsinwar, Y.K., Gupta, V.K., 2009. Yield parameters responses in a spreading (cv. M-13) and semi-spreading (cv. Girnar-2) types of groundnut to six growth regulators. American-Eurasian J. Agric. Environ. Sci. 6(1), 88-91.

Waqas, M., Shahzad, R, Khan, A.L., Asaf, S., Kim, Y.H., Kang, S.M., *Bilal, S., Hamayun*, M., Lee, I-J. 2016. Salvaging effect of triacontanol on plant growth, thermotolerance, macro-nutrient content, amino acid concentration and modulation of defense hormonal levels under heat stress, Plant Physiology and Biochemistry, 99; 118-125.doi: http://dx.doi.org/10.1016/j.plaphy.2015.12.012.

Wu, Z., Liu, S., Zhao, J., Wang, F., Du, Y., Zou, S., Li, H., Wen, D., Huang, Y. 2017. Comparative responses to silicon and selenium in relation to antioxidant enzyme system and the glutathione-ascorbate cycle in flowering Chinese cabbage (*Brassica campestris* L. ssp. *chinensis* var. *utilis*) under cadmium stress. Environ. Expt. Bot, 133, 1-11. doi: http://dx.doi.org/10.1016/j.envexpbot.2016.09.005.

Xiong, J., Fu, G., Tao, L., Zhu, C. 2010. Roles of nitric oxide in alleviating heavy metal toxicity in plants. Arch. Biochem. Biophys. 497, 13-20. doi: http://doi.org/10.1016/j.abb.2010.02.014.

Zare Dehabadi, S., Asrar, Z., Namaki Shoushtari, A., 2014. Investigation of synergistic action between coronatine and nitric oxide in alleviating arsenic-induced toxicity in sweet basil seedlings. Plant Growth Regul. 74, 119–130 doi: http://doi.org/10.1007/s10725-014-9903-2.

International Journal of *Molecular Sciences*

MDPI

The moss *Leptodictyum riparium* counteracts severe cadmium stress by activation of glutathione transferase and phytochelatin synthase, but slightly by phytochelatins

Erika Bellini [1,5#], Viviana Maresca [2#], Camilla Betti [3], Monica Ruffini Castiglione [1], Debora Fontanini [1], Antonella Capocchi [1], Carlo Sorce [1], Marco Borsò [4], Laura Bruno [5], Sergio Sorbo [6], Adriana Basile [2], and Luigi Sanità di Toppi [1*]

[1] Department of Biology, University of Pisa, 56126 Pisa, Italy; erika.bellini@biologia.unipi.it (E.B.); monica.ruffini.castiglione@unipi.it (M.R.C.); debora.fontanini@unipi.it (D.F.); antonella.capocchi@unipi.it (A.C.); luigi.sanita@unipi.it (L.S.d.T.)

[2] Department of Biology, University of Naples "Federico II", 80138 Naples, Italy; viviana.maresca@unina.it (V.M.); adriana.basile@unina.it (A.B.)

[3] Department of Medicine, University of Perugia, 06123 Perugia, Italy; camilla.betti@unipg.it (C.B.)

[4] Department of Surgery, Medical, Molecular, and Critical Area Pathology, University of Pisa, 56124 Pisa, Italy; marco.borso@student.unisi.it (M.B.)

[5] Department of Biology, University of Rome "Tor Vergata", 00133, Rome, Italy; laura.bruno@uniroma2.it (L.B.)

[6] Centro di Servizi Metrologici Avanzati (CeSMA), Microscopy Section, University of Naples "Federico II", 80126 Naples, Italy; sersorbo@unina.it (S.S.)

[#] These authors contributed equally.

[*] Correspondence: luigi.sanita@unipi.it; Tel.: +39-050-2211333

Abstract

In the present work, we investigated the response to Cd in *Leptodictyum riparium*, a cosmopolitan moss (Bryophyta) that can accumulate higher amounts of metals than other plants, even angiosperms, with absence or slight apparent damage. High-performance liquid chromatography followed by electrospray ionization tandem mass spectrometry of extracts from *L. riparium* gametophytes, exposed to 0, 36 μM and 360 μM Cd for 7 days, revealed the

presence of γ-glutamylcysteine (γ-EC), reduced glutathione (GSH), and phytochelatins up to PC_4. The increase in Cd concentrations progressively augmented reactive oxygen species levels, with activation of both antioxidant (catalase and superoxide dismutase) and detoxifying (glutathione-*S*-transferase) enzymes. After Cd treatment, cytosolic and vacuolar localization of thiol peptides was performed by means of the fluorescent dye monochlorobimane and subsequent observation with confocal laser scanning microscope. The cytosolic fluorescence observed with the highest Cd concentrations was also consistent with the formation of γ-EC-bimane in the cytosol, possibly catalyzed by the peptidase activity of the *L. riparium* phytochelatin synthase. Thus, in *L. riparium*, activation of phytochelatin synthase and glutathione-*S*-transferase, but minimally phytochelatin synthesis, play a role to counteract Cd toxicity, in this manner minimizing the cellular damage caused by the metal. This study strengthens previous investigations on the *L. riparium* ability to efficiently hinder metal pollution, hinting at a potential use for biomonitoring and phytoremediation purposes.

Keywords: Antioxidants; bryophytes; cadmium; γ-glutamylcysteine; glutathione; metals; *Leptodictyum riparium*; monochlorobimane; moss; phytochelatins; ROS.

1. Introduction

Trace metals, such as Cd, Hg, Pb, Cr(VI), etc., are important environmental pollutants, particularly in areas characterized by a strong anthropogenic pressure [1]. Their presence in the atmosphere, soil, and water, even at extremely low concentrations, can seriously damage all living organisms. Specifically, Cd is a widespread metal that is released into the environment by power stations, heating systems, electroplating, smelting, urban traffic, cement factories, and, sometimes, as a byproduct of some fertilizers [1]. By possessing a toxicity from 2- to 20-fold higher than many other metals, Cd is very harmful to a large number of organisms [2].

In plant cells, Cd ions are highly noxious even at low concentrations, with subsequent severe negative effects [3]. Unlike other metals, Cd does not directly induce oxidative stress [4,5] *via* Fenton and/or Haber-Weiss reactions [6], but rather disturbs the overall cellular redox balance and, consequently, affects the reactive oxygen species (ROS) levels [7]. In fact, Cd toxicity mainly originates from non-functional binding to various ligands that are meant to bind other divalent metals, i.e. Zn. Less known, a ligand may also be chlorophyll, where Cd^{2+} replaces Mg^{2+} as the central ion. Therefore, although not redox active, Cd exposure leads to enhanced production of ROS. Another reason is that Cd exposure reduces the capability of scavenging ROS [8, and references therein]. In this regard, Cd can activate or even inhibit several antioxidant enzymes, such as superoxide dismutase (SOD; EC 1.15.1.1), which catalyzes the production of O_2 and H_2O_2 from the radical anion superoxide ($\bullet O_2^-$); catalase (CAT; (EC 1.11.1.6), which decomposes H_2O_2 into O_2 and H_2O, and many others. Among these enzymes, the multifunctional enzyme glutathione-*S*-transferase (GST; EC 2.5.1.18) [9] can simultaneously counteract oxidative stress by enhancing ROS quenching, and detoxify a number of electrophilic xenobiotics or chemical elements, including Cd, both in yeast [10] and in plants [11–13]. Particularly, GST catalyzes an intracellular detoxification reaction of metals or noxious compounds by forming first a cytosolic conjugate between the thiol peptide glutathione (GSH) and the toxic element/substance, followed by sequestering this conjugate (GS conjugate) into the vacuolar compartment of the plant cell [14] by means of ATP binding cassette (ABC) transporters [15]. To detect xenobiotic or metal detoxification by conjugation,

and the subsequent translocation of the conjugate to various compartments, the dye monochlorobimane (MCB) can be useful, because it becomes fluorescent after conjugation to GSH and, to a lesser extent, to other thiol peptides [16,17]. Time course experiments with MCB can be monitored by confocal laser scanning microscopy (CLSM).

Besides, in higher plants an important metal detoxification system is based on the so-called phytochelatins (PCn) [1], directly derived from GSH. PCn are thiol peptide compounds with the general structure (γ-glutamylcysteine [EC])$_n$-glycine, with n usually ranging from 2 to 5. Due to the cysteine thiol groups, PCn chelate Cd or other metals and compartmentalize them in the vacuole [18], in order to quickly detoxify the cytosolic environment. From a biosynthetic point of view, PCn are synthetized from GSH by the activation of the enzyme phytochelatin synthase (PCS), a γ-EC dipeptidyl (trans)peptidase (EC 2.3.2.15) that is constitutively expressed in the plant cytosol [19]. PCS activation is self-regulated, because its reaction products (that is, PCn) chelate Cd, and the reaction stops when free Cd ions are no longer available [20]. However, other than being a γ-EC transpeptidase, PCS is also a cysteine peptidase that may regulate the cytosolic catabolism of GS-conjugates [21–23]. In this case, GS-conjugates with MCB (GS-bimane) can be cleaved into γ-EC and glycine, a reaction stimulated by some metals, particularly Cd, Zn, and Cu [21,23].

So far, the vast majority of studies on responses to metals (in particular Cd) in plants have been performed in higher plants, especially angiosperms, whereas only few aspects have been thoroughly investigated in bryophytes, considered the earliest-diverged lineages of land plants [24]. Because of their ancientness and their peculiar phylogenetic position [25,26], bryophytes (liverworts, mosses, and hornworts) are pivotal for reconstructing the origin of morphofunctional, ultrastructural, and cytohistological features of plants in the transition from water to land, including traits related to metal detoxification and homeostasis [24,27,28]. Moreover, bryophytes possess a very high surface/volume ratio, have an elevated cation exchange capacity, do not develop strong hydrophobic barriers, and, consequently, are prone to the absorption of (metal) contaminants from all environmental matrices. For these reasons, bryophytes are considered extraordinary systems for the monitoring of pollution and, more particularly, of metal contamination [29, and references therein].

Previous studies have demonstrated that the cosmopolitan moss *Leptodictyum riparium* (Bryophyta) can accumulate, and seemingly tolerate very high concentrations of toxic metals, including Cd [30–32], with a bioconcentration factor higher than that of other plants, even of some angiosperms [33]. Thanks to its apparent tolerance to metal stress and to its high efficiency for metal removal, *L. riparium* has therefore been proposed as an useful tool for biomonitoring metal contamination, as well as for carrying out phytoremediation projects in polluted areas [31–33]. Interestingly, *L. riparium* performs little Cd immobilization at the cell wall level, and therefore the metal enters the cytosol rather easily [31,34]. Thus, the apparent Cd tolerance showed by this moss in the open environment might be due to efficient intracellular (symplastic), rather than to cell wall (apoplastic), detoxification processes.

Although the *L. riparium* gametophytes collected in the open had seemingly an elevated tolerance level to Cd [31,32], until now no *ad hoc* studies have been carried out in the laboratory-confined environment. The latter experiments could therefore address the issue in mechanistic terms, when the moss is subjected to strong and prolonged Cd stress. Thus, in this work we hypothesize that the high ability of *L. riparium* gametophytes to effectively counteract Cd stress could rely on the activation of intracellular responses based on some antioxidant/detoxifying enzymes, such as SOD, CAT, and GST, as well as on the presence of thiol-peptide compounds, particularly γ-EC, GSH, and PCn. An in-depth observation of Cd effects in this moss is here provided by CLSM imaging of MCB-stained thiols, and by optical/transmission electron microscopy techniques. The overall results can be useful to understand the basis of the complex response mechanisms carried out by mosses and other early land plants when exposed, even outdoors, to severe metal stress.

2. Results

2.1. ROS production and antioxidant response to Cd

In Cd-treated gametophytes, the amount of ROS highly increased compared to controls (Figure 1a), and the antioxidant/detoxifying enzymes under investigation were also progressively activated by the two Cd concentrations. Actually, the SOD activity in 360-μM-treated moss samples was 20% and 60% higher than under the 36 μM treatment and the control, respectively (Figure 1b), whereas CAT increased up to 150 U/mg for 360 μM-treated samples (Figure 1c). Both Cd concentrations markedly enhanced the GST activity, reaching a value of 2.0 μmol ml^{-1} min^{-1} in the 360-μM-treated gametophytes (Figure 1d). Data are given in detail in Table S1.

2.2. *L. riparium* possesses a functional PCS that produces Cd-induced PCn *in vitro* and *in vivo*

The *in vitro* assay of the PCS from *L. riparium* gametophytes clearly revealed that the enzyme was activated already at the lowest Cd concentration supplied (36 μM). The increase in Cd concentration up to 100 μM led to an enhanced PCS activation, followed by a *plateau* state of the activity at the highest Cd concentration (360 μM) (Figure 2).

Both in control and in Cd-treated samples, the ability of *L. riparium* gametophytes to synthesize thiol peptides *in vivo* was demonstrated; in particular, the presence of γ-EC, GSH, and $PC_{2–4}$ was distinctly detected (Figure 3). The amount of PCn, although at trace levels, significantly increased only with the 360 μM $CdCl_2$ treatment, and not with 36 μM $CdCl_2$, as compared to controls. The highest Cd concentration led to an induced synthesis of all PCn oligomers (PC_2, PC_3, and PC_4) (Figure 3). Differently, the GSH levels progressively decreased with increase in Cd concentrations (Figure 3), and the γ-EC levels showed an upward trend between the controls and the 36-μM-treated samples, whereas the difference was significant only between the control and the 360 μM $CdCl_2$-treated samples (Figure 3).

The presence of PC_2, PC_3, and PC_4 oligomers was evident in the chromatograms obtained by high-performance liquid chromatography-electrospray ionization tandem mass spectrometry

(HPLC-ESI-MS-MS) of extracts from *L. riparium* gametophytes, exposed to Cd for 7 days (see Figure S1 for some exemplifying chromatograms).

2.3. Confocal imaging of MCB staining and chlorophyll autofluorescence

Control and Cd-treated *L. riparium* gametophytes (phylloids) were labeled *in situ* with 100 μM MCB for 30 min, 2 h, and 24 h (Figure 4). In controls, the mild MCB staining was localized in the cytosol and, partially, in the vacuoles, and remained at a fairly constant level at all exposure times (Figure 4a-c). In the 36 μM $CdCl_2$-treated gametophytes, MCB-stained for 30 min, a fluorescent labeling in the cytosol and vacuoles, not too dissimilar from that of the controls, was observed (Figure 4a). In contrast, after 2 h and 24 h, the MCB staining in the cytosol and vacuoles was much stronger than that in controls (Figure 4b, c). Concerning the 360 μM $CdCl_2$ treatments, the MCB staining after a 30-min incubation was mainly visible in the cytosol and minimally in the vacuoles (Figure 4a), but after 2 h and 24 h, it was localized only in the cytosol (Figure 4b, c). As negative control, incubation with methanol (instead of MCB) was carried out for each condition and treatment to avoid erroneous interpretations of the fluorescence labels (Figure 4d).

Additionally, in accordance with the TEM observations (see below), the chlorophyll autofluorescence imaging of the 360 μM Cd-treated gametophytes (Figure 4c) revealed a slight dilatation of the chloroplasts, possibly due to swelling of thylakoid membranes, in contrast to the round-shaped morphology of the chloroplasts in the control samples (Figure 4c).

2.4. Cd treatments caused only slight cytohistological damage to gametophytes

L. riparium gametophytes not exposed to Cd (controls) and stained with Evans Blue did not show any damage, particularly in phylloids (Figure 5a). Likewise, 36 and 360 mM Cd treatments did not show extensive damage (Figure 5b, c), but only slight injuries at the highest metal concentration (Figure 5c). By contrast, 1 h-exposure of gametophytes to pure ethanol (positive control) produced heavy alterations in the tissues (Figure 5d).

2.5. Cd treatment lowers photosynthetic activity in *L. riparium* gametophytes

In order to evaluate the effect of Cd treatments on the photosynthetic activity in gametophytes, the photochemical efficiency was assessed. Maximum PSII quantum yield (Fv/Fm) was negatively affected by both Cd concentrations (36 and 360 µM), compared to control (Figure 6).

2.6. Ultrastructural observations evidenced slight ultrastructure alteration in Cd-exposed gametophytes

TEM micrographs of control (untreated) *L. riparium* gametophyte sections revealed that phylloid cells were surrounded by a thick cell wall, and contained several lenticular chloroplasts in the peripheral cytoplasm, as well as a central vacuole (Figure 7a). The well-developed thylakoids, arranged as grana and intergrana, were packed and tidily placed along the chloroplast main axis, without signs of swelling (Figure 7b, c); starch grains and rare plastoglobules were also visible (Figure 7b, c). Mitochondria had a typical morphology with cristae and an electron-dense matrix. Nuclei showed classical eu- and heterochromatin (Figure 7b).

Conversely, in Cd-treated samples, some ultrastructural changes were observed that were more marked, albeit not severely, in the 360 µM Cd-treated phylloids. Samples exposed to 36 µM Cd had in fact a quite well-preserved ultrastructure, even though chloroplasts were slightly deformed (Figure 7d, e). The morphology of mitochondria was comparable to that of the controls (Figure 7f) and multilamellar bodies occurred in the cytoplasm (Figure 7fbis). By contrast, samples treated with 360 µM Cd had additional ultrastructural alterations, such as plasmolyzed cells with some cytoplasm vacuolization (Figure 7g). Although grana and intergrana thylakoids were still present in the chloroplasts, a diffuse swelling was visible (Figure 7j). Mitochondria seemed altered, with swollen cristae and an electron-clear matrix. In some cells, precipitated electron-dense material was also present (Figure 7i).

3. Discussion

The moss *L. riparium* is able to detoxify (extremely) elevated concentrations of Cd (36 and 360 μM $CdCl_2$) even when the metal is supplied for a prolonged time (7 days). The slight cytohistological and ultrastructural damage caused by Cd suggests very efficient metal detoxification processes functioning on the whole in this moss, despite that - as a general sign of suffering - photochemical efficiency was negatively affected by both Cd concentrations. Interestingly, the mechanisms based on Cd immobilization at the cell wall level have previously been demonstrated not to play a relevant role [31,34]. By contrast, intracellularly-synthesized stress proteins (such as the heat shock protein 70) might be important in repairing the damage caused by Cd, especially at high concentrations, possibly by allowing the correct refolding of Cd-impaired proteins [31,34].

Here, we found that to counteract (extremely) severe Cd stress, *L. riparium* gametophytes adopt a detoxification system employing, on the whole, thiol peptide compounds, such as γ-EC, GSH, and PCn. In particular, after 7 days of Cd treatment, PCn synthesis is induced only by the highest (360 μM Cd) and not by the lowest (36 μM Cd) metal concentration. This response demonstrates that PCn biosynthesis (in any case, present at trace levels) is only triggered by an extremely high Cd concentration. Accordingly, the *in vitro* PCS activity measured in the gametophyte extracts reaches a *plateau* only after treatment with the highest Cd concentrations (100 μM and 360 μM Cd), whereas its activation is approximately half as high with the lowest concentration (36 μM Cd). Thus, especially in the presence of 36 μM Cd, other metal detoxification systems, rather than PCn, seem to operate effectively at an intracellular level.

In this regard, it should be pointed out that, at least in higher plants, the PCS enzyme does not possess an exclusive transpeptidase activity (i.e., a polymerase activity directed to PCn biosynthesis) [18], but also has a peptidase activity [21–23], because PCS belongs to the papain-like Clan CA of the cysteine peptidases [35, and references therein]. Thus, the "bifunctional" enzyme PCS can convert GSH to γ-EC by deglycination of GS-conjugates [21–23] and, consistently, contribute to the degradation of xenobiotics and/or metal-thiolate complexes in the cytosolic compartments. In this way, the high levels of GSH found in *L.*

riparium gametophytes might be important catalytic promoters of the PCS activation in the peptidase instead of in the transpeptidase "direction" - even considering that Cd does not induce more PCn synthesis at 36 μM than in the controls, and induces only trace level-PCn at 360 μM.

Indeed, unlike PCn, high GSH levels are detected both in the controls and in Cd-treated *L. riparium* gametophytes. Mosses are already known to be able to synthesize GSH at high levels, as shown by control and 36 μM Cd-exposed gametophytes of *Polytrichastrum formosum*, *Fontinalis antipyretica*, and *Hypnum cupressiforme*, in which up to ca. 370 nmol g^{-1} FW of GSH were measured [27]. Likewise, Bleuel et al. (2011) [36] detected about 200 nmol g^{-1} FW of GSH in the moss *Physcomitrella patens*. Indeed, GSH *per se* can represent an efficient system for Cd detoxification, particularly in bryophytes [37], but also in higher plants [7,38]. Moreover, besides their direct metal detoxification capacity, high levels of GSH are essential to neutralize ROS production, together with antioxidant enzymes, such as SOD and CAT. In our samples, these enzymes are activated by the two Cd concentrations, thus indicating that *L. riparium* owns an enzymatic arsenal that is collectively able to quench ROS even after 7 days of severe metal exposure.

Last but not least, GSH is also an essential co-substrate for GST activation. This enzyme, with cytosolic, chloroplastic, and nuclear isoforms in the moss *P. patens* [39], catalyzes the conjugation of GSH and, to a much lesser extent, of γ-EC [16,17] with several endogenous substances, xenobiotics, metals, etc. [10–13,39–41]. This conjugation is usually followed by vacuolar compartmentalization [39,42] and further intravacuolar degradation [43,44]. Interestingly, an hemerythrin class of GST that can bind metals, such as Fe and Cd [45], by means of a thiolate complex, has been discovered in *P. patens* [39]. In our experiments, in contrast to the PCS enzyme, the GST from gametophytes exposed to both Cd concentrations is much more active than in controls. Hence, GST can be activated, together with SOD and CAT, both to limit ROS production and to contribute to Cd detoxification by its intravacuolar segregation. Consequently, the high levels of GSH found in *L. riparium* gametophytes might result, on the one hand, in a substrate for PCS activation in the cytosol toward the peptidase

"direction" and, on the other hand, in a Cd detoxifying *per se*, as well as a co-substrate for GST, the activation of which can lead to vacuolar compartmentalization of the GS-conjugates. The importance of the balance between cytosolic/vacuolar processes for Cd detoxification in *L. riparium* gametophytes, in particular in phylloids, is confirmed by the *in situ* labeling of the thiolic compounds with MCB at different time points (30 min, 2 h, and 24 h). After a 30-min treatment with MCB, in control and 36 □M Cd-exposed gametophytes, cytosolic and, in part, intravacuolar fluorescence is detected. After 2 h and 24 h of MCB staining, a marked increase in cytosolic and, above all, intravacuolar fluorescence is observed in the 36 □M Cd-exposed gametophytes, a possible sign of enhanced MCB staining due to the prolonged exposure. Accordingly, treatment of *P. patens* protonema cells with MCB led to labeling of the cytosol, followed by vacuolar internalization after 3 h of staining [36]. Moreover, the exposure of gametophytes to the highest concentration of Cd, deliberately supplied to burden the moss with an extremely severe metal stress, radically changes the scenario. Already after 30 min, and even after 2 h and 24 h, the MCB fluorescence is evident only in the cytosol of the phylloid cells, but it is almost completely absent inside the vacuoles.

Altogether, under 36 μM Cd treatment, the PCS enzyme *in vitro* is more active than in the controls, but it is still much less active, by approximately 50%, than in the presence of the higher metal concentrations (100 μM and 360 μM Cd); above all, the PCn synthesized *in vivo* are present at levels not significantly higher than those in controls. Thus, under these conditions, the high GST activity, due to the high GSH levels, allows the vacuolar compartmentalization of Cd. In this process, ABC tonoplast transporters are possibly involved [14]. At the same time, the trend of PCS activation toward the peptidase "direction" may lead to some γ-EC production, possibly contributing to slight increase in the cytosolic MCB staining [16,17]. In fact, γ-EC, at least in *Arabidopsis thaliana*, cannot be considered a suitable substrate for ABC tonoplast transporters [14], and, hence, its intravacuolar fluorescence might be overlooked. In any case, with 36 μM Cd, the GST activity of *L. riparium* gametophytes seem to overcome the peptidase activity of the PCS.

Despite a PCn production higher in the 360 μM than in the 36 μM Cd-exposed gametophytes (and in controls), the PCn levels synthesized under this extremely high metal

concentration are still very low, also when compared with those found in other bryophytes - specifically in *Sphagnum palustre* that, to our knowledge, is the only moss in which PCn were quantified and characterized [27]. Thus, in our samples, the direct contribution of PCn to Cd detoxification seems to be extremely limited. But, at the same time, at this Cd concentration, the PCS enzyme is fully active *in vitro*, having even reached a *plateau* in its activity. Thus, under this condition, PCS might reasonably be assumed to be mainly challenged for the cytosolic degradation of GS-Cd conjugates, i.e., the peptidase "direction", rather than for the biosynthesis of PCn, i.e, the transpeptidase "direction". Therefore, the MCB fluorescence constantly detected intracellularly might be a consequence of a PCS-dependent generation of the cleavage products in the cytosolic compartment. Indeed, when MCB is supplied together with Cd and other metals in *A. thaliana*, a significant amount of fluorescence is retained in the cytosol of the leaf cells [14]. Hence, a cytosolic formation of γ-EC-bimane may be postulated in this condition, through the Cd-triggered PCS activation, without or with a very low sequestration of this conjugate in the vacuolar compartment. All these processes suggest that PCS and GST play a joint role in the intracellular detoxification of Cd, at least when the metal is supplied at extremely elevated concentrations and for a long time.

Thus, *L. riparium* seems to be an effective system for the study of Cd detoxification, also thanks to anatomical features that facilitate metal uptake, such as lack of strong hydrophobic barriers and the absence of a vascular system *sensu proprio*. The main mechanisms underlying the high ability at counteracting the negative effects of (extremely) high Cd levels can be attributed to thiol peptide–mediated intracellular detoxification, as well as to activation of PCS and GST and, to some extent, to vacuolar compartmentalization. This study strengthens previous observations on the ability of *L. riparium* to tolerate strong metal pollution, clarifies its intracellular Cd detoxification mechanisms, and points to the potential use of this moss in biomonitoring and phytoremediation purposes.

4. Materials and Methods

4.1. Plant material and growth conditions

Samples of *Leptodictyum riparium* (Hedw.) Warnst. (Bryophyta) were collected from a tap water–filled basin in the Botanical Garden of the University of Naples "Federico II" (Italy). Single gametophytes were carefully washed with deionized water, then surface–sterilized in 7% (v/v) NaClO with a few drops of Triton X-100, and thoroughly rinsed with deionized water. Samples were individually put into Falcon tubes filled with 45 ml of sterile tap water (control) or $CdCl_2$ in two different concentrations (36 μM and 360 μM), for an overall metal exposure of 7 days. The cultures were placed in a growth chamber with night and day temperatures ranging, respectively, from 15 °C ± 1.3 °C to 20 °C ± 1.3 °C, 70% ± 4% relative humidity, a 16-h/8-h light/dark regime, and a photosynthetic photon flux density of 40 μmol m^{-2} s^{-1}. To confirm the absence of damage due to the sterilization process, *L. riparium* gametophytes were observed every 2 days with a Leitz Aristoplan microscope and a wild Heerbrugg M3Z binocular. The plant material was grown in triplicate and all the experiments were repeated at least three times.

4.2. Detection of ROS production and SOD, CAT, and GST activities

A spectrofluorometric assay employing 2',7'-dichlorofluorescein diacetate (DCFH–DA) was performed for measurements of ROS production; the assay is based on intracellular de-esterification of DCFH-DA and its conversion to nonfluorescent 2',7'-dichlorofluorescein (DCFH), which is then oxidized by ROS to the highly fluorescent 2',7'-dichlorofluorescein (DCF) [46]. Moss samples were immediately frozen in liquid nitrogen and ground thoroughly with prechilled mortar and pestle. The resulting powder (150 mg) was then resuspended in Tris HCl 40 mM pH 7.4, sonicated, and centrifuged at 12,000×*g* for 30 min. The supernatant (500 μl) was collected, and protein content determined according to the Bradford's method [47]. An aliquot (10 μl) of each sample was transferred to a 96-well plate, incubated with 5 μM DCFH–DA for 30 min at 37 °C ± 1 °C, and analyzed with an automatic plate reader.

ROS amounts were monitored by fluorescence (excitation wavelength of 530 nm and emission wavelength of 660 nm).

One gram of moss gametophytes was ground with 1 ml of chilled NaH_2PO_4/Na_2HPO_4 buffer (PBS, 50 mM, pH 7.8) containing 0.1 mM ethylenediaminetetraacetic acid (EDTA) and 1% (w/v) polyvinylpyrrolidone (PVP). The homogenate was centrifuged at 12,000×*g* for 30 min, and the supernatant (enzyme extract) was collected for protein quantification and determination of SOD, CAT, and GST activities. The protein concentration was quantified spectrophotometrically at 595 nm according to the Bradford method with bovine serum albumin (BSA) as the standard [47].

CAT activities were calculated and expressed as the absorbance decrease at 240 nm due to H_2O_2 consumption with a commercial kit (Sigma-Aldrich, St. Louis, MO, USA), according to the manufacturer's protocol. SOD activity was spectrophotometrically determined at 450 nm with a commercial kit (19160, Sigma-Aldrich). The assay utilizes a water-soluble tetrazolium salt that produces a formazan dye after reduction by the radical anion superoxide ($\bullet O_2^-$). The reduction rate with $\bullet O_2^-$ is linearly related to the xanthine oxidase activity, which is inhibited by SOD. The result was compared with a standard SOD curve. One unit of SOD activity was defined as the amount of enzyme that inhibited 50% of the $\bullet O_2^-$ reduction per min at 25 °C and pH 7. GST activity was measured with a commercial kit (CS0410, Sigma-Aldrich). The GST-catalyzed conjugation of GSH to 1-chloro-2,4-dinitrobenzene (CDNB) was monitored at 340 nm for 4 min. The reaction mixture contained 4 µl of extract and 196 µl of reaction solution (200 mM GSH and 100 mM CDNB in Dulbecco's buffer at pH 7). A GST unit was defined as the amount of enzyme that catalyzes the formation of 1 µmol of the GS-DNB conjugate per min at 25 °C and pH 7 ($\varepsilon = 9.6\ mM^{-1}\ cm^{-1}$ according to Habig and Jakoby 1981 [48]).

4.3. *In vitro* activity assay of PCS

L. riparium PCS activity was assayed in extracts of fresh Cd-untreated gametophytes (200 mg), as described in Petraglia et al. (2014) and Wojas et al. (2008) [27,49], with some

modifications. Briefly, each gametophyte sample was frozen with liquid nitrogen in a 2-ml Eppendorf tube containing two agate grinding balls (5 mm diameter); each tube was then placed in a mixer mill (MM200, Retsch, Haan, Germany) and shaken with a frequency of 30 Hz for 1 min. The powder obtained was added with 600 µl of extraction buffer (20 mM HEPES-NaOH pH 7.5; 10 mM ß-mercaptoethanol; 20% (w/v) glycerol; 100 mg ml^{-1} polyvinylpyrrolidone) and homogenized for 1 min with another cycle of mixer mill shaking. The homogenized samples were then centrifuged twice at 13,000×*g* (Hermle, Z 300 K, Wehingen, Germany) at 4 °C for 10 min; an aliquot of 400 µl of the supernatants was mixed with 100 µl of reaction buffer (250 mM HEPES-NaOH pH 8.0; 10% (w/v) glycerol; 25 mM GSH). The extraction and reaction buffers contained 36 µM Cd, 100 µM Cd, and 360 µM Cd supplied as $CdCl_2$. After an incubation time of 90 min at 35 °C, the reaction was terminated with 125 µl 20% (w/v) trichloroacetic acid. The PCS activity was immediately assayed by HPLC–ESI–MS–MS and expressed as pmol PCn g^{-1} FW min^{-1}.

4.4. γ–EC, GSH, and PCn extraction, characterization, and quantification

On the 7th day of growth, single gametophytes were carefully washed with deionized water and gently blotted dry with filter paper. Then, 100 mg of each sample were put into a 2-ml Eppendorf tube, briefly frozen in liquid nitrogen, and stored in the dark at –80 °C until further analysis.

Each sample was extracted as described in Bellini et al. (2019) [50]. Briefly, gametophytes were homogenized by a mixer mill (MM200, Retsch) with two agate grinding balls (5 mm diameter) at a vibrational frequency of 30 Hz for 2 min. Then 300 µl of ice-cold extraction buffer (5% (w/v) 5-sulfosalicylic acid (SSA), 6.3 mM diethylenetriamine-pentaacetic acid (DTPA), and 2 mM Tris (2-carboxyethyl) phosphine (TCEP)) were added to each homogenate, together with $^{13}C_2$,^{15}N-GSH, and $^{13}C_2$,^{15}N-PC_2 as internal standards (each at a concentration of 200 ng ml^{-1}). The powder was resuspended, kept in an ice bath for 15 min, and vortexed each 5 min. The extract was sedimented by centrifugation at 10,000×*g* (Z 300 K; Hermle, Wehingen, Germany) at 4 °C for 20 min. Each supernatant was filtered by a

Minisart RC4 0.45-µm filter (Sartorius, Goettingen, Germany) and samples were stored at –80 °C until analysis.

Thiol peptides (γ-EC, GSH, and PCn) were analyzed with an 1290 Infinity UHPLC (Agilent, Santa Clara, CA, USA), equipped with a thermostated autosampler, a binary pump, and a column oven, coupled to an API 4000 triple quadrupole mass spectrometer (AB Sciex, Concord, ON, Canada), equipped with a Turbo-V ion spray source (AB Sciex). Chromatographs were separated by a reverse-phase Phenomenex (Torrance, CA, USA) Kinetex 2.6 µm XB-C18 100 Å, 100×3 mm HPLC column, protected by a C18 3-mm ID security guard ULTRA cartridge, as described in Bellini et al. (2019) [50]. The separation was achieved by means of a gradient solvent system [solvent A, acetonitrile with 0.1% (v/v) formic acid; solvent B, water with 0.1% (v/v) formic acid] as follows: solvent A was set at 2% for 5 min, raised with a linear gradient to 44% in 4.5 min, and then raised with a linear gradient to 95% in 1 min. Solvent A was maintained at 95% for 1 min before column re-equilibration (2.5 min). Flow rate and column oven temperature were set to 300 µl min^{-1} and 30 °C, respectively. The injection volume was 20 µl. Thiol peptides were identified and quantified by tandem mass spectrometry (MS/MS) with certified standards (GSH, $PC_{2–4}$; AnaSpec Inc., Fremont, CA, USA) to build external calibration curves and certified glycine-$^{13}C_2$,^{15}N-labeled GSH (Sigma-Aldrich) and glycine-$^{13}C_2$,^{15}N-labelled PC_2 (AnaSpec Inc.) as internal standards. System control, data acquisition, and processing were carried out by an Analyst® version 1.6.3 software (AB Schiex). The method was validated as described in Bellini et al. (2019) [50].

4.5. Confocal laser imaging of MCB internalization

At least three samples of *L. riparium* gametophytes for each Cd treatment (36 and 360 µM $CdCl_2$) and control condition were treated on a rocking shaker with 100 µM MCB (Thermo Fisher Scientific, MA, USA) for 30 min, 2 h, and 24 h at 21 °C in the dark, at near-neutral pH conditions.

Phylloids from gametophytes were washed in sterile water and observed with a Zeiss 800 confocal caser scanning microscope (CLSM) using a 63× immersion objective. For the detection of MCB and chlorophyll fluorescence, excitation was set at 405 nm and 543 nm and emission was captured at 490 nm and 608 nm, respectively. MCB stock solutions were prepared at a 50 mM concentration in methanol, stored at –20 °C, and thawed immediately prior to use, with subsequent dilution up to 100 mM by adding sterile water. As control of the MCB staining, the same amount of methanol used for the 100 μM MCB treatments was added to the growth medium of the unstained *L. riparium* gametophytes.

4.6. Evans Blue staining and microscopy

Viability assay was performed using Evans Blue staining in order to detect cell damage/death as described in de León et al. (2007) [51]. At least three samples of *L. riparium* gametophytes for each growth condition (0, 36 and 360 μM $CdCl_2$) and three positive controls (100% ethanol for 1 h) were incubated for 2 h with 0.05% Evans Blue, and then washed 4 times with deionized water to remove excess dye. Material was then mounted on a slide in 100% glycerol and examined for Evans Blue staining using light microscope (Leitz Diaplan Wetzlar, Germany) equipped with a Leica DFC 420 camera (Leica Microsystems, Germany).

4.7. Photochemical efficiency

Maximum quantum yield of PSII (Fv/Fm) was measured by a chlorophyll fluorometer (Handy PEA, Hansatech Instruments, Ltd., UK) at 20 °C ± 1.3 °C temperature. Gametophytes were covered with a leaf clip to adapt them to darkness for 30 min and then exposed for 1 s to 3500 μmol photons m^{-2} s^{-1} (650 nm peak wavelength) and chlorophyll *a* fluorescence was recorded. Nine measurements were taken for each treatment and the fluorescence data were processed by PEA plus software (Hansatech Instruments, UK).

4.8. Ultrastructural observations

Gametophytes were fixed in 3% (v/v) glutaraldehyde in phosphate buffer solution (pH 7.2-7.4) for 2 h at room temperature, post-fixed with buffered 1% (w/v) OsO_4 for 1.5 h at room temperature, dehydrated with ethanol up to propylene oxide, and embedded in Spurr's epoxy medium [52]. Ultra-thin (40-nm thick) sections of gametophyte phylloids were put on 300-mesh Cu grids, stained with Uranyl Replacement Stain UAR (Electron Microscopy Science, Hatfield, PA, USA) and lead citrate, and observed under a Philips EM 208S TEM [52]. Fifty-four specimens were observed, with each set made up of three specimens collected twice and in triplicate from different dishes.

4.9. Statistical analysis

Data were analyzed by means of the Graph-Pad Prism 8.2.1 statistical program (GraphPad Software Inc., San Diego, CA, USA). Data were reported as the mean ± SE (standard error). The threshold of statistical significance was set at $p < 0.05$, unless otherwise specified. The effect of Cd concentrations in terms of ROS production, SOD, CAT, GST, and PCS activities, were examined by one-way analysis of variance (ANOVA), followed by Tukey's multiple comparison *post-hoc* test. Moreover, the data relating to PCn *in vivo* production were analyzed by two-way ANOVA, followed by Tukey's *post–hoc* test as above.

Author Contributions: Conceptualization, A.B. and L.S.d.T.; methodology, E.B., V.M., C.B., C.S., M.R.C., D.F., A.C., and S.S.; validation, E.B., V.M., M.B., and S.S.; formal analysis, D.F., A.B., and L.S.d.T.; investigation, A.B., and L.S.d.T.; data curation, E.B., A.B., and L.S.d.T.; writing-original draft preparation, E.B., C.B. M.R.C., and L.S.d.T.; supervision, L.S.d.T.; project administration, L.S.d.T.; funding acquisition, A.B., L.B., and L.S.d.T.

Funding: This research was partly funded by the Ministry of Education, University and Research-Research Projects of National Relevance (MIUR–PRIN 2015, grant number 20158HTL58 to L.S.d.T.).

Acknowledgments: The authors thank Dr. Alessandro Saba (University of Pisa) for the full availability of the HPLC-ESI-MS-MS system and Martine De Cock for English language check of the manuscript.

Conflicts of Interest: The authors declare no conflict of interest. The funder had no role in the design of the study; in the collection, analyses, or interpretation of data; in the writing of the manuscript, or in the decision to publish results.

Abbreviations

PCn	Phytochelatins
PCS	Phytochelatin synthase
GSH	Glutathione
GS–bimane	Glutathione–bimane
γ–EC	γ–glutamylcysteine
ROS	Reactive oxygen species
SOD	Superoxide dismutase
CAT	Catalase
GST	Glutathione-*S*–transferase
MCB	Monochlorobimane

Figure and Table

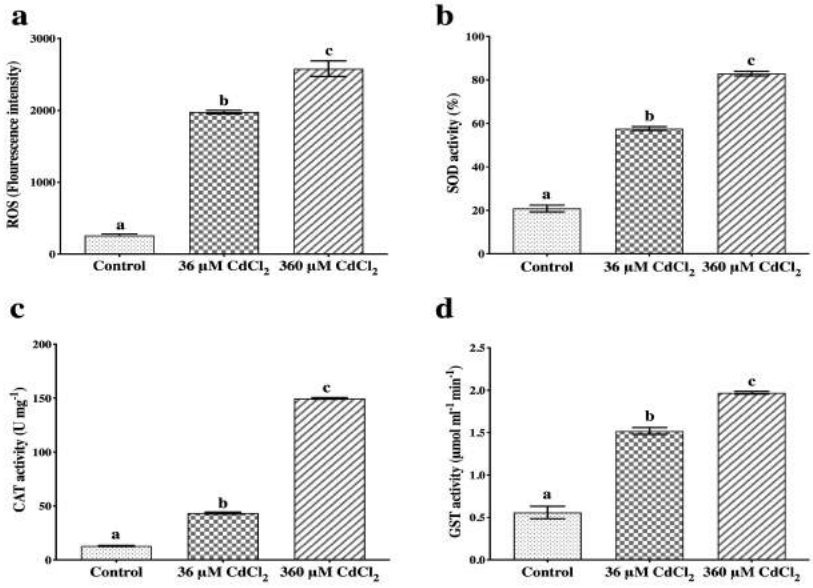

Figure 1. ROS amount and antioxidant/detoxifying enzyme activities in *L. riparium* gametophytes treated with 0 (Control), 36 or 360 µM $CdCl_2$ for 7 days. (**a**) ROS production; activities of (**b**) superoxide dismutase, SOD; (**c**) catalase, CAT; (**d**) glutathione-*S*-transferase, GST. Values are mean ± SE; bars not accompanied by the same letter are significantly different at $p < 0.05$.

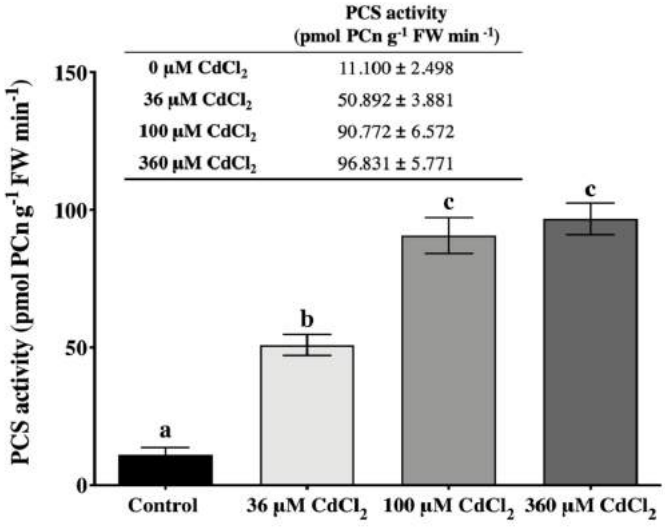

Figure 2. *In vitro* PCS activity of *L. riparium* gametophytes incubated with 0 (Control), 36, 100, and 360 µM $CdCl_2$ for 90 min. Values are mean ± SE; bars not accompanied by the same letter are significantly different at $p < 0.05$.

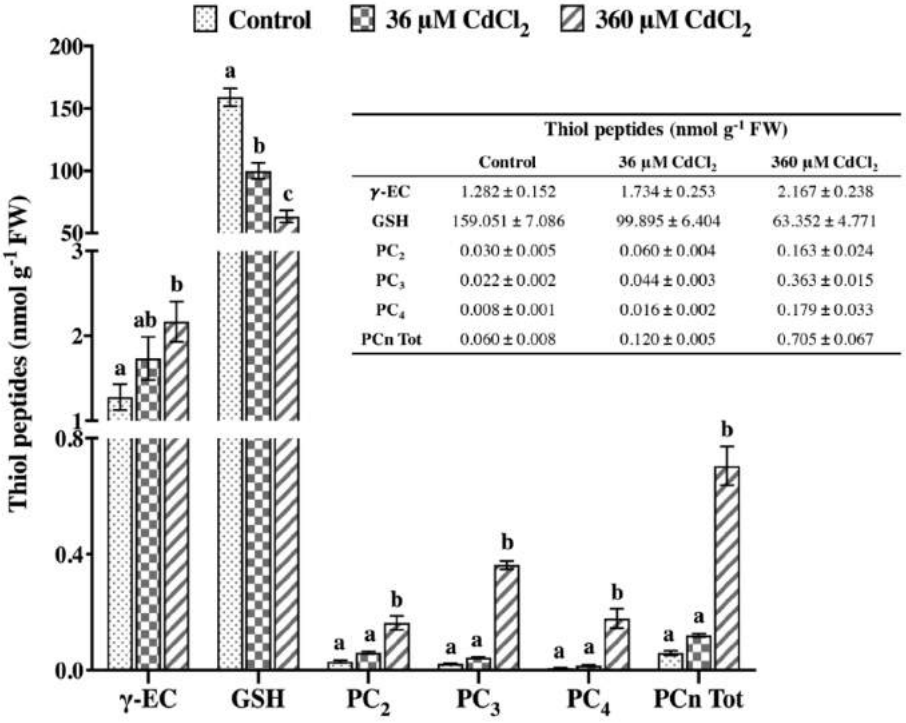

Thiol peptides (nmol g^{-1} FW)	Control	36 µM $CdCl_2$	360 µM $CdCl_2$
γ-EC	1.282 ± 0.152	1.734 ± 0.253	2.167 ± 0.238
GSH	159.051 ± 7.086	99.895 ± 6.404	63.352 ± 4.771
PC_2	0.030 ± 0.005	0.060 ± 0.004	0.163 ± 0.024
PC_3	0.022 ± 0.002	0.044 ± 0.003	0.363 ± 0.015
PC_4	0.008 ± 0.001	0.016 ± 0.002	0.179 ± 0.033
PCn Tot	0.060 ± 0.008	0.120 ± 0.005	0.705 ± 0.067

Figure 3. Content of γ-EC, GSH and PCn in *L. riparium* gametophytes, exposed to 0 (Control), 36 and 360 µM $CdCl_2$ for 7 days. Values are mean ± SE; within each group of thiol peptides, bars not accompanied by the same letter are significantly different at $p < 0.05$.

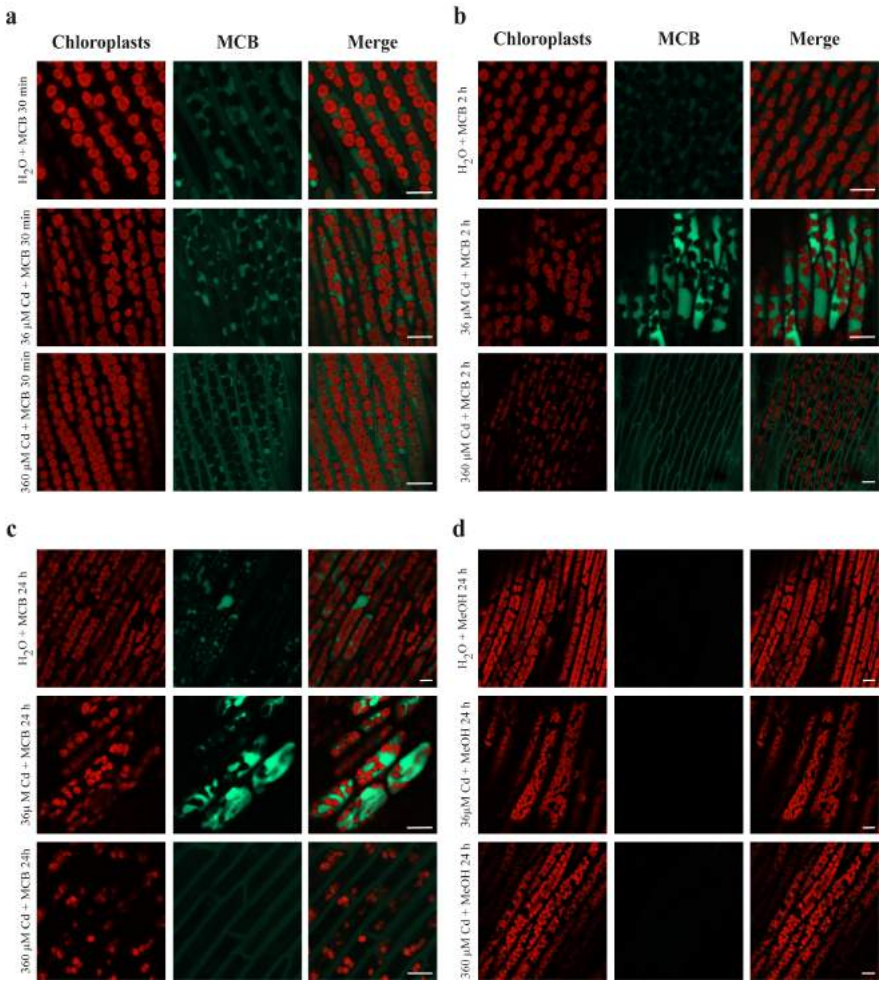

Figure 4. Confocal laser scanning microscopy (CLSM) imaging of *L. riparium* gametophytes (phylloids) from controls and samples exposed to 36 and 360 μM $CdCl_2$ for 7 days, followed by treatment with 100 μM MCB for 30 min, 2 h, and 24 h (green signal). Chlorophyll autofluorescence at the same exposure times is also visualized (red signal in chloroplasts), as well as the merge between MCB staining and chlorophyll autofluorescence. **(a)** MCB staining for 30 min. In control MCB-treated gametophytes, staining is visible in the cytosol and, partly, in the vacuoles. In samples treated with 36 μM $CdCl_2$, MCB staining occurs in the cytosol and the vacuoles, whereas in the samples treated with 360 μM $CdCl_2$, MCB fluorescence is predominantly present in the cytosol and much less in the vacuoles. **(b)** MCB staining for 2 h. Controls similar to (a). Differently, the 36-μM $CdCl_2$ samples show strong MCB staining inside the vacuoles, whereas in the 360-μM $CdCl_2$ samples the MCB signal is detected only in the cytosol. **(c)** MCB staining for 24 h. The overall situation is similar to (b) [(in controls also to (a)]. In addition, in the 360-μM $CdCl_2$ samples, the chloroplasts are slightly dilated, possibly because of thylakoid membrane swelling, when compared to the round–shaped morphology of chloroplasts from the control samples (a). **(d)** Representative negative controls treated

with methanol (MeOH) instead of MCB. All images were captured with a Zeiss LSM 800 CLSM at λ_{EX}: 405 nm, λ_{EM}: 490 nm for MCB (as for MeOH), and λ_{EX}: 543 nm, λ_{EM}: 608 nm for chlorophyll. Scale bars = 10 μm.

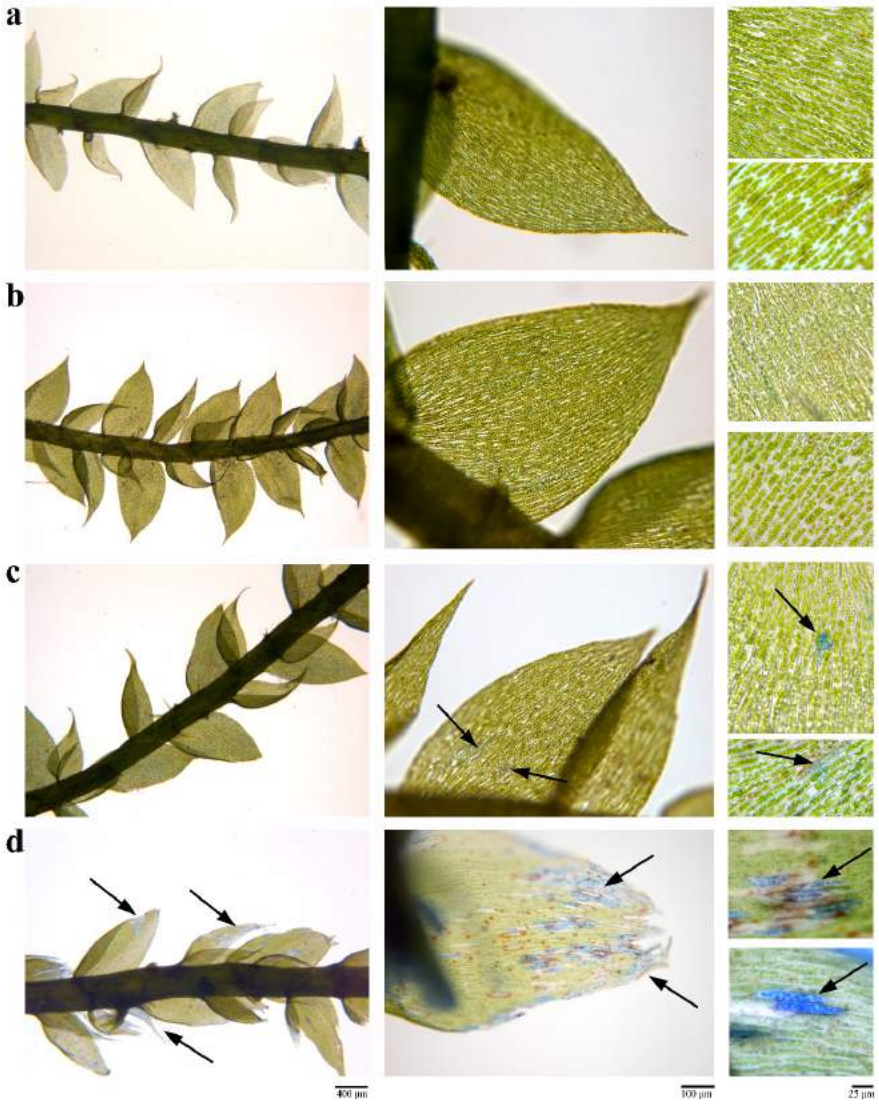

Figure 5. Evans Blue staining (2h-treatment) of *L. riparium* gametophytes. **(a)** controls; **(b)** exposed to 36 mM Cd for 7 days; **(c)** exposed to 360 mM Cd for 7 days; **(d)** exposed to 100% ethanol for 1 h (positive controls). Arrows indicate cytohistological damage.

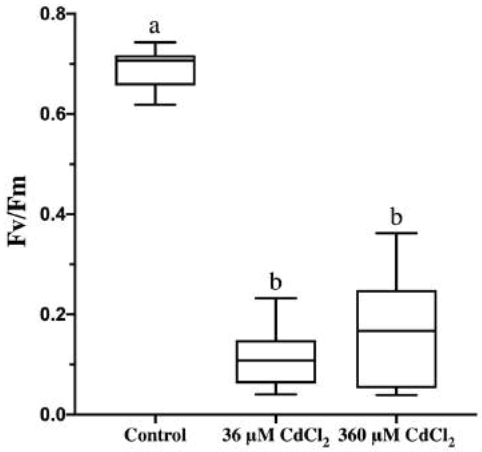

Figure 6. Photochemical efficiency (Fv/Fm) of *L. riparium* from control and Cd-exposed gametophytes for 7 days. Values are given by nine replicate measurements *per* treatment, and expressed as mean ± SE; bars not accompanied by the same letter are significantly different at $p < 0.05$.

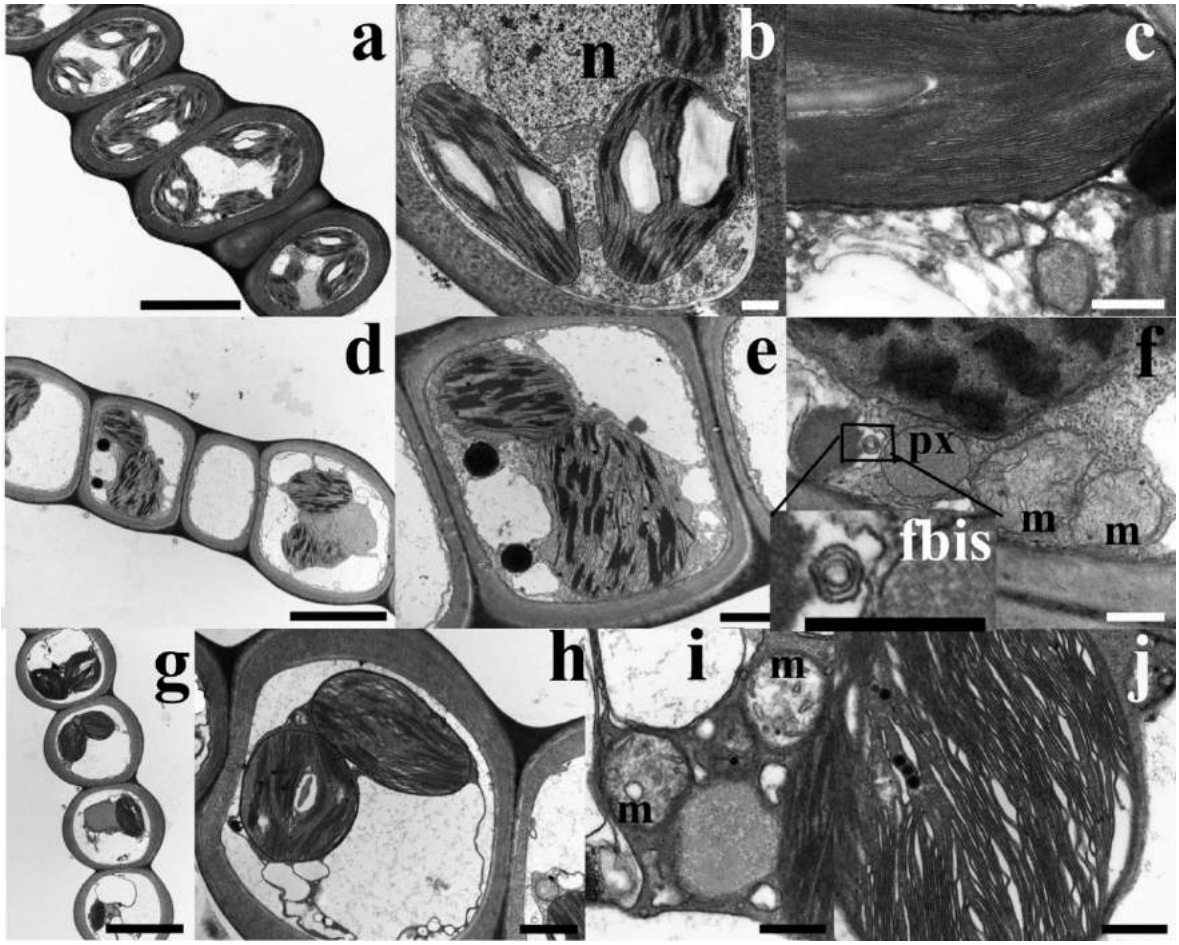

Figure 7. TEM micrographs of *L. riparium* gametophyte (phylloid) cells from samples untreated (control) (a–c) and treated with 36 μM Cd (d-f) and 360 μM Cd (g-j). **(a)** Low-magnification micrograph of a gametophyte section. Each cell is characterized by a thick cell wall, lenticular chloroplasts in the peripheral cytoplasm with grana and intergrana thylakoids and starch grains inside, and a large central and electron-transparent vacuole. **(b)** Detail of a single cell delimited by a thick cell wall. Chloroplasts with grana and intergrana thylakoids and starch grains are visible, as well as a central nucleus (n) containing eu- and heterochromatin. **(c)** Detail of a unswollen chloroplast in which the thylakoids are arranged in tightly packed straight bands. **(d)** Low-magnification micrograph of samples treated with 36 μM Cd revealing an overall cell ultrastructure similar to the controls. **(e)** Micrograph of a single cell with misshaped chloroplasts and well-preserved grana and intergrana thylakoids and vacuoles. **(f)** Micrograph of two mitochondria (m) with a regular morphology, next to a peroxisome (px). (**fbis**) Detail of the area outlined in (**f**) showing a multilamellar body. **(g)** Low-magnification micrograph of samples treated with 360 μM Cd in which plasmolyzed cells delimited by thick cell walls, chloroplasts, and vacuoles are visible. **(h)** Detail of a single cell showing plasmolysis and a vacuolated cytoplasm still containing chloroplasts with grana and intergrana

thylakoids and starch grains. **(i)** Detail of two mitochondria (m) with an electron-clear matrix and swollen cristae. **(j)** Detail of a chloroplast with diffuse thylakoid swelling. Scale bars = 5 μm (a, d, g), 1 μm (b, e, h), and 300 nm (c, f, fbis, i, j).

References

1. Sanità di Toppi, L.; Gabbrielli, R. Response to cadmium in higher plants. *Environ Exp Bot* **1999**, *41*, 105–130.

2. Vassilev, A.; Yordanov, I.; Vangronsveld, J. Cadmium phytoextraction from contaminated soils. **2006**. In: Khan, N.A., Samiullah (Eds.), Cadmium Toxicity and Tolerance in Plants. Narosa Publishers, New Delhi, India, 2006, 35–61.

3. White, P.J.; Brown, P.H. Plant nutrition for sustainable development and global health. *Ann Bot* **2010**, *105*, 1073–1080.

4. Hendry, G. a. F.; Baker, A.J.M.; Ewart, C.F. Cadmium tolerance and toxicity, oxygen radical processes and molecular damage in cadmium-tolerant and cadmium-sensitive clones of *Holcus lanatus* L. *Acta Bot Neerl* **1992**, *41*, 271–281.

5. Somashekaraiah, B.V.; Padmaja, K.; Prasad, A.R.K. Phytotoxicity of cadmium ions on germinating seedlings of mung bean (*Phaseolus vulgaris*): Involvement of lipid peroxides in chlorphyll degradation. *Physiol Plantarum* **1992**, *85*, 85–89.

6. Salin, M.L. Toxic oxygen species and protective systems of the chloroplast. *Physiol Plantarum* **1988**, *72*, 681–689.

7. Yadav, S.K. Heavy metals toxicity in plants: An overview on the role of glutathione and phytochelatins in heavy metal stress tolerance of plants. *S Afr J Bot* **2010**, *76*, 167–179.

8. Küpper, H.; Andresen, E. Mechanisms of metal toxicity in plants. *Metallomics* **2016**, *8*, 269–285.

9. Gallego, S.M.; Pena, L.B.; Barcia, R.A.; Azpilicueta, C.E.; Iannone, M.F.; Rosales, E.P.; Zawoznik, M.S.; Groppa, M.D.; Benavides, M.P. Unravelling cadmium toxicity and tolerance in plants: Insight into regulatory mechanisms. *Environ Exp Bot* **2012**, *83*, 33–46.

10. Adamis, P.D.B.; Gomes, D.S.; Pinto, M.L.C.C.; Panek, A.D.; Eleutherio, E.C.A. The role of glutathione transferases in cadmium stress. *Toxicol Lett* **2004**, *154*, 81–88.

11. Moons, A. *Osgstu3* and *osgtu4*, encoding tau class glutathione S-transferases, are heavy metal- and hypoxic stress-induced and differentially salt stress-responsive in rice roots 1. *FEBS Lett* **2003**, *553*, 427–432.

12. Mohanpuria, P.; Rana, N.K.; Yadav, S.K. Cadmium induced oxidative stress influence on glutathione metabolic genes of *Camellia sinensis* (L.) O. Kuntze. *Environ Toxicol* **2007**, *22*, 368–374.

13. Zhang, C.; Yin, X.; Gao, K.; Ge, Y.; Cheng, W. Non-protein thiols and glutathione S-transferase alleviate Cd stress and reduce root-to-shoot translocation of Cd in rice. *J Plant Nutr Soil Sci* **2013**, *176*, 626–633.

14. Grzam, A.; Tennstedt, P.; Clemens, S.; Hell, R.; Meyer, A.J. Vacuolar sequestration of glutathione S-conjugates outcompetes a possible degradation of the glutathione moiety by phytochelatin synthase. *FEBS Lett* **2006**, *580*, 6384–6390.

15. Rea, P.A.; Li, Z.-S.; Lu, Y.-P.; Drozdowicz, Y.M.; Martinoia, E. From vacuolar GS-X pumps to multispecific ABC transporters. *Annu Rev Plant Physiol* **1998**, *49*, 727–760.

16. Meyer, A.J.; May, M.J.; Fricker, M. Quantitative in vivo measurement of glutathione in Arabidopsis cells: In vivo measurement of glutathione. *Plant J* **2001**, *27*, 67–78.

17. Pasternak, M.; Lim, B.; Wirtz, M.; Hell, R.; Cobbett, C.S.; Meyer, A.J. Restricting glutathione biosynthesis to the cytosol is sufficient for normal plant development. *Plant J* **2008**, *53*, 999–1012.

18. Grill, E.; Winnacker, E.-L.; Zenk, M.H. Phytochelatins: The principal heavy-metal complexing peptides of higher plants. *Science* **1985**, *230*, 674–676.

19. Clemens, S.; Peršoh, D. Multi-tasking phytochelatin synthases. *Plant Sci* **2009**, *177*, 266–271.

20. Loeffler, S.; Hochberger, A.; Grill, E.; Winnacker, E.-L.; Zenk, M.H. Termination of the phytochelatin synthase reaction through sequestration of heavy metals by the reaction product. *FEBS Lett* **1989**, *258*, 42–46.

21. Beck, A.; Lendzian, K.; Oven, M.; Christmann, A.; Grill, E. Phytochelatin synthase catalyzes key step in turnover of glutathione conjugates. *Phytochemistry* **2003**, *62*, 423–431.

22. Blum, R.; Beck, A.; Korte, A.; Stengel, A.; Letzel, T.; Lendzian, K.; Grill, E. Function of phytochelatin synthase in catabolism of glutathione-conjugates: Catabolism of glutathione-conjugates. *Plant J* **2007**, *49*, 740–749.

23. Blum, R.; Meyer, K.C.; Wünschmann, J.; Lendzian, K.J.; Grill, E. Cytosolic action of phytochelatin synthase. *Plant Physiol* **2010**, *153*, 159–169.

24. Vanderpoorten, A.; Goffinet, B. *Introduction to Bryophytes*; Cambridge University Press, 2009; ISBN 978-1-107-37736-3.

25. Qiu, Y.-L.; Li, L.; Wang, B.; Chen, Z.; Knoop, V.; Groth-Malonek, M.; Dombrovska, O.; Lee, J.; Kent, L.; Rest, J.; et al. The deepest divergences in land plants inferred from phylogenomic evidence. *PNAS* **2006**, *103*, 15511–15516.

26. Qiu, Y.-L. Phylogeny and evolution of charophytic algae and land plants. *J Syst Evol* **2008**, *46*, 287–306.

27. Petraglia, A.; De Benedictis, M.; Degola, F.; Pastore, G.; Calcagno, M.; Ruotolo, R.; Mengoni, A.; Sanità di Toppi, L. The capability to synthesize phytochelatins and the presence of constitutive and functional phytochelatin synthases are ancestral (plesiomorphic) characters for basal land plants. *J Exp Bot* **2014**, *65*, 1153–1163.

28. Degola, F.; De Benedictis, M.; Petraglia, A.; Massimi, A.; Fattorini, L.; Sorbo, S.; Basile, A.; Sanità di Toppi, L. A Cd/Fe/Zn-responsive phytochelatin synthase is constitutively present in the ancient liverwort *Lunularia cruciata* (L.) Dumort. *Plant Cell Physiol* **2014**, *55*, 1884–1891.

29. Harmens, H.; Ilyin, I.; Mills, G.; Aboal, J.R.; Alber, R.; Blum, O.; Coşkun, M.; De Temmerman, L.; Fernández, J.Á.; Figueira, R.; et al. Country-specific correlations across Europe between modelled atmospheric cadmium and lead deposition and concentrations in mosses. *Environ Pollut* **2012**, *166*, 1–9.

30. Basile, A.; Sorbo, S.; Conte, B.; Cobianchi, R.C.; Trinchella, F.; Capasso, C.; Carginale, V. Toxicity, accumulation, and removal of heavy metals by three aquatic macrophytes. *Int J Phytoremediat* **2012**, *14*, 374–387.

31. Esposito, S.; Loppi, S.; Monaci, F.; Paoli, L.; Vannini, A.; Sorbo, S.; Maresca, V.; Fusaro, L.; Karam, E.A.; Lentini, M.; et al. In-field and in-vitro study of the moss *Leptodictyum riparium* as bioindicator of toxic metal pollution in the aquatic environment: Ultrastructural damage, oxidative stress and HSP70 induction. *PLOS ONE* **2018**, *13*, e0195717.

32. Maresca, V.; Fusaro, L.; Sorbo, S.; Siciliano, A.; Loppi, S.; Paoli, L.; Monaci, F.; Karam, E.A.; Piscopo, M.; Guida, M.; et al. Functional and structural biomarkers to monitor heavy metal pollution of one of the most contaminated freshwater sites in Southern Europe. *Ecotoxycol Environ Safety* **2018**, *163*, 665–673.

33. Basile, A.; Sorbo, S.; Pisani, T.; Paoli, L.; Munzi, S.; Loppi, S. Bioacumulation and ultrastructural effects of Cd, Cu, Pb and Zn in the moss *Scorpiurum circinatum* (Brid.) Fleisch. & Loeske. *Environ Pollut* **2012**, *166*, 208–211.

34. Esposito, S.; Sorbo, S.; Conte, B.; Basile, A. Effects of heavy Metals on ultrastructure and HSP70S induction in the aquatic moss *Leptodictyum riparium* Hedw. *Int J Phytoremediat* **2012**, *14*, 443–455.

35. Rea, P.A. Phytochelatin synthase: of a protease a peptide polymerase made. *Physiol Plantarum* **2012**, *145*, 154–164.

36. Bleuel, C.; Wesenberg, D.; Meyer, A.J. Degradation of glutathione S-conjugates in *Physcomitrella patens* is initiated by cleavage of glycine. *Plant Cell Physiol* **2011**, *52*, 1153–1161.

37. Bruns, I.; Friese, K.; Markert, B.; Krauss, G.-J. Heavy metal inducible compounds from *Fontinalis antipyretica* reacting with Ellman's reagent are not phytochelatins. *Sci Total Environ* **1999**, *241*, 215–216.

38. Wójcik, M.; Tukiendorf, A. Glutathione in adaptation of *Arabidopsis thaliana* to cadmium stress. *Biol Plant* **2011**, *55*, 125–132.

39. Liu, Y.-J.; Han, X.-M.; Ren, L.-L.; Yang, H.-L.; Zeng, Q.-Y. Functional divergence of the glutathione *S*-transferase supergene family in *Physcomitrella patens* reveals complex patterns of large gene family evolution in land plants. *Plant Physiol* **2013**, *161*, 773–786.

40. Huber, C.; Bartha, B.; Harpaintner, R.; Schröder, P. Metabolism of acetaminophen (paracetamol) in plants—two independent pathways result in the formation of a glutathione and a glucose conjugate. *Environ Sci Pollut Res* **2009**, *16*, 206.

41. Cummins, I.; Dixon, D.P.; Freitag-Pohl, S.; Skipsey, M.; Edwards, R. Multiple roles for plant glutathione transferases in xenobiotic detoxification. *Drug Metab Rev* **2011**, *43*, 266–280.

42. Kumar, S.; Trivedi, P.K. Glutathione S-Transferases: Role in combating abiotic stresses including arsenic detoxification in plants. *Front Plant Sci* **2018**, *9*, 1–9.

43. Grzam, A.; Martin, M.N.; Hell, R.; Meyer, A.J. γ-glutamyl transpeptidase GGT4 initiates vacuolar degradation of glutathione S-conjugates in Arabidopsis. *FEBS Lett* **2007**, *581*, 3131–3138.

44. Ohkama-Ohtsu, N.; Zhao, P.; Xiang, C.; Oliver, D.J. Glutathione conjugates in the vacuole are degraded by γ-glutamyl transpeptidase GGT3 in Arabidopsis. *Plant J* **2007**, *49*, 878–888.

45. French, C.E.; Bell, J.M.L.; Ward, F.B. Diversity and distribution of hemerythrin-like proteins in prokaryotes. *FEMS Microbiol Lett* **2008**, *279*, 131–145.

46. LeBel, C.P.; Ali, S.F.; McKee, M.; Bondy, S.C. Organometal-induced increases in oxygen reactive species: The potential of 2′,7′-dichlorofluorescin diacetate as an index of neurotoxic damage. *Toxicol Appl Pharm* **1990**, *104*, 17–24.

47. Bradford, M.M. A rapid and sensitive method for the quantitation of microgram quantities of protein utilizing the principle of protein-dye binding. *Anal Biochem* **1976**, *72*, 248–254.

48. Habig, W.H.; Jakoby, W.B. Glutathione S-transferases (rat and human). In *Methods in Enzymology*; Detoxication and Drug Metabolism: Conjugation and Related Systems; Academic Press, 1981; Vol. 77, pp. 218–231.

49. Wojas, S.; Clemens, S.; Hennig, J.; Sklodowska, A.; Kopera, E.; Schat, H.; Bal, W.; Antosiewicz, D.M. Overexpression of phytochelatin synthase in tobacco: distinctive effects of *AtPCS1* and *CePCS* genes on plant response to cadmium. *J Exp Bot* **2008**, *59*, 2205–2219.

50. Bellini, E.; Borsò, M.; Betti, C.; Bruno, L.; Andreucci, A.; Ruffini Castiglione, M.; Saba, A.; Sanità di Toppi, L. Characterization and quantification of thiol-peptides in *Arabidopsis thaliana* using combined dilution and high sensitivity HPLC-ESI-MS-MS. *Phytochemistry* **2019**, *164*, 215–222.

51. Ponce de León, I.; Oliver, J.P.; Castro, A.; Gaggero, C.; Bentancor, M.; Vidal, S. *Erwinia carotovora* elicitors and *Botrytis cinerea* activate defense responses in Physcomitrella patens. *BMC Plant Biol* **2007**, *7*, 52.

52. Basile, A.; Cogoni, A.E.; Bassi, P.; Fabrizi, E.; Sorbo, S.; Giordano, S.; Castaldo Cobianchi, R. Accumulation of Pb and Zn in gametophytes and sporophytes of the moss *Funaria hygrometrica* (Funariales). *Ann Bot* **2001**, *87*, 537–543.

Ecotoxicology and Environmental Safety 163 (2018) 665–673

Contents lists available at ScienceDirect

Ecotoxicology and Environmental Safety

journal homepage: www.elsevier.com/locate/ecoenv

Functional and structural biomarkers to monitor heavy metal pollution of one of the most contaminated freshwater sites in Southern Europe

Viviana Maresca[a], Lina Fusaro[b]*, Sergio Sorbo[c], Antonietta Siciliano[a], Stefano Loppi[d], Luca Paoli[d], Fabrizio Monaci[d], Elham Asadi karam[e], Marina Piscopo[a], Marco Guida[a], Emilia Galdiero[a], Marilena Insolvibile[f], Adriana Basile[a]*

[a] Dipartimento di Biologia, University of Naples Federico II, Complesso Univ. Monte Sant'Angelo, Via Cinthia 4, 80126 Napoli, Italy.

[b] Sapienza University of Rome, Department of Environmental Biology, P.le Aldo Moro 5 – 00185 Rome, Italy

[c] Ce.S.M.A, Section of Microscopy, University of Naples Federico II, Complesso Univ. Monte Sant'Angelo, Via Cinthia 4, 80126 Napoli, Italy

[d] Dipartimento di Scienze della Vita, University of Siena, via Mattioli 4, 53100 Siena, Italy

[e] Biology Department, Shahid Bahonar University of Kerman, Kerman, Iran

[f] Istituto Superiore per la Protezione e la Ricerca Ambientale, Via Vitaliano Brancati, 48 Roma

*Corresponding author. Email: *adbasile@unina.it*

Abstract

This study evaluated the biological effects of highly polluted freshwater environment (Regi Lagni channels, S Italy) on the aquatic moss *Leptodictyum riparium,* exposed in bags at three sites representative of different environmental conditions and characterized by different heavy metal burdens. Bioaccumulation, ultrastructural alterations, Reactive Oxygen Species (ROS) production, antioxidant enzymes activity and DNA damage were assessed. To better evaluate the biological response of the moss species to heavy metals, the same biological parameters

were assessed also in *L. riparium* samples cultured *in vitro* using metal mixtures at the same concentrations as measured at the 3 field exposure sites. Heavy metals were accumulated into the moss tissues causing severe ultra-structural damages at higher concentration case studies, and the ROS production as well as the activity of the enzyme followed a concentration-dependent increase. However, the DNA damage trend suggested a threshold effect that changed between field and in vitro experiment. The enrichment factor suggests that the concentration in the most polluted site is close to the upper limit of *L. riparium* to accumulate metals. Overall, combining measures of the morpho-functional traits at different level contribute to improving the knowledge about the tolerance of *L. riparium* to heavy metal stress, suggesting that this moss could be suitable for biomonitoring activity in field conditions.

Highlights

- Metal accumulation, ultrastructural damage, ROS production DNA damage were related to pollution in the highly contaminated Regi Lagni Channels.
- The biological effects were related to the toxic metal concentrations by both in the field and *in vitro* experiments.
- Comparing the oxidative pressure and DNA damages in the field and *in vitro* experiments highlighted a threshold-effect linked to moss resistance and biavailability of heavy metals.
- *L. riparium* was proposed as a model organism in biomonitoring projects also in extreme polluted situations.
- COMET as promising biomarkers of metal toxicity.

Keywords: Biomonitoring, *Leptodictyum riparium*, heavy metal pollution, biomarkers, oxidative stress, ultrastructure damage, DNA damages

Acknowledgements: This study was supported by the following grants: Sapienza Ateneo Research Project 2016 (Prot.No. RM116154C9CFDE3B).

1. Introduction

The Domizio-Flegreo Litoral (Campania Region, Southern Italy) and the nearby inner countryside, known as Agro Aversano, both including the Regi Lagni basin, have been declared as a National Concern Site (NCS) by the Italian Government, because of its huge contamination potential. The Regi Lagni channels are the product of a drainage and canalization work of the ancient Clanius River, acted by the Bourbons in the early 1600s. Since then, the areas surrounding the river have no longer been plagued by flooding, which previously affected the nearby territory. The Regi Lagni consists of a network of straight channels that, collecting meteoric, spring and also waste waters, carry them from the plain north of Naples to the Tyrrhenian Sea, covering a length of about 56 km (di Martino, 2014). Nowadays the Regi Lagni channels are in a completely careless condition and are affected by severe contamination caused by heavy urbanization and industrialization (mainly chemical industry) as well as intensive agriculture and buffalo farms (di Martino, 2014; Grezzi et al., 2011; Bove et al., 2011). In addition, their catchment area also includes the notorious "land of fires" and the "triangle of death", sadly known for the illegal waste dumping and the soot fallout from their uncontrolled burning causing harmful contamination of the groundwater and soil. This heavy pollution has been causing since a long time a strong impact on the health of the local population, with a significant increase in cerebrum-vascular diseases, lymphoma and cancers (Senior and Mazza, 2004). The district of Acerra (Naples, Southern Italy), one of the vertices of the "Italian triangle of death", emerged as plagued by severe air pollution caused by toxic metals, as shown by biomonitoring studies using mosses and lichens (Sorbo et al., 2008; Basile et al. 2008, 2009; 2012).

Depending on their chemical form and bioavailability, it is well-known that toxic metals affect plants, inducing different kinds and extents of damage, impairing anatomy, ultrastructure and molecules and adversely affecting their physiology and biochemistry (Nagajyoti et al. 2010). Ultrastructure damage in plants is a marker closely related to metal pollution (Barceló and Poschenrieder, 2004; Basile et al., 2015). Previous works demonstrated that *Bryophyta* developed ultrastructural changes in relation to metal pollution extent (Basile et al., 2011, 2012; Esposito et al. 2012; Basile et al., 2013). Furthermore, toxic metals lead to overproduction of Reactive Oxygen Species (ROS) in plants. This can trigger redox-sensitive pathways that lead to different alterations, such as protein carbonylation, DNA damage, activation of kinase cascades and transcription factors, which ultimately affect cellular essential metabolic activities and viability (Demidchik, 2015; Shahid et al., 2014). In particular, studies have shown that DNA damage measured in plants using the Comet assay is a good tool for the assessment of genotoxicity of polluted environment (Gichner et al., 2009; Al Khateeb, 2018; Nanda and Agrawal, 2018), detecting DNA single strand breaks and alkali-labile damage in individual cells (Gedik et al., 1992; Singh et al., 1988). Thus using the parameters obtained from Comet assay would allow implementing the intervention strategies to prevent or reduce the deleterious health effects in the sentinel species, as well as in humans. Indeed, assessment of environmental risk requires indicator organisms that quantitatively and qualitatively score the damage and have the capacity to counteract the oxidative pressure caused by heavy metals. To do this, plants have an efficient system of enzymatic and non-enzymatic antioxidants that work in synergy for scavenging the ROS in different compartments inside plant cells (Das and Roychoudhury, 2014). Among these enzymes,

superoxide dismutase (SOD) is the first line of defence against ROS, dismutating O^{2-} oxygen molecule and H_2O_2. Another enzyme is catalase (CAT) that breaks H_2O_2 to water and oxygen while peroxidase (POX) scavenges H_2O_2 in chloroplast and cytosol of plant cells. Glutathione S-transferase (GST) belongs to the family of detoxifying enzymes able to catalyse reactions of binding xenobiotics with GSH. GST plays an important role concerning the neutralization of lipid hydroperoxides generated by heavy metals exposure (Kaaya et al., 1999). Frame the changes in the intracellular redox state though these indicators (Inupakutika et al. 2016; Nath et al. 2016) could help to screen which species are able to accumulate and tolerate a large amount of metals, thus being suitable for biomonitoring and phytoremediation studies.

In previous studies *Leptodictyum riparium* (Hedw.) Warnst, an aquatic moss, showed a higher bioconcentration factor when exposed *in vitro* to Cu, Zn and Pb compared to two higher plants, *Lemna minor* and *Elodea Canadensis*, which are commonly used in bioindication and phytoremediation projects (Basile et al., 2012).

The aim of this study is to examine the effects that heavy metals can have on functional traits of the already proven *in vitro* bioaccumulator, *L. riparium* (Whitton et al., 1981; Basile et al.2011, 2012; Esposito et al. 2012). Moreover, the combination of experiments in the field and *in vitro* can allow evaluating if *L. riparium* could be a suitable bioindicator and could be used for phytoremediation in highly contaminated sites.

2. Materials and Methods

2.1. Plant material

Samples of *L. riparium* were collected from a tap water-filled basin in the Botanical Gardens of the University of Naples “Federico II,” Italy. These samples were used for both the field and *in vitro* experiments. The elemental analysis of initial mosses were performed and the results were reported in the Supplemetary Materials (SM 1).

2.2. Field experiment

After collection, homogeneous samples of *L. riparium* (ca. 2 g fw), were washed with deionized water and placed into >49 mm^2 – meshed nylon bags, as recommended by Kelly et al. (1987). Six bags were exposed for one week during July 2015 at a water depth of 25 cm in the Regi Lagni channels. The following three sites, characterized by different environmental conditions, were chosen for the moss bag experiment: Avella (Site 1, S_1) [40°57'48.5"N 14°35'36.9"E], Acerra (Site 2, S_2) 40°56'00.5"N 14°22'56.3"E] and Castel Volturno (Site 3, S_3) [40°59'01.8"N 13°58'10.3"E]. The selected sites represent three idealized territorial units: Avella (S_1), the control site, is upstream of pollution sources; Acerra (S_2) and Castel Volturno (S_3) are representative of the two most polluted areas of the area: the "triangle of death" and the "land of fires", respectively. The samples from the six bags exposed in each site, were pulled together the analysis described hereafter were carried out on three subsamples. At each site, three water samples were collected on the day of exposure and the day of retrieval of moss samples for subsequent heavy metal analysis. Physical and chemical properties of the

water in the three sites were provided by the national environmental agency are reported in the supplementary materials (SM 2).

2.3. In vitro experiment

The samples collected at the Botanical Gardens, washed with deionized water, were cultured in Petri dishes (10 cm diameter), 20 specimens per dish, using sterile modified Mohr medium, pH 7.5, (Esposito et al. 2012) and in the same medium with the addition of the metal salts. The cultures were maintained for 7 days in a climatic room and the environmental parameters were set according to the environmental conditions registered in the field. In particular: air temperature was maintained at 20 ± 1.5 ◦C, and 13 ± 1.3 ◦C, mean ± SD, during day and night, respectively; relative humidity was 70 ± 4% mean ± SD, 16 hours light (Photosynthetic Active Radiation 400 $\mu molm^2s^{-1}$)/8 hours dark photoperiod. These environmental parameters were chosen according to the period of the year, to obtain similar conditions between field and *in vitro* experiments. The samples were treated with heavy metals (Cd, Cu, Pb, Zn) adding to the medium the metals as soluble salts: $CdCl_2$, $CuSO_4$, $Pb(CH_3COO)_2$, and $ZnCl_2$ with the relative anions as K salts in control solutions. The heavy metals concentration administered to the *in vitro* cultured samples were the same as found in the three field sites, hereafter named as:

- C_1, for in vitro exposure using S_1 metals concentration;
- C_2, for in vitro exposure using S_2 metals concentration;
- C_3, for in vitro exposure using S_3 metals concentration.

The in vitro cultures were performed in triplicate and repeated three times. At each time, the moss exposed to the same concentration of heavy metals were pulled together and the analysis described hereafter were carried out on three subsamples.

2.4. *Analytical determination of metal in water samples and in moss*

Heavy metals were determinate in both water samples (from field experiment) and moss (field and *in vitro* experiment). The water samples collected in the field experimental sites were filtered through Whatman paper (no. 42) and analyzed by ICP-MS (Perkin-Elmer Sciex 6100) for the concentration of selected heavy metals: Cd, Cu, Pb, Zn. Analytical quality was checked by analysing the Standard Reference Material SRM 1463d 'river water'. The precision of analysis was estimated by the coefficient of variation of 3 replicates and was found to be <10% for all elements.

After both the field and *in vitro* experiments, apical leaflets (2 cm), were collected and then dried to constant weight at 40°C and then frozen in liquid nitrogen, pulverized and homogenized with a ceramic mortar and pestle.

About 300 mg of moss powder was mineralized with a mixture of 6 mL of 70% HNO_3, 0.2 mL of 60% HF and 1 mL of 30% H_2O_2 (ultra-pure reagent grade). Digestion of samples was carried out in a microwave digestion system (Milestone Ethos 900) for a total time of 30 min. Concentrations of selected toxic metals (Cd, Cu, Pb, Zn), expressed on a dry weight basis, were determined by ICP-MS (Perkin-Elmer Sciex 6100). Analytical quality was checked by analysing the Certified Reference Material BCR 61 "aquatic moss" (*Platyhypnidium*

riparioides, Hedw.) with a recovery percentage of 84%. The Precision of analysis was estimated by the coefficient of variation of 3 replicates and was found to be <10% for all elements. For both experiments, Enrichment Factor (EF) was calculated as the ratio between of the metal in the plant (mg g^{-1}) to the metal in the water (µg L^{-1}) (Ahmad et al., 2014).

2.5. Ultrastructural observations

Subapical leaflets, collected about 5 mm below the apex, were observed under TEM microscopy. Specimens were fixed in 3% glutaraldehyde in phosphate buffer solution (pH 7.2–7.4) for 2 h at room temperature and post-fixed with buffered 1% OsO_4 for 1.5 h at room temperature, dehydrated with ethanol up to propylene oxide and embedded in Spurr's epoxy medium (Basile et al., 2001). Ultra-thin (40 nm thick) sections were put on 300-mesh copper grids, then stained with Uranyl Replacement Stain UAR (Electron Microscopy Science) and lead citrate and observed under a Philips EM 208S TEM (Basile et al., 2001). 54 specimens (18 samples from each site; each set made up of 3 specimens in triplicate collected from different dishes) were observed.

2.6. Detection of ROS

A fluorescent technique using 2',7'-dichlorofluorescin diacetate (H2DCFDA) has been used for quantitative measurement of ROS production. H2DCFDA is de-esterified intracellularly and turns to nonfluorescent 2',7'-dichlorofluorescin (DCFH). DCFH is then oxidized by ROS to highly fluorescent 2′,7′-dichlorofluorescein (DCF) (LeBel et al 1990).

Homogenates were transferred to a 96- well plate, incubated with 5 μM H2DCFDA for 30 min at 37 ±1°C and analyzed using a with an automatic plate reader. ROS quantity was monitored by fluorescence (excitation wavelength of 350 nm and an emission wavelength of 600 nm).

2.7. Response to oxidative stress

One gram of plant material was ground with 1 mL of chilled NaH_2PO_4/ Na_2HPO_4 buffer (PBS, 50 mM, pH 7.8) containing 0.1 mM ethylenediaminetetraacetic acid (EDTA) and 1% polyvinylpyrrolidone (PVP). The homogenate was centrifuged at 12,000 g for 30 min, and the supernatant (enzyme extraction) was collected for protein assay and the determination of SOD, CAT, GST and PEROX activities. Protein concentration was quantified spectrophotometrically at 595 nm according to the Bradford method with bovine serum albumin (BSA) as the standard (Bradford, 1976).

CAT activities were calculated and expressed as a decrease in absorbance at 240 nm due to H_2O_2 consumption using a commercial kit (Sigma-Aldrich Co., St Louis, MO, USA) and according to the manufacturer's protocol. Superoxide dismutase (SOD, EC 1.15.1.1) activity was spectrophotometrically determined at 450 nm with a commercial kit (19160, Sigma). The assay utilizes a water-soluble tetrazolium salt that produces a formazan dye after reduction by the superoxide ($\bullet O_2^-$) radical. The rate of reduction with $\bullet O_2^-$ is linearly related to xanthine oxidase activity, which is inhibited by SOD. The result is compared with a standard curve of SOD. One unit of SOD activity is defined as the amount of enzyme that inhibits in 50 % of

the reduction of $\bullet O_2^-$ per minute at 25 °C and pH 7. Glutathione S-transferase (GST, EC 2.5.1.18) activity was measured using a commercial kit (CS0410, Sigma). The conjugation of GSH to 1-chloro-2,4-dinitrobenzene (CDNB) catalyzed by GST was monitored at 340 nm for 4 min. The reaction mixture contained 4 µL of extract and 196 µL of reaction solution (200 mM GSH and 100 mM CDNB in Dulbecco's buffer at pH 7). The activity was calculated with $\varepsilon = 9.6\ mM^{-1}\ cm^{-1}$ (Habig and Jakoby 1981). A GST unit is defined as the amount of enzyme that catalyzes the formation of 1 µmol of the GS-DNB conjugate per minute at 25 °C and pH 7.

Assay kits for Peroxidase Activity (Product No. MAK092) were purchased from Sigma–Aldrich (Castile Hill, NSW, Australia). The fluorometric peroxidase activity assay measures the reaction between hydrogen peroxide (H_2O_2) and the Fluorescent Peroxidase chemical probe (Product No. MAK092B), which is catalyzed by the presence of peroxidase in the sample (measured at $\lambda ex = 535/\lambda em = 585$ nm).

2.8. Comet assay

The protocol was performed according to Gichner et al. 2004 with some modifications. All operations were conducted under inactinic red light to avoid light-induced damage. After plant treatment, the excised organs (around 150mg) were placed in a 60-mm petri dish kept on ice and spread with 1.5mL of cold 400mM Tris buffer, pH 7.5. Plants have a cell wall that cannot be removed by a lysing step as used in the Comet assay protocol for animal and human cells to remove the cell membrane and to denature proteins. The nuclei for the plant cellular and

acellular Comet assay have to be isolated mechanically (Gichner et al., 1998). The material plant was gently sliced using a fresh razor blade. The plate was kept tilted on ice so that the isolated nuclei would collect in the buffer. A nuclear suspension (500 µl) and 1% low melting point (LMP) agarose (500 µl) prepared with PBS were added at 37°C. The nuclei and the LMP agarose were gently mixed and 80 µL aliquots placed on microscope slides which were pre-coated with 1% normal melting point (NMP) agarose. The drops were then recovered with a coverslip and the slides were placed on ice for 5 min. Then, the coverslips were removed and the slides were placed in a horizontal gel electrophoresis tank containing freshly prepared cold electrophoresis buffer (1 mM Na2EDTA and 300 mM NaOH, pH > 13). The nuclei were incubated for 15 min to allow the DNA to unwind prior to electrophoresis at 0.72 V/cm (26 V, 300 mA) for 5 min at 4°C. Finally, the slides were gently washed twice in a neutralization buffer (Tris–HCl 0.4 M, pH 7.5) for 5 min to remove alkali and detergent, and stained with 50 mL/mL DAPI (3 h).

A fluorescence microscope was used to examine the slides, analyzing a minimum of 50 randomly selected nuclei from each slide and avoiding overlapping figures. A computerized image-analysis system (CometScore) was employed. Twenty-five nuclei were scored per slide, three slides were evaluated per treatment and each treatment was repeated at least twice. From the repeated experiments, DNA damages, Tail moment and olive moment from each slide were calculated.

2.9. Statistical analysis

One-way ANOVA was applied for analysing the differences:

- among sites (S_1, S_2 and S_3) in the field experiment in terms of heavy metals concentration in the water as well as metals concentration, ROS production, functional traits such as anti-oxidant activity and DNA damage;
- among the concentration *in vitro* in terms of metals concentration, ROS production, functional traits such as anti-oxidant activity and DNA damage.

Two-way ANOVA was applied to indentify differences in the enrichment factor attributable to metals concentration in the water (X_1, X_2, X_3) and to the field and in vitro experiments. The assumptions of normality (the Kolmogorov–Smirnov test) and homogeneity of variances (Levene test) were tested and when necessary, the data were log-transformed.

The significance of differences was estimated using the post-hoc Student–Newman–Keuls test at $P < 0.05$. Data were analysed using the software Statistica, version 7.0 (StatSoft, Tulsa OK, USA).

3. Results

3.1. Heavy metals in water samples

The concentration of heavy metals in water samples (Table 1) varied greatly according to the sampling site, with the control site of Avella (S_1), showed the lowest concentrations, whereas the site of Castel Volturno (S_3) showed the highest concentration for all heavy metals investigated. Concentration at S_1 was within the Italian legal limit established for Pb (10 □g l^{-1}), but at S_2 and S_3 values were markedly above to these thresholds. At site S_3 concentrations of Cd and Zn were exceptionally high. The concentrations detected in the three sites were used in the water for the *in vitro* experiments ($S_1 = C_1$; $S_2 = C_2$; $S_3 = C_3$).

3.2. Concentration and bioaccumulation factor of heavy metals

The concentration of heavy metals (Table 2) significantly differed between the three sites following a general pattern: $S_1 < S_2 < S_3$ for all over the considered heavy metals. Likewise for the *in vitro* experiment the concentration pattern was $C_1 < C_2 < C_3$.

In the field experiment, the EF of Cu (Fig. 1a) reached the highest value in S_2, at the intermediate concentration of metals, whereas the lower EF occurred in S_3, where the highest metals concentration were detected. In the *in vitro* conditions EF decreased when metals concentration increased ($C_1 > C_2 \approx C_3$). Looking at the differences between in field and *in vitro* experiment, for the lower and the intermediate metals concentration the *in vitro* experiment had the higher EF values ($C_1 > S_1$; $C_2 > S_2$) whereas the EF of S_3 and C_3 did not show differences. For both Zn (Fig. 1b) and Cd (Fig. 1c), EF showed the same general pattern: as the metals

concentration increase, EF decreased in both field and *in vitro* experiments (S_1>S_2>S_3; C_1>C_2>C_3). For each level of metals concentration, the *in vitro* EF was higher relative to the field. In the field experiment the EF of Pb (Fig. 1d) decreased from S_2 to S_1, whereas the S_3 presented an intermediate EF. On the other hand, *in vitro* experiment the EF decreased as metals concentration increased (C_1>C_2>C_3). Looking at the differences between in field and *in vitro*, we highlighted that in the latter conditions the EF was tendentiously lower in respect to what found in the field experiment, even if S_3 and C_1 showed no significant differences.

It is interesting to notice that EF values between in field and in vitro are approximately equivalent, except for C_1 that for Cu, Zn and Cd reached values that are about twice those found in S_1.

3.3. Ultrastructure observations

3.3.1. Field experiment

Moss samples in field exposed at site Avella (Fig. 2. a-c), those in vitro C_1 (Fig. 3 a-c) and the unexposed specimens collected from the Botanical Gardens showed the same appearance (images not shown). The leaflet cells, surrounded by thick cell walls, contained lenticular chloroplasts beneath the cell wall. The protoplast is occupied in the middle by a large, clear, vacuole. The thylakoid system appeared well developed, arranged as grana and intergrana thylakoids extending along the main axis of the organelle (Fig. 2 b-c; Fig. 3 b). Starch grains and rare plastoglobules were also visible in the stroma. Mitochondria with electron dense matrix and clear cristae showed a typical appearance (Fig. 2. c; Fig. 3 c).

In comparison to the previous, samples in field exposed at the S_1 and S_3 appeared heavily changed, those from site S_3 being the most altered. After exposure at S_1, the leaflet cells appeared plasmolysed and chloroplasts were well recognizable in the protoplast (Fig. 2. d). The chloroplasts were swollen and showed dilated thylakoids (Fig. 2. e, f). Nuclei occurred as remnant structures (Fig. 2.e). Mitochondria are severely impaired and no clear cristae are still visible (Fig. 2. f).

In the samples exposed at site S_3, the cells contained few chloroplasts with respect to those exposed at site S_1 (Fig. 2. g). Those organelles appeared misshaped and the thylakoid system, and its typical arrangement in grana and intergrana membranes, is not yet discernible (Fig. 2. h-i). Site Avella (S_1). (a) The leaflet cross section shows thick walled cells with lenticular chloroplasts containing grana and starch grains. (b) A typical cell with a thick wall and chloroplasts featuring grana and intergrana membranes and starch grains. (c) A typical mitochondrion (m) with cristae is located between two chloroplasts.

Site Acerra (S_2). (d) The leaflet cross section shows plasmolysed cells with chloroplasts. (e) The plasmolysed cell contains swollen chloroplasts with dilated thylakoids. Remnants of a nucleus (n) are visible. (f) Remnants of two mitochondria (asterisks) next to a chloroplast with dilated thylakoids (arrows).

Site Castel Volturno (S_3). (g) The leaflet cross section shows the impaired protoplasts with only a few severely changed chloroplasts. (h) The cell contains severely altered chloroplasts. (i) A heavily modified chloroplast where the typical arrangement of the thylakoid system is no more visible.

Scala bars: 5 μ (a, d, g), 1 μ (b, e, h), 500 nm (i), 300 nm (c, f)

3.3.2. *In vitro* experiment

TEM observations of the samples cultured *in vitro* are consistent with the data from the field exposure. Those cultured in the C_1 mixture showed features comparable with the site Avella-exposed samples, with a regular appearance (Fig. 3 a-c). Differently, those cultured with the C_2 and C_3 mixtures showed changes similar to the corresponding field exposed ones (Fig. 3. d-f, g-i). The appearance of the specimens from the C_3 mixture is worse than those from the C_2 mixture, consistently with the field data.

3.4. Detection of ROS and activity of antioxidant enzymes

In the field experiment, the amount of ROS (Table 3) significantly changed among the sites and S_1 presented the lower value. The antioxidant activity expressed by SOD was comparable between S_1 and S_2 although the heavy metals concentration was higher in the latter site. CAT, GST and POX activity increased gradually following heavy metals concentration found in the water of the three sites ($S_1 < S_2 < S_3$, table 1). Looking at the results acquired during the *in vitro* experiment, the amount of ROS and the antioxidants activity followed the same pattern: $C_1 < C_2 < C_3$, except for CAT where C_2 presented higher value relative to C_3.

3.5. Comet assay

In field experiment, the DNA damage detected by comet assay (Table 4, SM 3), significantly increased in S_3 site, whereas no differences were detected between S_1 and S_2.

The results obtained from *in vitro* experiment showed that the % DNA damage, Tail and olive Moment are lower in C_1 concentration (equivalent to the heavy metals concentration detected in S_1 site) increasing in C_2 and C_3. In particular, no differences were detected between C_2 and C_3 for the % DNA damage and olive Moment whereas the tail moment presented a gradual increase from C_1 to C_3.

4. Discussion

The goodness of moss *L. riparium* as bioaccumulator of heavy metals, was tested combining field and *in vitro* experiments, verifying its tolerance through several structural and functional indicators. Compared with values reported for aquatic mosses from unpolluted or lightly polluted rivers (Gecheva et al., 2011; Siebert et al., 1996; Cesa et al., 2015), heavy metal concentrations measured in moss bags were already high at the control site S_1. Accumulation of toxic metals in the moss was notably different among sites, and the highest concentrations were reached at the most polluted sites, reflecting the metal content found in water samples. However, the bioavailability of metals could be different between experimental conditions as suggested by the EF that is generally higher *in vitro* relative to the field conditions. Moreover, the general pattern of EF was $X_1>X_2>X_3$, but in the field experiment this trend is present only for Zn and Cd. For Cu and Pb, EF varied without a fixed trend suggesting that for these two metals the site-specific conditions are the important drivers of bioaccumulation process (Dixit et al., 2015). Given the very high concentration of metals found in the field conditions, we can claim that *L. riparium* can proficiently accumulate the toxic compounds in its tissue (Basile et al., 2015). However, the EF of S_3 and C_3 were the lowest for all the considered metals, highlighting that the concentration of heavy metals found in the S_3 and used for built the *in vitro* experiment C_3, reaches values close to the upper limit of these species for accumulation. This is confirmed by the damages detected at both structural and functional level. Indeed, TEM observations showed that the samples exposed at the control site S_1 and the corresponding *in vitro* cultured ones have a regular appearance, with no signs of ultrastructure

damage. Compared with these samples, ultrastructural changes were evident at S_2 and S_3 and at the corresponding *in vitro* cultured ones. These results are consistent with the effects registered in terms of ROS production and comet assays tests related parameters.

The main ultrastructural changes occurred in the chloroplasts and mitochondria. In the samples exposed at the site S_2 and cultured in the corresponding metal mixture C_2, quite a few thylakoids appeared clearly dilated. Furthermore, also mitochondria appeared severely modified, with loss of cristae, and the shrinkage of the whole protoplast, known as plasmolysis, was also found. In the S_3-exposed and mixture C_3-cultured samples, the chloroplasts lost the typical arrangement of the thylakoid system, which is even not yet recognizable.

Swelling of organelle and plasmolysis in the plants are morphological hallmarks suggesting an incoming cell death caused by injury, which some Authors call necrosis (Van Doorn et al., 2011). By the way, chloroplasts, and mitochondria, are well-known targets of the toxic effect of heavy metals in plants and even in the moss *L. riparium* itself (Basile et al., 2012; Esposito et al., 2012). The structural damages can be directly ascribed to the overproduction of ROS, which eventually leads to lipid peroxidation in cell membranes (Blokhina et al., 2003; Farmer and Mueller, 2013), injury to thylakoids (Blokhina et al., 2003) and acceleration of cells senescence (Prochazkova et al., 2001). ROS even act as signals leading to cell death (Van Breusegem and Dat, 2006), a process that may also be a trigger in our study by toxic environmental conditions and substances (Schwartzman and Cidlowski, 1993; Van Breusegem and Dat, 2006; Van Doorn et al., 2011) (SM 4). Swelling of organelles or the opposite phenomenon, namelyorganelle or cell shrinkage, like plasmolysis, are caused by the loss of control of selective permeability in the membranes, which in turn is well known to

depend either on a direct damage to membrane or secondarily on a cellular energy depletion (Schwartzman and Cidlowski, 1993). Our finding of mitochondria with no cristae, along with plasmolysis and swelling and shrinkage of the organelles, suggests that energy depletion could play a central role in the occurrence of those phenomena. When the control of selective permeability is impaired, as ions move across the membrane along concentration gradients, the accompanying water shifting can cause swelling or shrinkage of organelles, part of them or the whole cell (Schwartzman and Cidlowski, 1993). Beyond structural damages, the evaluation of functional responses it is an important topic in the field of biomarkers, since the evaluation of environmental quality through the usage of suitable indicator organisms, can help to reach a fast and efficient environmental risk assessment (Huggett, 2018).

Both field studies and laboratory experiments have established that aquatic macrophytes (Maine et al., 2001; Fritioff et al., 2005) and mosses (Bruns et al., 1997; Samecka-Cymerman et al., 2002) can take up water contaminants. This ability and the wide distribution of aquatic bryophytes make them suitable organisms for monitoring metal contamination in aquatic environments (Mouvet, 1984).

Different studies have reported total metal contents accumulated by native and transplanted mosses (Siebert et al., 1996; Samecka-Cymerman et al., 2005; Fernandez et al., 2006) or maintained under laboratory conditions (Martins et al., 2004). In some cases, metals were measured both at extracellular and intracellular sites, suggesting possible toxic effects to occur at the cellular level (Vazquez et al., 1999; Fernandez et al., 2006).

However, none of these studies took into account the oxidative pressure exerted by heavy metals on the biomarker as well as their capacity to react. Examine in depth the anti-oxidant

capacity of *L. riparium* may help in clarifying the mechanisms involved in heavy-metal toxicity and/or elucidating the cellular basis of moss tolerance of these compounds. Even if some heavy metals (e.g. Cu, Zn) are essential micronutrients for plants, all may exert toxic effects, including alterations in photosynthetic and respiration processes or inhibition of plant growth (Vazquez et al., 1987; Kimbrough et al., 1999; Aravind and Prasad, 2005) and being a redox-active metals, they can stimulate the formation of ROS (Prasad, 1999; Wu et al., 2009) leading to multiple toxic effects like lipid peroxidation, protein cleavage or DNA damage (Unyayar et al., 2006).

To evaluate the oxidative pressure due to heavy metals and their oxidative effects, we measured ROS generation and antioxidant response both in the field and *in vitro* exposed samples. The low level of ROS production confirms that S_1 can be considered as a control site relative to S_2 and S_3, where ROS production is significantly higher. The obtained results underlined that heavy metals could generate ROS through various biochemical processes that lead to the development of a series of defense mechanisms such as SOD, CAT, GST and POX. It is interesting to notice that in the control site (S_1) the SOD activity is comparable to that found in concentration in vitro C_1, despite of the differences in ROS concentration. We hypothesized that in the field a multi-stress condition insists upregulating the first line of defense (Gill and Tuteja, 2010). In the highest heavy metals concentration (S_3 and C_3 for field and *in vitro* experiment respectively) ROS production was immediately balanced by enzyme activation with an increase of SOD, CAT, GST, and POX. Combing the bioaccumulation data with the biological responses it is interesting to highlight that *L. riparium* showed a clear heavy metal concentration-dependent increase on the response side (anti-oxidant enzymes activity)

in both field and *in vitro* experiment, but considering the damage side (DNA damage detected using comet assay) the results suggest a threshold effect that differed between in field and *in vitro* experiment.

Indeed in field experiment between S_1 and S_2 there were no significant differences for all over the parameters that quantify the DNA damage, despite the presence of heavy metals in the water was markedly higher in S_2. On the other side, the damage was evident in S_3, confirming the high polluted level of this site.

Looking at *in vitro* experiment, we distinguished a different pattern of damage: the C_1, a study case that contains a concentration of heavy metals equivalent to the control site in field condition (S_1), presented the lower damage level whereas no differences were detected between C_2 and C_3.

Despite of the concentration of metals are equivalent between field and in vitro experiment, the discrepancy found relative to the damage level, could be attributed to the bioavailability of the metals, higher in in vitro experiment (Nouri et al., 2011). The combination of field and *in vitro* experiments has highlighted that *L. riparium* can be used as a bioindicator for heavy metals and bioaccumulator, giving the responsiveness and its resistance to heavy metals, and other oxidative stresses that can occur in sites highly contaminated by human activities.

Based on the present results, we can conclude that not only higher, but also lower plants (mosses) can be used as an alternative first-tier assay system for the detection of possible genetic damage resulting from polluted waters. In this experimental work, we confirm the extraordinary sensitivity of the method to unveil the damage in *L. riparium* subject to different degrees of toxic metal pollution. Our results corroborate the fact that the occurrence of an

alarmingly high level of DNA damage in *L. riparium* exposed in site more pollution can be accounted for the presence of high concentration of heavy metals.

Figure and Table

	Water		
	S_1	S_2	S_3
Cu	113.83 ± 3.71^{a}	4743.46 ± 24.41^{b}	10812.52 ± 43.94^{c}
Zn	262.40 ± 11.51^{a}	4260.64 ± 11.02^{b}	396728.84 ± 1633.1^{c}
Cd	27.94 ± 2.60^{a}	1804.90 ± 9.38^{b}	278743.55 ± 685.84^{c}
Pb	7.54 ± 1.18^{a}	35.94 ± 4.50^{b}	943.77 ± 22.53^{c}

Table 1. The concentration of heavy metals (μg l^{-1}) in waters of river measured in the three experimental sites (Avella, S_1; Acerra, S_2; Castel Volturno, S_3). Values are presented as mean ± st. dev; numbers not accompanied by the same letter are significantly different at $P < 0.05$, using the post-hoc Student–Newman–Keuls test. The concentrations found in the water of the three sites in field experiment were used for the *in vitro* experiments ($S_1 = C_1$; $S_2 = C_2$; $S_3 = C_3$).

	Field			***in vitro***		
	S_1	S_2	S_3	C_1	C_2	C_3
Cu	225.87 ± 2.20^{a}	14802.85 ± 149.7^{b}	18307.30 ± 67.33^{c}	862.25 ± 3.22^{a}	12861.44 ± 12.37^{b}	28198.17 ± 89.79^{c}
Zn	2476.87 ± 15.35^{a}	7704.61 ± 5.34^{b}	21347.58 ± 130.6^{c}	9888.55 ± 321.5^{a}	14456.60 ± 258.58^{b}	125643.80 ± 3236.5^{c}
Cd	145.88 ± 2.24^{a}	2724.41 ± 16.18^{b}	13019.02 ± 163.8^{c}	286.66 ± 9.22^{a}	6353.90 ± 80.18^{b}	$109600.61 \pm 1471.98^{c}$
Pb	83.42 ± 1.77^{a}	742.21 ± 16.7^{b}	13723.70 ± 98.55^{c}	103.72 ± 3.47^{a}	271.87 ± 9.63^{b}	824.11 ± 44.41^{c}

Table 2. Concentration of metals (mg g-1) in L. riparium exposed in the field (S1, S2, S3) and in vitro (C1, C2, C3) experiments. Values are presented as mean ± st. dev; values not accompanied by the same letter are significantly different at $P < 0.05$, using the post-hoc Student–Newman–Keuls test.

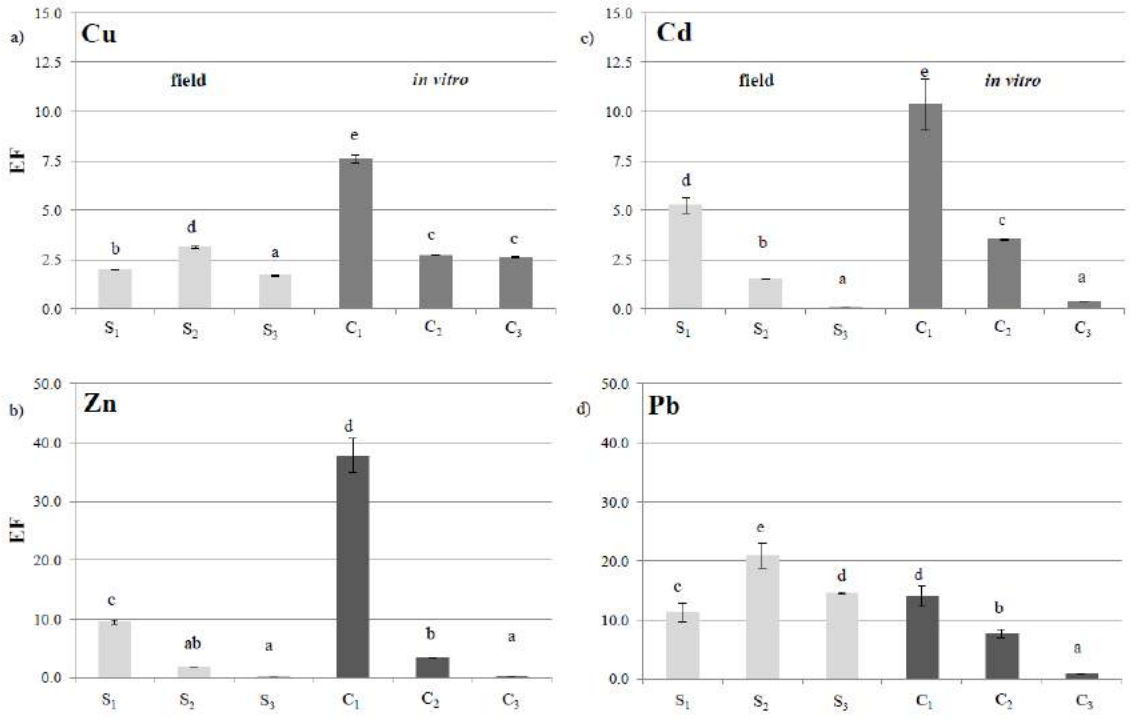

Figure. 1 Enrichment Factor (EF) of heavy metals in the field (light grey) and in vitro (dark grey) experiments. Values are presented as mean ± st. dev; bars not accompanied by the same letter are significantly different at $P < 0.05$, using the post-hoc Student–Newman–Keuls test.

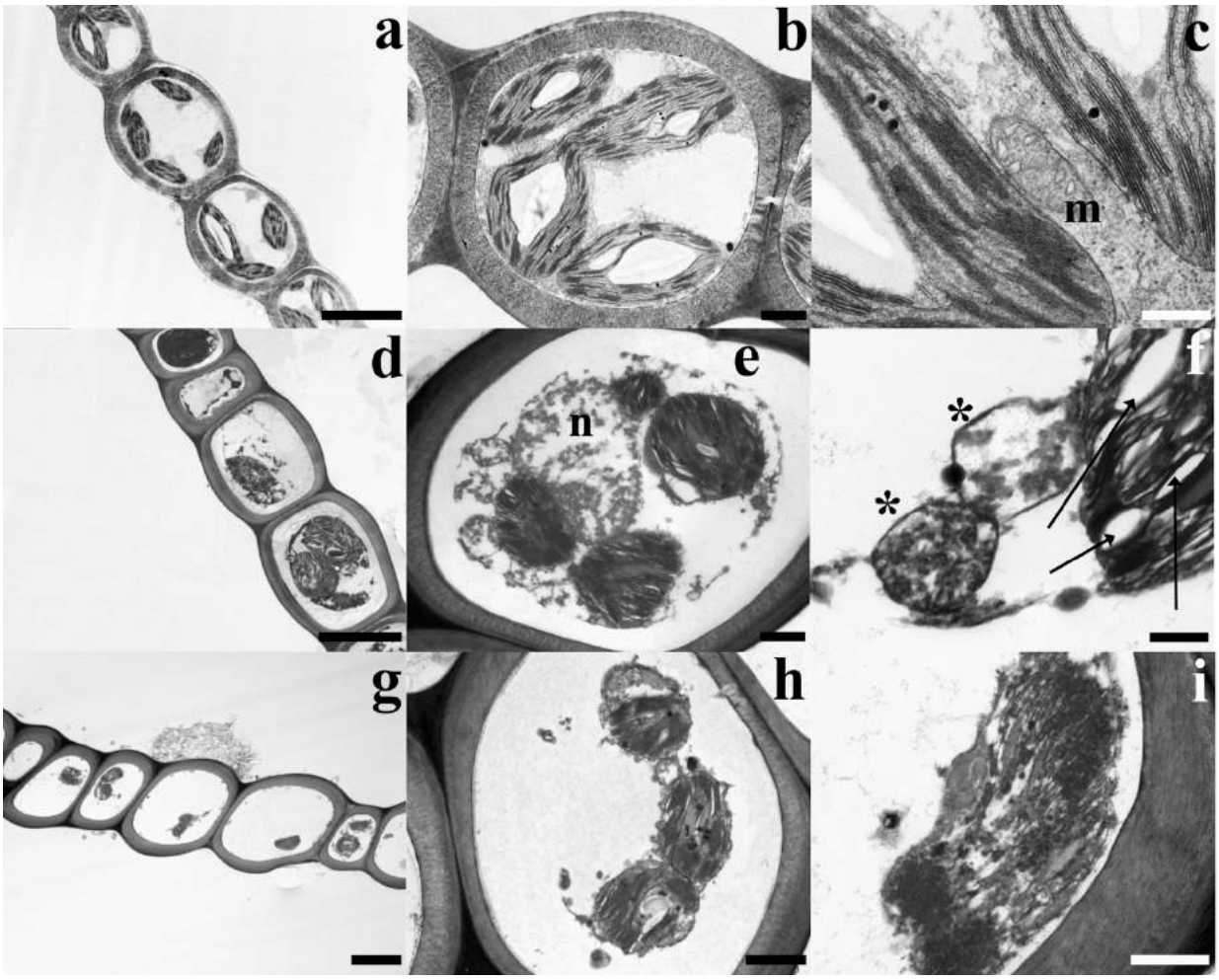

Figure 2. TEM micrographs from leaflets of *L. riparium* specimens in field exposed at the site Avella (a-c), site Acerra (d-f) and site Castel Volturno (g-i).

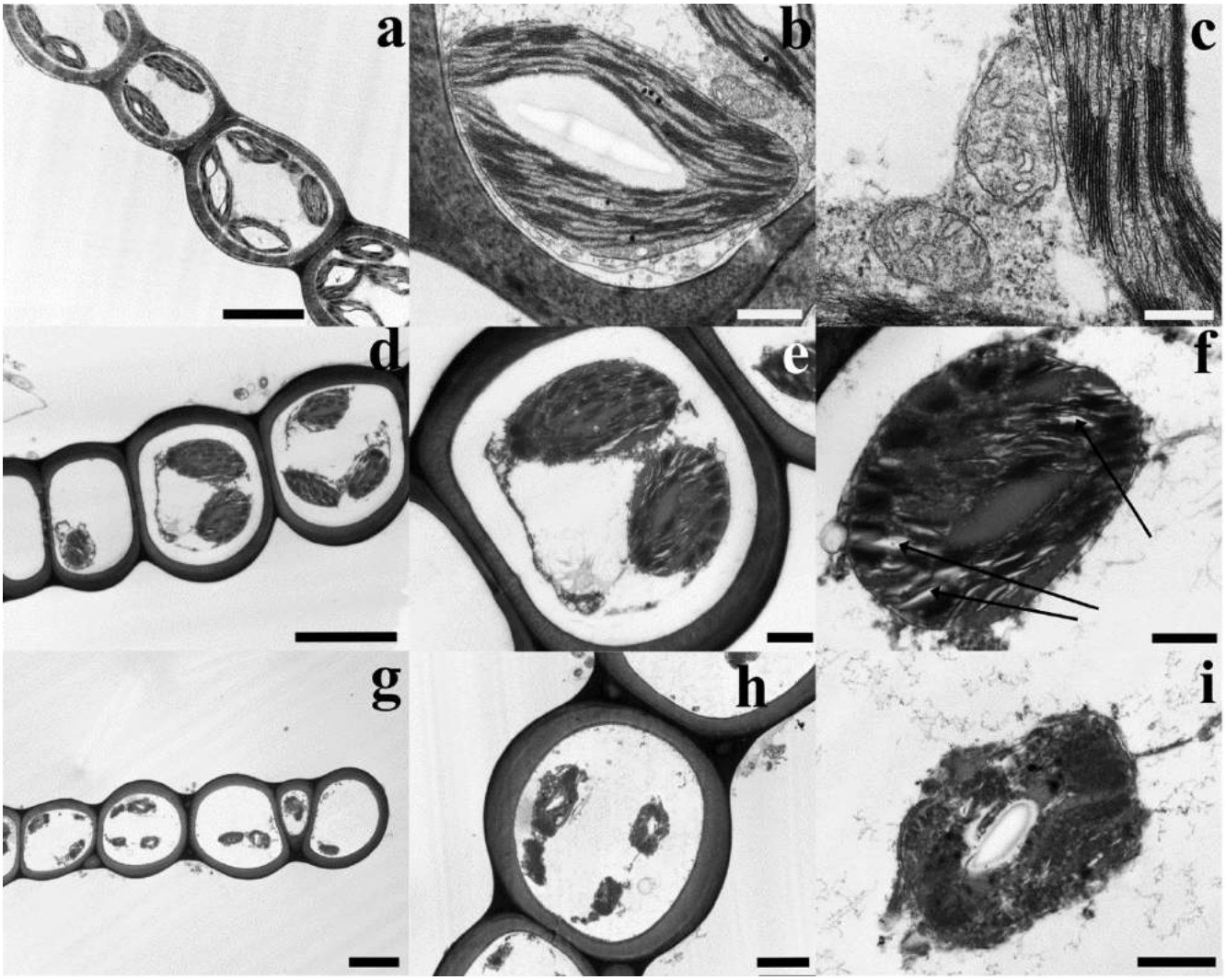

Figure. 3. The figure shows TEM micrographs from leaflets of *L. riparium* specimens *in vitro* cultured in the toxic metal mixture at the same concentrations as in the site Avella (C_1, a-c), site Acerra (C_2, d-f) and site Castel Volturno (C_3, g-i). C_1. (a) In the leaflet cross section typical thick walled cells show lenticular chloroplasts, with grana and starch grains. (b) The chloroplast contains a well-developed thylakoid system, starch grains and rare plastoglobules. (c) Section of mitochondria with cristae. C_2. (d) The leaflet cross section shows plasmolysed cells with chloroplasts. (e) A plasmolysed cell shows altered chloroplasts. (f) A changed chloroplast with dilated thylakoids (arrows). C_3. (g) The leaflet cross section shows severely impaired cells containing heavily changed chloroplasts. (h) A plasmolysed cell with severely altered chloroplasts. (i) A miss-shaped chloroplast. The typical arrangement of the thylakoid system is no more recognizable and a central starch grain is still visible. Scala bars: 5 µ (a, d, g), 2 µ (h), 1 µ (e), 500 nm (b, f, i), 300 nm (c)

Field	Sites	ROS	SOD	CAT	GST	POX
	S_1	60.94 ± 0.97^{a}	26.87 ± 6.73^{a}	12.94 ± 0.67^{a}	1.74 ± 0.33^{a}	0.012 ± 0.001^{a}
	S_2	431.15 ± 46.80^{b}	36.06 ± 4.27^{a}	35.78 ± 6.83^{b}	2.75 ± 0.04^{b}	0.029 ± 0.003^{b}
	S_3	506.72 ± 69.62^{b}	59.23 ± 0.19^{b}	102.99 ± 10.44^{c}	6.55 ± 1.26^{c}	0.122 ± 0.01^{c}
in vitro	**Concentration**					
	C_1	219.71 ± 12.84^{a}	30.65 ± 2.55^{a}	0.95 ± 0.001^{a}	2.43 ± 0.04^{a}	0.03 ± 0.001^{a}
	C_2	673.26 ± 49.14^{b}	47.87 ± 6.98^{b}	44.21 ± 1.80^{c}	6.24 ± 0.05^{b}	0.08 ± 0.005^{b}
	C_3	928.16 ± 57.6^{c}	66.87 ± 0.27^{c}	24.00 ± 2.10^{b}	7.70 ± 0.04^{c}	0.14 ± 0.01^{c}

Table 3. ROS production (fluorescence intensity) and antioxidant responses (SOD, SOD activity inhibition %, CAT, U/mg of protein, GST, umol/ml/min, POX, U/mg of protein) in the field (Avella, S_1; Acerra, S_2; Castel Volturno, S_3) and *in vitro* ($C_{1;}$ $C_{2;}$ C_3) experiments. Values are presented as mean ± st. err; numbers not accompanied by the same letter are significantly different at $P < 0.05$. One-way ANOVA was applied for analysing the differences among sites in field experiment, and among the concentration *in vitro*, followed by the post-hoc Student–Newman–Keuls test.

Field	Sites	% DNA damage	Tail Mom	olive mom
	S_1	4.32 ± 0.52^{a}	1.40 ± 0.19^{a}	1.01 ± 0.12^{a}
	S_2	4.94 ± 1.82^{a}	1.33 ± 1.00^{ab}	1.40 ± 0.20^{a}
	S_3	12.95 ± 0.93^{b}	6.36 ± 0.27^{b}	3.71 ± 0.54^{b}
in vitro	**Concentration**			
	C_1	6.38 ± 0.87^{a}	1.38 ± 0.16^{a}	1.72 ± 0.22^{a}
	C_2	10.81 ± 1.18^{b}	3.35 ± 0.46^{b}	3.74 ± 0.44^{b}
	C_3	13.02 ± 1.43^{b}	6.02 ± 0.70^{c}	4.06 ± 0.49^{b}

Table 4. Effects of heavy metals on comet assay results (DNA damages, Tail moment and olive moment) in the field (Avella, S_1; Acerra, S_2; Castel Volturno, S_3) and *in vitro* ($C_{1;}$ $C_{2;}$ C_3) experiments. Values are presented as mean ± st. err; numbers not accompanied by the same letter are significantly different at $P < 0.05$. One-way ANOVA was applied for analysing the differences among sites in field experiment, and among the concentration in vitro, followed by the post-hoc Student–Newman–Keuls test.

References

Ahmad SS, Reshi ZA, Shah MA, Rashid I, Ara R, Andrabi SMA. (2014). Phytoremediation potential of Phragmites australis in Hokersar wetland a Ramsar site of Kashmir Himalaya. Int J Phytorem 16, 1183-1191.

Al Khateeb, W. (2018). Plants genotoxicity as pollution bioindicator in Jordan using comet assay. Physiology and Molecular Biology of Plants, 24(1), 89-97.

Aravind, P., Prasad, M.N.V., 2005. Modulation of cadmium-induced oxidative stress in Ceratophyllum demersum by zinc involves ascorbate–glutathione cycle and glutathione metabolism. Plant Physiol. Biochem. 43, 107–116. https://doi.org/10.1016/j.plaphy.2005.01.002.

Barceló, J., Poschenrieder, C., 2004. Structural and Ultrastructural Changes in Heavy Metal Exposed Plants. In: Prasad M.N.V. (eds) Heavy Metal Stress in Plants. Springer, Berlin, Heidelberg; pp 223-248.

Basile A., Sorbo S., Conte B., Castaldo Cobianchi R., Trinchella F., Capasso C., Carginale V., 2012. Toxicity, Accumulation, and Removal of Heavy Metals by Three Aquatic Macrophytes. Int. J. Phytoremediation 14, 374-387. https://doi.org/10.1080/15226514.2011.620653

Basile, A., Cogoni, A.E., Bassi, P., Fabrizi, E., Sorbo, S., Giordano, S., Castaldo Cobianchi, R., 2001. Accumulation of Pb and Zn in gametophytes and sporophytes of the moss *Funaria hygrometrica* (Funariales). Ann. Bot. 87, 537-543. https://doi.org/10.1006/anbo.2001.1368

Basile, A., Sorbo, S., Aprile, G., Conte, B., Castaldo Cobianchi, R., Pisani, T., Loppi, S., 2009. Heavy metal deposition in the italian "Triangle of death" determined with the moss

Scorpiurium circinatum. Environ. Pollut. 157, 2255–2260. http://dx.doi.org/10.1016/j.envpol.2009.04.001.

Basile, A., Sorbo, S., Aprile, G., Conte, B., Castaldo Cobianchi, R., 2008. Comparison of the heavy metal bioaccumulation capacity of an epiphytic moss and an epiphytic lichen. Environ. Pollut. 151, 401– 407. http://dx.doi.org/10.1016/j.envpol.2007.07.004.

Basile, A., Sorbo, S., Cardi, M., Lentini, M., Castiglia, D., Cianciullo, P., Conte, B., Loppi, S., Esposito, S., 2015. Effects of heavy metals on ultrastructure and HSP70 induction in *Lemna minor* L. exposed to water along the Sarno River, Italy. Ecotox. Environ. Safe. 114, 93-101. http://dx.doi.org/10.1016/j.ecoenv.2015.01.009.

Basile, A., Sorbo, S., Conte, B., Cardi, M., Esposito, S., 2013. Ultrastructural changes and Heat Shock Proteins 70 induction upon urban pollution are similar to the effects observed under in vitro heavy metals stress in *Conocephalum conicum* (Marchantiales - Bryophyta). Environ. Pollut. 182, 209-216. http://dx.doi.org/10.1016/j.envpol.2013.07.014.

Basile, A., Sorbo, S., Conte, B., Golia, B., Montanari, S., Castaldo Cobianchi, R., Esposito, S., 2011. Antioxidant activity in extracts from *Leptodictyum riparium* (Bryophyta), stressed by heavy metals, heat shock, salinity. Plant Biosyst 175, 77-80. http://dx.doi.org/10.1080/11263504.2010.509935.

Basile, A., Sorbo, S., Pisani, T., Paoli, L., Munzi, S., Loppi, S., 2012. Bioacumulation and ultrastructural effects of Cd, Cu, Pb and Zn in the moss *Scorpiurum circinatum* (Brid.) Fleisch. & Loeske 166, 208-211. http://dx.doi.org/10.1016/j.envpol.2012.03.018.

Blokhina, O., Virolainene, E., Fagerstedt, K.V., 2003. Antioxidants, Oxidative Damage and Oxygen Deprivation Stress: a Review. Ann. Bot. 91, 179-194. https://doi.org/10.1093/aob/mcf118.

Bove, M.A., Ayuso, R.A., De Vivo, B., Lima, A., Albanese, S., 2011. Geochemical and isotopic study of soils and waters from an Italian contaminated site: Agro Aversano (Campania). J. Geochem. Explor. 109, 38–50. https://doi.org/10.1016/j.gexplo.2010.09.013.

Bradford, M.M., 1976. A rapid and sensitive method for the quantitation of microgram quantities of protein utilizing the principle of protein dye-binding. Anal. Biochem. 72, 248–254.

Bruns, I., Friese, K., Markert, B., Krauss, G.J., 1997. The use of *Fontinalis antipyretica* L. ex Hedw. as a bioindicator for heavy metals. 2. Heavy metal accumulation and physiological reaction of Fontinalis antipyretica L. ex Hedw. in active biomonitoring in the River Elbe. Sci. Total Environ. 204, 161–176.

Cesa, M., Bertossi, A., Cherubini, G., Gava, E., Mazzilis, D., Piccoli, E., Verardo, P., Nimis, P.L., 2015. Development of a standard protocol for monitoring trace elements in continental waters with moss bags: inter- and intraspecific differences. Environ. Sci. Pollut. Res. 2(7), 5030-5040. http://dx.doi.org/10.1007/s11356-015-4129-z.

Das, K., & Roychoudhury, A. (2014). Reactive oxygen species (ROS) and response of antioxidants as ROS-scavengers during environmental stress in plants. Front Environ Sci, 2, 53.

Demidchik, V. (2015). Mechanisms of oxidative stress in plants: from classical chemistry to cell biology. Environ. Exp Bot, 109, 212-228.

Di Martino, D., 2014. Ecologie dell'inquinamento Progetto di territorio attraverso la bonifica. Fedoa Università degli Studi di Napoli Federico II - Open Archive.

Dixit, R., Malaviya, D., Pandiyan, K., Singh, U. B., Sahu, A., Shukla, R., ... & Paul, D. (2015). Bioremediation of heavy metals from soil and aquatic environment: an overview of principles and criteria of fundamental processes. Sustainability, 7(2), 2189-2212.

Esposito, S., Sorbo, S., Conte, B., Basile, A., 2012. Effects of heavy metals on ultrastructure and HSP70s induction in the aquatic moss *Leptodictyum riparium* Hedw. Int. J. Phytoremediation 14, 443–455. http://dx.doi.org/10.1080/15226514.2011.620904.

Farmer, E.E., Mueller, M.J., 2013. ROS-Mediated Lipid Peroxidation and RES-Activated Signaling. Annu. Rev. Plant Biol. 64, 429–450. https://doi.org/10.1146/annurev-arplant-050312-120132.

Fernandez, J. A., Vazquez, M. D., Lopez, J., & Carballeira, A. (2006). Modelling the extra and intracellular uptake and discharge of heavy metals in Fontinalis antipyretica transplanted along a heavy metal and pH contamination gradient. Environ Pollut, 139(1), 21-31.

Fritioff, A., Kautsky, L., Greger, M., 2005. Influence of temperature and salinity on heavy metal uptake by submersed plants. Environ Pollut 133, 265–274. http://dx.doi.org/10.1016/j.envpol.2004.05.036.

Gecheva, G., Yurukova, L., Ganeva, A., 2011. Assessment of pollution with aquatic bryophytes in Maritsa River (Bulgaria). Bull. Environ. Contam. Toxicol. 87, 480-485. . http://dx.doi.org/10.1007/s00128-011-0377-x.

Gedik, C. M., Ewen, S.W.B., Collins, A.R., 1992. Single-cell gel electrophoresis applied to the analysis of UV-C damage and its repair in human cells. Int. J. Radiat. Biol. 62, 313-320.

Gichner, T., Patková, Z., Száková, J., Demnerová, K., 2009. Cadmium induces DNA damage in tobacco roots, but no DNA damage, somatic mutations or homologous recombination in tobacco leaves. Mutat. Res. 559,49-57. http://dx.doi.org/10.1016/j.mrgentox.2003.12.008.

Gichner, T., Plewa, M.J., 1998. Induction of somatic DNA damage as measured by single cell gel electrophoresis and point mutation in leaves of tobacco plants, Mutat. Res. 401, 143–152.

Gichner, T., Patková, Z., Száková, J., & Demnerová, K. 2004. Cadmium induces DNA damage in tobacco roots, but no DNA damage, somatic mutations or homologous recombination in tobacco leaves. Mutat Res-Gen Tox En, 559(1), 49-57.

Gill, S. S., & Tuteja, N. (2010). Reactive oxygen species and antioxidant machinery in abiotic stress tolerance in crop plants. Plant Physiol Biochem, 48(12), 909-930.

Grezzi, G., Ayuso, R.A., De Vivo, B., Lima, A., Albanese, S., 2011. Lead isotopes in soils and groundwaters as tracers of the impact of human activities on the surface environment: the DomizioFlegreo Littoral (Italy) case study. J Geochem. Explor. 109, 51–58. http://dx.doi.org/10.1016/j.gexplo.2010.09.12.

Habig, W.H., Jakoby, W.B., 1981. Assays for differentiation of glutathione S-transferases. Method Enzymology 77, 398–405. http://dx.doi.org/10.1016/S0076-6879(81)77053-8.

Huggett, R. J. (2018). Biomarkers: biochemical, physiological, and histological markers of anthropogenic stress. CRC Press.

Inupakutika, M.A., Sengupta, S, Devireddy AR, Azad RK, Mittler R., 2016. The evolution of reactive oxygen species metabolism. J. Exp. Bot. 67(21), 5933-5943. http://dx.doi.org/10.1093/jxb/erw382.

Kaaya, A., Najimi, S., Ribera, D., Narbonne, J.F., Moukrim, A., 1999. Characterization of glutathione S-transferase (GST) activities in Perna perna and Mytilus galloprovincialis used as a biomarker of pollution in the Agadir marine bay (south of Morocco). Bull. Environ. Contam. Toxicol. 62, 623/629.

Kelly, M.G., Girton, C., Whittion, B.A., 1987. Use of moss-bags for monitoring heavy metals in rivers. Water Res. 21, 1429-1435. http://dx.doi.org/10.1016/0043-1354(87)90019-4.

Kimbrough, D.E., Cohen, Y., Winer, A.M., Creelman, L., Mabuni, C., 1999. A critical assessment of chromium in the environment. Critical Reviews in Environmental Science and Technology 29, 1–46. https://doi.org/10.1080/10643389991259164.

LeBel, C.P., Ali, S.F., McKee, M., Bondy, S.C., 1990. Organometal-induced increases in oxygen reactive species: the potential of 2′,7′-dichlorofluorescin diacetate as an index of neurotoxic damage. Toxicol. Appl. Pharmacol. 104, 17–24. http://dx.doi.org/10. 1016/0041-008X(90)90278-3.

Maine, M.A., Duarte, M.V., Sune, N.L., 2001. Cadmium uptake by floating macrophytes. Water Research 35(11), 2629-2634.

Martins, R.J.E., Pardo, R., Boaventura, R.A.R., 2004. Cadmium(II) and zinc(II) adsorption by the aquatic moss Fontinalis antipyretica: effect of temperature, pH and water hardness. Water Res. 38, 693–699.

Mouvet ,C., 1984. Accumulation of chromium and copper by the aquatic moss Fontinalis antipyretica L. ex. Hedw. transplanted in a metal-contaminated river. Environ. Technol. Lett. 5, 541–8.

Nagajyoti, P. C., Lee K. D., Sreekanth T. V. M., 2010. Heavy metals, occurrence and toxicity for plants: a review Environ Chem. Lett. 8, 199–216.

Nanda, R., & Agrawal, V. (2018). Piriformospora indica, an excellent system for heavy metal sequestration and amelioration of oxidative stress and DNA damage in Cassia angustifolia Vahl under copper stress. Ecotoxicology and environmental safety, 156, 409-419.

Nath, M., Bhatt, D., Prasad, R., Gill, S.S., Anjum, N.A., Tuteja, N., 2016. Reactive Oxygen Species Generation-Scavenging and Signaling during Plant-Arbuscular Mycorrhizal and Piriformospora indica Interaction under Stress Condition. Front. Plant Sci. 7, 1574. http://dx.doi.org/10.3389/fpls.2016.01574.

Nouri, J., Lorestani, B., Yousefi, N., Khorasani, N., Hasani, A. H., Seif, F., & Cheraghi, M. (2011). Phytoremediation potential of native plants grown in the vicinity of Ahangaran lead–zinc mine (Hamedan, Iran). Environ Earth Sci, 62(3), 639-644.

Prasad, M.N.V., 1999. Heavy metal stress in plants: from biomolecules to ecosystems.(Springer-Verlag: Berlin).

Prochazkova, D., Sairam, R.K., Srivastava, G.C., Singh, D.V., 2001. Oxidative stress and antioxidant activity as the basis of senescence in maize leaves. Plant Science 161, 765–771.

Samecka-Cymerman, A., Kolon, K., Kempers, A.J., 2002. Heavy metals in aquatic bryophytes from the Ore Mountains (Germany). Ecotoxicol. Environ. Saf. 52, 203–210. https://doi.org/10.1006/eesa.2002.2175.

Samecka-Cymerman, A., Kolon, K., Kempers, A.J., 2005. A comparison of native and transplanted Fontinalis antipyretica Hedw. as biomonitors of water polluted with heavy metals. Sci. Total Environ. 341, 97–107. https://doi.org/10.1016/j.scitotenv.2004.09.026.

Schwartzman, R.A., Cidlowski, J.A., 1993. Apoptosis: the biochemistry and molecular biology programmed cell death. Endocr. Rev. 14, 133-151.

Senior, K., Mazza, A., 2004. Italian "Triangle of death" linked to waste crisis. Lancet. Oncol. 5, 525-527. http://dx.doi.org/10.1016/S1470-2045(04)01561-X.

Shahid, M., Pourrut, B., Dumat, C., Nadeem, M., Aslam, M., & Pinelli, E. (2014). Heavy-metal-induced reactive oxygen species: phytotoxicity and physicochemical changes in plants. In Reviews of Environmental Contamination and Toxicology Volume 232 (pp. 1-44). Springer International Publishing.

Siebert, A., Bruns, I., Krauss, G., Miersch, J., Markert, B., 1996. The use of the aquatic moss Fontinalis antipyretica L. ex Hedw. as a bioindicator for heavy metals: 1. Fundamental investigations into heavy metal accumulation in Fontinalis antipyretica Lex Hedw. Sci. Total Environ. 177, 137–144.

Singh, N.P., McCoy, M.T., Tice, R.R., Schneider, E.L., 1988. A simple technique for the quantitation of low levels of DNA damage in individual cells. Exp. Cell Res. 175, 184-191.

Sorbo, S., Aprile, G., Strumia, S., Castaldo Cobianchi, R., Leone, A., Basile, A., 2008. Trace element accumulation in *P. furfuracea* (L.) Zopf exposed in Italy's so-called Triangle of Death. Sci. Total Environ. 407, 647–654. https://doi.org/10.1080/11263504.2011.558722.

Ünyayar, S., Celik, A., Cekic, F.O., Gözel, A., 2006. Cadmium-induced genotoxicity, cytotoxicity and lipid peroxidation in Allium sativum and Vicia faba. Mutagenesis 21, 77–81. https://doi.org/10.1093/mutage/gel001.

Van Breusegem, F., Dat, J.F., 2006. Reactive Oxygen Species in Plant Cell Death. Plant Physiology 141, 384–390. https://doi.org/10.1104/pp.106.078295.

Van Doorn W.G., Beers E.P., Dangl J.L., Franklin-Tong V.E., Gallois P., Hara-Nishimura I., Jones A.M., Kawai-Yamada M., Lam E., Mundy J., Mur L.A.J., Petersen M., Smertenko A., Taliansky M., Van Breusegem F., Wolpert T., Woltering E., Zhivotovsky B., Bozhkov P.V., 2011. Morphological classification of plant cell deaths. Cell Death Differ 18, 1241–1246. https://doi.org/10.1038/cdd.2011.36.

Vazquez, M.D., Poschenrieder, C., Barcelo, J., 1987. Chromium VI induced structural and ultrastructural changes in bush bean plants (*Phaseolus vulgaris* L.). Ann. Bot. 59, 427–438.

Vazquez, M.D., Lopez, J., Carballeira, A., 1999. Uptake of heavy metals to the extracellular and intracellular compartments in three species of aquatic bryophyte. Ecotoxicol. Environ. Saf. 44, 12–24. https://doi.org/10.1006/eesa.1999.1798.

Whitton, B., Say, P., Wehr, J., 1981. Use of plants to monitor heavy metals in rivers. In: Say P. & Whitton B. (eds.) Heavy metals in Northern England: environmental and biological aspects. University of Durham, Dept. of Botany, Durham.

Wu, Y., Chen, Y., Yi, Y., & Shen, Z. (2009). Responses to copper by the moss Plagiomnium cuspidatum: hydrogen peroxide accumulation and the antioxidant defense system. Chemosphere, 74(9), 1260-1265.

PLOS ONE

In-field and in-vitro study of the moss *Leptodictyum riparium* as bioindicator of toxic metal pollution in the aquatic environment: ultrastructural damage, oxidative stress and HSP70 induction.

[a]Esposito Sergio, [b]Loppi Stefano, [b]Monaci Fabrizio, [b]Paoli Luca, [b]Vannini Andrea, [c*]Sorbo Sergio, [a]Maresca Viviana, [d]Fusaro Lina, [e]Elham Asadi karam, [a]Lentini Marco, [a]De Lillo Alessia, [a]Conte Barbara, [b]Cianciullo Piergiorgio, [a*]Basile Adriana

[a] Dipartimento di Biologia, University of Naples Federico II, Complesso Univ. Monte Sant'Angelo, Via Cinthia, 80126 Napoli, Italy

[b] Dipartimento di Scienze della Vita, University of Siena, via Mattioli 4, 53100 Siena, Italy

[c] Ce.S.M.A, Section of Microscopy, University of Naples Federico II, Complesso Univ. Monte Sant'Angelo, Via Cinthia, 80126 Napoli, Italy

d Dipartimento di Biologia Ambientale, Università Sapienza, Roma, Italy

[e] Biology Department, Shahid Bahonar University of Kerman, Kerman, Iran

*Corresponding authors:

Adriana Basile
Dipartimento di Biologia
Complesso Universitario Monte Sant'Angelo
Via Cinthia - Edificio 7
80126 – Napoli - ITALY
++39-081-2538508 (Office)
email: adbasile@unina.it

Sergio Sorbo
Ce.S.M.A, Section of Microscopy,
University of Naples Federico II,
Complesso Univ. Monte Sant'Angelo,
Via Cinthia - Edificio 7,
80126 Napoli,
Italy

Abstract

This study evaluates the effects of toxic metal pollution in the highly contaminated Sarno River (South Italy), by using the aquatic moss *Leptodictyum riparium* in bags at 3 representative sites of the river. Biological effects were assessed by metal bioaccumulation, ultrastructural changes, oxidative stress, as Reactive Oxygen Species (ROS) production and Glutathione S-transferase (GST) activity, as well as Heat Shock Proteins 70 (HSP70s) induction. The results showed that *L. riparium* is a valuable bioindicator for toxic metal pollution of water ecosystem, accumulating different amounts of toxic metals from the aquatic environment. Toxic metal pollution caused severe ultrastructural damage, as well as increased ROS production and induction of GST and HSP70s, in the samples exposed at the polluted sites. To assess the role and the effect of toxic metals on *L. riparium*, were also cultured *in vitro* with Cd, Cr, Cu, Fe, Ni, Pb, Zn at the same concentrations as measured at the 3 sites. Ultrastructure, ROS, GST, and HSP70s resulted severely affected by toxic metals. Based on our findings, we confirm *L. riparium* as a model organism in freshwater biomonitoring surveys, and GST and HSP70s as promising biomarkers of metal toxicity.

Keywords: Biomonitoring, Toxic metals, Freshwater pollution, Ultrastructure, Oxidative stress, ROS, GST, Heat Shock Proteins.

1. Introduction

The contamination of rivers is of special concern, since they may transport contaminants, among which toxic metal, to areas far removed from any local pollution source, thus posing at risk even pristine ecosystems.

Toxic metal pollution is a major concern worldwide, and the use of living organisms for monitoring these pollutants is widely accepted [1]. Whitton et al. [2] suggested the use of ten macrophytes for biomonitoring toxic metals in European rivers and streams; among them, the aquatic moss *Leptodictyum riparium* (Hedw.) Warnst (*Bryophyta*). Bioaccumulation ability, tissue localization, toxic effects of metals and antioxidant activity in this species were investigated in previous studies [3-5], confirming its suitability for biomonitoring freshwater pollution. Furthermore, *L. riparium* resulted the most effective among 3 freshwater plant species in bioaccumulating metals *in vitro* [4].

Among the damages induced by environmental stress, and namely by toxic metal pollution, the disruption of main metabolic pathways, primarily due to the unfolding of enzymes and proteins, represents one of the first, and most devastating, effects on living organisms. As a consequence, cells react by activating a number of defense mechanisms: the induction, synthesis and activation of chaperons represent the most evident and widespread of them [6]. Among the different groups and families of chaperons, exhibiting different functions and roles, it is widely accepted that Heat Shock Proteins 70 (HSP70s) represent the most conserved and widespread protectants of protein structures in all cells. Their role as cell protectants under pollution stress has already been demonstrated [3,7]

Various abiotic stressors lead to the overproduction of Reactive Oxygen Species (ROS) in plants. These molecular species are highly reactive and can play a dual role in plants. In fact, they can either act as toxic agents or work as signals, which then trigger and regulate biological processes, such as cell death or adaptation responses to environmental stress, or even main physiological processes, such as cell proliferation and differentiation [8-10]. As toxicants, they can cause severe damage, which ultimately results in an oxidative stress [11-13]. This can trigger redox-sensitive pathways that lead to different alterations, such as protein carbonylation, DNA damage, activation of kinase cascades and transcription factors, which ultimately affect cellular essential metabolic activities and viability. Thus, given the need of maintaining ROS concentrations within specific ranges, plants have very

efficient enzymatic and non-enzymatic antioxidant machinery, able to control ROS overproduction [11-13]. Therefore, measurement of the intracellular ROS content and/or the measure of the activity of antioxidant enzymes, e.g. glutathione S-transferase (GST), are considered valuable indicators of overall changes of the intracellular redox state [14,15]. The Sarno River (Campania region, Southern Italy), is known as one of the most polluted rivers in Europe: the whole basin (25 km long, 500 km2 wide, hosting 700,000 inhabitants) has been declared as "area with high risk of environmental crisis" [16]. The heavy urbanization and industrialization of this area caused a strong impact on the health of the local population, with significant increase in cerebrum-vascular diseases, lymphoma and cancers [17].

This study aimed at proposing an experimental protocol that allows determining contribution of the different pollutants to the overall biological effect, by carefully comparing in field and *in vitro* results. To this purpose, we evaluated the biological effects of water pollution by toxic metals in one of the most polluted river in Europe using the aquatic cosmopolitan moss *L. riparium*, a species able to strongly accumulate toxic metals [6]. Biological effects were studied in field and *in vitro*, considering metal bioaccumulation, oxidative stress (content of ROS and GST antioxidant enzyme activity), ultrastructural damage and HSP70s induction.

2. Materials and Methods

L. riparium was widely present in the Mediterranean area, and in the Sarno river basin from springs to the river mouth; in order to use similar specimens for the experimental design, samples were collected at the Botanical Gardens of the University of Naples "Federico II," Italy. Moss grew in a basin at a depth of 20-25 cm and temperature of 17-20°C. Homogeneous samples of about 2 g fresh weight (fw) were washed with deionized water and placed into 1 mm^2 meshed nylon bags, as recommended by Kelly et al. [18]. Six bags for each site were exposed for one week during July 2013 at a water depth of 25 cm in the River Sarno (the average temperature of the water was 17.5-19.0°C). The moss bags were exposed along the Sarno river path in three sites (S1 Table) characterized by different metal concentrations, as detailed in Basile et al. [19], and featured with good, poor, and very poor water quality respectively [20].

A summary of the three selected sites are provided below:

- "Rio Foce" (site A) near the spring, before pollution sources, as control site; 40°49'56.269" N, 14°35'27.103° E. Sarno River spring is located at 30 m asl, at the slope of the Saro Mount. This represents the Western extremity of Picentini Mounts, characterized by a forest extension of over 40,000 hectares, rich in beech, maple, alder, and chestnut, and numerous streams that make the area the richest potable drinking water tank in southern Italy.
- "San Marzano sul Sarno" (site B), before the confluence with the Alveo Comune Nocerino; this site is affected mainly by urban pollution. The Alveo Comune Nocerino is originated by the confluence of Solofrana and Cavaiola, and is the main Sarno tributary; 40°46'47.971" N, 14°34'23.296" E.
- "Scafati" (site C), the heavily polluted site, after the confluence of Alveo Comune Nocerino collecting Cavaiola e Solofrana streams, affected by heavy industrial (leather tannery; agri-food) and agricultural (tomatoes; fruit trees; vineyards) wastewaters. 40°44'48.812" N, 14°31'37.653" E.

No specific permissions were required for these locations/activities because they were not necessary and we confirm that the field studies did not involve endangered or protected species.

In parallel with in-situ toxic metal exposition, a twin experiment was performed to further evaluate the effects on ultrastructure and biochemistry of metals using manipulative laboratory infrastructure. For this purpose we exposed *in vitro* the moss to the same metal concentrations water solution and in the same condition measured in the experimental 3 sites. In addition, to assess the effects of the single metals, the moss was exposed *in vitro* to single toxic metal concentrations as measured at the most polluted environment (site C). Treatments consisted in the addition to the growth medium of the metals as soluble salts: $CdCl_2$, $Cr(Cl)_3$, $CuSO_4$, $FeCl_2$, $NiCl_2$, $Pb(CH3COO)_2$, $ZnCl_2$. In this way the studied metals were readily available to the moss.

In vitro cultures were done as previously reported [7]; after collection, single gametophytes were carefully cleaned and washed with deionised water and then the surface was sterilized with ethanol 70% and NaClO 2%. Then samples were then put into Petri dishes (10 cm diameter), 20 specimens per dish. The specimens were cultured with sterile modified Mohr medium, pH 7.5 [7] and in the same medium with the addition of the metal salts. The

cultures were kept in a climatic room with a temperature of 13/20°C, 70% constant RH, and photoperiod of 16/8 hours of light/dark. The specimens were maintained in the growth chamber for 7 days.

Experiments on gametophyte cultures were run in triplicate and repeated three times.

2.1. Bioaccumulation of toxic metals

After exposure along the River Sarno, moss samples were air-dried at 40 °C to constant weight and then frozen in liquid nitrogen, pulverized and homogenized with a ceramic mortar and pestle. About 300 mg of moss powder was mineralized with a mixture of 6 mL of 70% HNO_3, 0.2 mL of 60% HF and 1 mL of 30% H_2O_2 (ultra-pure reagent grade). Digestion of samples was carried out in a microwave digestion system (Milestone Ethos 900) for a total time of 30 min. Concentrations of selected toxic metals (Cd, Cr, Cu, Fe, Ni, Pb, Zn), expressed on a dry weight basis, were determined by ICP-MS (Perkin-Elmer Sciex 6100) on three subsamples for each site. Analytical quality was checked by analysing the Certified Reference Material BCR 61 "aquatic moss". Precision of analysis was estimated by the coefficient of variation of 3 replicates and was found to be <10% for all elements.

2.2. Ultrastructural observations

Leaflets on the moss stem ca. 5 mm below the apex were used for TEM observations. Samples were fixed in 3% glutaraldehyde in phosphate buffer (pH 7.2–7.4) for 2 h at room temperature and post-fixed with buffered 1% OsO_4 for 1.5 h at room temperature, dehydrated with ethanol and propylene oxide and embedded in Spurr's epoxy medium [21]. Ultra-thin (50 nm thick) sections were mounted on 300-mesh copper grids, then stained with uranyl acetate and lead citrate, and observed with a Philips EM 208S TEM [21].

2.3. HSP70s analysis

L. riparium samples of 1-5 g fw were frozen and powdered in liquid nitrogen using a mortar and pestle. HSP70s were extracted in 50 mM phosphate buffer at pH 7.5 with 10% glycerol; the homogenate was then filtered through four layers of muslin and centrifuged for 20 min at 20,000g at 4°C. The supernatant fraction was designated as the crude extract and used

for SDS-PAGE analysis and Western blots. SDS-PAGE was performed using 10% acrylamide resolving gel with a 4% stacking gel. Before loading, samples were boiled for 10 min, in the presence of BBF to ensure protein denaturation. Proteins were subjected to electrophoresis under a constant voltage of 180 V, 40 mA for 90 min. For Western blot analysis, the separated polypeptides were transferred from gels to a nitrocellulose membrane (Hybond, Amersham Biosciences) soon after the SDS-PAGE run, then incubated for 2 h at room temperature with antibodies raised against bovine heart HSP70 (Sigma). Western blotting on the same extracts using anti-tubulin antisera (Sigma) were made to check the equal loading of the sample lanes, as previously described [22]. The results bands were analysed with densitometric analyses using Quantity-One software (Bio-Rad) (not shown). After washing, the membranes were incubated with secondary antibodies coupled to horseradish peroxidase and polypeptides immunoreacting were revealed by enhanced chemiluminescence using the ECL Prime kit (Ge Healthcare) as described in Cardi et al. [23]. As control, the same samples were tested against anti-alfa-tubulin antibodies, to check the equal loading of the lanes. All electrophoresis and western blotting analyses were performed with in a Mini-PROTEAN Tetra cell electrophoresis chamber (Bio-Rad), equipped with EPS 301 power supply (Ge Healthcare).

2.4. ROS content

A fluorescent technique using 2',7'-dichlorofluorescin diacetate (DCFH-DA) has been used for quantitative measurement of ROS production. DCFH-DA is de-esterified intracellularly and turns to nonfluorescent 2',7'-dichlorofluorescin (DCFH). DCFH is then oxidized by ROS to highly fluorescent 2′,7′-dichlorofluorescein (DCF) [24]. Briefly, leaf samples were immediately frozen in liquid nitrogen and ground thoroughly with prechilled mortar and pestle. The resulting powder (150 mg) was then resuspended in TrisHCl 40 mM pH 7.4, sonicated, and centrifuged at 12,000g for 30 min. The supernatant (500 μL) was collected and protein content determined. An aliquot (10 μL) of each sample was incubated with 5 μM DCFH-DA for 30 min at 37°C followed by recording of the final fluorescence value, which was detected at excitation (488 nm) and emission (525 nm) wavelength (SyneryTM HTX Multi-Mode). DCF formation was quantified from a standard curve (0.05-1.0 μM). The analysis were carried out on five subsamples for each site.

2.5. Glutathione S-transferase activity

Glutathione S-transferase (GST, EC 2.5.1.18) activity was measured using a commercial kit (CS0410, Sigma). The conjugation of GSH to 1-chloro-2,4-dinitrobenzene (CDNB) catalyzed by GST was monitored at 340 nm for 4 min (SyneryTM HTX Multi-Mode). The reaction mixture contained 4 μL of extract and 196 μL of reaction solution (200 mM GSH and 100 mM CDNB in Dulbecco's buffer at pH 7). The activity was calculated with ε = 9.6 mM−1 cm−1 [25]. A GST unit is defined as the amount of enzyme that catalyzes the formation of 1 μmol of the GS-DNB conjugate per minute at 25 °C and pH 7. All reagents for oxidative stress detection were analytical grade from Sigma-Aldrich (St. Louis, MO, USA). The analysis were carried out on five subsamples for each site.

2.6. Statistical analysis

One-way ANOVA was used to analyse the differences in metals concentration between sites (in-field experiment), and differences in ROS content and GST activity between treatments in-vitro experiment. The one-way ANOVA was followed by Student-Neuman-Keuls test for post hoc comparisons. Prior to analysis, data not matching a normal distribution (Shapiro–Wilk W test, $p < 0.05$) were log-transformed to correct for skewed distributions. Results were reported as mean ± standard deviation. For the in-field experiment, the relationships between toxic metals content, ROS and GST were assessed using Pearson correlation analysis. Data from all sites (A, B, C) were analysed together.

3. Results

3.1. Accumulation of toxic metals

Metal concentrations measured in moss bags exposed at site A (Table 1) are significantly lower than the concentrations measured at sites B and C. In comparison with site A, only Pb significantly ($P<0.05$) increased at site B and the same occurred at site C compared with site B (Table 1). At site C, Cd, Cu, Cr and Fe concentrations significantly increased compared with sites A and B. Only Ni and Zn concentrations remained significantly unchanged at the three sites (Table 1).

3.2. Ultrastructural observations

In field.

Moss samples exposed at site A showed an ultrastructure comparable with control, unexposed samples, collected at the Botanical Gardens (data not shown) (Fig 1, 1-5). The leaflet cells were delimited by thick cell walls, and contained lenticular chloroplasts beneath the cell wall. The thylakoid system was well developed, and arranged as grana and intergrana thylakoids extending along the longitudinal axis of the organelle: starch grains and rare plastoglobules were visible in the chloroplasts. Large clear vacuoles occupied the centre of the protoplast. Mitochondria with cristae, nucleus with eu- and heterochromatin, endoplasmic reticulum, and dictyosomes were regular.

Samples exposed at sites B and especially C showed severe alterations. After a 7-day exposure at site B, the cells, delimited by a thick cell wall, contained few chloroplasts with respect to those exposed at site A (Fig 1, 6-7). These organelles appeared misshaped, but they still preserved grana and intergrana thylakoids; plastoglobules increased (Fig 1, 8-9). The cytoplasm showed lipid droplets, vesicles with an electron dense content, and multivesicular bodies (Fig 1, 10). Moss samples exposed at site C were severely damaged: the thick cell walls were highly fissured (Fig 1, 11). The chloroplasts were swollen and contained numerous large plastoglobules; grana were still noticeable (Fig 1, 11-15). Large lipid droplets were present in the cytoplasm (Fig 1, 13-14).

In vitro

Toxic metals mixture-treatment

Samples exposed to the toxic metal mixture at the same concentrations as at site A showed the same appearance as control specimens, with no visible ultrastructural damage (Fig 2, 1-5). In contrast, samples treated with the toxic metal mixture as at site B appeared severely damaged: heavy plasmolysation, swelling of the chloroplasts and the thylakoids occurred (Fig 2, 6-10). Membranes had a thick appearance. In the samples treated with the toxic metals at the same concentrations as at site C, the chloroplasts were severely misshaped and developed plastoglobules in the stroma; multilamellar bodies occurred in the cytoplasm (Fig 2, 11-14). Nuclei and mitochondria were unchanged (Fig 2, 11-15).

Single toxic metal-treatments

Cd-treated samples. Cd-treated samples maintained a regular ultrastructure arrangement (Fig 3, 1). Leaflet cells showed chloroplasts with a well-developed thylakoid system (Fig 3, 2). Chloroplasts appeared misshaped as their profile was wavy, with bulges and invaginations (Fig 3, 3-4). Nuclei and mitochondria were comparable to the control (Fig 3, 5).

Cr-treated samples. Cr-treatment induced cytoplasm vacuolization with the occurrence of both clear and electron dense vacuoles (Fig 3, 6-8). Chloroplasts, even though still maintaining a regular grana and intergrana arrangement, showed irregular profiles (Fig 3, 8-9). Mitochondria with clear matrix and very few cristae, and cytoplasmic lipid droplets occurred (Fig 3, 10).

Cu-treated samples. Cu-treatment induced changes of the ultrastructure. The leaflet cells appeared heavily plasmolysed, or even empty (Fig 3, 11-12). Chloroplasts were swollen, even though grana and intergrana thylakoids and starch grains were still visible (Fig 3, 13-14). Membranes had a thick appearance. Multilamellar bodies occurred in the cytoplasm (Fig 3, 15).

Fe-treated samples. Fe-treated samples maintained the ultrastructure arrangement, but chloroplast shape was changed (Fig 3, 16-18). Nuclei and mitochondria were comparable to the control (Fig 3, 19-20).

Ni-treated samples. In Ni-treated samples, chloroplasts still maintained grana and intergrana arrangement (Fig 3, 21-24). Electron dense and electro clear vacuoles were observed. (Fig 3, 21-24). Other organelles such as mitochondria still preserved their regular ultrastructure (Fig 3, 25).

Pb-treated samples. Pb treatment induced chloroplast misshaping (Fig 3, 26-28); a swelling of the space between the outer and inner membranes occurred (Fig 3, 28). Furthermore, cytoplasm showed vesicles filled with electron dense material (Fig 3, 29). The other organelles were comparable with the control (Fig 3, 30).

Zn-treated samples. Zn treatment induced the presence of cytoplasm vesicles, and multilamellar bodies (Fig 3, 34-35). Chloroplasts conserved a well-developed thylakoid system and starch grains (Fig 3, 31-32); no other changes were observed in the other organelles (Fig 3, 35).

3.3. Oxidative stress

In field

ROS levels were low in *L. riparium* field-exposed at site A, but they significantly increased from site B to site C, by 9.4- and 26-fold respectively, compared with site A (Fig 4A). GST activity in field-exposed samples increased significantly from site B to site C, reaching the maximum at site C (Fig 5A).

In vitro

The treatment with the metal mix as measured at sites A and B did not show significant differences in ROS concentrations and GST activity measured in field-exposed samples (data not shown). *In vitro* treatment with the same metal mixture as site C gave a lower ROS value than field-exposure at the corresponding site, with a 31% lower value. Among the toxic metals tested, using concentrations as at site C, Pb, Cr and Cd caused the highest increase in ROS content, by 4-, 10-, and 4-fold respectively, compared with site A (Fig 4B). Treatment with the same metal mixture as at site C increased GST activity 7-fold, compared with the mixture as at site A (data not shown). As for the single metal treatments, similarly to ROS, treatments with Pb, Cr and Cd showed the maximum GST activities (Fig 5B).

3.4. HSP70s induction

In field

Moss samples of *L. riparium* exposed in bags along the Sarno River for 7 d showed strong differences in the amount of proteins reacting vs HSP70 antisera (Fig 6). At site A two pale bands of proteins were detected. At site B a strong increase was observed in two bands at 72 and 70 kDa MW. These bands further increased at site C, confirming the high and increasing degree of water pollution along the river.

In vitro

The figure 7 shows that HSP70s also increased exposing *L. riparium in vitro* to the toxic metals: the most severe increase was induced by the metal mixture as at site C and by Pb, Cr and Ni, when tested as single metals.

Pearson's correlation

In Table 2, data collected for in-field experiment were pooled together and the correlation between heavy metals and ROS and GST were derived. The amount of ROS, proportional to the oxidative stress experienced in the sample, resulted directly correlated with the concentration of all metals measured, except for Ni and Zn. In agreement with this result, the antioxidant activity was not related with the concentration of Ni and Zn. All metals were directly intercorrelated (i.e. Cd increases with increasing of Cr), with the exception of Ni and Zn.

4. Discussion

The use of living organisms to survey water ecosystems has been recommended by the European Union (Water Framework Directive, 2000/60/CE), and aquatic mosses are known to be suitable bioaccumulators of trace elements [28]. Mosses react to toxic metals excess in a complex way, activating a number of pathways at physiological and morphological levels and in the present work both have been studied and related to bioaccumulation shown both in the field and in vitro experiments.

The Sarno River, one of the most polluted in Europe, is known for having been subjected to illegal disposal of waste from the leather industry [27]. Toxic metals concentrations measured in moss bags exposed at site A (Tab. 1) were generally in line with values reported for aquatic mosses from unpolluted or lightly polluted rivers [28, 29]. This

confirmed that site A, at the springs of the Sarno River, is not affected by toxic metal pollution. On the contrary moss bags bioaccumulation in site B and C confirmed the the high degree of pollution of these sites, pinpointing at toxic metals as polluting the waters of the Sarno River. The pollution source is connected with the widespread presence of leather factories, massively using Cr and Fe for tanning, and the possible illegal waste disposal. Nowadays, Cr is largely replaced by Al in tanning manufacturing. At sites B and C the concentrations of Cd, Cu, and Pb were high as well, claiming for environmental and human health concern, and suggesting that the use of untreated river waters, e.g. for irrigation of agricultural products, should be avoided to prevent toxic metal accumulation along the food chain, with possible effects on human health. The ultrastructural observations of samples cultured *in vitro* and exposed to the toxic metal mixture, confirmed that low toxic metal concentrations as measured at the site A did not induce ultrastructure damage [19]. On the contrary, also from *in vitro* data we can conclude that the toxic metal concentrations measured at sites B and C cause severe and increasing alterations; this is consistent with our previous studies [6,7,19,22]. In addition, it should be considered that not all the metals, or not all fractions, present in the river waters may be readily available to the moss, because toxic metals could be not available to biological organisms, and thus not harmful [30,31]. The use for the *in vitro* test of fully soluble salts could also explain the more visible plasmolysis in the *in vitro*-treated samples compared with the in field-exposed ones. Intriguingly, samples treated with the metal mixture similar to the water of site B are all plasmolysed, but samples exposed at site B were not: this could be possibly caused by a different forms and bioavailability of pollutants. This hypothesis has been supported by Sassmann et al. [32], who found free metal ion availability as a major factor for tolerance and growth of plant under metal treatments.

Culturing *in vitro* with single toxic metals induced harmful effects on the moss, resulting in plasmolysis, swollen chloroplasts, and thick membrane appearance; moreover, empty cells appeared along the leaflet section. Toxic metals induced harmful effects, possibly in relation to their toxicity, concentration and/or availability.

The ultrastructural analyses of *L. riparium* cells showed that the most damaged organelles were the chloroplasts. In our samples these organelles became heavily swollen and developed large plastoglobules in the stroma. Chloroplasts are a common target of metal toxicity in different plant taxa, as comparable damage was already reported for toxic metal-

treated *L. riparium* [5], and other bryophytes, like the mosses *Funaria hygrometrica* (Hedw.) [33] and *Scorpiurum circinatum* (Brid) [34] the liverworts *Pellia neesiana* (Gottsche) Limpr. [35] and *Lunularia cruciata* L. Dum [36], as well as the aquatic Angiosperms *L. minor* and *Elodea canadensis* Michx. [19, 37].

Toxic metal exposure is known to induce oxidative stress [30] and lipid peroxidation [38]; thus, cell membranes and membrane-rich organelles, such as chloroplasts, and their functionality, such as selective permeability, are expected targets of harmful effects. All that could also cause swelling or shrinkage of the whole cell or its organelles, observed in our treated samples, relating to membrane impairment.

Damaged membranes could be the source for the lipid droplets and plastoglobules [38, 39], which increase in our treated samples. In plastoglobules these lipids could be recycled for the synthesis of tocopherols and vitamin E [41], which are also able to scavenge ROS [42].

Metal-induced toxicity and oxidative stress could also explain the occurrence of multivesicular bodies. These ultrastructures, which were observed in our treated samples, originate as an accretion of undigested membranes from endocytosis phenomena, probably related to autophagy recycling damaged cell components [43, 44].

Plant vacuoles, which are also increased in some of our treated samples, are also known to be involved in autophagy phenomena and are reported to be a major site for the degradation of macromolecules (42; 45).

L. riparium samples exposed along the Sarno river path showed strong GST activity, increasing from site A to site C. This can enable the cells to better scavenge the pollution-induced ROS increase. Therefore, it can be suggested that plant adaptive response(s) to pollution-induced oxidative stress may involve antioxidants like GST. The correlation between GST activity and ROS levels implies that the induction of activity of this enzyme by pollution is attributable to enhanced ROS. Therefore, activation of glutathione-S-transferases could enhance ROS quenching.

Heavy metals stimulated the GST activity. Notably this effect seems not being species-specific, since it has been found in several studies, also on pumpkin (*Curbita maxima*) subjected to metal stress [46, 47] and in rice in response to Cd stress [48].

Antioxidant activities linearly and progressively increased along the Sarno river path; in contrast, antioxidant activities observed in *in vitro* metal-treated samples showed a lower increase. This suggests that the antioxidant activity in the field-exposed samples could be

inducted by others, but not yet measured, pollutants as well. This is in agreement with the trend of the ultrastructure damage revealed by our TEM observations, and HSP70s induction. *L. riparium* GST activity trend along the Sarno river suggests that many sources of pollution are present along the river path [49, 50].

On the other hand, the correlation between metal pollution and ROS/GST levels is very strong (>92%).

Increased levels of HSP70s are usually resulting from the toxic action of pollutants taken up by living organisms, which have not been scavenged by detoxification systems, and negatively influence the correct folding of native proteins [51]. The moss *L. riparium* increased the activity of HSP70s in parallel with a higher accumulation of toxic metals. This result is consistent with the increased HSP70s and antioxidant activity found in experiments with the same moss exposed *in vitro* to toxic metals [5]. It is assumed that this response could be induced by toxic metal stress and has a protective role against toxic effects.

A previous experiment was carried out in Sarno River using the aquatic macrophyta *Lemna minor* L. [19] and a comparable pollution was detected. In that case both ultrastructure and HSPs responded consistently with the metallic concentrations measured in the same 3 sites. Compared to *L minor*, *L. riparium*, although presenting a simpler anatomical organization, typical of mosses, presents a surprising more preserved ultrastructure. In particular, the thylakoid system still appears recognizable even in the samples exposed in the most polluted site and /or at the highest metal concentrations. In addition, the measured bioaccumulation confirms that the moss is not able to avoid the presence of metals, but rather it accumulates them. The relative "resistance" of the moss is explained by the biochemical responses measured. In particular both HSPs and antioxidant response could protect the moss from proteotoxic and oxidative stresses respectively. The observed strong responses of *L riparium* could explain its hard resistance to pollutants and suggest it as an excellent bioindicator of pollution in aquatic systems.

In conclusion, for the first time to our knowledge, a comprehensive study has described the effects of pollution in moss in a river, by comparing both ultrastructural damage with biochemical and physiological parameters observed *in situ* and carefully measuring pollution in river waters. Always for the first time, these alterations have been validated by comparing the response in field with the parameters measured in the laboratory under

controlled conditions. Overall, our results suggest that *L. riparium* is able to respond to pollution by modifying biological parameters, such as HSP70s, ultrastructural organization, enzyme and antioxidant activity, suggesting that this species may be used as an effective bioindicator and bioaccumulator of water toxic metal pollution.

Figure and table

Elements	Site A	Site B	Site C	*p*
Cd	0.11 ± 0.02 a	0.147 ± 0.04 a	0.34 ± 0.04 b	**0.000**
Cr	0.26 ± 0.03 a	0.91 ± 0.13 a	5.65 ± 1.19 b	**0.000**
Cu	29.1 ± 6 a	29.1 ± 5.9 a	39.2 ± 3.71 b	**0.050**
Fe	174.8 ± 2 a	387.7 ± 56.9 a	1715.7 ± 442.4 b	**0.000**
Ni	7.9 ± 1.3	7.5 ± 1.9	10.07 ± 4.01	0.425
Pb	2.8 ± 0.1 a	3.9 ± 0.05 b	8.4 ± 0.94 c	**0.000**
Zn	457.8 ± 133.4	464.2 ± 98.3	467.47 ± 80.9	0.992

Table 1. Concentrations (µg g^{-1} dw) of toxic metals in moss bags of *L. riparium* exposed for 7 days at the 3 sites (A, B, C) along the river Sarno.

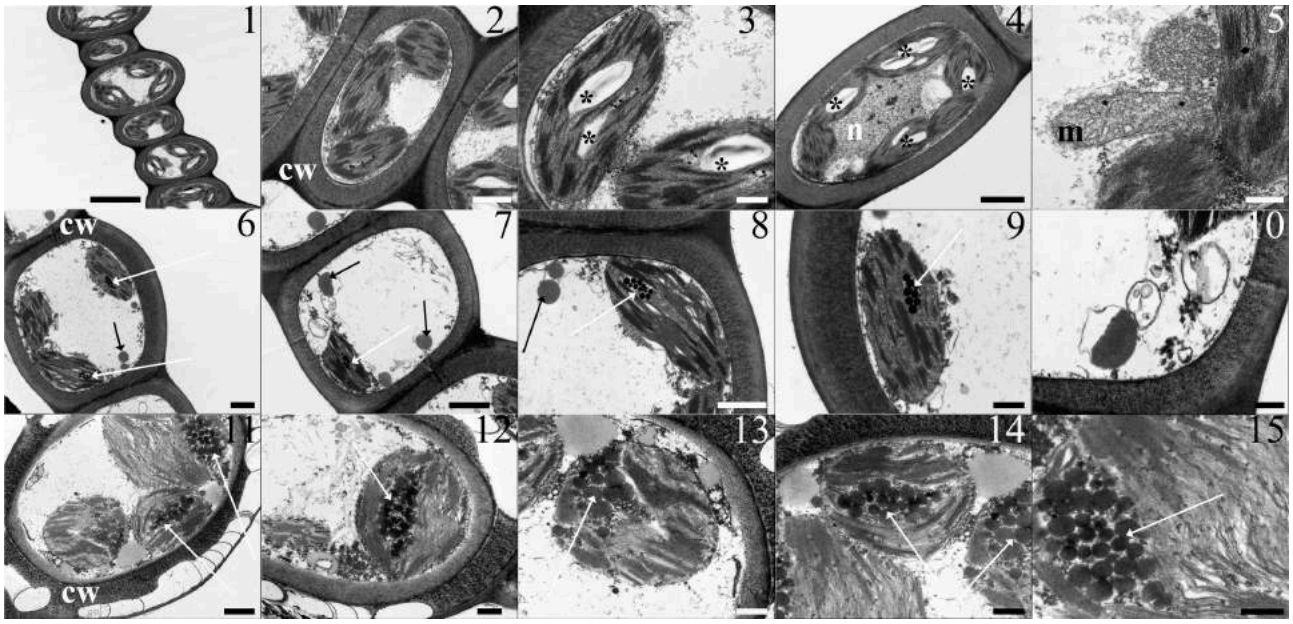

Figure 1. TEM micrographs from leaflets of *L. riparium* specimens exposed in the river Sarno at the site A (1-5), site B (6-10) and site C (11-15).

Site A. (1) Thick wall delimited cells showing lenticular chloroplasts, with grana and starch grains, and large clear vacuoles occupying the centre of the protoplast. (2) A thick walled cell with regular chloroplasts and vacuole. The chloroplasts show well-developed grana. (3) The chloroplasts contain a well-developed thylakoid system, starch grains and rare plastoglobules. (4) The thick wall delimited cell shows regular chloroplasts, with grana and starch grains, and a central nucleus, with eu- and heterochromatin. (5) A section of a mitochondrion with cristae.

Site B. (6) A thick wall delimited cell containing chloroplasts, with grana and plastoglobules, and cytoplasm lipid droplets. (7) The cell contains a miss-shaped chloroplast with grana and plastoglobules, cytoplasm lipid droplets and vesicles. (8) A miss-shaped chloroplast with a well-developed thylakoid system and

plastoglobules. Lipid droplets and a mitochondrion with no cristae are between the chloroplasts. (9) A chloroplast with a well-developed thylakoid system and plastoglobules. (10) Vesicles at high magnification.
Site C. (11) A severely altered cell featured by a highly fissured thick wall. The chloroplasts, still showing a developed thylakoid system with grana, are swollen and filled with large plastoglobules. Large lipid droplets are in the cytoplasm. (12) The altered cell shows cytoplasm lipid droplets and a swollen chloroplast with plastoglobules and thylakoids. (13-14) Chloroplasts showing large plastoglobules and thylakoid systems with still recognizable grana and intergrana membranes. Large lipid droplets around the chloroplast. (15) Magnified plastoglobules and thylakoids.
Scala bars: **5 µm** (1), **2 µm** (4), **1 µm** (2, 6, 7, 11, 15), **500 nm** (3, 9, 12, 13, 14), **300 nm** (5, 10)
Lettering and marks: **cw** cell wall; **m** mitochondrion; **n** nucleus; ***** starch grain; **black arrow** cytoplasm lipid droplet; **white arrow** plastoglobules.

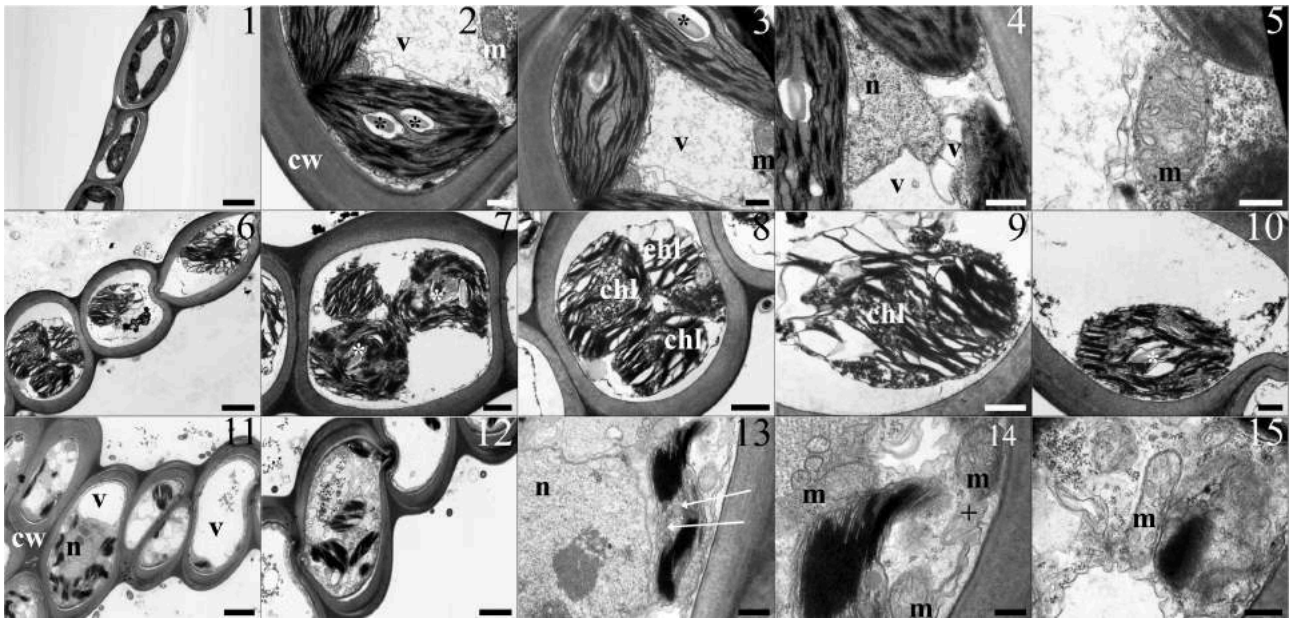

Figure 2. The table shows TEM micrographs from leaflets of *L. riparium* specimens cultured in the toxic metal mixture at the same concentrations as in the site A (1-5), site B (6-10) and site C (11-15).
Site A. (1) Thick wall delimited cells containing lenticular chloroplasts, with grana and starch grains, and large clear vacuoles. (2, 3) Regular chloroplasts featured by a well-developed thylakoid system and mitochondria. (4) A central nucleus (N) with eu- and heterochromatin, surrounded by chloroplasts and vacuoles. (5) A section of a mitochondrion with cristae.
Site B. (6) Thick wall delimited cells showing plasmolysed protoplasts with severely swollen chloroplasts. (7, 8) Severely plasmolysed cells containing swollen chloroplasts with swollen thylakoids. (9, 10) Swollen chloroplasts with swollen thylakoids and small starch grains. Membranes have a thicker and not sharp appearance.
Site C. (11) Inside the thick wall delimited cells are changed chloroplasts, vacuoles and a nucleus. (12) A cell with chloroplasts and plenty of cytoplasm vesicles. (13) A detail of a cell showing a misshaped

chloroplast with grana and large plastoglobules in the stroma. A nucleus with eu- and etherochromatin is on the left. (14) Details of a misshaped chloroplast with grana, mitochondria and a multilamellar body. (15) A section of a mitochondrion with cristae.

Scale bars: 5 µm (1), **3 µm** (11), **2 µm** (6, 12), **1 µm** (4, 7, 8), **500 nm** (2, 3, 9, 10, 13, 14), **300 nm** (5, 15)

Lettering and marks: cw cell wall; **m** mitochondrion; **n** nucleus; **v** vacuole; ***** starch grain; **white arrow** plastoglobules; **+** multilamellar body.

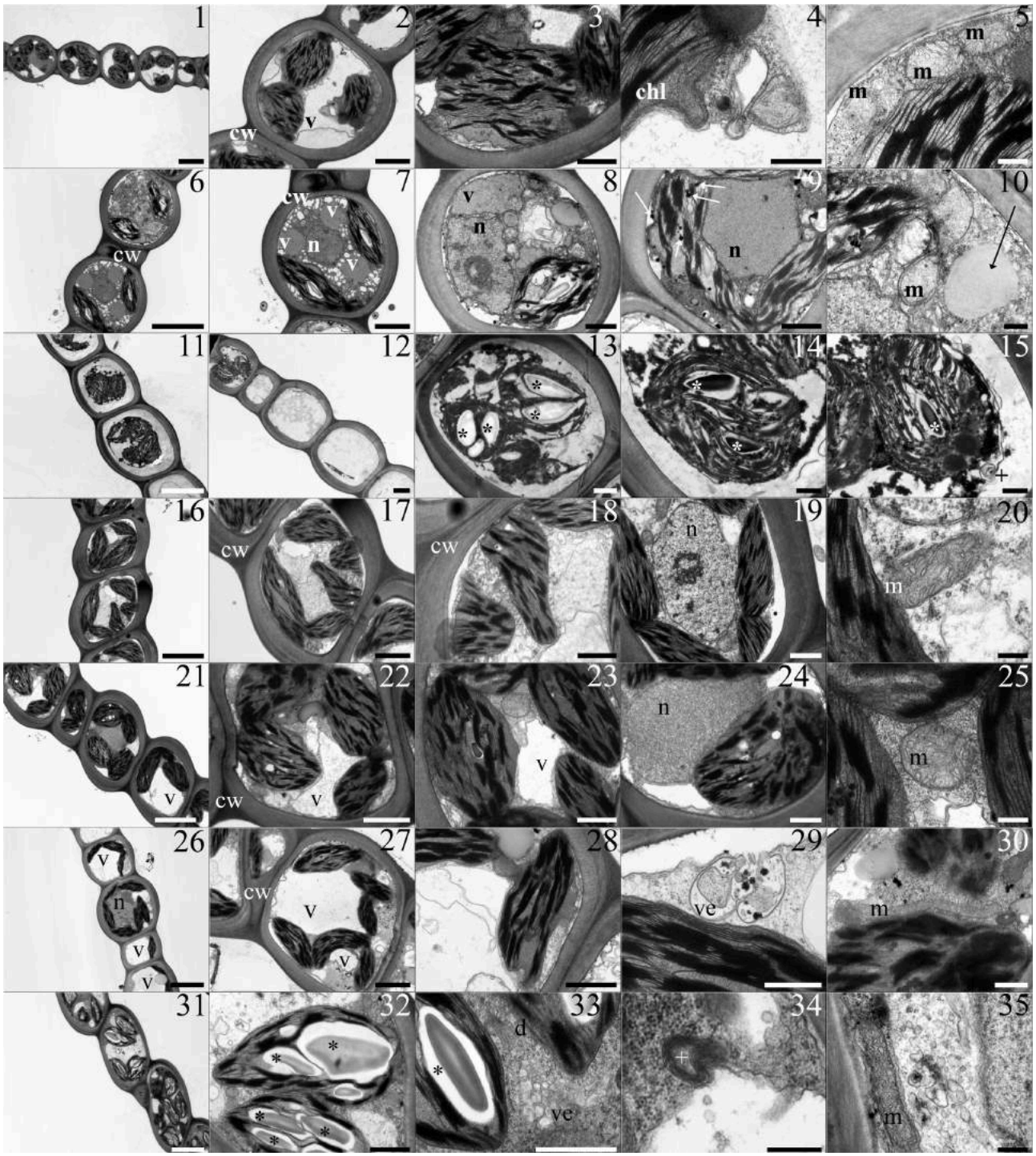

Figure 3. The table shows TEM micrographs from *L. riparium* leaflets of samples treated with the single toxic metals. (1-5) Cd-treated samples. (1) Thick wall delimited cells with chloroplasts, nucleus and

vacuoles. (2) A plasmolysed cell showing a large vacuole and chloroplasts with grana. (3) A misshaped chloroplast with grana and integrana thylakoids. (4) A bulge from a misshaped chloroplast. (5) Beside a chloroplast mitochondria with cristae. **(6-10) Cr-treated samples.** (6) Thick wall delimited cells with highly vacuolated cytoplasm, chloroplasts and nuclei. (7) The cell cytoplasm contains clear and electron dense vacuoles, chloroplasts and a nucleus. (8) The plasmolysed cell presents a misshaped chloroplast, with grana and a starch grain, clear and electron dense vacuoles, a nucleus and a large lipid droplet in the cytoplasm. (9) The cell contains a central nucleus surrounded by misshaped chloroplasts with a poorly developed thylakoid system and visible plastoglobules. (10) A diving mitochondrion, with clear matrix and no cristae, located beside a cytoplasm lipid droplet. **(11-15) Cu-treated sample.** (11-12) Severely plasmolysed cells with swollen chloroplasts and empty cells are shown. (13) A plasmolysed cell filled with swollen chloroplasts provided by starch grains. (14-15) Plasmolysed cells containing swollen chloroplasts with visible grana and starch grains. A multilamellar body near the plasma membrane. All the membranes appear poorly sharp. **(16-20) Fe-treated samples.** (16-18) Thick wall delimited cells with misshaped chloroplasts containing grana. (19) A normal nucleus with eu- and heterochromatin and a nucleolus. (20) A section of a mitochondrion with cristae. **(21-25) Ni-treated samples.** (21) The thick wall delimited cells show chloroplasts with grana and clear vacuoles. (22-23) Cells containing clear vacuoles and chloroplasts with grana. (24) A nucleus next to a chloroplast. (25) A section of a mitochondrion with developed cristae. **(26-30) Pb-treated samples.** (26) Thick wall delimited cells with chloroplasts and large clear vacuoles. (27) A cell contains chloroplasts with grana and clear vacuoles. Some of the chloroplasts appear misshaped. (28) A misshaped chloroplast with grana. (29) A vesicle filled with material fuses with plasma membrane. (30) A longitudinal section of a mitochondrion with cristae **(31-35) Zn-treated samples.** (31) Cells with chloroplasts containing starch grains. (32) A chloroplast with grana and starch grains. (33) Plenty of vesicles in the cytoplasm beside dictyosomes and chloroplasts. (34) A multilamellar body. (35) A longitudinal section of a mitochondrion with cristae, next to cytoplasm vesicles.

Scale bars: 5 µm (1, 6, 11, 16, 21, 26, 31), **2 µm** (2, 7, 12, 17, 22, 27), **1 µm** (3, 8, 9, 13, 18, 19, 23, 24, 28, 32, 33), **500 nm** (4, 14, 15, 29, 30), **300 nm** (5, 10, 20, 25, 34, 35)

Lettering and marks: **chl** chloroplast; **cw** cell wall; **d** dictyosomes; **m** mitochondrion; **n** nucleus; **v** vacuole; **ve** vesicles; ***** starch grain; **white arrow** plastoglobules; **+** multilamellar body.

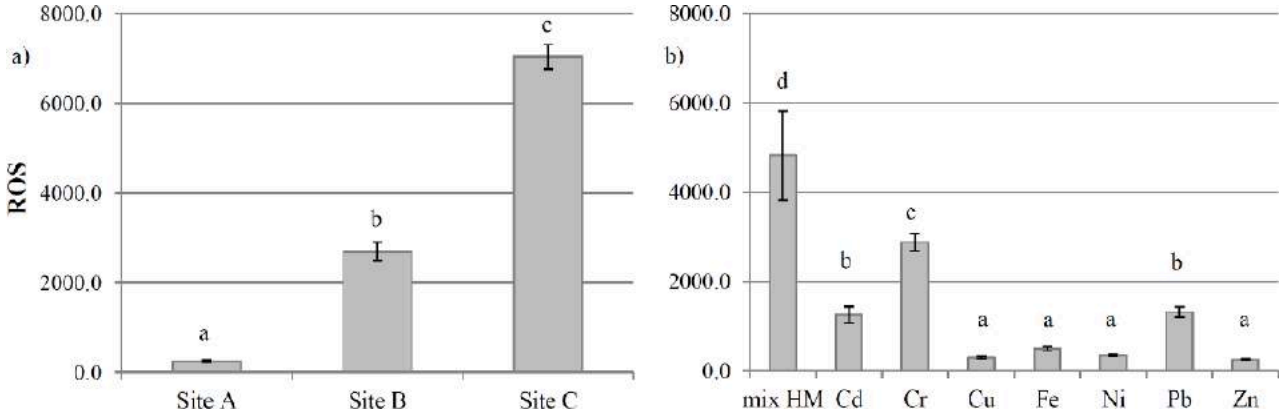

Figure 4. ROS content in *L. riparium* exposed in bags at sites A, B and C of Sarno River (in-field experiment, left panel, a) and *in vitro* cultured with mixtures of toxic metal or with the single toxic metal at the concentrations measured in site C ($CdCl_2$ 0.14 mg l^{-1}, Cr(Cl) 3 9.05 mg l^{-1}, $CuSO_4$ 2.45 mg l^{-1}, $FeCl_2$ 308.0 mg l^{-1}, $NiCl_2$ 3.4 mg l^{-1}, $Pb(CH3COO)_2$ 0.85 mg l^{-1}, $ZnCl_2$ 46.76 mg l^{-1}) (right panel, b).

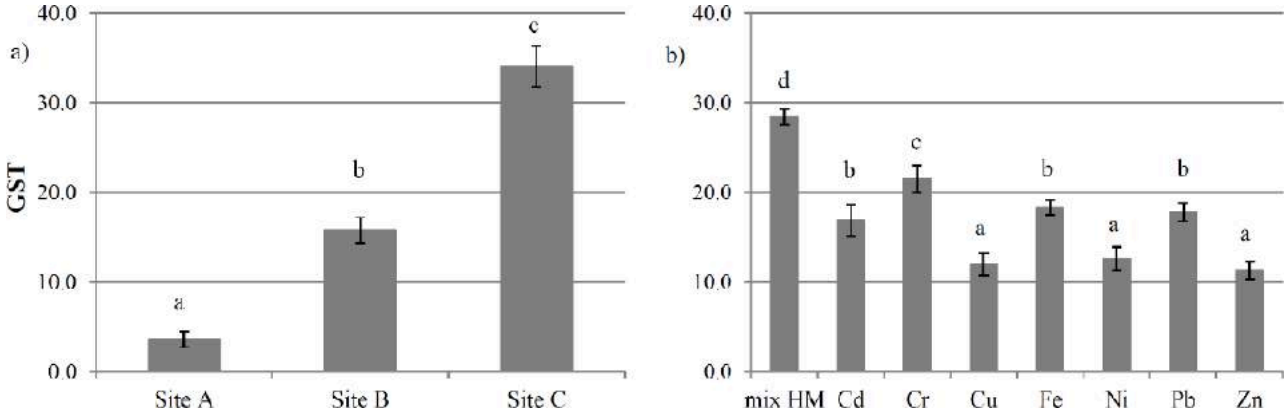

Figure 5. GST activity in *L. riparium* exposed in bags and *in vitro* cultured. GST activity in *L. riparium* exposed in bags at sites A, B and C of Sarno River (in-field experiment, left panel, a) and *in vitro* cultured with mixtures of toxic metal or with the single toxic metal at the concentrations measured in site C ($CdCl_2$ 0.14 mg l^{-1}, Cr(Cl) 3 9.05 mg l^{-1}, $CuSO_4$ 2.45 mg l^{-1}, $FeCl_2$ 308.0 mg l^{-1}, $NiCl_2$ 3.4 mg l^{-1}, $Pb(CH3COO)_2$ 0.85 mg l^{-1}, $ZnCl_2$ 46.76 mg l^{-1}) (right panel, b). Data are shown as the mean ± standard deviation (n = 5). The GST activity was expressed as micromoles/ml min^{-1}. Bars not accompanied by the same letter are significantly different at $p < 0.05$, using post hoc Student-Neuman-Keuls test.

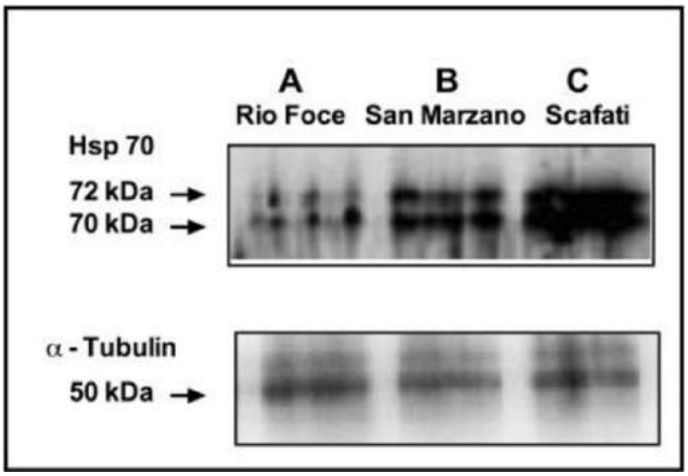

Figure 6. Western blotting using Hsp70 antibodies (Sigma) of *L.riparium* samples exposed along the Sarno River at sites A, B and C.

The lower figure shows Western Blotting of the same samples using alfa-tubulin to check the equal loading of electrophoretic lanes.

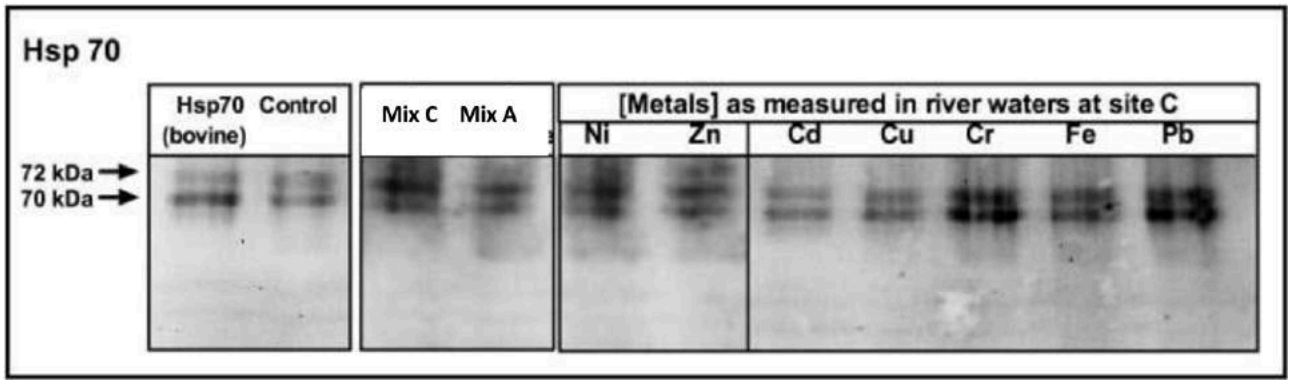

Figure 7. Western blotting using Hsp70 antibodies (Sigma) of *L. riparium* samples exposed *in vitro*.

Western blotting using Hsp70 antibodies (Sigma) of *L. riparium* samples exposed *in vitro* to metal mixtures of site C and site A, and to the single metal concentrations as measured in the site C: $CdCl_2$ 0.14 mg l^{-1}, Cr(Cl) 3 9.05 mg l^{-1}, $CuSO_4$ 2.45 mg l^{-1}, $FeCl_2$ 308.0 mg l^{-1}, $NiCl_2$ 3.4 mg l^{-1}, $Pb(CH_3COO)_2$ 0.85 mg l^{-1}, $ZnCl_2$ 46.76 mg l^{-1}.

	GST	ROS	Cd	Cr	Cu	Fe	Ni	Pb	Zn
GST	1	**0.989**	**0.889**	**0.935**	**0.616**	**0.927**	0.412	**0.956**	0.024
ROS		1	**0.928**	**0.934**	**0.642**	**0.920**	0.420	**0.971**	0.030
Cd			1	**0.951**	**0.685**	**0.942**	0.529	**0.937**	-0.01
Cr				1	**0.738**	**0.995**	0.473	**0.943**	0.087
Cu					1	**0.733**	0.337	**0.657**	**0.656**
Fe						1	0.540	**0.937**	0.062
Ni							1	0.545	-0.27
Pb								1	-0.03
Zn									1

Table 2. Pearson correlation coefficients (r) obtained for the linear correlations between GST and ROS and metals concentrations measured in-field experiment.
Data from all experimental sites were analyzed together. Correlations with $p< 0.05$ are marked in bold.

Table S1. Concentrations of metals as mg l^{-1} in waters of Sarno River, measured at the three different exposure sites.

	Cd	Cr	Cu	Fe	Ni	Pb	Zn
Site A	0.20±0.04	1.8±0.18	0.92±0.07	218.7±9.6	2.45±0.20	0.65±0.03	< 0.01
Site B	< 0.01	17.97±0.39	11.23±0.34	222.3±12.1	2.6±0.19	<0.01	29.94±2.83
Site C	0.14±0.02	9.05±0.27	2.45±0.15	308.0±13.0	3.4±0.27	0.85±0.05	46.76±1.81

References

1. Zhou Q, Zhang J, Fu J, Shi J, Jiang G. Biomonitoring: An appealing tool for assessment of metal pollution in the aquatic ecosystem. Anal. Chim. Acta. 2008;606: 135-150. https://doi.org/10.1016/j.aca.2007.11.018.
2. Whitton B, Say P, Wehr J. Use of plants to monitor heavy metals in rivers. In: Say P. & Whitton B. (eds.) Heavy metals in Northern England: environmental and biological aspects. University of Durham, Dept. of Botany, Durham. 1981.
3. Basile A, Sorbo S, Conte B, Golia B, Montanari S, Castaldo Cobianchi R, et al. Antioxidant activity in extracts from *Leptodictyum riparium* (*Bryophyta*), stressed by heavy metals, heat shock, salinity. Plant Biosyst. 2011;175: 77-80. http://dx.doi.org/10.1080/11263504.2010.509935.
4. Basile A, Sorbo S, Pisani T, Paoli L, Munzi S, Loppi S. Bioacumulation and ultrastructural effects of Cd, Cu, Pb and Zn in the moss *Scorpiurum circinatum* (Brid.) Fleisch. & Loeske. Environ Pollut. 2012;166: 208-211. http://dx.doi.org/10.1016/j.envpol.2012.03.018.
5. Esposito S, Sorbo S, Conte B, Basile A. Effects of heavy metals on ultrastructure and HSP70s induction in the aquatic moss *Leptodictyum riparium* Hedw. Int. J. Phytoremediation. 2012;14: 443–455. http://dx.doi.org/10.1080/15226514.2011.620904
6. Hartl FU. Molecular chaperons in cellular protein folding. Nature. 1996;381: 571–580. http://dx.doi.org/10.1038/381571a0.
7. Basile A, Sorbo S, Conte B, Cardi M, Esposito S. Ultrastructural changes and Heat Shock Proteins 70 induction upon urban pollution are similar to the effects observed under *in vitro* heavy metals stress in *Conocephalum conicum* (Marchantiales - *Bryophyta*). Environ. Pollut. 2013; 182: 209-216. http://dx.doi.org/10.1016/j.envpol.2013.07.014.
8. Dat J, Vandenabeele S, Vranová E, Van Montagu M, Inzé D, Van Breusegem F. Dual action of the active oxygen species during plant stress responses. Cell. Mol. Life Sci. 2000;57: 779–795
9. Mullineaux PM, Baker NR. Oxidative Stress: Antagonistic Signaling for Acclimation or Cell Death? Plant Physiol. 2010;154: 521–525.

10. Mittler R. ROS Are Good. Trends in Plant Sci. 2017;22: 11-19.
11. Pinto E, Sigaud-kutner TCS, Leitão MAS, Okamoto OK, Morse D, Colepicolo P. Heavy metal–induced oxidative stress in algae. J. Phycol 2003;39: 1008–1018. doi: 10.1111/j.0022-3646.2003.02-193.x
12. Dazy M, Masfaraud JF, Férard JF. Induction of oxidative stress biomarkers associated with heavy metal stress in *Fontinalis antipyretica* Hedw. Chemosphere. 2009;75: 297–302.
13. Gill SS, Tuteja N. Reactive oxygen species and antioxidant machinery in abiotic stress tolerance in crop plants. Plant Physiol. Biochem. 20104;8: 909-930. http://dx.doi.org/10.1016/j.plaphy.2010.08.016.
14. Inupakutika MA, Sengupta S, Devireddy AR, Azad RK, Mittler R. The evolution of reactive oxygen species metabolism. J. Exp. Bot. 2016;67(21): 5933-5943. http://dx.doi.org/10.1093/jxb/erw382.
15. Nath M, Bhatt D, Prasad R, Gill SS, Anjum NA, Tuteja N. Reactive Oxygen Species Generation-scavenging and signalling during plant-arbuscular mycorrhizal and Piriformospora indica interaction under stress condition. Front. Plant Sci. 2016;7: 1574. http://dx.doi.org/10.3389/fpls.2016.01574.
16. Ministry Council's Decree; 1995. Available: http://dx.doi.org/http://www.protezionecivile.gov.it/resources/cms/documents/DPCM_14_4_95_Sarno.pdf.
17. Senior K, Mazza A. Italian "Triangle of death" linked to waste crisis. Lancet Oncol. 2004;5 (9): 525-527.
18. Kelly MG, Girton C, Whittion BA. Use of moss-bags for monitoring heavy metals in rivers. Water Res. 1987;21: 1429-1435. http://dx.doi.org/10.1016/0043-1354(87)90019-4.
19. Basile A, Sorbo S, Cardi M, Lentini M, Castiglia D, Cianciullo P, et al. Effects of heavy metals on ultrastructure and HSP70 induction in *Lemna minor* L. exposed to water along the Sarno River, Italy. Ecotoxicol. Environ. Saf. 2015; 114; 93-101. http://dx.doi.org/10.1016/j.ecoenv.2015.01.009.
20. Goletta del fiume Sarno. Analisi, numeri e riflessioni sull'ecosistema del bacino del fiume Sarno. Castellamare di Stabia (NA). Legambiente; 2014. Available:

http://legambiente.campania.it/files/Goletta%20del%20Fiume%20Sarno%202016.pdf

21. Basile A, Cogoni AE, Bassi P, Fabrizi E, Sorbo S, Giordano S, et al. Accumulation of Pb and Zn in gametophytes and sporophytes of the moss *Funaria hygrometrica* (Funariales). Ann. Bot. 2001;87: 537-543. https://doi.org/10.1006/anbo.2001.1368
22. Basile A, Loppi S, Piscopo M, Paoli L, Vannini, Monaci F, et al. The biological response chain to pollution: a case study from the "Italian Triangle of Death" assessed with the liverwort *Lunularia cruciate*. Environ. Sci. Pollut. Res. 2017;24: 26185–26193. http://dx.doi.org/10.1007/s11356-017-9304-y.
23. Cardi M, Chibani K, Castiglia D, Cafasso D, Pizzo E, Rouhier N, et al. Overexpression, purification and enzymatic characterization of a recombinant plastidial glucose-6-phosphate dehydrogenase from barley (Hordeum vulgare cv. Nure) roots. Plant Physiol Biochem. 2013;73: 266-273. http://dx.doi.org/10.1016/j.plaphy.2013.10.008.
24. LeBel CP, Ali SF, McKee M, and Bondy SC. Organometal-induced increases in oxygen reactive species: The potential of 2',7'-dichlorofluorescin diacetate as an index of neurotoxic damage. Toleicol. Appl. Pharmacal. 1990; 104: 17-24.
25. Habig WH, Jakoby WB. Assays for differentiation of glutathione S-transferases. Methods Enzymol. 1981;77: 398–405. http://dx.doi.org/10.1016/S0076-6879(81)77053-8.
26. Ceschin S, Aleffi M, Bisceglie S, Savo V, Zuccarello V. Aquatic bryophytes as ecological indicators of the water quality status in the Tiber River basin (Italy). Ecol. Indic. 2012;14: 74-81. http://dx.doi.org/10.1016/j.ecolind.2011.08.020.
27. Albanese S, Iavazzo P, Adamo P, Lima A, De Vivo B. Assessment of the environmental conditions of the Sarno river basin (south Italy): a stream sediment approach. Environ. Geochem. Health. 2013;35: 283–297. https://doi.org/10.1007/s10653-012-9483-x
28. Gecheva G, Yurukova L, Ganeva A. Assessment of pollution with aquatic bryophytes in Maritsa River (Bulgaria). Bull. Environ. Contam. Toxicol. 2011;87: 480-485. http://dx.doi.org/10.1007/s00128-011-0377-x.
29. Cesa M, Bertossi A, Cherubini G, Gava E, Mazzilis D, Piccoli E. et al. Development of a standard protocol for monitoring trace elements in continental waters with moss

bags: inter- and intraspecific differences. Environ. Sci. Pollut Res. 2015; 22: 5030-5040. http://dx.doi.org/10.1007/s11356-015-4129-z.

30. Schützendübel A, Polle A. Plant responses to abiotic stresses: heavy metal-induced oxidative stress and protection by mycorrhization. J. Exp. Bot. 2002; 53: 1351-1365. https://doi.org/10.1093/jexbot/53.372.1351.
31. Uchimyia M, Lima IM, Klasson KT, Wartelle LH. Contaminant immobilization and release by biochar soil amendment: Roles of natural organic matter. Chemospere. 2010; 80: 935–940. https://doi.org/10.1016/j.chemosphere.2010.05.020.
32. Sassmann S, Adlassnig W, Puschenreiter M, Palomino-Cadenas J, Leyvas M, Lichtscheidl I, et al. Free metal ion availability is a major factor for tolerance and growth in *Physcomitrella patens*. Environ. Exp. Bot. 2014; 110: 1-10. http://dx.doi.org/10.1016/j.envexpbot.2014.08.010.
33. Basile A, Sorbo S, Bassi P, Napolitano E, Cogoni AE, Castaldo Cobianchi R. Effects of heavy metals on protonemal development and ultrastructure in populations of the moss *Funaria hygrometrica* Hedw. (Bryophyta) from a mine and an unpolluted site. Fresen. Environ. Bull. 2008; 17: 1956-1963.
34. Basile A, Sorbo S, Pisani T, Paoli L, Munzi S, Loppi S. Bioacumulation and ultrastructural effects of Cd, Cu, Pb and Zn in the moss *Scorpiurum circinatum* (Brid.) Fleisch. & Loeske Environmental Pollution 2012; 166: 208-211
35. Basile A, Sorbo S, Lentini M, Conte B, Esposito S. Water pollution causes ultrastructural and functional damages in *Pellia neesiana* (Gottsche) Limpr. J. Trace. Elem. Med. Biol. 2016;43: 80-86. https://doi.org/10.1016/j.jtemb.2016.11.014.
36. Carginale V, Sorbo S, Capasso C, Trinchella F, Cafiero G, Basile A. Accumulation, localisation, and toxic effects of cadmium in the liverwort *Lunularia cruciata*. Protoplasma. 2004;223: 3-61. http://dx.doi.org/10.1007/s00709-003-0028-0.
37. Esposito S, Castaldo Cobianchi R, Sorbo S, Conte B, Basile A. Ultrastructural alterations and HSP 70 induction in *Elodea canadensis* Michx. exposed to heavy metals. Caryologia. 2007;60: 115-120. http://dx.doi.org/10.1080/00087114.2007.10589557.
38. Zhang FQ, Wang YS, Lou ZP, Dong JD. Effect of heavy metal stress on antioxidative enzymes and lipid peroxidation in leaves and roots of two mangrove

plant seedlings (Kandelia candel and Bruguiera gymnorrhiza). Chemosphere. 2007;67: 44–50. https://doi.org/10.1016/j.chemosphere.2006.10.007.

39. Ghosh S, Mahoney SR, Penterman JN, Peirson D, Dumbroff EB. Ultrastructural and biochemical changes in chloroplasts during *Brassica napus* senescence. Plant Physiol. Biochem. 2001;39: 777–784.
40. Dalla Vecchia F, La Rocca N, Moro I, De Faveri S, Andreoli C, Rascio N. Morphogenetic, ultrastructural and physiological damages suffered by submerged leaves of *Elodea canadensis* exposed to cadmium. Plant Sci. 2005; 168: 329–338.
41. Vidi PA, Kanwischer M, Baginsky S, Austin JR, Csucs G, Dörmann P, et al. Tocopherolcyclase (VTE1) localization and vitamin E accumulation in chloroplast plastoglobule lipoprotein p.articles. J. Biol. Chem. 2006;281: 11225-11234. https://doi.org/10.1074/jbc.M511939200.
42. Bréhélin C, Kessler F, Van Wijk KJ. Plastoglobules: versatile lipoprotein particles in plastids. Trends Plant Sci. 2007;12: 1360-1385. http://dx.doi.org/10.1016/j.tplants.2007.04.003.
43. Thompson AR, Vierstra RD. Autophagic recycling: lessons from yeast help define the process in plants. Curr. Opin. Plant Biol. 2005; 8: 165-173. https://doi.org/10.1104/pp.105.060673.
44. Todeschini V, Lingua G, D'Agostino G, Carniato F, Roccotiello E, Berta G. Effects of high zinc concentration on poplar leaves: a morphological and biochemical study. Environ. Exp. Bot. 2011;71: 50-56. https://doi.org/10.1016/j.envexpbot.2010.10.018
45. Bassham DC Function and regulation of macroautophagy in plants. Biochim. Biophys. Acta 2009; 1793:1397–1403.
46. Fujita M, Hossain MZ. Molecular cloning of three tau-type glutathione S-transferases in pumpkin (*Cucurbita maxima*) and their expression. Physiol. Plant. 2003;117: 85-92.
47. Hossain MZ, Hossain MD, Fujita M. Induction of pumpkin glutathione S-transferases by different stresses and its possible mechanisms. Biologia Plantarum 2006; 50 (2): 210–218. http://dx.doi.org/10.1007/s10535-006-0009-1.

48. Hu Y, Ge Y, Zhang C, Ju T, Cheng W. Cadmium toxicity and translocation in rice seedlings are reduced by hydrogen peroxide pretreatment. Plant Growth Regul. 2009;59: 51–61. http://dx.doi.org/10.1007/s10725-009-9387-7.
49. Arienzo M, Adamo P, Bianco MR, Violante P. Impact of land use and urban runoff on the contaminationof the Sarno river basin in southwestern Italy. Water, Air, and Soil pollution. 2001; 131: 349–366.
50. Trocchia S, Labar S, Abdel Gawad FK, Rabbito D, Ciarcia G, Guerriero G. Frog Gonad as bio-indicator of Sarno River Health. J. sci. eng. res. 2015; 6 (1): 449-456.
51. Gupta SC, Sharma A, Mishra M, Mishra RK, Chowdhuri DK. Heat shock proteins in toxicology: How close and how far?. Life Sciences. 2010;86: 377-384. http://dx.doi.org/10.1016/j.lfs.2009.12.015.

Biological effects from environmental pollution by toxic metals in the "land of fires" (Italy) assessed using the biomonitor species *Lunularia cruciata* L. (Dum).

Viviana Maresca[a], Sergio Sorbo[b], Stefano Loppi[c] , Federica Funaro[a], Davide Del Prete[a], Adriana Basile[a]*

[a]Dipartimento di Biologia, Università di Napoli "Federico II" - Complesso Universitario Monte Sant'Angelo, Via Cinthia 4, I-80126 Napoli, Italy

[b]Ce.S.M.A, Università di Napoli "Federico II" - Complesso Universitario Monte Sant'Angelo, Via Cinthia 4, I-80126 Napoli, Italy

[c] Dipartimento di Scienze della Vita, Università di Siena, Via Pier Andrea Mattioli, 453100, Siena, Italy

*Corresponding author:

Prof. Adriana Basile

Dipartimento di Biologia - Università di Napoli "Federico II",

Complesso Universitario di Monte Sant'Angelo

Via Cinthia 4

80126 - Naples – ITALY

Email: adbasile@unina.it

Tel ++39-081-25-38508

Fax ++39-081-6-79233

Abstract

'Land of Fires' is a large area in the eastern part of Campania region of Italy affected by burning of waste and fraudulent dumping. The liverwort *Lunularia cruciata*, widespread in urban areas due to its tolerance to pollution, was collected from the town of Acerra, in the heart of the so-called "land of fires" and one of the vertices of the "Italian Triangle of Death" so said for the high incidence and mortality from tumors. The data obtained from these samples were compared with those collected from the village of Riccia, (Molise, Southern Italy) a site far removed from known sources of local pollution and samples collected in the center of Naples (a big metropolitan city of about 5 million people). The soil below the samples, and gametophytes, were collected and analysed for the concentration of Al, As, Ba, Cd, Cr, Cu, Fe, Hg, Mn, Ni, Pb, Se, V. DNA damage (using

the comet assay), oxidative damage (ROS production and localization) and related response mechanisms (activity of antioxidant enzymes), presence of chelating molecules (glutathione and phytochelatins) were investigated. All biomarkers provided an answer closely related to the pollution conditions at the 3 sites. We discuss the data considering the possibility of using these biological changes as environmental pollution biomarkers. Finally, it is underlined the importance of phytochelatins in spite of their specificity for metal pollution.

Keywords: Biomarkers, Environmental pollution, heavy metals, “land of fires”, *Lunularia cruciata*

1. Introduction

A health and environmental great concern has been raised about the notorious "Land of fires", in Campania Region (Southern Italy), so called because of the burning of waste and fraudulent dumping. In fact vast areas to the east of Campania Region (Naples and Caserta Province) have been involved for decades in illegal and uncontrolled spilling of industrial and urban waste and an alarming increase in the incidence of chronic-degenerative diseases and tumors has been recorded.

Although it has been hypothesized, a specific causal relation has not yet established between the toxic waste exposure and the increased development and mortality for cancer (Maselli et al., 2019). A recent paper studied blood concentrations of As, Cd, Cr and Pb metals in 95 patients with different kinds of cancer and in 27 healthy individuals; cancer patients from municipalities affected by the toxic fires showed higher blood concentrations of the heavy metals than healthy individuals (Forte et al., 2019).

Taking into account the well-known cause-effect relationship between tumor and metal exposure, the metal high levels detected in patients with cancer demand an accurate evaluation of the biological effects of pollution in the whole affected area, possibly by the means of fast, reliable and cost-effective methods, such as the evaluation of pollution biomarkers in biological organisms.

Bryophytes, due to the lacking of a root system and a thick cuticle, taking advantage of a high surface/volume ratio and a high cation-exchange capacity, absorb nutrients through their whole surface. All that makes them sensitive to the atmospheric deposition and effective at absorbing and sometimes bioaccumulating metals and other pollutants from the environment.

All those reasons explain why they are regarded as extraordinary system and have been used since the 1960s to monitor environmental pollution and heavy metal contamination, even more considering their wide distribution in the most diverse habitats (Bargagli, 1998; Harmens et al., 2012; Ruhling, 1968; Steinnes, 1995).

The liverwort *Lunularia cruciata* L. (Dum.) was employed to estimate the in vitro effects of heavy metals on different cellular responses, such as tissue localization, ultrastructural alteration and changes in gene expression and transcription (Basile et al., 2005; Carginale et al., 2004). Samples of *L. cruciata* collected in the heart of the land of fires showed alarming concentrations of toxic heavy metals as Cd, Cr, Pb as well as changes in:

ultrastructure, vitality, chlorophyll degradation, photosynthetic efficiency, expression and occurrence of heat shock protein 70 (Hsp70) (Basile et al., 2017).

It is well-known that reactive oxygen species (ROS) are involved in almost all abiotic stresses, including heavy metals, as signals in downstream responses (Maresca et al., 2018). ROS overproduction in plants can trigger redox-sensitive pathways such as enzymatic and non-enzymatic antioxidant mechanisms that have the capacity to counteract the oxidative stress.

Enzymatic antioxidant mechanisms include the interaction of different enzymes. Antioxidant enzymes that intervenes to defend the cell from the effects of ROS are superoxide dismutase (SOD), catalase (CAT), peroxidase (POX) and the detoxifying enzyme glutathione S-transferase (GST). In addition to trigger defense mechanisms, ROS induce different alterations including DNA damage. In particular, recent studies have shown that DNA damage measured in plants using the Comet assay is a suitable tool for the assessment of genotoxicity of metal polluted environments (Maresca et al., 2018).

In plants, phytochelatins (PCn) play an important role in metal detoxification system (Sanità di Toppi and Gabbrielli, 1999), directly obtained from GSH. PCn, (γ-glutamylcysteine [EC])n-glycine, are thiolic peptide that chelate metals and compartmentalize them in the vacuole (Grill et al., 1985), in order to quickly detoxify the cytosolic environment.

This study was carried out to study the effects of environmental pollution on the liverwort *L. cruciata* collected from the heart of the land of fires, in terms of DNA damage, oxidative damage (ROS), activity of antioxidant enzymes, and the synthesis of phytochelatins, in comparison with samples of the same species from two other sites characterized by different contamination of heavy metal pollution.

2. Materials and Methods

2.1. Study sites

Three sites were chosen as representative of three different pollution conditions:

Site Ri: Riccia (Molise, Italy) town of 3500 inhabitants surrounded by green hills and far from known sources of pollution.

Site Na: The city center of Naples (Campania, Italy): at the Botanical Garden of the University, in a central area affected by heavy metal pollution, mainly originating from vehicular traffic.

Site Ac: Acerra (Campania, Italy), in the "land of fires", where organized crime and "less conscientious citizens" burn outdoors waste of all kinds, which is also characterized by a high traffic load, heavy industry and intensive agriculture.

2.2. Plant material

The metal-tolerant liverwort *L. cruciata* L. (Dum.) was randomly collected at three sampling points for each site. The collection points should satisfy the following characteristics: *L. cruciata* present on at least 20 cm deep soil and with a cover of at least 10 cm^2, distance from a roads of at least 5 meters. Samples were collected from moist soil and were maintained in Petri dishes and processed in the laboratory within 6 h from collection. While considering protocol European moss survey (Harmens et al., 2008), We could not follow it closely, as it considers monitoring by moss on a large scale. At each point, the superficial (5 cm) soil beneath *L. cruciata* was also collected and analyzed.

2.3. Soil analysis

We followed the protocol of Mao et al., (2017) with some modifications. Approximately 0.2g (dry weight) of soil samples were weighed into a beaker. A combination of 6 mL of HNO_3, 2 mL of HCl and 2 mL of HF was used for the simultaneous extraction of many metals in soils. The solution was digested in a Microwave digestion system (CEM, MARS 6, USA).

The determination of metals was performed by ICP-MS with internal standard method and standard addition method as reported in Maisto et al., (2011)

2.4. Metal bioaccumulation

After collection of 125 mg of *L. cruciata* from each site, we removed soil particles and other material from samples. Successively, we dried samples at 105 °C for 24 h, and homogenized in an agate mortar in according to Basile et al., (2017). The digested material was analyzed by inductively coupled plasma-mass spectrometry (Perkin Elmer Elan 600) for Al, As, Cd, Cr, Cu, Fe, Mn, Pb, V, Hg and Ni content.

2.5. Imaging of peroxides with 2',7'-dichlorofluorescein diacetate

Fluorescent probe 2'- 7'dichlorofluorescein diacetate DCF-DA (Sigma) was solubilized in dimethyl sulfoxide and then diluted in 10 mM Tris-HCl (pH 7.4) to obtain a 25 μM solution. Thin cross sections of sample thalli were incubated in the DCF-DA solution for 30', then washed three times for 10 min each in the same buffer. As negative control, pieces of thalli from Acerra were incubated in the buffer solution with no DCF-DA and then washed as before. For confocal microscopy observation, the sections from *L. cruciata* samples were analyzed with a laser-scanning confocal microscope (Leica TCS SP5, Wetzlar, Germany). An excitation source at 496 nm was employed; the emission bandwidths were 506/585 nm (green light) and 615/715 nm (red light) (begin - end). Objectives were used as reported in Degola et al., (2014). Data were collected and processed with the software LAS AF (Leica).

2.6. Detection of ROS

A fluorescent technique using 2',7'-dichlorofluorescin diacetate (DCFH-DA) has been used for quantitative measurement of ROS production. ROS quantity was evaluated according to Maresca et al., (2018).

2.7. Antioxidant activity enzyme

Enzyme extraction and the determination of SOD, CAT, and GST activities was performed as reported in Maresca et al., (2018).

2.8. DNA damage

The typical Comet assay for animal and human cells is not able to lyse plant cell wall, so plant nuclei have to isolated mechanically (Gichner and Plewa, 1998). The plant material was cut into thin slices using a razor blade on a plate kept on ice, tilted so that the removed

nuclei collect in the buffer. The protocol was performed as reported in Maresca et al., (2018). A computerized image-analysis system (CometScore) was employed. Twenty-five nuclei per slide were isolated, three slides per treatment were observed and each treatment was repeated at least twice.

From the repeated experiments, DNA damages, Tail moment and Olive moment from each slide were calculated.

2.9. Thiol-peptides extraction, characterization and quantification by HPLC-ESI-MS-MS

Thiol-peptides extraction, characterization and quantification by HPLC-ESI-MS-MS was performed as reported in Bellini et al., (2019).

2.10. Statistical analysis

Owing to the limited dataset, non-parametric statistics were used. Kruskal-Wallis ANOVA was run to check for differences ($p<0.05$) among the three sites, and the Spearman rank correlation coefficient was calculated among parameters. Data analysis was performed using the software Statistica 7.0 (StatSoft, Inc., Tulsa OK, USA).

3. Results

3.1. Soil analysis

The most interesting data that can be observed in the Table 1 is the alarming increase in toxic metals such as Ba, Cd, Cr and Pb which follow a significant increasing trend from Riccia to Naples up to Acerra, and in particular cadmium which is almost ten-fold compared to the uncontaminated site. Differences did not emerge for Al, Cu, Hg, Mn and Ni between Riccia and Napoli, while these elements were significantly higher at Acerra.

3.2. Metal bioaccumulation

Al, Cd, Cr, Cu, Pb, Hg and Ni concentrations were significantly ($P < 0.05$) lower at Riccia and higher at Acerra, and intermediate at Naples (Table 2).

Concentrations of Fe and As were higher at Acerra and Naples and significatively lower at Riccia; concentrations of Mn and V were higher at Acerra and did not show up significantly difference between Riccia and Napoli.

3.3. Imaging of peroxides with 2',7'-dichlorofluorescein diacetate

Confocal microscopy observations after ROS labeling with DCF showed emission signals from *L. cruciata* samples from all sites. Under the excitation at 496 nm, two different signals were recorded: the green light from DFC-ROS conjugates and the red one from unstained chloroplasts. All the 3 panels (Fig. 1.) showed clear red signals, while evident differences were recorded in the green light emissions, with the Riccia (Fig1 a-c) samples emitting the least and the Acerra (Fig1. g-i) ones the highest. The samples from Naples (Fig1. d-f) showed an intermediate green signal. Unstained negative control samples from Acerra gave no green light signal.

3.4. Detection of ROS and activity of antioxidant enzymes

Low ROS values were measured in the samples collected at Riccia, while higher values were measured at Naples, and the highest at Acerra (Fig. 2).

The antioxidant activity expressed by CAT showed low values in the samples collected at Riccia, while high values were measured both in the samples collected at Naples and

Acerra (Fig. 2). SOD and GST activity increased gradually from Riccia to Naples up to Acerra (Fig. 2).

3.5. Comet Assay

The results showed that DNA damage, detected by the %DNA damage, Tail and Olive Moment, was lower at Riccia and increased at Naples and especially at Acerra (Fig. 3)

3.6. GSH and Phytochelatins

HPLC-ESI-MS-MS analysis detected the presence of thiol peptides (GSH and PC_{2-4}), in samples collected at the three investigated sites (Fig. 4). The amount of GSH was not different across sites. On the other hand, the levels of PCn increased considerably from Riccia to Naples up to Acerra (Fig. 4). In detailed, PC_2 was responsible of this trend while PC_3 and PC_4 were synthesized in comparable amount at the three sites (Fig. 4).

3.7. Correlations

In the soil: the Table S1 shows that the metals Al, Cd, Cr, Hg and Pb are strongly correlated with each other. Furthermore, they are all strongly correlated with ROS, CAT, SOD, GST, %DNA in Tail, Tail Moment, Olive Moment and PC_2 and PCtot. Biological activities such as ROS, CAT, SOD, GST, %DNA in Tail, Tail Moment, Olive Moment and PC_2 and PCtot are all strongly correlated to each other. GSH, PC_3, and PC_4 showed no correlation with any of the measured parameters.

As for as metal bioaccumulation the table S1 shows that the biological activities such as ROS, CAT, SOD, GST, %DNA in Tail, Tail Moment, Olive Moment and PC_2 and PCtot except GSH, PC_3, and PC_4, are strongly correlated to all the metals considered.

4. Discussion

Studies carried out on bryophytes and lichens could be used in epidemiological investigations. However, since bryophytes, as the other plants, are sessile organisms are influenced by parameters other than those that affect human health, the comparison between the data must therefore be carried out with caution. Nevertheless, biomonitors can provide information on the effects that pollution could have on human health, giving

indications useful for risk areas. An important example of this is the paper of Cislaghi and Nimis, (1997) which compares the biodiversity of epiphytic lichens with mortality from lung cancer in the Veneto region (N Italy).

There are several studies showing that bioindicator organisms capable of bioaccumulating polluting substances or responding to them in a coherent way, can give precise and useful indications of the health of a given environment that reflects on human health (e.g. (Lequy et al., 2019). The liverwort *L. cruciata* lives anchored to the ground, and it usually uptakes water and minerals both from the atmosphere and the solution circulating in the soil.

In this work, chemical soil analysis clearly showed a marked pollution by Ba, Cd, Cr, and Pb at Acerra and Naples, and also by Al, Cu, Hg, Mn and Ni at Acerra. In addition, the biological responses considered, were strongly correlated with these heavy metals both present in the soil and bioaccumulated within the gametophyte. It is noteworthy that Cd and Cr exceed the legal limits for heavy metals in soils. Notwithstanding the small number of measurements carried out, this outcome should be regarded as a sentinel prompting for a systematic soil analysis in that area.

On the other hand, the contribution of air pollution cannot be excluded, as it certainly influences both the concentrations of pollutants in the soil and in the liverwort through direct absorption (Basile et al., 2017). Our data on the concentration of metals in the soil, although extremely limited, agree with the results shown in the paper of (Forte et al., 2019) in which the presence heavy metals as Cd, Hg and Pb were demonstrated in patients from the land of fires. Considering the data on the accumulation of metals in *L. cruciata* (Basile et al., 2017) and the bioaccumulation in moss and lichen bags (Basile et al., 2012, 2009, 2008) find that in all cases the bioindicator organism considered, liverwort, moss or lichen, showed an accumulation of these metals in relation to environmental pollution, confirming the possibility of using a bioindicator organism as a sentinel for pollution conditions.

The confocal microscopy observations showed evident differences in the fluorescence emissions among the three samples, with Riccia samples emitting only a barely visible green light, Acerra samples giving the highest signal, Naples samples being intermediate. Differently, the red light signals were comparable in all the three samples. The latter red signal is related to the natural autofluorescence of chloroplasts due to chlorophyll and other naturally occurring pigments; the green signals depend on the DCF-ROS conjugates. DCF-DA has been used to show intracellular oxidants in plant tissues (Rodríguez-Serrano et al.,

2006; Shapiro and Zhang, 2001). This molecule can enter the cell, where it is modified to DCF, which is trapped inside the cell and, upon reaction with ROS, detected as fluorescent DCF-derived compound (Sandalio et al., 2008). Our confocal microscopy observations are consistent with ROS analyses, which showed the lowest ROS content at Riccia and the highest at Acerra.

In this work, both oxidative stress including the activity of antioxidant enzymes, and DNA damage were strongly correlated to the degree of pollution of the most heavy metal such as Pb, Cr and Cd. Although some heavy metals (Cu, Zn) are essential micronutrients for plants, they can all give a toxic effect (Aravind and Prasad, 2005; Kimbrough et al., 1999; Vázquez et al., 1987). Heavy metals, as Pb, Cd, and Cr, Hg, As can directly or indirectly induce ROS generation (Valko et al., 2006). Oxygen radicals H_2O_2, ·OH and O_2^-, are very reactive compounds produced during different types of abiotic and biotic stress (Apel and Hirt, 2004). When in excess, ROS can lead to manifold toxic effects such as lipid peroxidation, damage to DNA and proteins (Ünyayar et al., 2006).

Our results showed that ROS production and the antioxidant activity of scavenger enzymes in *L. cruciata,* underlined the fact that in the most polluted sites (Acerra and Naples) the production of ROS was immediately balanced by enzymatic activation with an increase in SOD activity, CAT, and GST. These results indicate that organisms exposed to high pollution conditions can generate ROS which through different biochemical processes can lead to the development of defense mechanisms such as the activation of antioxidant enzymes SOD, CAT and GST. As far as ROS levels, a statistically significant increase was measured from Riccia to Naples to Acerra. With respect to the activity of antioxidant enzymes there are two different trends: the activity of GST and SOD undergo a significant increase from Riccia in Naples to Acerra; CAT activity is significantly lower in Riccia, but no statistically significant differences in this activity were measured between the two polluted sites, Naples and Acerra. We can therefore state that the activity of catalase have not proved to be extremely sensitive biomarkers such as to discriminate between two different polluted sites.

The Comet Assay is a sensitive technique in estimating DNA damage on the single and the double strand (Gedik et al., 1992; Singh et al., 1988). The determination of DNA damage using the Comet assay in indicator organisms provides us with early information on the genotoxic potential of the environment in which they live, making it possible to improve

environmental intervention strategies. Using three of the many parameters available to evaluate DNA damage through a comet assay, in particular the Olive Moment, Tail Moment and percentage of DNA in tail, we evaluated that DNA damage level increases statistically significantly from Riccia to Naples to Acerra following the trend of presence of heavy metals in the soil and bioaccumulation of toxic metals in the *L. cruciata* (Basile et al., 2017). Studies have shown that DNA damage, measured in plants, using comet assay, is an excellent biomarker, extremely sensitive for estimating the genotoxic potential of environmental contaminants, both in environmental monitoring studies and for environmental screening. Our data, for the first time, confirmed the use of Comet assay also in liverworts, as reliable biomarker of environmental pollution. Furthermore, it should not surprise to find a strong correlation between the quantity of ROS and the damage to DNA as an excess of ROS can, among other effects, also cause damage to DNA including its breakdown, which, however, can also depend on a direct effect of heavy metals on the nucleotide (Roldán-Arjona and Ariza, 2009).

From the characterization and quantification of the tiol peptides, it was found that the phytochelatins 3 (PC_3) and the phytochelatins 4 (PC_4) were found to be low at all sites, while the phytochelatins 2 (PC_2) showed increasing values from Riccia to Naples to Acerra. This outcome is at some variance with other results. (Degola et al., 2014) showed that *in vitro* exposure of *L. cruciata* to heavy metals for one week caused an increase in PC_2, but also in PC_3 and PC_4. Interestingly, the only metals that were able to increase the activity of PC_3 and PC_4 *in vitro* were Cd, Fe and Zn, while As, Cu, Hg, Pb and Sb were not, at any concentration. Similarly, (Fontanini et al., 2018) reported an increase in PC_2, PC_3 and PC_4 in the alga *Nitella mucronata* following treatment with Cd and Fe. Based on these outcomes, we may speculate that the three phytochelatins take part in the heavy metal detoxification process with different roles: PC_3 and PC_4 (alert) could be regarded as a "short-term response", as they are mainly produced in response to an unexpected stress situation and to which the plant has not had time to adapt; in addition such response is triggered by a limited number of metals. On the other hand, PC_2 (adaptation) could play a "long-term" response, being abundant in the case of long-lasting sources of pollution; in addition they seem to respond to a wider number of metals.

5. Conclusions

The results of the present study suggest that the site located inside the “land of fires” has an alarming soil pollution from toxic metals; the biological responses considered, oxidative stress, DNA damage and the synthesis of phytochelatins, responded consistently with the expected environmental stress and were related to the concentrations of the most toxic metals found in the soil. In the context of heavy metal pollution, among the parameters investigated, the biomarker of greatest interest is probably PC_2, since its increase is specifically related to toxic metal occurrence.

Table and Figure

		Ri	Na	Ac
Al	g/Kg	14.19 ± 0.68 a	15.3 ± 1.07 a	19.66 ± 1.23 b
V	mg/Kg	26.77 ± 0.49 a	27.58 ± 2.83 a	31.27 ± 3.39 a
Cr	mg/Kg	2.59 ± 0.35 a	4.63 ± 0.44 b	6.75 ± 0.78 c
Mn	mg/Kg	286 ± 1.89 a	287 ± 6.89 a	346 ± 6.46 b
Fe	g/Kg	9.16 ± 1.05 a	9.92 ± 1.80 a	10.72 ± 1.26 a
Ni	mg/Kg	2.85 ± 0.21 a	3.01 ± 0.44 a	4.61 ± 0.53 b
Cu	mg/Kg	23 ± 2 a	21 ± 2.05 a	27 ± 1.77 b
As	mg/Kg	5.04 ± 0.94 a	6.02 ± 1.23 a	7.11 ± 0.85 a
Se	mg/Kg	0.92 ± 0.07 a	1.02 ± 0.25 a	1.37 ± 0.38 a
Cd	mg/Kg	0.20 ± 0.02 a	0.92 ± 0.28 b	1.89 ± 0.09 c
Ba	mg/Kg	115 ± 0.90 a	122 ± 2.53 b	149 ± 5.51 c
Hg	mg/Kg	0.05 ± 0.01 a	0.06 ± 0.01 a	0.08 ± 0.01 b
Pb	mg/Kg	30.16 ± 1.51 a	39.31 ± 2.31 b	49.01 ± 4.26 c

Table 1. Concentration (mean±st.dev, mg/kg) of heavy metals measured in soil samples. Values not followed by the same letter are significantly different ($p<0.05$).

	Ri	Na	Ac
Al	1111 ± 191a	2544 ± 114b	3386 ± 168c
As	0.45 ± 0.05a	1.13 ± 0.32b	1.49 ± 0.35b
Cd	0.18 ± 0.01a	1.46 ± 0.11b	3.36 ± 0.25c
Cu	3.9 ± 0.72a	12.7 ± 2.30b	20.13 ± 0.36c
Cr	0.88 ± 0.02a	1.53 ± 0.15b	3.96 ± 0.41c
Fe	624 ± 56a	804 ± 28.53b	843 ± 10.44b
Pb	3.1 ± 0.2a	13.26 ± 0.92b	19.22 ± 0.09c
Mn	32.73 ± 2.34a	36.24 ± 2.62a	39.49 ± 0.55b
V	1.73 ± 0.20a	2.06 ± 0.66ab	2.53 ± 0.15b
Hg	0.19 ± 0.03a	0.26 ± 0.02b	0.39 ± 0.02c
Ni	2.06 ± 0.4a	4.71 ± 0.15b	12 ± 0.33c

Table 2. Mean concentration (±standard deviation; µg/g dw) of heavy metals bioaccumulated in *Lunularia cruciata* samples collected at the three sampling sites.

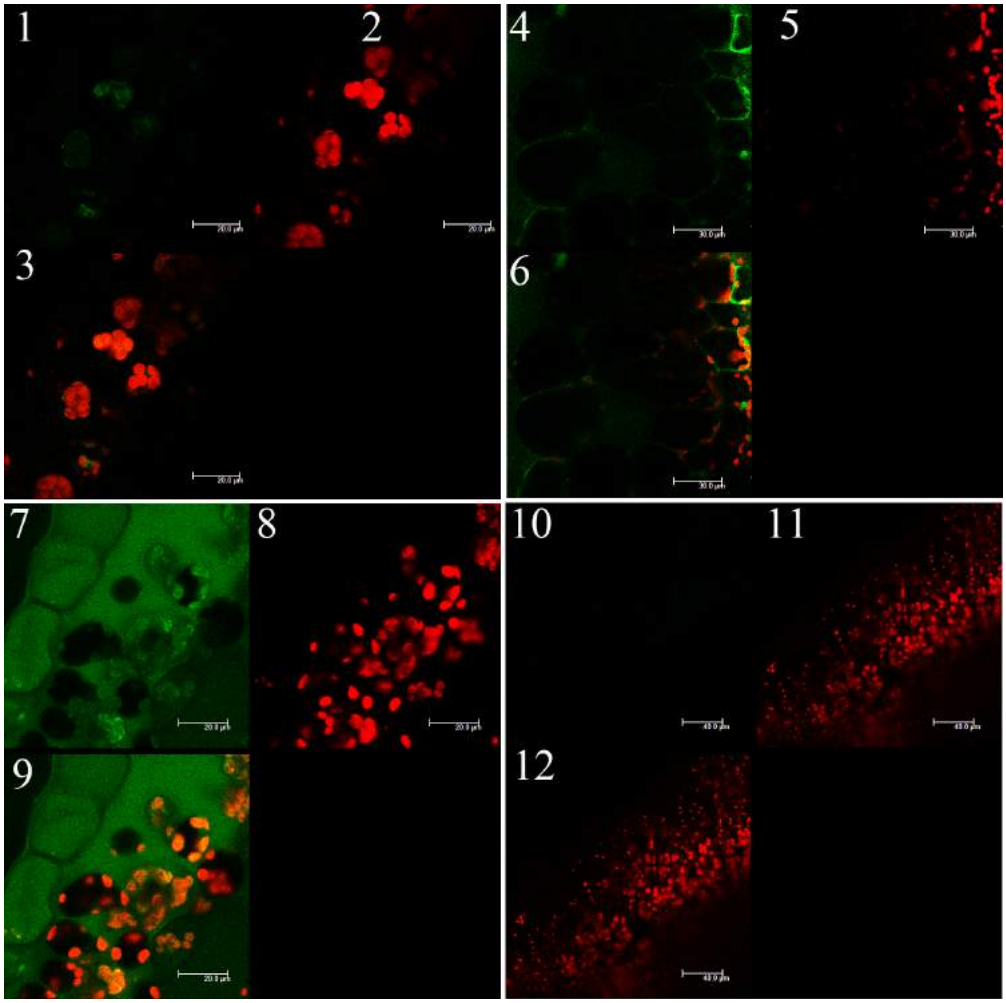

Figure 1. Upper thalli of *L. cruciata* samples observed under the confocal laser microscope. Each panel (figs.a-c, figs.d-f, figs.g-i, and figs. l-n) is composed of 3 figures representing green light from DFC-ROS conjugates, red light from autofluorescent chloroplasts and a merge of the two emissions, respectively. Figs.a-c show *L. cruciata* samples from Riccia with a faint green light and a clear red light emission. Figs.d-f show *L. cruciata* samples from Naples with a green light intermediate between Riccia and Acerra samples and a clear red light signal. Figs.g-i show *L. cruciata* samples from Acerra with clear green and red light signals. Figs. l-n show unstained *L. cruciata* samples from Acerra with no green light, but red signal. **Scale bars:** 20 µm (figs a-c and g-i); 30 µm (figs. d-f); 40 µm (figs. l-n).

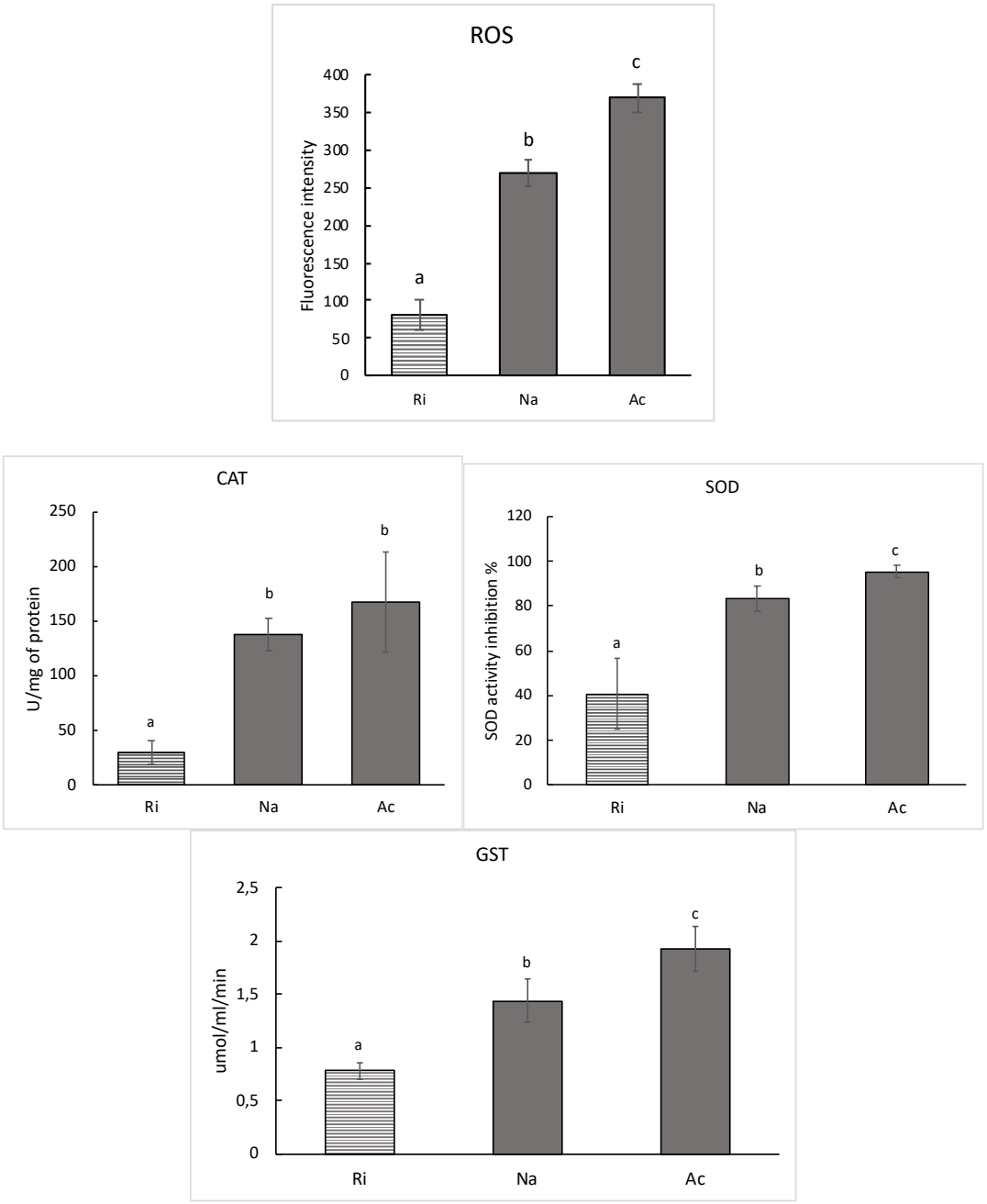

Figure 2. ROS production (fluorescence intensity) and antioxidant responses (SOD, SOD activity inhibition %, CAT, U/mg of protein, GST, umol/ml/min,) in the sample (Riccia, Ri; Napoli, Na; Acerra, Ac). Values are presented as mean ± st. dev. Means not accompanied by the same letter are significantly different at $p < 0.05$.

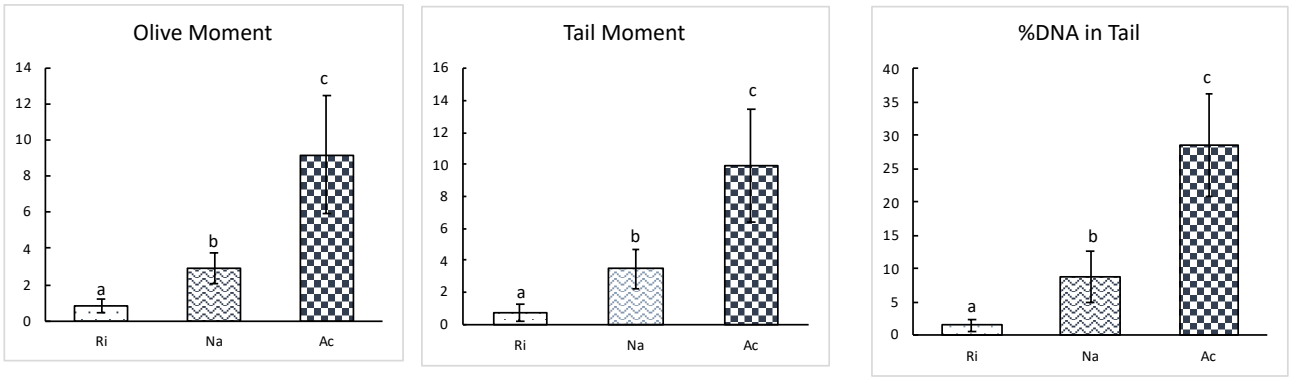

Figure 3. Comet assay results (DNA damages, Tail moment and Olive moment) in the sample (Riccia, Ri; Napoli, Na; Acerra, Ac). Values not followed by the same letter are significantly ($p<0.05$) different.

Thiol-peptides (nmol g^{-1}FW)					
	GSH	PC_2	PC_3	PC_4	PCn Tot
ACERRA	0.199 ± 0.026	3.672 ± 0.172	0.047 ± 0.006	0.022 ± 0.001	3.741 ± 0.170
NAPOLI	0.238 ± 0.039	2.474 ± 0.185	0.046 ± 0.004	0.026 ± 0.002	2.547 ± 0.187
RICCIA	0.257 ± 0.032	1.802 ± 0.194	0.051 ± 0.007	0.028 ± 0.002	1.881 ± 0.200

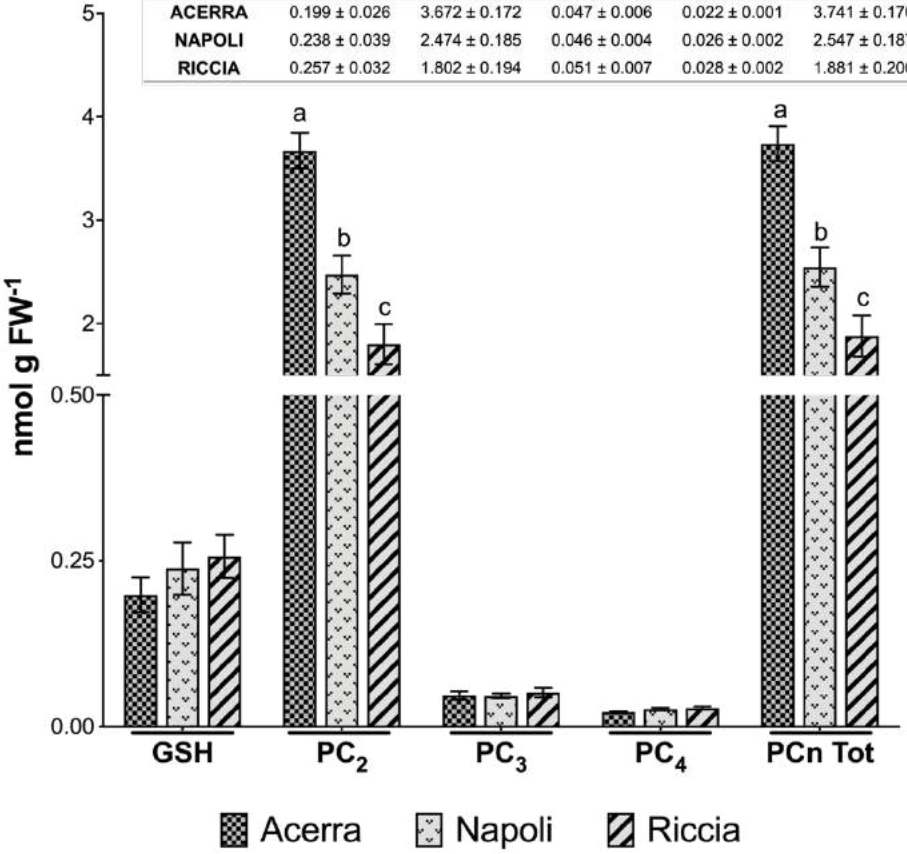

Figure 4. Content (mean±SE, nmol/g fw) of GSH and PCn in *L. cruciata* samples collected at the three sites investigated. Values not marked by the same letter are significantly ($p<0.05$) different.

Reference

Apel, K., Hirt, H., 2004. REACTIVE OXYGEN SPECIES: Metabolism, Oxidative Stress, and Signal Transduction. Annu. Rev. Plant Biol. 55, 373–399. https://doi.org/10.1146/annurev.arplant.55.031903.141701

Aravind, P., Prasad, M.N.V., 2005. Modulation of cadmium-induced oxidative stress in Ceratophyllum demersum by zinc involves ascorbate–glutathione cycle and glutathione metabolism. Plant Physiol. Biochem. 43, 107–116. https://doi.org/10.1016/j.plaphy.2005.01.002

Bargagli, R., 1998. Trace elements in terrestrial plants. Springer.

Basile, A., Alba di Nuzzo, R., Capasso, C., Sorbo, S., Capasso, A., Carginale, V., 2005. Effect of cadmium on gene expression in the liverwort Lunularia cruciata. Gene 356, 153–159. https://doi.org/10.1016/j.gene.2005.04.017

Basile, A., Loppi, S., Piscopo, M., Paoli, L., Vannini, A., Monaci, F., Sorbo, S., Lentini, M., Esposito, S., 2017. The biological response chain to pollution: a case study from the "Italian Triangle of Death" assessed with the liverwort Lunularia cruciata. Environ. Sci. Pollut. Res. 24, 26185–26193. https://doi.org/10.1007/s11356-017-9304-y

Basile, A., Sorbo, S., Aprile, G., Conte, B., Castaldo Cobianchi, R., 2008. Comparison of the heavy metal bioaccumulation capacity of an epiphytic moss and an epiphytic lichen. Environ. Pollut., Proceedings of the 4th International Workshop on Biomonitoring of Atmospheric Pollution (With Emphasis on Trace Elements) 151, 401–407. https://doi.org/10.1016/j.envpol.2007.07.004

Basile, A., Sorbo, S., Aprile, G., Conte, B., Castaldo Cobianchi, R., Pisani, T., Loppi, S., 2009. Heavy metal deposition in the Italian "triangle of death" determined with the moss Scorpiurum circinatum. Environ. Pollut. 157, 2255–2260. https://doi.org/10.1016/j.envpol.2009.04.001

Basile, A., Sorbo, S., Conte, B., Cobianchi, R.C., Trinchella, F., Capasso, C., Carginale, V., 2012. Toxicity, Accumulation, and Removal of Heavy Metals by Three Aquatic Macrophytes. Int. J. Phytoremediation 14, 374–387. https://doi.org/10.1080/15226514.2011.620653

Bellini, E., Borsò, M., Betti, C., Bruno, L., Andreucci, A., Ruffini Castiglione, M., Saba, A., Sanità di Toppi, L., 2019. Characterization and quantification of thiol-peptides

in Arabidopsis thaliana using combined dilution and high sensitivity HPLC-ESI-MS-MS. Phytochemistry 164, 215–222. https://doi.org/10.1016/j.phytochem.2019.05.007

Carginale, V., Sorbo, S., Capasso, C., Trinchella, F., Cafiero, G., Basile, A., 2004. Accumulation, localisation, and toxic effects of cadmium in the liverwort Lunularia cruciata. Protoplasma 223, 53–61. https://doi.org/10.1007/s00709-003-0028-0

Cislaghi, C., Nimis, P.L., 1997. Lichens, air pollution and lung cancer. Nature 387, 463–464. https://doi.org/10.1038/387463a0

Degola, F., De Benedictis, M., Petraglia, A., Massimi, A., Fattorini, L., Sorbo, S., Basile, A., Sanità di Toppi, L., 2014. A Cd/Fe/Zn-Responsive Phytochelatin Synthase is Constitutively Present in the Ancient Liverwort Lunularia cruciata (L.) Dumort. Plant Cell Physiol. 55, 1884–1891. https://doi.org/10.1093/pcp/pcu117

Fontanini, D., Andreucci, A., Ruffini Castiglione, M., Basile, A., Sorbo, S., Petraglia, A., Degola, F., Bellini, E., Bruno, L., Varotto, C., Sanità di Toppi, L., 2018. The phytochelatin synthase from Nitella mucronata (Charophyta) plays a role in the homeostatic control of iron(II)/(III). Plant Physiol. Biochem. 127, 88–96. https://doi.org/10.1016/j.plaphy.2018.03.014

Forte, I.M., Indovina, P., Costa, A., Iannuzzi, C.A., Costanzo, L., Marfella, A., Montagnaro, S., Botti, G., Bucci, E., Giordano, A., 2019. Blood screening for heavy metals and organic pollutants in cancer patients exposed to toxic waste in southern Italy: A pilot study. J. Cell. Physiol. https://doi.org/10.1002/jcp.29399

Gedik, C.M., Ewen, S.W.B., Collins, A.R., 1992. Single-cell Gel Electrophoresis Applied to the Analysis of UV-C Damage and Its Repair in Human Cells. Int. J. Radiat. Biol. 62, 313–320. https://doi.org/10.1080/09553009214552161

Gichner, T., Plewa, M.J., 1998. Induction of somatic DNA damage as measured by single cell gel electrophoresis and point mutation in leaves of tobacco plants. Mutat. Res. Mol. Mech. Mutagen. 401, 143–152. https://doi.org/10.1016/S0027-5107(98)00003-7

Grill, E., Winnacker, E.-L., Zenk, M.H., 1985. Phytochelatins: The Principal Heavy-Metal Complexing Peptides of Higher Plants. Science 230, 674–676. https://doi.org/10.1126/science.230.4726.674

Harmens, H., Ilyin, I., Mills, G., Aboal, J.R., Alber, R., Blum, O., Coşkun, M., De Temmerman, L., Fernández, J.Á., Figueira, R., Frontasyeva, M., Godzik, B., Goltsova, N., Jeran, Z., Korzekwa, S., Kubin, E., Kvietkus, K., Leblond, S., Liiv, S., Magnússon, S.H., Maňkovská, B., Nikodemus, O., Pesch, R., Poikolainen, J., Radnović, D., Rühling, Å., Santamaria, J.M., Schröder, W., Spiric, Z., Stafilov, T., Steinnes, E., Suchara, I., Tabors, G., Thöni, L., Turcsányi, G., Yurukova, L., Zechmeister, H.G., 2012. Country-specific correlations across Europe between modelled atmospheric cadmium and lead deposition and concentrations in mosses. Environ. Pollut. 166, 1–9. https://doi.org/10.1016/j.envpol.2012.02.013

Harmens, H., Norris, D., Cooper, D., Hall, J., Kubin, E., Piispanen, J., Poikolainen, J., Karhu, J., 2008. Spatial trends in nitrogen concentrations in mosses across Europe in 2005/2006. Report on Nitrogen in European Mosses. Work package 4. The UNECE International Cooperative Programme on Vegetation. Centre for Ecology & Hydrology, Wales, UK, Saint Ives (41 authors, participants of the moss survey, from Metla Kubin, E., Piispanen, J., Poikolainen, J., Karhu, J.).

Kimbrough, D.E., Cohen, Y., Winer, A.M., Creelman, L., Mabuni, C., 1999. A Critical Assessment of Chromium in the Environment. Crit. Rev. Environ. Sci. Technol. 29, 1–46. https://doi.org/10.1080/10643389991259164

Lequy, E., Siemiatycki, J., Leblond, S., Meyer, C., Zhivin, S., Vienneau, D., de Hoogh, K., Goldberg, M., Zins, M., Jacquemin, B., 2019. Long-term exposure to atmospheric metals assessed by mosses and mortality in France. Environ. Int. 129, 145–153. https://doi.org/10.1016/j.envint.2019.05.004

Maisto, G., Manzo, S., Nicola, F.D., Carotenuto, R., Rocco, A., Alfani, A., 2011. Assessment of the effects of Cr, Cu, Ni and Pb soil contamination by ecotoxicological tests. J. Environ. Monit. 13, 3049–3056. https://doi.org/10.1039/C1EM10496A

Mao, J., Liu, X., Chen, B., Luo, F., Wu, X., Jiang, D., Luo, Z., 2017. Determination of heavy metals in soil by inductively coupled plasma mass spectrometry (ICP-MS) with internal standard method. Electron. Sci. Technol. Appl. 4. https://doi.org/10.18686/esta.v4i1.36

Maresca, V., Fusaro, L., Sorbo, S., Siciliano, A., Loppi, S., Paoli, L., Monaci, F., karam, E.A., Piscopo, M., Guida, M., Galdiero, E., Insolvibile, M., Basile, A., 2018.

Functional and structural biomarkers to monitor heavy metal pollution of one of the most contaminated freshwater sites in Southern Europe. Ecotoxicol. Environ. Saf. 163, 665–673. https://doi.org/10.1016/j.ecoenv.2018.07.122

Maselli, V., Maresca, V., Fusco, L., Petrelli, S., Galdiero, E., Guida, M., Fulgione, D., 2019. Frog as Sentinel of Human Cancer Incidence in Southern Italy's So-Called 'Terra dei Fuochi.' Pol. J. Environ. Stud. 28, 3527–3532. https://doi.org/10.15244/pjoes/94051

Rodríguez-Serrano, M., Romero-Puertas, M.C., Zabalza, A., Corpas, F.J., Gómez, M., Río, L. a. D., Sandalio, L.M., 2006. Cadmium effect on oxidative metabolism of pea (Pisum sativum L.) roots. Imaging of reactive oxygen species and nitric oxide accumulation in vivo. Plant Cell Environ. 29, 1532–1544. https://doi.org/10.1111/j.1365-3040.2006.01531.x

Roldán-Arjona, T., Ariza, R.R., 2009. Repair and tolerance of oxidative DNA damage in plants. Mutat. Res. Mutat. Res. 681, 169–179. https://doi.org/10.1016/j.mrrev.2008.07.003

RUHLING, A., 1968. An ecological approach to the lead problem. Bot. Not. 121, 321–342.

Sandalio, L.M., Rodríguez-Serrano, M., Romero-Puertas, M.C., del Río, L.A., 2008. Imaging of Reactive Oxygen Species and Nitric Oxide In Vivo in Plant Tissues, in: Methods in Enzymology, Nitric Oxide, Part F. Academic Press, pp. 397–409. https://doi.org/10.1016/S0076-6879(07)00825-7

Sanità di Toppi, L., Gabbrielli, R., 1999. Response to cadmium in higher plants. Environ. Exp. Bot. 41, 105–130. https://doi.org/10.1016/S0098-8472(98)00058-6

Shapiro, A.D., Zhang, C., 2001. The Role of NDR1 in Avirulence Gene-Directed Signaling and Control of Programmed Cell Death in Arabidopsis. Plant Physiol. 127, 1089–1101. https://doi.org/10.1104/pp.010096

Singh, N.P., McCoy, M.T., Tice, R.R., Schneider, E.L., 1988. A simple technique for quantitation of low levels of DNA damage in individual cells. Exp. Cell Res. 175, 184–191. https://doi.org/10.1016/0014-4827(88)90265-0

Steinnes, E., 1995. A critical evaluation of the use of naturally growing moss to monitor the deposition of atmospheric metals. Sci. Total Environ., Ecological Effects of

Arctic Airborne Contaminants 160–161, 243–249. https://doi.org/10.1016/0048-9697(95)04360-D

Ünyayar, S., Çelik, A., Çekiç, F.Ö., Gözel, A., 2006. Cadmium-induced genotoxicity, cytotoxicity and lipid peroxidation in Allium sativum and Vicia faba. Mutagenesis 21, 77–81. https://doi.org/10.1093/mutage/gel001

Valko, M., Rhodes, C.J., Moncol, J., Izakovic, M., Mazur, M., 2006. Free radicals, metals and antioxidants in oxidative stress-induced cancer. Chem. Biol. Interact. 160, 1–40. https://doi.org/10.1016/j.cbi.2005.12.009

Vázquez, M.D., Poschenrieder, C., Barceló, J., 1987. Chromium VI Induced Structural and Ultrastructural Changes in Bush Bean Plants (Phaseolus vulgaris L.). Ann. Bot. 59, 427–438. https://doi.org/10.1093/oxfordjournals.aob.a087331

CHAPTER 2

Heat stress

antioxidants

MDPI

Salicylic Acid and Melatonin Alleviate the Effects of Heat Stress on Essential Oil Composition and Antioxidant Enzyme Activity in *Mentha* × *piperita* and *Mentha arvensis* L.

Milad Haydari [1,†], Viviana Maresca [2,†],Daniela Rigano [3,†], Alireza Taleei [1], Ali Akbar Shahnejat Bushehri [1], Javad Hadian [4], Sergio Sorbo [5], Marco Guida [2], Caterina Manna [6], Marina Piscopo [2], Rosaria Notariale [6], Francesca De Ruberto [2], Lina Fusaro [7] and Adriana Basile [2,*]

[1] Department of Agronomy and Plant Breeding, Collage of Agriculture and Natural Resources, University of Tehran, P.O. Box 31787-316 Karaj,Iran; milad.heydari@ut.ac.ir(M.H.); ataleei@ut.ac.ir(A.T.); ashah@ut.ac.ir(A.A.S.B.)

[2] Department of Biology—University of Naples "Federico II", 80126 Naples, Italy; viviana.maresca@unina.it(V.M.); marco.guida@unina.it(M.G.); marina.piscopo@unina.it(M.P.); francesca.deruberto@gmail.com(F.D.R.)

[3] Department of Pharmacy, School of Medicine and Surgery, University of Naples Federico II, 80126 Naples, Italy; drigano@unina.it

[4] Medicinal Plants and Drug Research Institute, ShahidBeheshti University, G.C. Tehran 11369, Iran; j_hadian@sbu.ac.ir(J.H.)

[5] C.e.S.M.A. University of Naples "Federico II", 80126 Naples, Italy; sersorbo@unina.it

[6] Department of Precision Medicine, School of Medicine, University of Campania "Luigi Vanvitelli",via Luigi de Crecchio, 80138 Naples, Italy; caterina.manna@unicampania.it(C.M.); notarialer@gmail.com(R.N.)

[7] Department of Environmental Biology, Sapienza University of Rome, P.le Aldo Moro 5, 00185 Rome, Italy;

* Correspondence: adbasile@unina.it; Tel.: +39-0812538508

† These authors contributed equally to this work.

Abstract

The aim of this study was to evaluate changes in the chemical profile of essential oils and antioxidant enzymes activity (catalase CAT, superoxide dismutase SOD, Glutathione *S*-transferases GST, and Peroxidase POX) in *Mentha* × *piperita* L. (Mitcham variety) and *Mentha arvensis* L. (var. *piperascens*), in response to heat stress. In addition, we used salicylic acid (SA) and melatonin (M), two brassinosteroids that play an important role in regulating physiological processes, to assess their potential to mitigate heat stress. In both species, the heat stress caused a variation in the composition of the essential oils and in the antioxidant enzymatic activity. Furthermore both Salicylic acid (SA) and melatonin (M) alleviated the effect of heat stress.

Keywords: mentha; heat stress; antioxidant enzyme activity; salicylic acid; melatonin; essential oil.

1. Introduction

The Lamiaceae family encompasses various genera, including aromatic herbs such as mint. Embracing half a dozen cultivated species, mint genus includes more than 30 species that are scattered worldwide, chiefly in temperate and tropical/subtropical regions. One of the distinctive features is that mint species possess essential oils [1].

Japanese mint or Cornmint (*Mentha arvensis* L. var. *piperascens* (Malinv. ex Holmes) Malinv. ex L.H.Bailey) is a fundamental natural source of monoterpenes, particularly L-menthol (up to 80% menthol), and it was already cultivated in ancient Japan as well as in China, India, and Brazil.

Mentha × *piperita* is an abortive hybrid of the species *M. aquatica* L. and *M. spicata.* Ecumenically, peppermint is one of the most commercial odorous scented herbs. The peppermint leaves have not only a peculiar, sweet, and strong odor, but also a redolent, warm, and spicy taste, with a cooling aftertaste. The supremacy of the essential oils of *Mentha* × *piperita* is due to the presence of menthone, isomenthone, and different isomers of menthol. Nowadays, extensive usage of peppermint oil in flavoring chewing gums, sugar confectioneries, ice creams, desserts, baked goods, tobacco, and alcoholic beverages is just one of the most prevalent applications of such oils. Furthermore, it is also commonly employed in the flavoring of pharmaceutical and oral preparations [2].

Menthol shows various biological activities, such as sedative, anesthetic, antiseptic, gastric, and antipruritic. It is also one of the few natural monocyclic monoterpene alcohols that have characteristics conducive to fragrances. As such, it has been used to flavor various goods such as candies, chewing gums, and toothpaste [3,4].

Heat stress has effects on metabolite synthesis in aromatic plants, changing phenolic and antioxidants concentrations [5]. Heat stress induces the generation of reactive oxygen species (ROS), such as superoxide radicals ($\cdot O_2^-$), hydrogen peroxide (H_2O_2), and hydroxyl radicals ($\cdot OH$), in plants, thereby creating a state of oxidative stress in them. This increased ROS level in plants causes oxidative damage to biomolecules such as lipids, proteins, and nucleic acids, thus altering the redox homeostasis [6,7]. To avoid potential damage by ROS, a balance between production and elimination of ROS at the intracellular level must be regulated. This equilibrium between production and detoxification of ROS is sustained by enzymatic and nonenzymatic antioxidants [8,9]. The enzymatic components comprise

several antioxidant enzymes, such as superoxide dismutase (SOD), catalase (CAT), glutathione peroxidase (GPX), guaiacol peroxidase (POX), and peroxiredoxins.

Salicylic acid (SA) and melatonin (M) are two brassinosteroids playing an important role in regulating physiological processes. SA is a phenolic compound with antioxidant properties, involved in the regulation of physiological processes in plants [10]. SA can modulate plant responses to a wide range of oxidative stresses [11]. When applied exogenously at suitable concentrations, SA was found to enhance the efficiency of antioxidant system in plants [12]. M (N-acetyl-5-methoxytryptamine) is an indole hormone involved in multiple biological processes [13]. According to a lot of findings, M plays an important role in the regulation of plant growth and development [14] and provides a defense against abiotic stresses such as extreme temperature, excess copper, salinity, and drought [15–17]. A lot of studies have proven that M may act as a plant growth regulator in rooting, seed germination, and delay in leaf senescence and other morphogenetic features [18–20]. M has been observed to improve tolerance for multiple stresses including heat stress, and in particular, exogenous M treatments protect plants from temperature extremes [21].

The aim of this study was to evaluate the response of *M. arvensis* L. var. *piperascens* and *M.* × *piperita* to heat stress in relation to the production of essential oils in general and in particular of menthol, menthone, and isomenthone, which have considerable economic importance and play an important role in the industrial field. In particular, our goal was to investigate the potential of SA and M to mitigate the heat stress effects on the two plants, focusing on the variation of essential oils composition and antioxidant enzymes activity.

2. Materials and Methods

2.1. Plant Material, Culture, and Treatment

M. × *piperita* L. var. Mitcham and *M. arvensis* var. *piperascens* Malinv. ex L. H. Bailey were obtained from the "Safiabad agricultural and natural resources research and education center". Planting and cultivation conditions were carried out in the growth chambers. The method is described in detail in Heydari et al. [22].

After 40 culturing days, plants were sprayed with SA (2, 3, and 4 mM, reported as SA2 , SA3, and SA4, respectively) and M (10 and 30 M, reported as M1 and M3), together with M and SA at the highest concentrations (M3SA4). Tap water was used for controls.

For each treatment, we selected 50 sample plants for subsequent experiments.

The abbreviation used to antioxidant enzyme activity and GC and GC-MS (Gas chromatography - Mass spectrometry) analysis are:

MpH1C = *M.* x *piperita* at the H1 temperature without treatment; MpH1M3 = *M.* x *piperita* at the H1 temperature treated with melatonin 3 mM; MpH1SA4 = *M.* x *piperita* at the H1 temperature treated with 4 mM salicylic acid; MpH1M3SA4 = *M.* x *piperita* at the H1 temperature treated with melatonin 3 mM and 4 mM salicylic acid; MpH2C = *M.* x *piperita* at the H2 temperature without treatment; MpH2M3 = *M.* x *piperita* at the H2 temperature treated with melatonin 3 mM; MpH2SA4 = *M.* x *piperita* at the H2 temperature treated with 4 mM salicylic acid; MpH2M3SA4 = *M.* x *piperita* at the H2 temperature treated with melatonin 3 mM and 4 mM salicylic acid; MpH3C = *M.* x *piperita* at the H3 temperature without treatment; MpH3M3 = *M.* x *piperita* at the H3 temperature treated with melatonin 3 mM; MpH3SA4 = *M.* x *piperita* at the H3 temperature treated with 4 mM salicylic acid; MpH3M3SA4 = *M.* x *piperita* at the H3 temperature treated with melatonin 3 mM and 4 mM salicylic acid; MaH1C = *M. arvensis* L. var. *piperascens* at the H1 temperature without treatment; MaH1M3 = *M. arvensis* L. var. *piperascens* at the H1 temperature treated with melatonin 3 mM; MaH1SA4 = *M. arvensis* L. var. *piperascens* at the H1 temperature treated with 4 mM salicylic acid; MaH1M3SA4= *M. arvensis* L. var. *piperascens* at the H1 temperature treated with melatonin 3 mM and 4 mM salicylic acid; MaH2C = *M. arvensis* L. var. *piperascens* at the H2 temperature without treatment; MaH2M3 = *M. arvensis* L. var. *piperascens* at the H2 temperature treated with melatonin 3 mM; MaH2SA4 = *M. arvensis* L. var. *piperascens* at the H2 temperature treated with 4 mM

salicylic acid; MaH2M3SA4 = *M. arvensis* L. var. *piperascens* at the H2 temperature treated with melatonin 3 mM and 4 mM salicylic acid; MaH3C = *M. arvensis* L. var. *piperascens* at the H3 temperature without treatment; MaH3M3 = *M. arvensis* L. var. *piperascens* at the H3 temperature treated with melatonin 3 mM; MaH3SA4 = *M. arvensis* L. var. *piperascens* at the H3 temperature treated with 4 mM salicylic acid; MaH3M3SA4 = *M. arvensis* L. var. *piperascens* at the H3 temperature treated with melatonin 3 mM and 4 mM salicylic acid.

2.2. Relative Water Content (RWC)

*Relative Water Content (*RWC) was calculated according to Dhopte and Manuel [23]:

$$RWC = (FW-DW)/(TW-DW) \times 100$$

where FW is leaf fresh weight, DW is dry weight, and TW is leaf turgor mass of leaf samples [24] obtained measuring the leaf weight after 10–12 h in water saturating conditions.

2.3. Antioxidant Enzyme Activity

Protein extraction and the activity of antioxidant enzymes(SOD, CAT, GST ans PEROX) was carried out according to Maresca et al. [25].

2.4. Isolation of Essential Oils

Samples' shoots were air-dried in dark conditions at room temperature and were used for essential oils extraction. Each sample (50 g in three replications) was extracted using hydro-distillation for 3 h and Clevenger-type apparatus based on the standard procedure described by Russo et al. [26]. The essential oils were obtained with different yields (0.97 ± 0.02–3.26 ± 0.02%) on dry mass (w/w) and results were yellowish with a pleasant smell. The oils were dried with anhydrous sodium sulfate and stored under N2 at +4 °C in the dark for subsequent tests and analyses.

2.5. GC and GC-MS Analysis

Analytical gas chromatography was carried out on a Perkin-Elmer Sigma 115 gas chromatograph fitted with an Agilent HP-5 MS capillary column (30 m × 0.25 mm), 0.25 μm film thickness. The analysis was also performed by using a fused silica HP Innowax polyethylene glycol capillary column (50 m × 0.20 mm), 0.20 μm film thickness. Gas chromatography analysis was performed as done previously and described in detail by Rigano et al. [27]. Compounds identification and components relative percentages were carried out as described by Rigano et al. [27].

2.6. Statistical Analysis

For each species, the differences between treatments were analyzed by factorial ANOVA (Analysis of Variance) using the hormones and temperature as categorical predictors. The factorial ANOVA was followed by Student-Neuman-Keuls test for post hoc comparisons. Results were reported as mean ± standard deviation.

3. Results

3.1. Relative Water Content (RWC)

Significant decrease of Relative Water Contents (RWC%) in H2 and H3 suggested that plants could be under stress. *M. arvensis* L. var. *piperascens* lost more water than *M.* × *piperita* L. SA and M restored water content in a dose-dependant way (Figure 1). For this reason, for the next experiments, we only used the highest concentration for both treatments: melatonin 30 M (M3) and salicylic acid 4 mM (SA4).

3.2. Antioxidant Enzyme Activity

As for the activity of antioxidant enzymes, heating determined a temperature-dependent increase, and treatments with SA4 and M3 determined a further increase, which proved to be extremely significant with the two hormones used simultaneously at their maximum concentrations.

In *M.* × *piperita*, the activity of all the measured antioxidant enzymes increased with increasing temperature both in the absence and presence of SA and M (M3, SA4). The only exception was the POX activity of samples C, which did not increase with increasing temperature but only under H3 conditions.

Moreover, in most cases the treatment with SA4 had a synergistic effect with the temperature compared to M3 on the activity of all the measured enzymes.

In general, for all the enzymatic activities measured, the samples treated with SA4M3 maintained a significantly higher enzyme activity compared to the C control samples and in the samples treated individually with SA and M3.

In *M. arvensis* L. var. *piperascens* the antioxidant enzymes activity in relation to temperature and treatment with M3, SA4, and M3SA4 followed the same trend shown in *M.* × *piperita* (Table 1).

3.3. Essential Oil Yield

Essential oil yields in *M.* × *piperita* and *M. arvensis* L. var. *piperascens* were not statistically different (Figure 2.). Heat stress had a similar effect on both species, determining a significant reduction of essential oils as the temperature increased. In

addition, both the treatments with SA4 and M3 determined an increase in the yield of essential oils in samples exposed to H3 heat stress conditions, even if there was no statistically significant difference between SA4 and M3.

The oxygenated monoterpenes amount in *M. arvensis* L. var. *piperascens* increased by using SA4, M3, and the two of them used simultaneously in normal condition (H1). In H2 conditions, only SA4 increased the oxygenated monoterpenes, while in H3 conditions only M3 increased them. In *M.* × *piperita* SA, M, and the two hormones used simultaneously increased the oxygenated monoterpenes in H1, and the major effect was observed by using M3. In H2 the oxygenated monoterpenes increased only by using S4 and M3 together. Unfortunately, we could not observe an increase of the oxygenated monoterpenes in H3 (Figure 3).

A different trend was observed for monoterpene hydrocarbons on respect to oxygenated monoterpenes. In *M. arvensis* L. var. *piperascens* monoterpene hydrocarbons concentration was 4.3% for H1, 3.6% for H2, and 7.4% for H3 in control plants. Their amounts were decreased by using S4 (1.4%), M3 (1.3%), and both simultaneously (S4M3) (1.1%) in H1 conditions. In H2 they decreased by using M3 (0.8%), SA4 (0.8%), and the two of them simultaneously (1.0%), and the same applied for H3 by using SA4 (3.5%), M3 (2.5%) and the two of them simultaneously (4.8%). In *M.* × *piperita* the monoterpene hydrocarbons concentrations were in H1 4.0%, in H2 3.6% and in H3 5.2% in control plants. In H1 treatment by hormones decreased their amount (about 0.8%), and the same trend of reduction was observed for the other temperature conditions for all the treatments (data not shown).

Oxygenated sesquiterpenes were observed in very low concentrations in both the essential oils. Generally, in *M. arvensis* L. var. *piperascens* and in *M.* × *piperita* they were reduced or depleted by heat stress.

The dominant secondary metabolite in mint is menthol. Menthol dramatically decreased by heat stress, more than twice (in H1 56.6%, H2 39.0%, and H3 28.0%) in *M. arvensis* L. var. *piperascens* and about 4.5 fold (in H1 25%, H2 12.2%, and H3 5.6%) in *M.* × *piperita.* In *M. arvensis* L. var. *piperascens* only using SA4 and M3 simultaneously in H2 conditions the menthol concentration increased. In *M.* × *piperita* under H1 both SA4 and/or M3 increased the menthol concentration. In H3 by using SA4 and M3 simultaneously, the menthol concentration increased (14.3%) in comparison to control in H3 (Figure 4).

Menthone is a precursor of menthol. The menthone concentration decreased in *M. arvensis* L. var. *piperascens* in H2 (7.6%) and H3 (12.0%), compared to H1 (14.5%). In *M.* × *piperita* the menthone concentration increased in H2 (15.9%) and decreased in H3 (9.5%), compared to H1 (13.0%). In normal condition (H1) in *M. arvensis* L. var. *piperascens* M3 decreased and SA4 increased menthone concentration. But in *M.* × *piperita* all the treatments increased menthone in H1 and H3 conditions. In H2 SA4 and M3 reduced menthone, but using both of them simultaneously increased menthone concentration (data not shown).

The menthofuran concentration in *M. arvensis* L. var. *piperascens* increased (in H1 7.8%, H2 34.0%, H3 13.0%) and in *M.* × *piperita* decreased (in H1 35.0%, H2 25.4%, H3 34.0%) under heat stress; the highest differences were observed in H2 condition. In *M. arvensis* L. var. *piperascens*, M3 increased, SA4 decreased, and the simultaneous use of both increased the menthofuran concentration, especially in the H1 condition. In H3 all treatments increased the menthofuran concentration. As regards *M.* × *piperita*, all treatments dramatically decreased the menthofuran concentration in H1. In H2, SA4 and M3 increased the menthofuran concentration. In H3, all the treatments decreased the menthofuran concentration, especially during simultaneous use (data not shown).

The pulegone concentrations increased for both the essential oils under heat stress condition. Particularly, the pulegone concentrations in *M. arvensis* L. var. *piperascens* were in H1 5.6%, in H2 8.0%, and in H3 11.0% and for *M.* × *piperita* in H1 15.0%, in H2 24.3% and in H3 28.1%. In *M. arvensis* L. var. *piperascens* SA4 and the simultaneous use of the two brassinosteroids caused an increase in the pulegone concentration in normal condition (H1). In H2, all treatments increased the pulegone amount. In H3, M3 and the simultaneous use of multiple treatments increased pulegone. In *M.* × *piperita*, all treatments decreased the pulegone concentration in H1. But as for the heat conditions, in H2 all treatments increased the pulegone amount, while in H3 only M3 increased the pulegone concentration. (Figure 5).

In general, menthol has a significant negative correlation with menthofuran ($r = -0.459$ **) and pulegone ($r = -0.912$ **), that is to say that menthol is reduced and the pulegone increased under the heat stress. Also, menthofuran had a significant negative correlation with menthone ($r = -0.527$ **). The pulegone had a significant positive correlation with menthofuran ($r = 0.345$ *) (Table 2).

4. Discussion

In the mid-1980s, the relative water content (RWC) was introduced as the best reference point for the state of water in plants, expressing the balance between water absorption and consumption by transpiration [28]. The heat stress induces an increase of transpiration, with the effect of cooling and adapting the plant to heat. However a further transpiration dries up the tissues and the cells [29]. Generally, osmoregulation is one of the main mechanisms preserving turgor pressure in most plants against water loss; it causes the plant to continue to absorb water and maintain metabolic activity [30]. The RWC leaf may be the best biochemical growth / activity parameter that reveals the severity of stress [31]. Our data show a significant decrease in relative water content (RWC%) in both plants treated with different temperatures, suggesting that both plants were under stress. *M. arvensis* L. var. *piperascens* has lost more water than *M.* × *piperita* L.

Heat stress disturbs the stable physiological condition in plants and for this reason scientists are trying to find a way to relieve stress. Brassinosteroids such as SA and M have recently been studied in relation to this issue. Coban and Baydar [32] have shown that brassinosteroids reduce salt stress. He et al. [33] inhibited heat stress in bluegrass using SA. In particular, SA stimulates the production and/or an increase of secondary metabolites from polyphenols by acting as an elicitor [34,35]. SA activates phenylalanine ammonia lyase (PAL) [36] and plays a role in the regulation of physiological processes [37]. M also alleviates stress damage, and this has been reported in cucumber in the germination phase [38] and in *Arabidopsis* in which it compensates for heat stress [39]. Our data show that both plants undergo a strong heat stress reducing RWC in a temperature-dependent way. Treatment with SA and M in both plants significantly reduce heat stress effect on RWC, confirming the protective role of these two hormones against heat stress.

In a previous work, we have shown that heat stress determines a change in oxygenated monoterpenes, monoterpene hydrocarbons, oxygenated sesquiterpenes, sesquiterpene hydrocarbons, and other components in *M.* × *piperita* L. (Mitcham variety) and *M. arvensis* L. (var. *piperascens*) essential oils [22]. In this study, brassinosteroids treatments in both the oils subjected to heat stress determined a variation in the composition of the essential oils and in the antioxidant enzymatic activity.

Saharkhiz and Goudarzi [40], showed that application of 150 mgL^{-1} SA in *M.* × *piperita* L. significantly ($p < 0.05$) increased the oil content compared to control plants. In particular the treatment with different SA concentrations mostly increased menthone (15.8%–18.1%) and menthol (46.3%–47.4%) content.

In particular, monoterpenes (synthesized in Methylerythritol phosphate [MEP] pathway) and sesquiterpenes (synthesized in mevalonate [MVA] pathway) were the most important components. In the MEP pathway, menthol is synthesized in the cytoplasm and menthofuran is synthesized in the endoplasmic reticulum [41]. In particular, isopiperitenone from mitochondria is transferred to the cytoplasm and converts to pulegone. Pulegone can continue two branches of the MEP pathway: 1: It remains in the cytoplasm, is converted to menthone and finally to menthol; 2: it is transferred to the endoplasmic reticulum to be converted in menthofuran. So, in the MEP pathway, pulegone, menthone, menthofuran, and menthol have a crucial role and we should consider how they change under heat stress. In general, menthol and menthone have a significant negative correlation with menthofuran and pulegone, (menthol and menthone are reduced and the pulegone and menthofuran increased under the heat stress). Considering the (−)-Menthol biosynthesis pathway (Figure 6), we can hypothesize that under heat stress, pulegone reductase (PR) reduces its activity, leading to a decrease of the conversion of pulegone to menthone (that is the precursor of menthol). The increase of pulegone, due to the reduction of the activity of the enzyme that converts it in menthone, could also explain the increase of the mentofuran, which is synthesized from pulegone in the endoplasmic reticulum. In fact, pulegone had a significant positive correlation with menthofuran (Figure 6). In future studies, it will be necessary to verify the activity of the enzyme PR under heat stress and after treatment with the brassinosteroids.

As for the antioxidant activity, our studies have shown that SA and M have a positive effect on *M. arvensis* L. var. *piperascens* and *M.* × *piperita* L., increasing the activity of antioxidant enzymes in both species when used alone, but even more if applied simultaneously, demonstrating a synergistic effect.

On the other hand, an enhanced activity of CAT and SOD was observed in heat stressed plants of *Poa pratensis*, after the treatment with SA [33]. Xu et al. [42] reported that external M applications caused a significant increase in enzymatic antioxidants such as SOD, POX, CAT, and APX peroxidase and non enzymatic antioxidants such as ascorbic

acid and vitamin E, resulting in decreased ROS levels and lipid peroxidation in cucumber under high temperature stress. Our data therefore not only confirms the effect of the two hormones on the activity of antioxidant enzymes and therefore the mitigating effect against the heat stress, but also show their ability to act in a synergistic way, which has not been demonstrated so far.

5. Conclusion

M and SA alleviate the effects of heat stress in *M. arvensis* L. var. *piperascens* and *M.* × *piperita* L. by changing the yield of essential oils and the activity of antioxidant enzymes. It is possible that the activity of the brassinosteroids highlighted by us occurs through an action by the enzymatic game involved in the metabolism of the studied essential oils. Future studies will aim to highlight a possible modification of enzymatic activity and/or a different expression of the genes involved in their synthesis in response to the presence of M and SA.

Our results can be considered for future applications in the cosmetics, food, and pharmacological fields, given the extreme importance of menthol and menthone in these areas.

Author Contributions: Conceptualization, M.H, V.M. and D.R; methodology, M.H., V.M., D.R., A.T., A.A.S.B., J.H., S.S., M.G., C.M., M.P., R.N., F.D.R., L.F., A.B.; investigation, M.H, V.M., D.R and A.B.; data curation, L.F. and R.N.; formal analysis, A.T., A.A.S.B. and J.H.; writing—original draft preparation, A.B.; writing—review and editing, M.H, V.M., D.R and A.B.; supervision, A.B.; project administration, A.B.

Funding: This research received no external funding.

Conflicts of Interest: The authors declare no conflict of interest.

Figure and Table

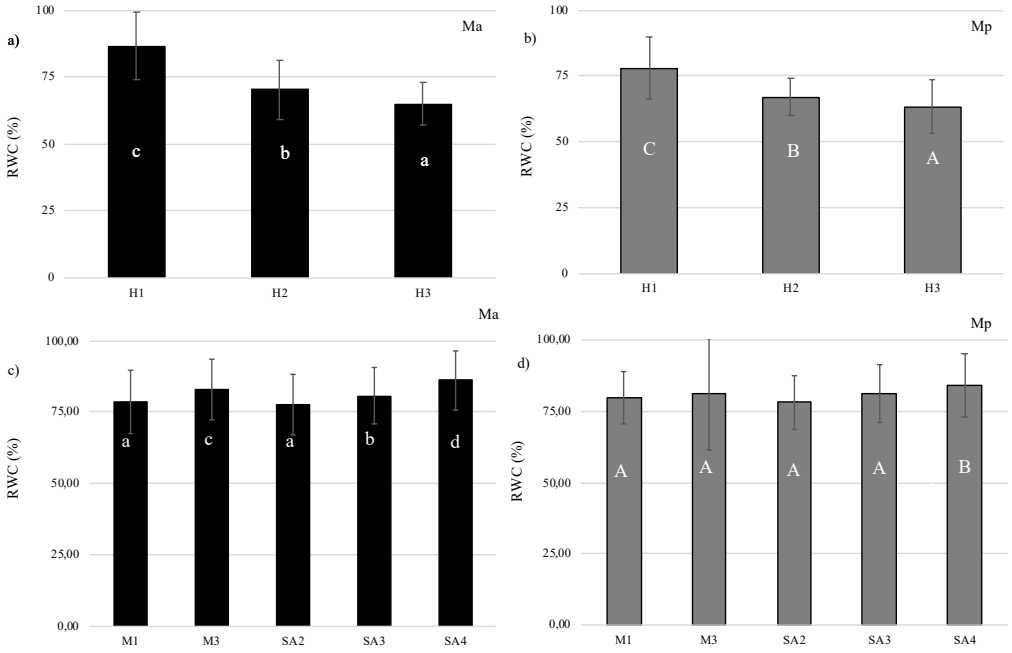

Figure 1. Relative Water Content for (**a**) and (**c**) *M. arvensis* L. var. *piperascens* (Ma) and for (**b**) and (**d**) *M.* × *piperita* (Mp). Values are presented as means ± standard deviation (n = 15); values not accompanied by the same letter are significantly different at $p < 0.05$, using the post-hoc Student–Newman–Keuls test. Lowercase letters(a–d) indicate significant differences between treatments for Ma; uppercase letters(A–C) indicate significant differences between treatments for Mp.

Table 1. Enzyme activity in *M.* × *piperita* L. and *M. arvensis* L. var. *piperascens* for each treatment.

	Temperature	Hormons	CAT	GST	POX	SOD
Ma	H1	C	3.188 ± 0.89a	1.02 ± 0.08 a	19.39 ± 1.25 a	6.88 ± 0.21a
Ma		M3	34.76 ± 1.94a	1.78 ± 0.08 c	126.42 ± 1.25c	12.98 ± 1.03b
Ma		SA4	42.56 ± 2.05a	1.49 ± 0.06b	98.12 ± 3.69c	10.33 ± 1.05bc
Ma		M3SA4	66.42 ± 2.45d	2.54 ± 0.06d	226.77 ± 5.11 d	18.45 ± 1.13bc
Ma	H2	C	9.46 ± 1.83b	1.52 ± 0.03d	22.73± 1.04a	9.98 ± 1.01c
Ma		M3	63.86 ± 2.95c	2.01 ± 0.08e	245.13 ± 9.46d	43.79 ± 1.13d
Ma		SA4	98.73 ± 2.83b	2.67 ± 0.08h	108.42 ± 3.14f	19.07 ± 1.16e
Ma		M3SA4	134.52 ± 2.54e	4.29 ± 0.08 i	269.67 ± 1.22g	54.53 ± 1.51f
Ma	H3	C	19.61 ± 1.67d	2.28 ± 0.02f	4.96 ±1.45b	16.88 ± 0.71d
Ma		M3	92.37± 2.04e	2.67 ± 0.04g	316.91± 7.70e	49.07 ± 0.73g
Ma		SA4	129.04 ± 3.75e	3.74 ± 0.06l	146.95 ± 4.22h	49.12 ± 0.87g
Ma		M3SA4	130.33 ± 2.16f	4.61 ± 0.09m	491.12 ± 11.77i	58.77 ± 0.89h
Mp	H1	C	9.53 ± 1.33 a	0.92 ±0.04 a	11.49 ± 1.25 a	5.64 ± 0.55a
Mp		M3	10.51 ± 1.07 a	1.70 ± 0.03 c	61.50 ± 1.42c	18.61 ± 1.62b
Mp		SA4	12.54 ± 1.46 a	1.57 ± 0.07b	66.26 ± 2.38c	20.61 ± 0.83bc
Mp		M3SA4	41.15 ± 2.03 d	1.93 ± 0.1d	103.57 ±5.45 d	20.54 ± 0.53bc
Mp	H2	C	19.42 ± 1.47b	1.93 ± 0.03d	15.19 ± 1.52a	22.06 ± 0.90c
Mp		M3	29.54 ± 1.19c	2.28 ± 0.07e	95.12 ± 1.20d	28.75 ± 2.23d
Mp		SA4	22.39 ± 1.54 b	3.12 ± 0.08h	154.46 ± 4.56f	33.48 ± 0.82e
Mp		M3SA4	54.49 ± 2.50e	3.74 ± 0.07 i	343.70 ± 6.38g	51.21 ± 1.31f
Mp	H3	C	42.75 ± 1.6d	2.63 ± 0.04f	36.79 ± 0.82b	29.81 ± 1.19d
Mp		M3	53.12 ± 2.04e	2.99 ± 0.08g	138.90 ± 7.00e	56.40 ± 1.47g
Mp		SA4	51.76 ± 2.26e	6.13 ± 0.08l	417.25 ± 13.36h	54.50 ± 1.52g
Mp		M3SA4	130.33 ± 2.16f	6.52 ± 0.08m	466.18 ± 16.72i	66.61 ± 1.27h

Values are presented as means ± standard deviation (n = 15); values not accompanied by the same letter(a–i,l), are significantly different at $p < 0.05$using the post-hoc Student–Newman–Keuls test. For treatment details, see the Material and Methods section (2.1).

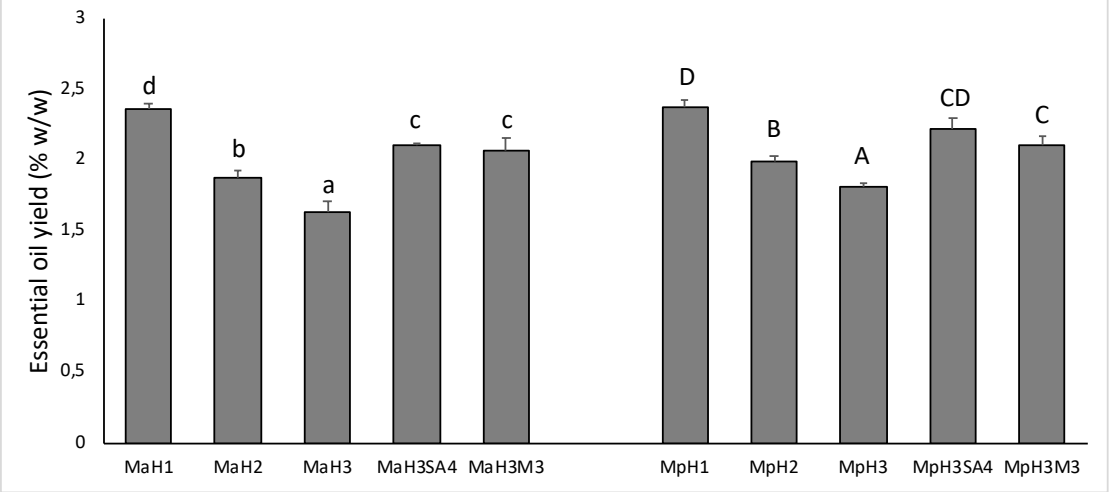

Figure 2. Essential oil yield in *M. arvensis* L. var. *piperascens* (Ma) and *M.* × *piperita* (Mp) shown in H1, H2, and H3 conditions, and the effect of melatonin (M3) and salicylic acid (SA4) at their highest concentrations on essential oil yield in H3 condition.Values are presented as means ± standard deviation (n = 15); values not accompanied by the same letter are significantly different at $p < 0.05$, using the post-hoc Student–Newman–Keuls test. Lowercase letters(a–d) indicate significant differences between treatments for Ma; uppercase letters(A–D) indicate significant differences between treatments for Mp. For treatments details see Material and Methods section (2.1).

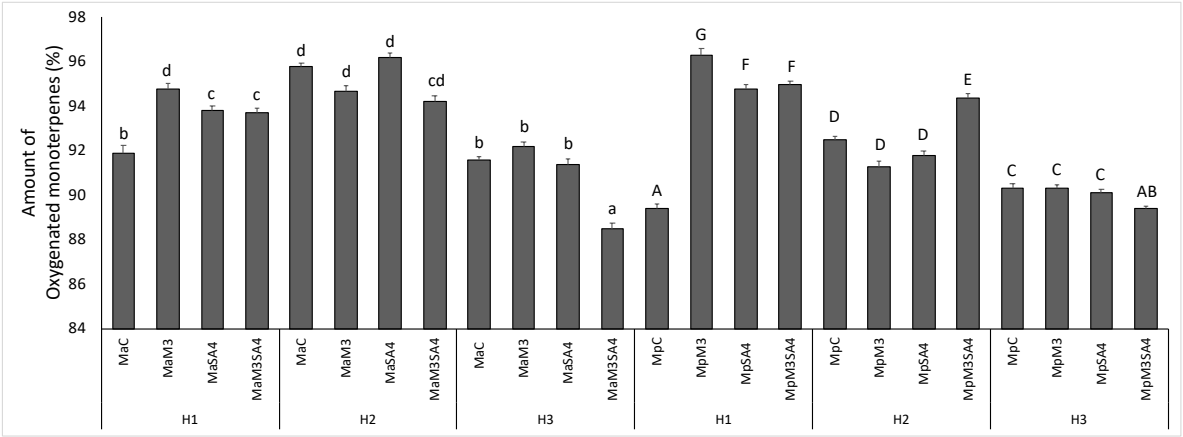

Figure 3. The amount of oxygenated monoterpenes in *M. arvensis* L. var. *piperascens* (Ma) and *M.* × *piperita* (Mp) under heat stress in H1, H2, and H3 and effects of melatonin (M3) and salicylic acid (SA4) on oxygenated monoterpenes. Values are presented as means ± standard deviation (n = 15); values not accompanied by the same letter are significantly different at $p < 0.05$, using the post-hoc Student-Newman-Keuls test. Lowercase letters(a–d) indicate significant differences between

treatments for Ma; uppercase letters(A–G) indicate significant differences between treatments for Mp. For treatment details, see the Material and Methods section (2.1).

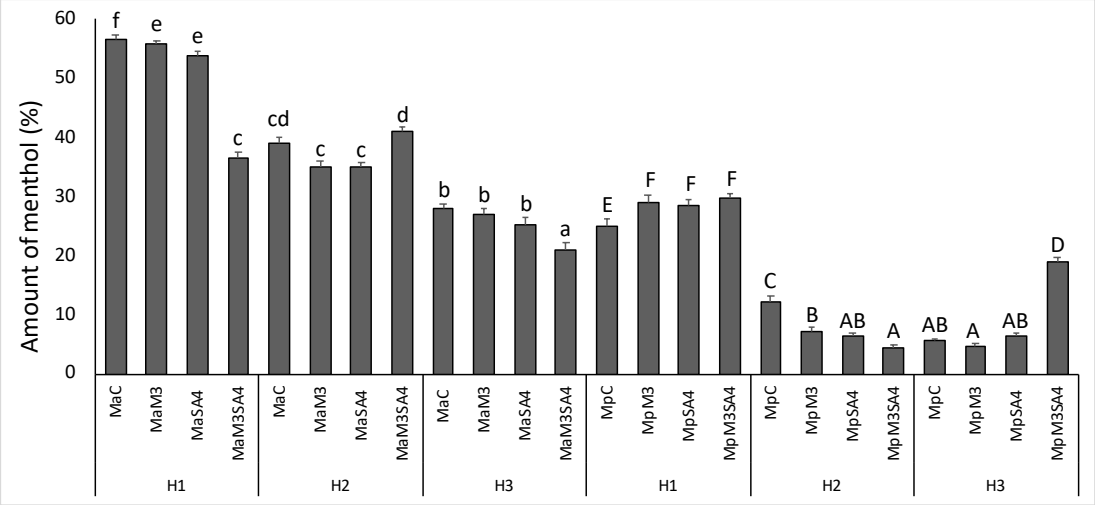

Figure 4. The amount of menthol in *M. arvensis* L. var. *piperascens* (Ma) and *M.* × *piperita* (Mp) under heat stress in H1, H2, and H3 and effect of melatonin (M3) and salicylic acid (SA4) on menthol. Values are presented as means ± standard deviation (n = 15); values not accompanied by the same letter are significantly different at $p < 0.05$, using the post-hoc Student-Newman-Keuls test. Lowercase letters(a–f) indicate significant differences between treatments for Ma; uppercase letters(A–F) indicate significant differences between treatments for Mp. For treatment details, see the Material and Methods section (2.1).

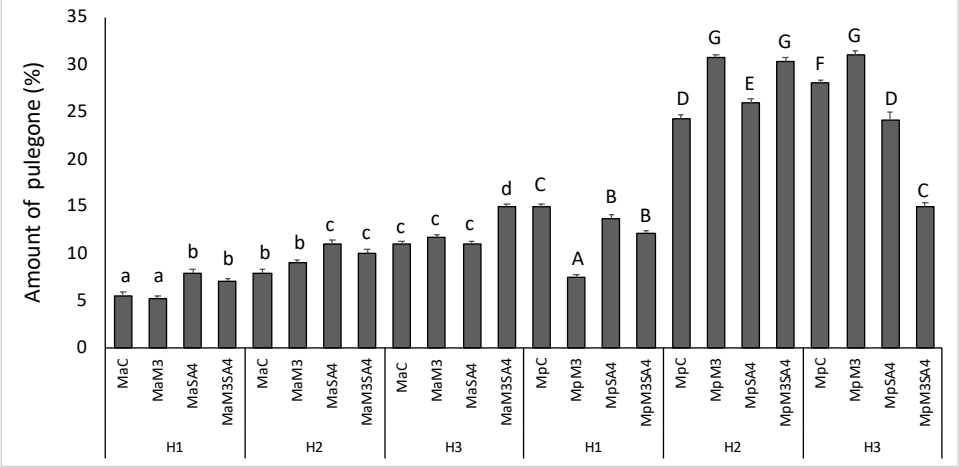

Figure 5. The amount of pulegone in *M. arvensis* L. var. *piperascens* (Ma) and *M.* × *piperita* (Mp) under heat stress in H1, H2, and H3 and effect of melatonin (M3) and salicylic acid (SA4) on pulegone. Values are presented as means ± standard deviation (n = 15); values not

accompanied by the same letter are significantly different at $p < 0.05$, using the post-hoc Student-Newman-Keuls test. Lowercase letters(a–d) indicate significant differences between treatments for Ma; uppercase letters (A–G) indicate significant differences between treatments for Mp. For treatment details, see the Material and Methods section (2.1).

Table 2. Pearson correlation coefficients found among four important secondary metabolites (menthofuran, menthol, pulegone, and menthone) in the menthol pathway in *M. arvensis* L. var. *piperascens* and *M.* × *piperita* under the long-term extreme heat stress by using SA and M as a compensator of stress.

	Menthofuran	Menthol	Pulegone	Menthone
Menthofuran	1	−0.459 **	0.345 *	−0.527 **
Menthol		1	−0.912 **	−0.054
Pulegone			1	0.009
Menthone				1

** Correlation is significant at the 0.01 level (2-tailed).* Correlation is significant at the 0.05 level (2-tailed).

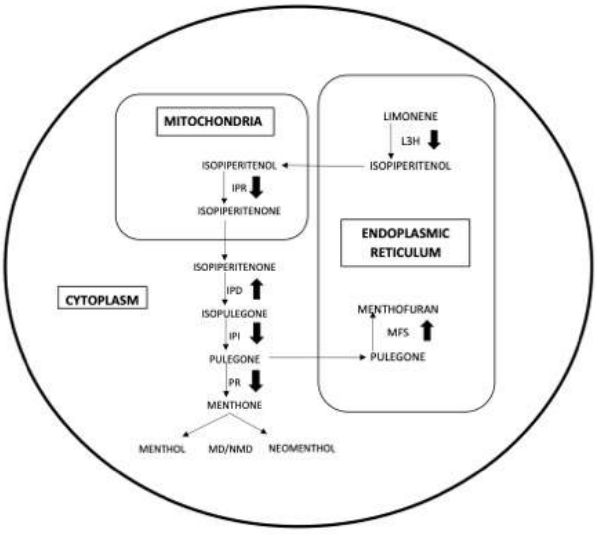

Figure 6. Menthol biosynthesis pathway. IPD: isopiperitenol dehydrogenase, IPR: isopiperitenone reductase, IPI: Isopentenyl diphosphate isomerase, PR: pulegone reductase, LH3:limonene 3-hydroxylase, MFS: menthofuran synthase, NMD: neomenthol reductase, MD: menthol dehydrogenases.

References

1. Lawrence, B.M. *Mint: The Genus Mentha*; CRC Press: Boca Raton, FL, USA, 2006; ISBN 978-0-429-12587-4.
2. Kokkini, S.; Karousou, R.; Hanlidou, E. HERBS|Herbs of the Labiatae. In *Encyclopedia of Food Sciences and Nutrition*; Academic Press: Cambridge, MA, USA, 2003; pp. 3082–3090; ISBN 978-0-12-227055-0.
3. Taneja, S.C.; Chandra, S. 20 - Mint. In *Handbook of Herbs and Spices (Second Edition)*; Peter, K.V., Ed.; Woodhead Publishing Series in Food Science, Technology and Nutrition; Woodhead Publishing: Sawston/Cambridge, UK, 2012; pp. 366–387; ISBN 978-0-85709-039-3.
4. Mander L., Liu H.W. *Comprehensive Natural Products II: Chemistry and Biology*; Elsevier: Amsterdam, The Netherlands, 2010; ISBN 978-0-08-045382-8.
5. Fletcher, R.S.; Slimmon, T.; McAuley, C.Y.; Kott, L.S. Heat stress reduces the accumulation of rosmarinic acid and the total antioxidant capacity in spearmint (*Mentha spicata* L). *J. Sci. Food Agric.* **2005**, *85*, 2429–2436.
6. Smirnoff, N. The role of active oxygen in the response of plants to water deficit and desiccation. *New Phytol.* **1993**, *125*, 27–58.
7. Gille, G.; Sigler, K. Oxidative stress and living cell. *Folia Microbiol.* **1995**, *40*, 131–152.
8. Mittler, R. Oxidative stress, antioxidants and stress tolerance. *Trends Plant Sci.* **2002**, *7*, 405–410.
9. Mittler, R.; Vanderauwera, S.; Gollery, M.; Van Breusegem, F. Reactive oxygen gene network of plants. *Trends Plant Sci.* **2004**, *9*, 490–498.
10. Moghaddam, N.M.; Arvin, M.J.; Nezhad, G.R.K.; Maghsoudi, K. Effect of salicylic acid on growth and forage and grain yield of maize under drought stress in field conditions. *Seed Plant Prod. J.* **2011**, *272*, 41–55.
11. Shirasu, K.; Nakajima, H.; Rajasekhar, V.K.; Dixon, R.A.; Lamb, C. Salicylic acid potentiates an agonist-dependent gain control that amplifies pathogen signals in the activation of defense mechanisms. *Plant Cell* **1997**, *9*, 261–270.
12. Knörzer, O.C.; Lederer, B.; Durner, J.; Böger, P. Antioxidative defense activation in soybean cells. *Physiol. Plant.* **1999**, *107*, 294–302.

13. Calvo, J.R.; González-Yanes, C.; Maldonado, M.D. The role of melatonin in the cells of the innate immunity: A review. *J. Pineal Res.* **2013**, *55*, 103–120.
14. Manchester, L.C.; Coto-Montes, A.; Boga, J.A.; Andersen, L.P.H.; Zhou, Z.; Galano, A.; Vriend, J.; Tan, D.-X.; Reiter, R.J. Melatonin: An ancient molecule that makes oxygen metabolically tolerable. *J. Pineal Res.* **2015**, *59*, 403–419.
15. Wang, P.; Sun, X.; Li, C.; Wei, Z.; Liang, D.; Ma, F. Long-term exogenous application of melatonin delays drought-induced leaf senescence in apple. *J. Pineal Res.* **2013**, *54*, 292–302.
16. Zhang, N.; Sun, Q.; Zhang, H.; Cao, Y.; Weeda, S.; Ren, S.; Guo, Y.-D. Roles of melatonin in abiotic stress resistance in plants. *J. Exp. Bot.* **2015**, *66*, 647–656.
17. Gao, W.; Zhang, Y.; Feng, Z.; Bai, Q.; He, J.; Wang, Y. Effects of Melatonin on Antioxidant Capacity in Naked Oat Seedlings under Drought Stress. *Molecules* **2018**, *23*, 1580.
18. Nawaz, M.A.; Huang, Y.; Bie, Z.; Ahmed, W.; Reiter, R.J.; Niu, M.; Hameed, S. Melatonin: Current Status and Future Perspectives in Plant Science. *Front. Plant Sci.* **2016**, *6*, 1230.
19. Arnao, M.B.; Hernández-Ruiz, J. Melatonin: Plant growth regulator and/or biostimulator during stress? *Trends Plant Sci.* **2014**, *19*, 789–797.
20. Arnao, M.B.; Hernández-Ruiz, J. Melatonin and its relationship to plant hormones. *Ann. Bot.* **2018**, *121*, 195–207.
21. Tan, D.-X.; Hardeland, R.; Manchester, L.C.; Paredes, S.D.; Korkmaz, A.; Sainz, R.M.; Mayo, J.C.; Fuentes-Broto, L.; Reiter, R.J. The changing biological roles of melatonin during evolution: From an antioxidant to signals of darkness, sexual selection and fitness. *Biol. Rev.* **2010**, *85*, 607–623.
22. Heydari, M.; Zanfardino, A.; Taleei, A.; Bushehri, A.A.S.; Hadian, J.; Maresca, V.; Sorbo, S.; Napoli, M.D.; Varcamonti, M.; Basile, A.; et al. Effect of Heat Stress on Yield, Monoterpene Content and Antibacterial Activity of Essential Oils of Mentha x piperita var. Mitcham and Mentha arvensis var. piperascens. *Molecules* **2018**, *23*, 1903.
23. Dhopte, A.M.; Livera-M, M. *Principles and Techniques for Plant Scientist [s]*; Agrobios: Jodhpur, India, 2002.
24. Arjenaki, F.G.; Morshedi, A.; Jabbari, R. Evaluation of Drought Stress on Relative

Water Content, Chlorophyll Content and Mineral Elements of Wheat (*Triticum aestivum* L.) Varieties. *Int. J. Agric. Crop Sci.* **2012**, *4*, 726–729.

25. Maresca, V.; Fusaro, L.; Sorbo, S.; Siciliano, A.; Loppi, S.; Paoli, L.; Monaci, F.; Karam, E.A.; Piscopo, M.; Guida, M.; et al. Functional and structural biomarkers to monitor heavy metal pollution of one of the most contaminated freshwater sites in Southern Europe. *Ecotoxicol. Environ. Saf.* **2018**, *163*, 665–673.
26. Russo, A.; Formisano, C.; Rigano, D.; Cardile, V.; Arnold, N.A.; Senatore, F. Comparative phytochemical profile and antiproliferative activity on human melanoma cells of essential oils of three lebanese Salvia species. *Ind. Crop. Prod.* **2016**, *83*, 492–499.
27. Rigano, D.; Arnold, N.A.; Conforti, F.; Menichini, F.; Formisano, C.; Piozzi, F.; Senatore, F. Characterisation of the essential oil of Nepeta glomerata Montbret et Aucher ex Bentham from Lebanon and its biological activities. *Nat. Prod. Res.* **2011**, *25*, 614–626.
28. Schonfeld, M.A.; Johnson, R.C.; Carver, B.F.; Mornhinweg, D.W. Water Relations in Winter Wheat as Drought Resistance Indicators. *Crop Sci.* **1988**, *28*, 526–531.
29. Jiang, Y.; Huang, B. Drought and Heat Stress Injury to Two Cool-Season Turfgrasses in Relation to Antioxidant Metabolism and Lipid Peroxidation. *Crop Sci.* **2001**, *41*, 436–442.
30. Gunasekera, D.; Berkowitz, G.A. Evaluation of contrasting cellular-level acclimation responses to leaf water deficits in three wheat genotypes. *Plant Sci.* **1992**, *86*, 1–12.
31. Alizadeh, A. *Soil, Water, Plants Relationship*; Emam Reza University Press: Mashhad, Iran, 2002; Volume 3.
32. Çoban, Ö.; Göktürk Baydar, N. Brassinosteroid effects on some physical and biochemical properties and secondary metabolite accumulation in peppermint (*Mentha piperita* L.) under salt stress. *Ind. Crop. Prod.* **2016**, *86*, 251–258.
33. He, Y.; Liu, Y.; Cao, W.; Huai, M.; Xu, B.; Huang, B. Effects of Salicylic Acid on Heat Tolerance Associated with Antioxidant Metabolism in Kentucky Bluegrass. *Crop Sci.* **2005**, *45*, 988–995.
34. Edreva, A.; Velikova, V.; Tsonev, T.; Dagnon, S.; Gürel, A.; Aktaş, L.; Gesheva, E. Stress-protective role of secondary metabolites: Diversity of functions and mechanisms. *Gen. Appl. Plant Physiol.* **2008**, *34*, 67–78.

35. Cohen, S.D.; Kennedy, J.A. Plant metabolism and the environment: Implications for managing phenolics. *Crit. Rev. Food Sci. Nutr.* **2010**, *50*, 620–643.
36. Klessig, D.F.; Malamy, J. The salicylic acid signal in plants. *Plant Mol. Biol.* **1994**, *26*, 1439–1458.
37. Raskin, I. Role of Salicylic Acid in Plants. *Annu. Rev. Plant Physiol. Plant Mol. Biol.* **1992**, *43*, 439–463.
38. Zhang, H.-J.; Zhang, N.; Yang, R.-C.; Wang, L.; Sun, Q.-Q.; Li, D.-B.; Cao, Y.-Y.; Weeda, S.; Zhao, B.; Ren, S.; et al. Melatonin promotes seed germination under high salinity by regulating antioxidant systems, ABA and GA4 interaction in cucumber (*Cucumis sativus* L.). *J. Pineal Res.* **2014**, *57*, 269–279.
39. Bajwa, V.S.; Shukla, M.R.; Sherif, S.M.; Murch, S.J.; Saxena, P.K. Role of melatonin in alleviating cold stress in Arabidopsis thaliana. *J. Pineal Res.* **2014**, *56*, 238–245.
40. Saharkhiz, M.J.; Goudarzi, T. Foliar Application of Salicylic acid Changes Essential oil Content and Chemical Compositions of Peppermint (*Mentha piperita* L.). *J. Essent. Oil Bear. Plants* **2014**, *17*, 435–440.
41. Croteau, R.B.; Davis, E.M.; Ringer, K.L.; Wildung, M.R. (−)-Menthol biosynthesis and molecular genetics. *Naturwissenschaften* **2005**, *92*, 562–577.
42. Xu, X.; Sun, Y.; Guo, X.; Sun, B.; Zhang, J. Effects of exogenous melatonin on ascorbate metabolism system in cucumber seedlings under high temperature stress. *Yingyong Shengtai Xuebao* **2010**, *21*, 2580–2586.

CHAPTER 3

Ozone stress

PLOS ONE

Functional indicators of response mechanisms to nitrogen deposition, ozone and their interaction in two Mediterranean tree species

Lina Fusaro [1,*], Adriano Palma [1], Elisabetta Salvatori [1], Adriana Basile [2], Viviana Maresca[2], Elham Asadi karam[3], Fausto Manes [1].

[1] Sapienza University of Rome, Department of Environmental Biology, P.le Aldo Moro, 5, 00185 Rome, Italy

[2] University of Naples "Federico II", Biology Department, via Cinthia, 80126, Naples, Italy

[3] University of Kerman, Biology Department, Shahid Bahonar Kerman, Iran

* Corresponding author

E-mail lina.fusaro@uniroma1.it

Abstract

The effects of nitrogen (N) deposition, tropospheric ozone (O_3) and their interaction were investigated in two Mediterranean tree species, *Fraxinus ornus* L. (deciduous) and *Quercus ilex* L. (evergreen), having different leaf habits and resource use strategies,. An experiment was conducted under controlled condition to analyze how nitrogen deposition can affect ecophysiological and biochemical traits, and to explore how the nitrogen-induced changes would influence the response to O_3. For both factors we chose realistic exposures (20 kg ha^{-1} yr^{-1} and 80 ppb h for N and O_3, respectively), in order to elucidate the mechanisms implemented by the plants. Nitrogen addition resulted in higher nitrogen concentration at the leaf level in *F. ornus*, whereas a slight increase was detected in *Q. ilex*. Nitrogen enhanced the maximum rate of assimilation and ribulose 1,5-bisphosphate regeneration in both the species, whereas influenced the light harvesting complex only in the deciduous *F. ornus*. that was also affected by O_3 (reduced assimilation rate and accelerated senescence-related processes). Conversely, *Q. ilex* developed an avoidance mechanism to cope with O_3, confirming a substantial O_3 tolerance of this species. Nitrogen seemed to ameliorate the harmful effects of O_3 in *F. ornus*: the hypothesized mechanism of action involved the production of nitrogen oxide as the first antioxidant barrier followed by enzymatic

antioxidant response. In *Q. ilex*, the interaction was not detected, but in this specie nitrogen might stimulate an alternative antioxidant response such as the emission of volatile organic compound: antioxidant enzymes activity was lower in plants treated with both O_3 and nitrogen even though reactive oxygen species production did not differ between the treatments.

Keywords: tropospheric ozone; nitrogen deposition; rubisco activity; photosystems functionality; antioxidant activity; leaf nitrogen and carbon concentration; functional traits.

1. Introduction

Mediterranean forests are subjected to challenging environmental conditions in the current global change context, since many stressors, individually or in combination, affect plants functionality simultaneously or successively over time [1]. Of more recent concern are the combined effects of ozone (O_3) and nitrogen (N) on vegetation [2]. Monitoring activities in European countries have indicated that studies on O_3 exposure effects are essential in Mediterranean regions [3], where the concurrence of high temperature and radiation promote the photo-stationary cycle toward high O_3 concentration during the late spring and summer seasons [4].

O_3 impacts forests by increasing the oxidation load, thereby triggering the production of Reactive Oxygen Species (ROS) that lead to alterations of functional processes at different levels [5,6]. The production of ROS activates the detoxifying barrier in the apoplast and enzymatic activity at the symplastic level that have high metabolic cost [7,8], and the capacity to increase antioxidant defences is recognized as a key factor in determining O_3 tolerance [9–12].

Leaf gas exchanges are also affected by O_3 through a direct impact on stomatal guard cell functionality [13,14], or stomatal number [15], as well as owing to a decrease in the photochemical and carboxylation efficiency [15–18]. Leaf structural traits such as leaf mass area (LMA), in addition to leaf nitrogen and carbon concentrations, have been found to reveal ozone sensitivity and tolerance in different species [19,20], where species with low LMA and high leaf nitrogen concentration show higher O_3 sensitivity [11,21]. Further, O_3 can adversely influence these functional traits, accelerating leaf senescence processes [22–24].

Nitrogen deposition represents an additional threat for Mediterranean forests adapted to low nitrogen availability [25]. During the last decades many studies have evaluated the effects of nitrogen on plant biodiversity and carbon balance or assimilation capacity [26–30], but many of them have been conducted on pastures [31], boreal temperate forest species [26], or in Chaparral species [32,33]. The implications concerning Mediterranean forests are still scarce [34], and knowledge regarding the response of the large plethora of functional traits to increasing nitrogen deposition for forest species is lacking [15,35,36]. In Italy, the average nitrogen throughfall, in terms of NO_3NH_4, measured using the network

of permanent monitoring stations, ranges between 4 and 29 kg ha^{-1} yr^{-1} [37], and the critical loads indicated for Mediterranean forest ecosystems, that fall within the range of 10 to 15 kg ha^{-1} yr^{-1}, have low reliability owing to the lack of experimental evidence [26].

Previous studies have shown that higher nitrogen availability can increase stomatal conductance [38,39], entailing a potential harmful increase in O_3 uptake. However the effects of nitrogen on hydraulic architecture and stomatal conductance are still contradictory [40]. Therefore, experiments under controlled conditions are required to better elucidate the mechanisms underlying the influence of nitrogen on key functional traits that are involved in pollutant uptake or antioxidant defence mechanisms, to better elucidate the possible interaction between nitrogen and other stressors such as O_3 [2]. Recent studies on the interaction between O_3 and nitrogen deposition have highlighted that O_3 reduced the nitrogen availability for photosynthesis [41]; further, the positive effect on root development owing to nitrogen, is lost at higher O_3 levels [42]. An antagonistic effect was detected on root starch concentrations, where higher nitrogen levels alleviated the negative impact of ozone [39]. Recent findings suggested that the interactions between O_3 and nitrogen depend on the concentration of these two factors and can change throughout the growing season [2].

Moreover, species can remarkably differ in nitrogen absorption depending on the successional stage and resource allocation strategy [43,44]. Deciduous species tend to allocate nitrogen to ribulose-1, 5-bisphosphate carboxylase/oxygenase (Rubisco) or to light-harvesting components in order to enhance the photosynthetic capacity; in contrast, in evergreen species, nitrogen is preferentially allocated to the cell walls, leading to an increase in the persistence of leaves [45,46], as well as toughness and chemical defence [47].

In this framework, we performed an experiment under controlled conditions to investigate how *Fraxinus ornus* L. and *Quercus ilex* L. react to nitrogen addition, and how nitrogen availability can influence the response mechanisms to O_3. For both factors we selected realistic exposures (20 kg ha^{-1} yr^{-1} and 80 ppb h for N and O_3, respectively), since an acute exposure could hinder the elucidation of mechanisms implemented by the plants [2]. We focused on these two species that typically co-occur in Mediterranean forests [48], and have different functional traits and ecological role. *F. ornus* is typical of early successional stages, with a rapid growing strategy, whereas *Q.ilex* belongs to the mature stage of a

succession, with a slow growth strategy, and a conservative patterns of nutrient use [49]. Moreover, previous studies suggested that *F. ornus* is moderately sensitive to O_3 [50], whereas *Q. ilex* was considered to be tolerant to this pollutant [11,15,51]; however, to the best of our knowledge, these two species have never been compared directly thus far.

We hypothesize that *F. ornus* uptakes a large amount of nitrogen, allocating higher fraction to the leaves and photosynthetic tissues, unlike that in *Q. ilex*. Accordingly, we expected that nitrogen addition would lead to higher mitigation of O_3 detrimental effects in *F.ornus*, owing to leaf habit and more flexible patterns of nitrogen uptake, than in *Q. ilex* [52]. This study provides new data on *F. ornus* and *Q. ilex* that would be useful to improve the risk assessment for Mediterranean forests subjected to nitrogen deposition and ozone. Furthermore, understanding the mechanisms underlying functional trait shifts under multistress environments could allow the forecasting of forests' responses to global change and addressing biodiversity conservation in the future.

2. Materials and Methods

2.1. Growth conditions

Two-years-old seedlings of *F. ornus* and *Q. ilex*, obtained from the nursery of Aurunci Regional Park (Central Italy), were transported to the experimental garden of the Department of Environmental Biology, Sapienza University of Rome on 18 May, 2016. Plants were transferred to 7 L pots along with their clods and the remaining pot volume was filled with a mixture of sand, turf and perlite. The experiment was conducted in a "walk-in" chamber facility, consisting of two closed chambers (2.5 m × 3.9 m × 3 m h): one was used as control and one for O_3 fumigation [53]. Air temperature was maintained at 27.9 ± 1.8 °C during the day and at 22.7 ± 0.9 °C at night. The relative humidity was 61 ± 6.1%.

In each chamber, a photosynthetic active radiation of approximately 700 $\mu molm^{-2}s^{-1}$ was provided for 12 h per day by using 6 metal halide lamps (1000 W, Philips HPI-T). The microclimatic conditions were monitored at 5-min interval, and did not differ significantly between the chambers. In each chamber, plants were randomly relocated daily to reduce possible position effects. During the entire experimental period, all plants were watered in order to maintain soil close to field capacity and avoid water stress.

2.2. Experimental design

After the plants were acclimated for 30 days to the chamber environmental conditions, 20 plants per species were randomly divided into four experimental sets (C, N, O_3 and O_3N). Ten plants per species were assigned to the control chamber and thus randomly divided as follows: five plants to the control experimental set (C, -O_3 -N), and five plants to nitrogen addition experimental set (N, -O_3 + N). Ten plants per species were assigned to the fumigated chamber and thus randomly divided as follows: five plants to the O_3 treatment (O_3, +O_3 -N), and five plants to the interaction experimental set, treated with both N and O_3 (O_3N, +O_3 +N).

The fertilizer was divided into 7 aliquots and applied throughout the experimental period as an aqueous solution. For this, 100 mL of deionised water was weekly added to each pot with different doses of ammonium nitrate (NH_4NO_3): 0 mg for C plants and 0.031 mg for N treatment. The final nitrogen dose was equal to 20 Kg N ha^{-1} yr^{-1} based on the soil surface

area. The ozone fumigation was started after five nitrogen additions, when was reached the cumulative dose roughly equivalent to 14 kg ha^{-1} yr^{-1}, which falls in the upper limit of the threshold load currently indicated as critical for Mediterranean vegetation. The acclimation to N addition phase and fumigation period lasted 30 days and 15, respectively.

During the fumigation period, the C and N experimental sets were kept in the control chamber under filtered air (O_3 = 0 to maximal 5.8 ppb). The O_3 and O_3N sets were placed in the fumigation chamber and exposed for 10 consecutive days to a mean hourly O_3 concentration of 87.00 ± 0.5 ppb for 5 h per day simulating a concentration found in the Mediterranean rural area during the summer period [54,55]. The cumulative exposure was 2585.47 ppb h, expressed as AOT40, i.e. the sum of the differences between the hourly mean ozone concentration in ppb and 40 ppb for each hour when the concentration exceeds 40 ppb, accumulated during daylight hours [55]. O_3 in the fumigation chamber was generated by flowing pure oxygen on a UV light source (Helios Italquartz, Milan, Italy), and then added to the chamber air inlet via a Teflon tube. The O_3 concentration at plant height was continuously monitored using a photometric O_3 detector (Model 205, 2B Technologies, Boulder, CO, USA).

Leaf gas exchange and chlorophyll (Chl) *a* fluorescence were measured every three days, particularly on first, fourth, seven and tenth day of fumigation (DOF). At the end of the experimental period, leaves for biochemical analysis and structural measurements (nitrogen and carbon concentration, leaf mass area) were sampled immediately after the end of fumigation; P_N/C_i curves were performed within two days.

2.3. Gas exchanges measurements

Steady state measurements of gas exchanges were performed using a portable infrared gas analyzer (CIRAS-2, PP-System International, Amesbury, MA). The net photosynthesis (P_N, $\mu molCO_2$ m^{-2} s^{-1}), leaf transpiration (E, $mmolH_2O$ m^{-2} s^{-1}), stomatal conductance (gs, $mmolH_2O$ m^{-2} s^{-1}) and sub-stomatal CO_2 concentration (C_i, ppm) were simultaneously measured. The instantaneous water use efficiency (WUE, µmol CO_2 mmol H_2O^{-1}) was calculated as the ratio between net photosynthetic rates and transpiration rates, and the ratio of substomatal and ambient CO_2 concentration, C_i/C_a, was determined. All measurements were performed using fully developed leaves.

2.4. Chl *a* fluorescence measurements and application of the JIP-test

The Chl *a* fluorescence was measured using a Handy PEA direct fluorometer (Hansatech Instruments, Norfolk, UK) on the same days, hours, and leaves as those used for steady state gas exchange measurements. After a dark adaptation period of 40 min, obtained using specific leaf clips, the leaf samples were exposed to a saturating red light pulse (peak 650 nm) of 3000 μmol photons m^{-2} s^{-1}, for 1 s, thus generating a fluorescence transient (FT). The FT, plotted on a logarithmic timescale, shows a polyphasic behaviour, the different steps of which corresponded to a specific stage in the electron chain between reaction centres of photosystem II (PSII) and end acceptors of photosystem I (PSI). The first part of the transient curve (O–J) is called 'single turnover region'. It expresses the photochemical events, providing information regarding the reduction of plastoquinone. The J–I–P region of the FT is called 'multiple turnover region' and reflects the velocity of ferredoxin reduction beyond PSI. In particular, the I–P region reflects the velocity and quantity of ferredoxin and NADP reduction via electron donation of PSI. The JIP test was applied to the FT, and the following parameters were calculated from each curve:

- φ_{Po}: maximum quantum yield of primary photochemistry expresses the probability that an absorbed photon will be trapped by the PSII reaction centre;
- J-phase: expression of the efficiency with which a trapped exciton can move an electron into the electron transport chain from plastoquinone to the intersystem electron acceptors;
- IP-phase: expression of the efficiency of electron transport around PSI to reduce the final acceptors of the electron transport chain, i.e. ferredoxin and $NADP^+$
- PI_{tot}: a multiparametric expression that synthesizes the potential for energy conservation from photons absorbed by PSII to the reduction of PSI end acceptors.

2.5. P_N/C_i response curves

The response of net photosynthesis to the variation of substomatal CO_2 concentration was measured on the same leaves sampled for steady state gas exchanges. Two intercalibrated CIRAS2 were used for simultaneous measurements. The P_N/C_i curves were constructed following Long and Bernacchi, 2003 [56]. Cuvette environment was maintained at 60% relative humidity and at 28°C; photosynthetic active radiation was mantained at the

saturating value of 1000 μmol $m^{-2}s^{-1}$. The assimilation rate under CO_2 saturation (P_{Nmax}) was measured and the maximum electron transport rate driving regeneration of ribulose 1,5-bisphosphate (J_{max}, mol m^{-2} s^{-1}) was calculated according to Loustau et al., 1999 [57]. The CO_2 compensation point Γ (ppm) was derived and the *in vivo* apparent Rubisco activity (V_{cmax}, mol $m^{-2}s^{-1}$) was calculated as the angular coefficient of the linear part of the curve. Data at very low [CO_2], which can be limited by Rubisco deactivation, were excluded from the analysis [58].

2.6. Leaf chemistry and derivation of the photosynthetic nitrogen use efficiency

The total leaf nitrogen and carbon concentrations (N_L, C_L, % dry mass) were determined using the Dumas micro-combustion technique (Eurovector EA 3000, Milan, Italy) on the same dried leaf samples used for the calculation of sclerophylly degree (see paragraph Leaf structural and total biomass traits). Samples were ground in liquid nitrogen, and five subsamples were weighed using a precision balance (MJ-300, d=0.001g) before the analysis. Photosynthetic Nitrogen-Use Efficiency (PNUE) was calculated as the ratio of instantaneous P_{Nmax} to N on an area basis.

2.7. Antioxidant enzymes

Antioxidant enzyme activities were determined using fresh leaf material, which was extracted as described previously [59]. All reagents for oxidative stress detection were purchased from Sigma-Aldrich (St. Louis, MO, USA). ROS production was detected using the general oxidative stress cell-permeant 2′,7′dichlorodihydrofluorescein diacetate dye. This dye passively diffuses into the cells and interacts with endogenous esterases, which cleave the diacetate groups. The stock solution of the dye (25 μM in DMSO) was diluted to a final concentration of 5 μM. Fluorescence was monitored using a fluorescence spectrophotometer, with an excitation wavelength of 350 nm and an emission wavelength of 600 nm. The increase in fluorescence intensity yielded the ROS quantity.

The Superoxide dismutase (SOD) activity was determined using an SOD assay kit – WST (Sigma–Aldrich) – according to manufacturer's instructions. The SOD activity (inhibition of activity) was calculated by measuring the decrease in the colour development at 440 nm. Catalase (CAT, EC 1.11.1.6) activity was measured using a commercial CAT assay kit

(Sigma–Aldrich) following manufacturer's protocol. CAT activities were calculated and expressed as a decrease in absorbance at 240 nm due to H_2O_2 consumption. Total ascorbate peroxidase (APX, EC 1.11.1.11) activity of leaves was assayed by monitoring the decrease in absorbance at 290 nm due to ascorbate oxidation [60]. The concentration of ascorbic acid (ASC) was measured as described by [61]. Briefly, total ascorbate was determined after the reduction of oxidised ascorbic acid (DHA) to ASC with 1,4-dithiothreitol, and the concentration of DHA was estimated from the difference between the total ascorbate pool (ASA plus DHA) and ASC. Glutathione (GSH) content was determined at 412 nm by using 5,5′-dithiobis(2-nitrobenzoic acid), according to the spectrophotometric method of [62].

2.8. Leaf structural traits

The degree of sclerophylly was estimated by assessing the leaf mass area (LMA, g cm^{-2}). After petiole exclusion, the leaf area was measured using Image Lab software (http://en.freedownloadman-ager.org/Windows-PC/Image-Lab.html), and after the samples were dried at 80°C to constant weight, the leaf dry weight (g) was measured.

2.9. Statistical analysis

The effect of time on ecophysiological measurements (gas exchanges and Chl *a* fluorescence) was analyzed using repeated measurement ANOVA with nitrogen and O_3 treatments as between-subjects factors. Two-way ANOVA, with nitrogen and O_3 as fixed factors, with their interaction factor, was used to analyze the ecophysiological measurements during each sampling date (DOF1, DOF 4, DOF 7 and DOF 10), and to test the differences between treatments on the P_N/C_i curve parameters and on the biochemical and structural measurements obtained at the end of the experiment. Two-way ANOVA was followed by post hoc Student–Neuman–Keuls test at $p < 0.05$ when necessary. All analyses were performed using Statistica software, version 7.0 (StatSoft, Tulsa OK, USA).

3. Results

3.1. Steady-state gas exchanges

Advancement of time (e.g plant developmental stage) affected the gas exchanges parameters for both species, with the exception of WUE in *F. ornus*, in which a significant time × nitrogen interaction was noted (Table 1, A) for all parameters. Time × O_3 interaction was significant for WUE and C_i/C_a in *Q.ilex*, whereas the three level interaction was significant for WUE and C_i/C_a in both species and for g_s only in *Q. ilex*.

In particular, comparison of the gas exchange parameters of *F.ornus* for each sampling date (Fig 1) revealed that nitrogen affected all the assayed parameters at DOF 1, with a decrease in P_N, g_s, and C_i/Ca and an increase in WUE. However, at DOF4, only P_N was affected and at the following sampling dates, no difference from C values was found.

O_3 began to affect P_N and g_s (-75 and - 82 % compared to those in the control, respectively) on DOF 4, lasting with the same order of magnitude through DOF 7 to 10. The interaction significantly affected P_N and g_s for low or high O_3 exposure (DOF 1 and 10, AOT40 254.22 and 2585.47 ppb h respectively); the direction of the interaction remained the same, where the decrease of P_N and g_s relative to the control was less pronounced in O_3N plants than in O_3 alone.

For *Q. ilex* nitrogen increased both P_N and g_s relative to those in C (from +5 to 15 % depending on DOF); however the variability in the data led to $p > 0.05$ at each DOF (Fig 2). The main factor affecting gas exchanges was O_3, entailing a decrement of P_N (-60% at DOF 4, - 28% at DOF 7 and – 23% at DOF10) because of stomatal limitation as indicated by C_i/C_a reduction. The interaction was present on DOF 1, for low O_3 exposure (AOT40 254.22 ppb h), only for g_s where the reduction in O_3N experimental set was higher than in the O_3 set. At DOF 4 and DOF 10 the reduction of P_N and g_s in O_3N was less pronounced than O_3, even if the interaction effect was not significant (Table 1, B).

3.2. Chl *a* fluorescence measurements

The repeated measures ANOVA showed that the photosystems functionality was not affected by time in both the species (Table 2, A).

In *F. ornus*, nitrogen enhanced the primary reactions characterizing the single turnover region of the fluorescence transient (Fig 3 A, B). A slight but significant increase of φ_{Po}

occurred at DOF 4 and DOF 10, and the J-phase was affected from DOF 1 to DOF 7 (Table 2, B). Nitrogen influenced the IP-phase (rate of reduction of end acceptors ferredoxin and NADP) on DOF 4 and 10, and the overall functionality of photosystems as showed by the trend of PI_{tot}. O_3 affected the JIP-test parameters since DOF 1, decreasing both IP-phase and PI_{tot} relative to those in control. The interaction between nitrogen and O_3 was evident on PI_{tot} (DOF 4, 10), with nitrogen ameliorating the detrimental effect of O_3 photosystem functionality (Fig 3 D).

In *Q. ilex* the effect of nitrogen and interaction between factors on photosystems functionality was marginal (Fig 4; Table 2), affecting IP-phase and PI_{tot} on DOF1 only. The main driver of photosystems functionality was O_3 which influenced the primary photochemistry (Fig 4 B) only during the final phase of O_3 exposure (DOF 7 and 10), whereas IP-phase and PI_{tot} (Fig 4 C, D) were affected by O_3 since DOF1.

3.3. P_N/Ci response curves

The parameters derived from P_N/C_i curves, together with PNUE, chemical and structural leaf traits such as nitrogen and carbon concentration for the two species (N_L C_L), their ratio, and LMA are shown in Table 3.

In *F. ornus*, P_{Nmax} increased significantly after nitrogen addition (final dose 20 kg ha^{-1} yr^{-1}), decreasing in response to O_3 (Table 3). The Nitrogen concentration at the leaf level increased in +N experimental set, although slightly significant ($p = 0.058$). The main driver of photosynthesis was O_3, leading to a reduction of P_{Nmax}, V_{cmax} and J_{max} relative to those in C plants. The N_L decreased because of O_3 fumigation, entailing a significant change in the C_L/N_L ratio. The interaction between factors significantly affected J_{max}: O_3 limited the positive effect of nitrogen. In *F. ornus*, nitrogen did not affect the LMA, whereas this parameter was reduced by O_3 (Table 3).

Interestingly, in *Q. ilex* the response curves parameters were affected by nitrogen, thereby enhancing P_{Nmax} as well as the apparent maximum electron transport rate contributing to RuBP regeneration (J_{max}). Nitrogen addition resulted in an increase of N_L (+14 and +8 % in N and O_3N experimental sets respectively); however, because of high variability in the data, no significant N effect ($p > 0.05$) was detected. However, C_L significantly increased in the evergreen species.

O_3 caused the reduction in PNUE, because of slight, but not significant ($p > 0.05$), reduction of P_{Nmax} and N_L, and an increase in C_L concentration. No interaction was detected. LMA decreased in *Q. ilex* after nitrogen addition, since leaf area increased (data not shown), influencing in the same direction as the LMA of O_3N experimental set.

3.4. Antioxidant enzyme activities

In both the species, N addiction increased SOD, CAT and GSH activities, the key enzymatic components of the first antioxidant defense mechanisms involved in O_2^- and H_2O_2 scavenging (Fig 5).

In *F. ornus* the ROS amount increased significantly under O_3 exposure; however, compared to that in C, their concentration in the O_3 experimental set was higher than that in the O_3N experimental set. Accordingly, the activity of the first line of ROS scavengers, such as SOD and CAT were higher in O_3 than in the O_3N experimental set, but the antioxidants involved in the conversion of H_2O_2 to O_2 or H_2O (i.e APX, ASA, DHA and GSH) were upregulated in the O_3N plants. Conversely, in *Q. ilex*, even if ROS were produced to the same extent as in O_3 and O_3N plants, SOD and CAT were lower in O_3N than in O_3. All the antioxidants related to ascorbate-glutathione cycle were higher in O_3N than in O_3 plants.

4. Discussion

The impacts of atmospheric nitrogen deposition and O_3 on Mediterranean forests have been of increasing concern, and experimental data are needed to elucidate the mechanisms of action, or identify specific functional traits affected by interacting stress factors. Thus, the present study aimed to measure the effects of realistic exposure of nitrogen and O_3 on a broad range of traits of two Mediterranean species with different leaf habits to characterize their response. The study was performed under controlled condition in a medium-term experiment, in order to determine the traits that are first affected by nitrogen and how the potential nitrogen effects can influence the response to O_3. Moreover, to our knowledge, this is the first study to compare *F. ornus* and *Q .ilex* directly after O_3 exposure, with important implication for assessing the risk for these co-occurring species.

4.1. Response patterns to nitrogen deposition

An overview of available literature highlights that results for the effects of nitrogen deposition at the leaf and plant levels are contradictory [37,63]. The numerous processes involved in nitrogen assimilation and metabolism might bring high variability in the assayed data. In our experiment, after an acclimation period to nitrogen, when the cumulative dose was roughly equivalent to 14 kg ha yr^{-1}, thereby within the threshold load considered as critical for Mediterranean vegetation, nitrogen concentration at the leaf level did not increase in both species and no negative effect was detected on photosynthetic traits (data not shown). When nitrogen exposure exceed this level, between 14 and 17 kg ha yr^{-1} (DOF 1), assimilation rate measured under steady state conditions was adversely affected in *F.ornus* possibly because of the decrease that nitrogen caused on stomatal conductance, as documented in several species [64,65]. Indeed nitrogen can affect g_s by changing the hydraulic conductivity [40], or by increasing nitric oxide (NO) that is emitted from different plant species as a side-reaction of the nitrate assimilation process [66]. In fact, NO is required in the ABA-induced stomatal closure process [65,67]. Since the first mechanism has been observed in long-lasting fertilisation experiments (from 2 to 5 years of nitrogen addition), we argue that in our study the nitrogen effect on g_s could be mediated by NO signalling.

Interestingly, in both the species P_{Nmax} and J_{max}, increased because of nitrogen, whereas V_{cmax} did not change, namely the electron transport driving RuBP regeneration was more affected than carboxylation. This result also explains why the assimilation rate measured under steady state condition, i.e in the Rubisco-limited phase [56], did not show variations. Moreover, this evidence and the Chl a fluorescence measurement, indicate that, while in *Q. ilex* a higher fraction of nitrogen was allocated to components related to biochemical phase of assimilation process than to light-harvesting elements [68], this hypothesis is not completely applicable to *F. ornus*. In fact, in the former species nitrogen significantly affects only the parameters related to the functionality of the end acceptors (i.e IP-phase and PI_{tot}), whereas in *F. ornus*. also primary photochemistry (φ_{Po} and J-phase) was enhanced by nitrogen, confirming that the partitioning pattern can differ depending on leaf habit [46].

In agreement with ecophysiological measurements, at the end of the experimental period, the concentration of nitrogen on mass basis increased to a different extent between the species. In *F. ornus*, nitrogen addition resulted in 25% higher N_L relative to that in the control (p= 0.058), whereas in *Q. ilex* the variation was less pronounced (+ 14%). It is worth to notice that in both species PNUE did not change because of nitrogen addition. This could be because the value of PNUE changes according to many factors such as assimilation rate, Rubisco activity, nitrogen concentration on area basis, and LMA [69], and thus resulting in no difference in PNUE between treatments, as in our study. If we expressed nitrogen per leaf area (data not shown) in *F. ornus* the percentage of variation between plants treated with nitrogen and control ones, decreased (+ 16%), whereas the variation remained around the + 14 % for *Q. ilex*. These changes could be because of the effect of nitrogen supply on leaf structural traits [28]. In *F. ornus* nitrogen treatment decreased both leaf area and dry mass, resulting in no LMA variation relative to that in the control plants. However, in *Q. ilex*, the LMA decreased because of nitrogen, since the leaf area increased, thus the evergreen species did not invest resources in the cell wall to increase leaf toughness as has been reported in other studies [70,71].

4.2. Response patterns to ozone

Ozone effect was assessed using a wide range of traits to allow defining thoroughly the differences in the response patterns between the species. Plant sensitivity to O_3 cannot be identified based on the extent of leaf injury alone, because impairments to photosystem functionality and photochemistry occur before the appearance of visible injury [53,72]. In our experiment, although we adopted a realistic O_3 exposure (80 ppb h, AOT40 2458), *F. ornus* seemed to be sensitive to this pollutant because it did not trigger an active physiological response to O_3, such as avoidance mechanisms, determining instead an incoming injury. The gas exchange reduction occurred since the first day of fumigation (-55 and -33 % for g_s and P_N respectively), remaining around this order of magnitude for the entire fumigation period. Furthermore, in this species the P_N reduction was not merely owing to stomatal limitation, since the P_N/Ci response curves highlighted a decrease of P_{Nmax} and of both carboxylation efficiency (V_{cmax}) and maximum electron transport rate driving RuBP regeneration (J_{max}). The reduction of nitrogen concentration, i.e. increase of

leaf senescence, can also be a good indicator of O_3 injury helping to define the scale of tolerance between species [23]. In *F. ornus* O_3 exposure accelerated the processes related to senescence because of the decrease of leaf nitrogen and dry matter, as showed by the decrease of LMA. Although the results from controlled conditions cannot be extended to natural ecosystems, the sensitivity found in this experiment should be considered for risk assessment of tree species in a Mediterranean climate. The response pattern of *Q. ilex* to O_3 can be attributed to an avoidance mechanism, as shown by traits related to photochemistry, photosystems functionality or structural traits. The reduction of P_N in O_3 treated plants relative to controls was less pronounced in *Q. ilex* than in *F. ornus*, starting on DOF 4, and was related to stomatal limitation more than to biochemical impairments. Indeed, the parameters derived from P_N/Ci curves did not indicate detrimental effect on Rubisco activity because of O_3, whereas the analysis of photosystems functionality highlighted a down-regulation mechanisms (i.e reduction of end-acceptors activity). The differences in the response strategies implemented by the two species could be strictly associated with a different antioxidant potential [11]. Indeed the inherent amount of CAT, responsible for the removal of H_2O_2 [73] was higher in *Q. ilex*. Moreover, the components involved in the ascorbate-glutathione cycle (APX, ASA, DHA and GSH) showed high concentration or activity in *Q. ilex* relative to *F. ornus*, but these could be related to the higher stomatal conductance (that is, high O_3 fluxes) in the former species. Furthermore, in both the species, the finding that in O_3 treated plants the increase in DHA/ASA ratio was lower than the increases in APX activity suggests that recycling of DHA to ASA was not compromised by O_3.

Response patterns to the interaction between nitrogen deposition and ozone

Information on the interactive effects of nitrogen deposition and ozone pollution on vegetation is still scarce [34]. Many of the studies on nitrogen and O_3 have focused on the changes in community structure or species abundance in grasslands ecosystems [30,31,74]. However, few studies have determined the consequences of nitrogen and O_3 interaction on tree species [24,38,42]. The results highlighted by previous studies suggested that the interactive effects could be dynamic, changing throughout the growing season, and the effects on key ecophysiological parameters, such as P_N and g_s, can remarkably change depending on the concentration of nitrogen and O_3 exposure. In the present study, the interaction followed different patterns in the two species, confirming our hypothesis that

leaf habit plays a crucial role in determining the way of interaction between the two factors. In particular, in *F. ornus* the interaction was detectable on several traits indicating that nitrogen addition can ameliorate the detrimental effects owing to O_3. Nitrogen had a positive effect on the processes related to photochemistry, resulting in enhanced carbon assimilation rate in the O_3N experimental set relative to that in O_3 experimental set. The mechanisms involved in this type of response could be associated with the investment of available nitrogen to proteins that play a crucial role in enhancing the photosynthetic activity [75]. We argue that nitrogen was partially allocated to light-harvesting components, increasing the capacity to manage the energy flow thorough the photosystems [76]. The positive effect of nitrogen on the functionality of plants treated with O_3 could also be attributed to the upregulation of antioxidant response to O_3 implemented by nitrogen addition [77]. In particular, in O_3N plants the APX activity, ASA and DHA were almost doubled compared to that after treatment with O_3 alone. Moreover, in *F. ornus*, the O_3N experimental set led to lower ROS production relative to that in O_3 plants, that is, lower exposure to oxidative stress, even if the O_3 fluxes remained almost the same. On average, during the entire experimental period g_s was about to 96.9 ± 21.2 and 92.5 ± 12.3 in O_3 and O_3N respectively. This could be because of NO synthesis. Plants can emit NO under a series of stresses [78], in particular under ozone exposure [7], and several studies revealed that high N availability can promote NO production [79]. NO is involved in triggering antioxidant response, and can react directly with free radicals such as H_2O_2 and O_2^-, thereby decreasing their concentrations. We argue that, in the presence of high nitrogen availability, *F. ornus* can cope with incoming oxidative stress via the production of NO, which owing to the rapid synthesis and prompt availability, allows prompt scavenging of free radicals and concomitantly increases the photosynthesis rate [80]. We called into question this response mechanism to O_3 only for *F. ornus* because of NO synthesis should be favored in plants that do not emit VOCs, such as *F. ornus*, explaining the difference in the response patterns between the two species used in this study. We have to consider that *Q. ilex* is a strong monoterpene emitter species [81]. As shown by Velikova et al., [78], higher NO is emitted in the leaves that are isoprene-inhibited, and considering the similarity in biochemistry of isoprene and monoterpenes, we speculated that in *Q. ilex* the response to oxidative compounds is attributed to VOCs [82] than to NO.

Most importantly, in both the species nitrogen increased the constitutive amount of antioxidant enzymes such as SOD, CAT, but did not affect their activity (GST did not change, data not shown).

Unlike in *F. ornus*, in *Q. ilex* the interaction between nitrogen and O_3 was weak, and appeared only on DOF 1, when nitrogen seems to aggravate the stomatal limitation owing to O_3. g_s of O_3N plants recovered at the following sampling times to the level in the O_3 experimental set.

Photosystems functionality was not affected by the interaction and Rubisco related parameters did not show any nitrogen effect (positive or negative) when plants were exposed to O_3. However, interestingly, enzymes such as SOD and CAT, which play a crucial role in determining a suitable level of ROS in different cell compartments [73], were lower in O_3N plants than in O_3 plants, although the ROS production did not differ between the treatments. This evidence suggests that, in *Q. ilex*, nitrogen addition could enhance secondary metabolism promoting the production of VOCs, that can quench O_3 directly without activating an enzymatic antioxidant response. Conversely, similar to that in *F. ornus*, nitrogen upregulated the activity of the ascorbate-glutathione cycle in *Q. ilex*, indicating that nitrogen deposition can largely protect against oxidative stressors and to multi-stress condition experienced by Mediterranean vegetation.

5. Conclusion

Nitrogen deposition differently affected the functional traits of the two studied species. Influence of nitrogen on gas exchange parameters measured under the steady state condition had an unclear trend, confirming a complex mechanism of action of nitrogen on stomatal conductance. In both species photosynthetic traits as photosystems functionality, maximum assimilation and maximum electron transport rate were enhanced by nitrogen at the end of the experiment, when 20 kg N ha^{-1} y^{-1} had reached. However, chlorophyll *a* fluorescence measures revealed that nitrogen supply in *F. ornus* had also affected photochemical reactions, suggesting that nitrogen was allocated to the light harvesting components. *F. ornus* should be defined as an O_3-sensitive species, since biochemical limitation to photosynthesis as well as senescence processes were noted. Even if a significant effect of interaction was evident on photosynthetic processes in *F. ornus* only,

in both species nitrogen enhanced antioxidant activity, thus ameliorating O_3-related impacts. However, different mechanisms might be highlighted in the two species. In the deciduous specie *F. ornus*, the lower ROS production in the interaction experimental set (O_3N) might be related to the enhanced nitrogen oxide production, whereas in *Q. ilex* nitrogen might have upregulated the secondary metabolism promoting high VOCs production. This hypothesis is based on the fact that, although no difference was noted in ROS production between O_3 and O_3N plants in this species, the activity of the first level scavenging enzymes such SOD or CAT was lower in the interaction experimental set. These results indicate that nitrogen deposition could counteract the detrimental effect of O_3, thus suggesting that nitrogen is an important factor for assessing the critical level of O_3 for Mediterranean vegetation.

Acknowledgments

This study was supported by the following grants: MIUR, Rome, Project PRIN 2010-2011 "TreeCity" (Prot. no. 20109E8F95); Avvio alla Ricerca, Sapienza Research Project 2015 (Prot.No. C26N15CHHN); Sapienza Ateneo Research Project 2016; Accademia Nazionale delle Scienze detta dei XL (2012 Grants). Authors thank Dr. Antonietta Siciliano for providing support for antioxidant analysis.

Figure and Table

Table 1. Analysis of variance of the gas exchanges parameters for *F. ornus* and *Q. ilex*.

		F. ornus				*Q. ilex*			
Factors		**P_N**	**g_s**	**WUE**	**C_i/C_a**	**P_N**	**g_s**	**WUE**	**C_i/C_a**
a) *Repeated measures ANOVA*									
Time		**0.000**	**0.003**	0.077	**0.023**	**0.001**	**0.000**	**0.000**	**0.000**
Time × N		0.058	**0.004**	**0.000**	**0.000**	0.612	0.752	0.594	0.559
Time × O_3		0.435	0.589	0.173	0.069	0.606	0.070	**0.017**	**0.047**
Time × N × O_3		0.521	0.109	0.052	**0.025**	0.124	**0.010**	**0.005**	**0.006**
b) *Two-way ANOVA*									
DOF 1	N	**0.033**	**0.002**	**0.000**	**0.000**	0.992	0.867	0.715	0.813
	O_3	0.212	0.055	0.672	0.936	0.076	0.177	0.678	0.861
	N × O_3	**0.013**	**0.008**	**0.004**	**0.005**	0.509	**0.050**	**0.036**	0.055
DOF 4	N	**0.018**	0.071	0.640	0.370	0.256	0.299	0.335	0.355
	O_3	**0.001**	0.051	0.885	0.900	**0.009**	**0.006**	**0.025**	**0.032**
	N × O_3	0.050	0.202	0.970	0.670	0.151	0.469	0.505	0.560
DOF 7	N	0.969	0.922	0.901	0.540	0.074	0.160	0.995	0.706
	O_3	0.058	**0.035**	**0.022**	**0.001**	**0.029**	**0.004**	**0.026**	**0.012**
	N × O_3	0.389	0.728	0.927	0.950	1.000	0.915	0.790	0.754
DOF 10	N	0.432	0.725	0.185	0.162	0.146	0.117	0.496	0.658
	O_3	**0.013**	**0.014**	0.230	0.354	**0.006**	**0.000**	**0.001**	**0.004**
	N × O_3	**0.008**	0.050	0.748	0.944	0.597	0.316	0.858	0.757

Analysis of variance on steady-state gas exchange parameters: Repeated measures ANOVA (a) and two-way ANOVA (b) of time, nitrogen, O_3 and their interaction effects are reported for each measurement date. DOF = day of fumigation. Significant ($p < 0.05$) factors are marked in bold; 'quasi' significant factors ($0.1 > p > 0.05$) are underlined.

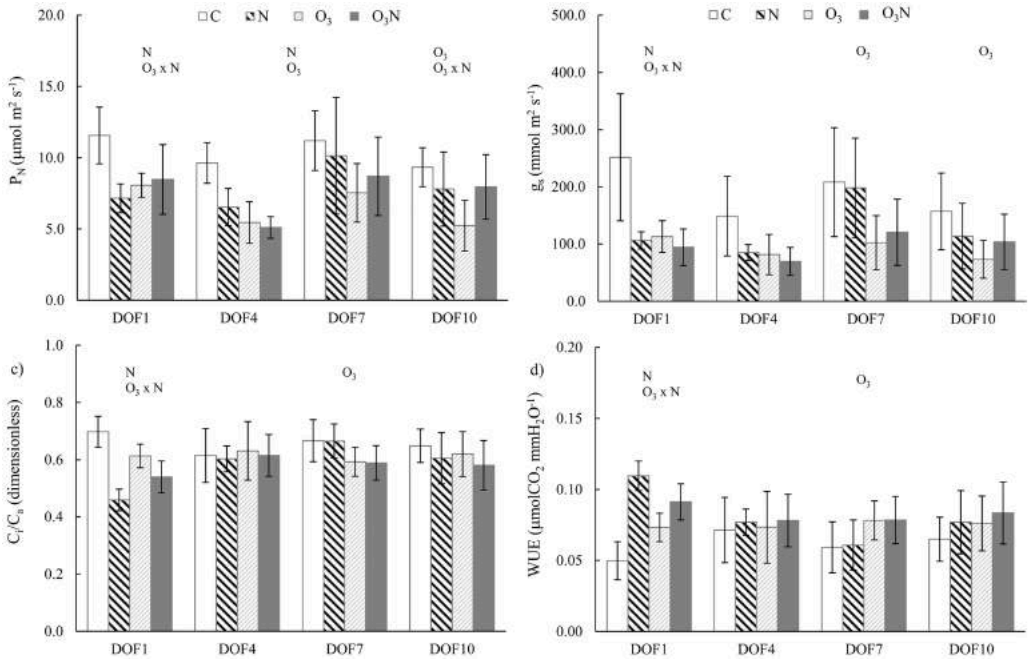

Figure 1. Trend of steady-state gas exchanges parameters in *F. ornus*. The trend is shown as the mean and standard deviation (n=5) for each treatment. Measurements were performed at the first, fourth, seventh, and tenth day of fumigation (DOF). Symbols over the bars indicate the significant factors ($p < 0.05$) affecting the gas exchanges parameters: N, nitrogen effect; O_3, ozone effect; $O_3 \times N$, interaction.

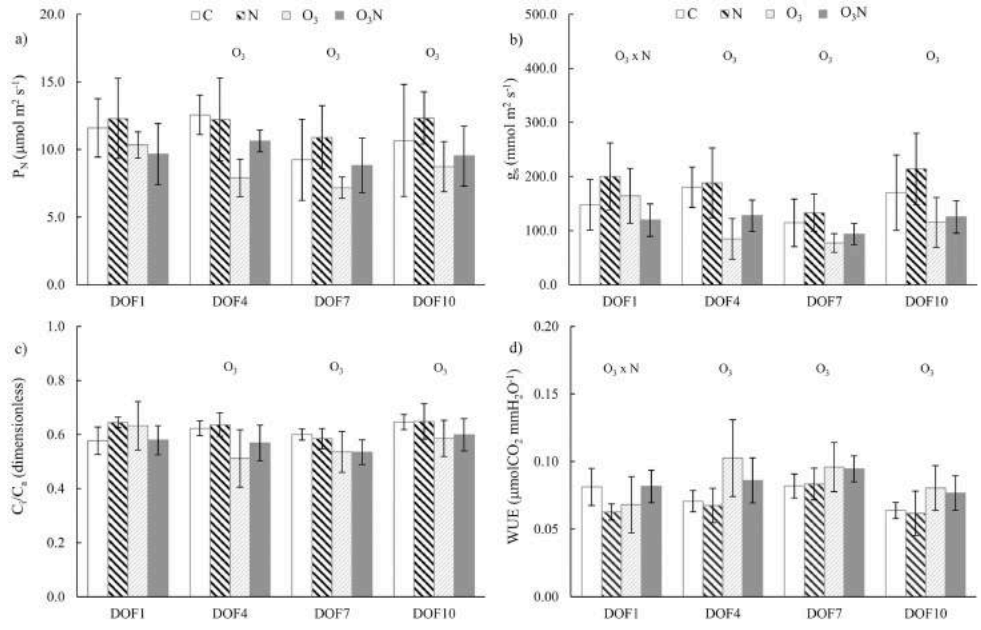

Figure 2. Trend of steady-state gas exchanges parameters in *Q.ilex*. The trend is shown as the mean and standard deviation (n=5) for each treatment. Measurements were performed at the first, fourth, seventh, and tenth day of fumigation (DOF). Symbols over the bars indicate the significant factors ($p < 0.05$) affecting the gas exchanges parameters: N, nitrogen effect; O_3, ozone effect; $O_3 \times N$, interaction.

Table 2 Analysis of variance of JIP-test parameters for *F. ornus* and *Q. ilex*.

		F. ornus				*Q. ilex*			
Factors		**φ_{P0}**	**J-phase**	**IP-phase**	**PI_{tot}**	**φ_{P0}**	**J-phase**	**IP-phase**	**PI_{tot}**
a) *Repeated measures ANOVA*									
Time		0.576	0.781	<u>0.082</u>	0.141	0.249	0.369	0.363	0.419
Time × N		0.670	0.959	0.359	0.250	0.739	0.753	0.565	0.286
Time × O_3		0.853	0.979	0.832	0.478	0.879	0.604	0.662	0.521
Time × N × O_3		0.062	0.588	0.092	0.220	0.184	0.204	0.788	0.670
b) *Two-way ANOVA*									
DOF 1	N	0.016	**0.000**	0.075	**0.000**	0.788	0.213	**0.044**	**0.044**
	O_3	0.625	**0.004**	0.726	**0.005**	0.118	0.077	**0.001**	**0.002**
	N × O_3	0.683	0.589	0.321	0.361	0.630	0.870	**0.016**	0.156
DOF 4	N	**0.000**	**0.042**	**0.000**	**0.000**	0.987	0.991	0.973	0.816
	O_3	**0.000**	0.570	0.443	**0.1**	0.022	0.365	**0.002**	**0.001**
	N × O_3	0.552	0.435	**0.000**	**0.000**	0.521	0.313	0.789	0.776
DOF 7	N	0.072	**0.025**	**0.056**	**0.028**	0.734	0.114	0.151	0.209
	O_3	0.467	0.781	0.267	0.187	0.056	**0.013**	**0.001**	**0.001**
	N × O_3	0.064	**0.014**	0.456	0.820	0.126	0.268	0.936	0.282
DOF 10	N	**0.038**	0.765	**0.000**	**0.000**	0.744	0.374	0.834	0.178
	O_3	0.795	0.179	**0.016**	0.114	0.195	**0.053**	**0.003**	**0.000**
	N × O_3	0.239	0.723	**0.009**	**0.001**	0.436	0.642	0.424	0.397

Analysis of variance on JIP-test parameters: Repeated measures ANOVA (a) and two-way ANOVA (b) of time, nitrogen, O_3 and their interaction effects,reported for each measurement date. DOF = day of fumigation. Significant ($p < 0.05$) factors are marked in bold; 'quasi' significant factors ($0.1 > p > 0.05$) are underlined.

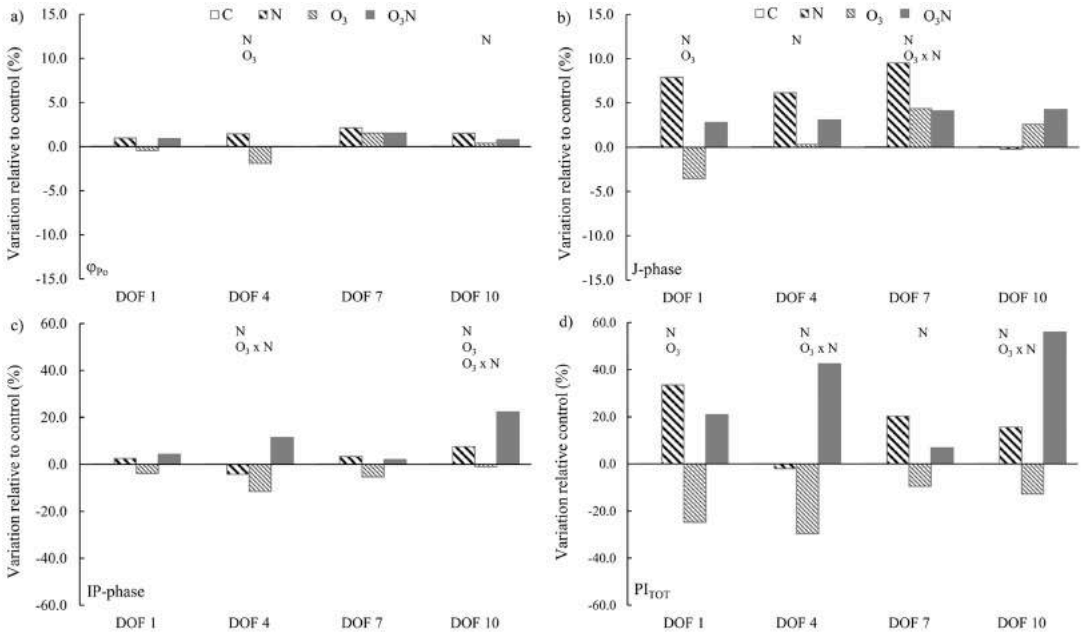

Figure 3. Trend of JIP-test parameters in *F. ornus*. The histograms indicate the percentage variation of each parameter of all treatments in relation to control plants. Measurements were performed at the first, fourth, seventh, and tenth day of fumigation (DOF). Symbols over the bars indicate the significant factors ($p< 0.05$) affecting the gas exchanges parameters: N, nitrogen effect; O_3, ozone effect; $O_3 \times N$, interaction.

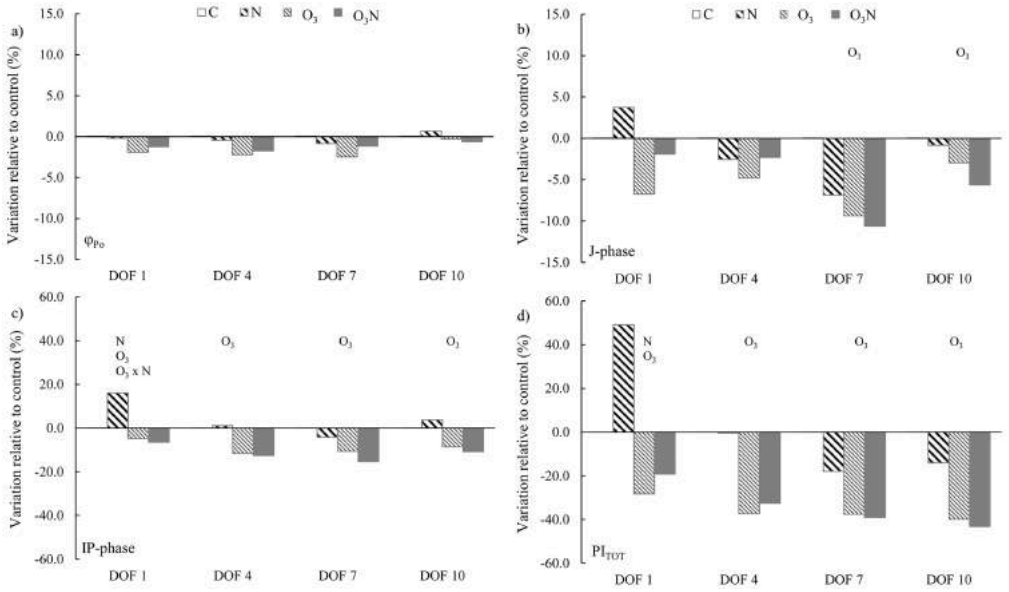

Figure 4. Trend of JIP-test parameters in *Q. ilex.* The histograms indicate the relative variation of each parameter of all treatments in relation to control plants. Measurements performed at the first, fourth, seventh, and tenth day of fumigation (DOF). Symbols over the bars indicate the significant factors ($p< 0.05$) affecting the gas exchanges parameters: N, nitrogen effect; O_3, ozone effect; $O_3 \times N$, interaction.

Table 3. Parameters derived from the P_N/Ci response curves performed out at the end of the experimental period and chemical and structural leaf traits.

	Fraxinus ornus				*p*		
Parameters	**C**	**N**	**O_3**	**O_3N**	**N**	**O_3**	**O_3N**
P_{Nmax}	25.64 ± 4.40	32.23 ± 4.24	22.73 ± 0.19	22.14 ± 3.65	**0.015**	**0.01**	0.09
V_{Cmax}	0.078 ± 0.01	0.067 ± 0.01	0.051 ± 0.00	0.057 ± 0.01	0.742	**0.03**	0.23
J_{max}	106.6 ± 18.44	136.5 ± 13.93	98.32 ± 6.26	91.58 ± 15.58	**0.012**	**0.01**	**0.04**
Γ	48.67 ± 3.68	56.2 ± 18.02	70.65 ± 23.13	52.20 ± 1.68	0.555	0.34	0.18
PNUE	1.9 ± 0.64	1.55 ± 0.28	1.40 ± 0.44	2.19 ± 1.07	0.59	0.86	0.19
N_L	1.71 ± 0.09	2.14 ± 0.45	1.26 ± 0.1	1.56 ± 0.32	0.058	**0.01**	0.71
C_L	44.73 ± 0.27	45.31 ± 0.6	44.25 ± 0.45	44.66 ± 0.42	0.094	0.06	0.76
C_L/N_L	26.15 ± 1.21	21.7 ± 3.97	35.21 ± 2.75	29.49 ± 6.66	0.067	**0.01**	0.8
LMA	0.013 ± 0.001	0.013 ± 0.001	0.011 ± 0.001	0.012±0.001	0.081	**0.003**	0.539
	Quercus ilex				***p***		
	C	**N**	**O_3**	**O_3N**	**N**	**O_3**	**O_3N**
P_{Nmax}	24.73 ± 3.91	29.9 ± 1.50	23.54 ± 5.41	28.67 ± 3.10	**0.003**	0.370	0.989
V_{Cmax}	0.076 ± 0.01	0.086 ± 0.009	0.074 ± 0.014	0.10 ± 0.017	0.059	0.498	0.368
J_{max}	105.9 ± 12.72	125.8 ± 4.19	102.3 ± 0.99	129.7 ± 8.64	**0.000**	0.982	0.438
Γ	67.69 ± 1.67	60.06 ± 13.14	67.11 ± 1.92	74.36 ± 12.98	0.972	0.238	0.204
PNUE	3.44 ± 0.97	3.00 ± 0.94	1.84 ± 0.13	2.2 ± 0.54	0.925	**0.021**	0.372
N_L	1.26 ± 0.14	1.44 ± 0.35	1.14 ± 0.07	1.36 ± 0.23	0.158	0.479	0.888
C_L	44.43 ± 0.48	45.24 ± 0.37	45.28 ± 0.21	45.55 ± 0.35	**0.036**	**0.026**	0.243
C_L/N_L	35.6 3± 4.03	32.57 ± 7.51	39.79 ± 2.36	34.01 ± 5.45	0.178	0.378	0.663
LMA	0.014 ± 0.001	0.13 ± 0.001	0.015 ± 0.001	0.012 ± 0.001	**0.000**	0.98	**0.01**

P_{Nmax}, (μmol m^{-2} s^{-1}) = maximum rate of net photosynthesis; V_{Cmax}, (mol m^{-2} s^{-1}) = in vivo apparent Rubisco activity; J_{max}, (μmol m^{-2} s^{-1}) = maximum rate of electron transport; Γ, (ppm) = CO_2 compensation point; PNUE, photosynthetic nitrogen use efficiency (μmol mol^{-1} s^{-1}); N_L, nitrogen at leaf level (%); C_L, carbon concentration at leaf level (%); C_L/N_L, ratio between carbon and nitrogen at leaf level; Leaf Mass Area (LMA, g cm^{-2}). Data are shown as the mean ± standard deviation (n=5) for each treatment. On the right panel, results of two-way ANOVA for each parameter are shown. Significant ($p < 0.05$) factors are marked in bold; quasi 'significant' values ($0.1 > p > 0.05$) are underline.

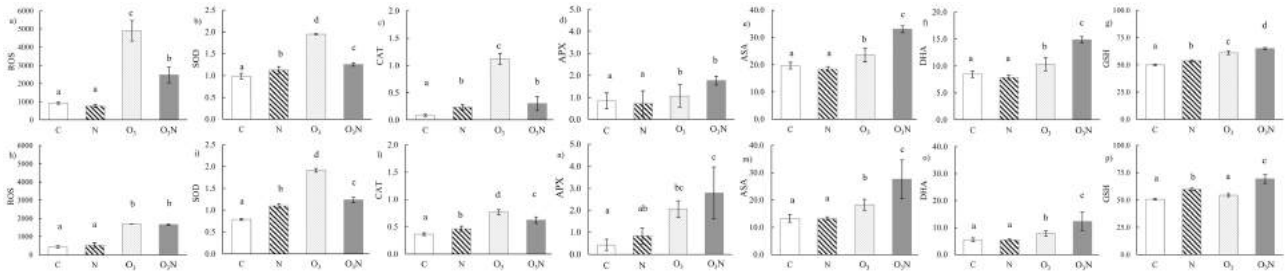

Figure 5. The outputs of biochemical analysis. They are shown for each treatment at the end of the experimental period for *F. ornus* (upper panel, from a to g) and *Q. ilex* (below panel, from h to p). Reactive oxygen species (ROS, %); superoxide dismutase, (SOD, inhibition rate %); catalase (CAT, U mg^{-1} of protein); ascorbate peroxidase (APX, U mg^{-1} of protein); total concentration of ascorbic acid (ASA, mg g^{-1}); oxidised ascorbic acid (DHA, mg g^{-1}); and glutathione (GSH, mg g^{-1}). Data are means ± standard deviation (n = 5) and bars not accompanied by the same letter are significantly different at $p < 0.05$, by using post hoc Student–Neuman–Keuls test.

References

1. Niinemets Ü. Cohort-specific tuning of foliage physiology to interacting stresses in evergreens. Tree Physiol. 2014;34: 1301–1304. doi:10.1093/treephys/tpu099

2. Mills G, Harmens H, Wagg S, Sharps K, Hayes F, Fowler D, et al. Ozone impacts on vegetation in a nitrogen enriched and changing climate. Environ Pollut. 2016;208, Part B: 898–908. doi:10.1016/j.envpol.2015.09.038

3. Manual on Methodologies and Criteria for Modelling and Mapping Critical Loads and Levels and Air Pollution Effects, Risks and Trends — European Environment Agency [Internet]. [cited 26 Apr 2017]. Available: http://www.eea.europa.eu/data-and-maps/indicators/exposure-of-ecosystems-to-acidification-2/manual-on-methodologies-and-criteria

4. Santurtún A, González-Hidalgo JC, Sanchez-Lorenzo A, Zarrabeitia MT. Surface ozone concentration trends and its relationship with weather types in Spain (2001–2010). Atmos Environ. 2015;101: 10–22. doi:10.1016/j.atmosenv.2014.11.005

5. Bytnerowicz A, Omasa K, Paoletti E. Integrated effects of air pollution and climate change on forests: A northern hemisphere perspective. Environ Pollut. 2007;147: 438–445. doi:10.1016/j.envpol.2006.08.028

6. Vries W de, Dobbertin MH, Solberg S, Dobben HF van, Schaub M. Impacts of acid deposition, ozone exposure and weather conditions on forest ecosystems in Europe: an overview. Plant Soil. 2014;380: 1–45. doi:10.1007/s11104-014-2056-2

7. Vainonen JP, Kangasjärvi J. Plant signalling in acute ozone exposure. Plant Cell Environ. 2015;38: 240–252. doi:10.1111/pce.12273

8. Das P, Nutan KK, Singla-Pareek SL, Pareek A. Oxidative environment and redox homeostasis in plants: dissecting out significant contribution of major cellular organelles. Front Environ Sci. 2015;2. doi:10.3389/fenvs.2014.00070

9. Cotrozzi L, Remorini D, Pellegrini E, Landi M, Massai R, Nali C, et al. Variations in physiological and biochemical traits of oak seedlings grown under drought and ozone stress. Physiol Plant. 2016;157: 69–84. doi:10.1111/ppl.12402

10. Guidi L, Degl'Innocenti E, Giordano C, Biricolti S, Tattini M. Ozone tolerance in Phaseolus vulgaris depends on more than one mechanism. Environ Pollut. 2010;158: 3164–3171. doi:10.1016/j.envpol.2010.06.037

11. Nali C, Paoletti E, Marabottini R, Della Rocca G, Lorenzini G, Paolacci AR, et al. Ecophysiological and biochemical strategies of response to ozone in Mediterranean evergreen broadleaf species. Atmos Environ. 2004;38: 2247–2257. doi:10.1016/j.atmosenv.2003.11.043

12. Scalet M, Federico R, Guido MC, Manes F. Peroxidase activity and polyamine changes in response to ozone and simulated acid rain in Aleppo pine needles. Environ Exp Bot. 1995;35: 417–425. doi:10.1016/0098-8472(95)00001-3

13. Calatayud V, Cerveró J, Sanz MJ. Foliar, Physiologial and Growth Responses of Four Maple Species Exposed to Ozone. Water Air Soil Pollut. 2007;185: 239–254. doi:10.1007/s11270-007-9446-5

14. Mills G, Hayes F, Wilkinson S, Davies WJ. Chronic exposure to increasing background ozone impairs stomatal functioning in grassland species. Glob Change Biol. 2009;15: 1522–1533. doi:10.1111/j.1365-2486.2008.01798.x

15. Fusaro L, Gerosa G, Salvatori E, Marzuoli R, Monga R, Kuzminsky E, et al. Early and late adjustments of the photosynthetic traits and stomatal density in Quercus ilex L. grown in an ozone-enriched environment. Plant Biol. 2016;18: 13–21. doi:10.1111/plb.12383

16. Calatayud V, Cerveró J, Calvo E, García-Breijo F-J, Reig-Armiñana J, Sanz MJ. Responses of evergreen and deciduous Quercus species to enhanced ozone levels. Environ Pollut. 2011;159: 55–63. doi:10.1016/j.envpol.2010.09.024

17. Manes F, Donato E, Vitale M. Physiological response of Pinus halepensis needles under ozone and water stress conditions. Physiol Plant. 2001;113: 249–257. doi:10.1034/j.1399-3054.2001.1130213.x

18. Ribas À, Peñuelas J, Elvira S, Gimeno BS. Contrasting effects of ozone under different water supplies in two Mediterranean tree species. Atmos Environ. 2005;39: 685–693. doi:10.1016/j.atmosenv.2004.10.022

19. Bussotti F. Functional leaf traits, plant communities and acclimation processes in relation to oxidative stress in trees: a critical overview. Glob Change Biol. 2008;14: 2727–2739. doi:10.1111/j.1365-2486.2008.01677.x

20. Li P, Calatayud V, Gao F, Uddling J, Feng Z. Differences in ozone sensitivity among woody species are related to leaf morphology and antioxidant levels. Tree Physiol. 2016;36: 1105–1116. doi:10.1093/treephys/tpw042

21. Zhang W, Feng Z, Wang X, Niu J. Responses of native broadleaved woody species to elevated ozone in subtropical China. Environ Pollut. 2012;163: 149–157. doi:10.1016/j.envpol.2011.12.035

22. Karnosky DF, Skelly JM, Percy KE, Chappelka AH. Perspectives regarding 50 years of research on effects of tropospheric ozone air pollution on US forests. Environ Pollut. 2007;147: 489–506. doi:10.1016/j.envpol.2006.08.043

23. Ribas À, Peñuelas J, Elvira S, Gimeno BS. Ozone exposure induces the activation of leaf senescence-related processes and morphological and growth changes in seedlings of Mediterranean tree species. Environ Pollut. 2005;134: 291–300. doi:10.1016/j.envpol.2004.07.026

24. Yamaguchi M, Watanabe M, Matsumura H, Kohno Y, Izuta T. Experimental Studies on the Effects of Ozone on Growth and Photosynthetic Activity of Japanese Forest Tree Species. Asian J Atmospheric Environ. 2011;5: 65–78. doi:10.5572/ajae.2011.5.2.065

25. Uscola M, Oliet JA, Villar-Salvador P, Díaz-Pinés E, Jacobs DF. Nitrogen form and concentration interact to affect the performance of two ecologically distinct Mediterranean forest trees. Eur J For Res. 2014;133: 235–246. doi:10.1007/s10342-013-0749-3

26. Bobbink R, Hicks K, Galloway J, Spranger T, Alkemade R, Ashmore M, et al. Global assessment of nitrogen deposition effects on terrestrial plant diversity: a synthesis. Ecol Appl. 2010;20: 30–59. doi:10.1890/08-1140.1

27. Dirnböck T, Grandin U, Bernhardt-Römermann M, Beudert B, Canullo R, Forsius M, et al. Forest floor vegetation response to nitrogen deposition in Europe. Glob Change Biol. 2014;20: 429–440. doi:10.1111/gcb.12440

28. Fleischer K, Rebel KT, van der Molen MK, Erisman JW, Wassen MJ, van Loon EE, et al. The contribution of nitrogen deposition to the photosynthetic capacity of forests. Glob Biogeochem Cycles. 2013;27: 187–199. doi:10.1002/gbc.20026

29. García-Gómez H, Garrido JL, Vivanco MG, Lassaletta L, Rábago I, Àvila A, et al. Nitrogen deposition in Spain: Modeled patterns and threatened habitats within the Natura 2000 network. Sci Total Environ. 2014;485–486: 450–460. doi:10.1016/j.scitotenv.2014.03.112

30. Volk M, Enderle J, Bassin S. Subalpine grassland carbon balance during 7 years of increased atmospheric N deposition. Biogeosciences. 2016;13: 3807–3817. doi:10.5194/bg-13-3807-2016

31. Calvete-Sogo H, González-Fernández I, Sanz J, Elvira S, Alonso R, García-Gómez H, et al. Heterogeneous responses to ozone and nitrogen alter the species composition of Mediterranean annual pastures. Oecologia. 2016;181: 1055–1067. doi:10.1007/s00442-016-3628-z

32. Fenn ME, Allen EB, Weiss SB, Jovan S, Geiser LH, Tonnesen GS, et al. Nitrogen critical loads and management alternatives for N-impacted ecosystems in California. J Environ Manage. 2010;91: 2404–2423. doi:10.1016/j.jenvman.2010.07.034

33. Pardo LH, Fenn ME, Goodale CL, Geiser LH, Driscoll CT, Allen EB, et al. Effects of nitrogen deposition and empirical nitrogen critical loads for ecoregions of the United States. Ecol Appl. 2011;21: 3049–3082. doi:10.1890/10-2341.1

34. Ochoa-Hueso R, Munzi S, Alonso R, Arróniz-Crespo M, Avila A, Bermejo V, et al. Ecological impacts of atmospheric pollution and interactions with climate change in terrestrial ecosystems of the Mediterranean Basin: Current research and future directions. Environ Pollut. 2017;227: 194–206. doi:10.1016/j.envpol.2017.04.062

35. Borghetti M, Gentilesca T, Leonardi S, van Noije T, Rita A, Mencuccini M. Long-term temporal relationships between environmental conditions and xylem functional traits: a meta-analysis across a range of woody species along climatic and nitrogen deposition gradients. Tree Physiol. 2017;37: 4–17. doi:10.1093/treephys/tpw087

36. Camarero JJ, Carrer M, Way D. Bridging long-term wood functioning and nitrogen deposition to better understand changes in tree growth and forest productivity. Tree Physiol. 2017;37: 1–3. doi:10.1093/treephys/tpw111

37. Ferretti M, Marchetto A, Arisci S, Bussotti F, Calderisi M, Carnicelli S, et al. On the tracks of Nitrogen deposition effects on temperate forests at their southern European range – an observational study from Italy. Glob Change Biol. 2014;20: 3423–3438. doi:10.1111/gcb.12552

38. Azuchi F, Kinose Y, Matsumura T, Kanomata T, Uehara Y, Kobayashi A, et al. Modeling stomatal conductance and ozone uptake of Fagus crenata grown under different nitrogen loads. Environ Pollut. 2014;184: 481–487. doi:10.1016/j.envpol.2013.09.025

39. Thomas VFD, Braun S, Flückiger W. Effects of simultaneous ozone exposure and nitrogen loads on carbohydrate concentrations, biomass, and growth of young spruce trees (Picea abies). Environ Pollut. 2005;137: 507–516. doi:10.1016/j.envpol.2005.02.002

40. Pivovaroff AL, Santiago LS, Vourlitis GL, Grantz DA, Allen MF. Plant hydraulic responses to long-term dry season nitrogen deposition alter drought tolerance in a

Mediterranean-type ecosystem. Oecologia. 2016;181: 721–731. doi:10.1007/s00442-016-3609-2

41. Yamaguchi M, Watanabe M, Iwasaki M, Tabe C, Matsumura H, Kohno Y, et al. Growth and photosynthetic responses of Fagus crenata seedlings to O3 under different nitrogen loads. Trees. 2007;21: 707–718. doi:10.1007/s00468-007-0163-x

42. Marzuoli R, Monga R, Finco A, Gerosa G. Biomass and physiological responses of Quercus robur (L.) young trees during 2 years of treatments with different levels of ozone and nitrogen wet deposition. Trees. 2016;30: 1995–2010. doi:10.1007/s00468-016-1427-0

43. Catovsky S, Bazzaz FA. Nitrogen Availability Influences Regeneration of Temperate Tree Species in the Understory Seedling Bank. Ecol Appl. 2002;12: 1056–1070. doi:10.1890/1051-0761(2002)012[1056:NAIROT]2.0.CO;2

44. Tulloss EM, Cadenasso ML. The Effect of Nitrogen Deposition on Plant Performance and Community Structure: Is It Life Stage Specific? PLOS ONE. 2016;11: e0156685. doi:10.1371/journal.pone.0156685

45. Wright IJ, Reich PB, Westoby M, Ackerly DD, Baruch Z, Bongers F, et al. The worldwide leaf economics spectrum. Nature. 2004;428: 821–827. doi:10.1038/nature02403

46. Takashima T, Hikosaka K, Hirose T. Photosynthesis or persistence: nitrogen allocation in leaves of evergreen and deciduous Quercus species. Plant Cell Environ. 2004;27: 1047–1054. doi:10.1111/j.1365-3040.2004.01209.x

47. Feng Y-L, Lei Y-B, Wang R-F, Callaway RM, Valiente-Banuet A, Inderjit, et al. Evolutionary tradeoffs for nitrogen allocation to photosynthesis versus cell walls in an invasive plant. Proc Natl Acad Sci. 2009;106: 1853–1856. doi:10.1073/pnas.0808434106

48. Tretiach M. Photosynthesis and transpiration of evergreen Mediterranean and deciduous trees in an ecotone during a growing season. Acta Oecologica. 1993;14: 341–360.

49. Valladares F, Martinez-Ferri E, Balaguer L, Perez-Corona E, Manrique E. Low leaf-level response to light and nutrients in Mediterranean evergreen oaks: a conservative resource-use strategy? New Phytol. 2000;148: 79–91. doi:10.1046/j.1469-8137.2000.00737.x

50. Paoletti E, Contran N, Bernasconi P, Günthardt-Goerg MS, Vollenweider P. Erratum to "Structural and physiological responses to ozone in Manna ash (Fraxinus ornus L.) leaves of seedlings and mature trees under controlled and ambient conditions" [Science of the Total Environment 407 (2009) 1631–1643]. Sci Total Environ. 2010;408: 2013. doi:10.1016/j.scitotenv.2010.01.022

51. Manes F, Vitale M, Maria Fabi A, De Santis F, Zona D. Estimates of potential ozone stomatal uptake in mature trees of Quercus ilex in a Mediterranean climate. Environ Exp Bot. 2007;59: 235–241. doi:10.1016/j.envexpbot.2005.12.001

52. Bazzaz FA, Carlson RW. Photosynthetic acclimation to variability in the light environment of early and late successional plants. Oecologia. 1982;54: 313–316. doi:10.1007/BF00379999

53. Salvatori E, Fusaro L, Strasser RJ, Bussotti F, Manes F. Effects of acute O3 stress on PSII and PSI photochemistry of sensitive and resistant snap bean genotypes (Phaseolus vulgaris L.), probed by prompt chlorophyll "a" fluorescence and 820 nm modulated reflectance. Plant Physiol Biochem. 2015;97: 368–377. doi:10.1016/j.plaphy.2015.10.027

54. Fares S, Schnitzhofer R, Jiang X, Guenther A, Hansel A, Loreto F. Observations of Diurnal to Weekly Variations of Monoterpene-Dominated Fluxes of Volatile Organic Compounds from Mediterranean Forests: Implications for Regional Modeling. Environ Sci Technol. 2013;47: 11073–11082. doi:10.1021/es4022156

55. Manes F, De Santis F, Giannini MA, Vazzana C, Capogna F, Allegrini I. Integrated ambient ozone evaluation by passive samplers and clover biomonitoring mini-stations. Sci Total Environ. 2003;308: 133–141. doi:10.1016/S0048-9697(02)00633-2

56. Long SP, Bernacchi CJ. Gas exchange measurements, what can they tell us about the underlying limitations to photosynthesis? Procedures and sources of error. J Exp Bot. 2003;54: 2393–2401. doi:10.1093/jxb/erg262

57. Loustau D, Brahim MB, Gaudillère J-P, Dreyer E. Photosynthetic responses to phosphorus nutrition in two-year-old maritime pine seedlings. Tree Physiol. 1999;19: 707–715. doi:10.1093/treephys/19.11.707

58. Sharkey TD, Bernacchi CJ, Farquhar GD, Singsaas EL. Fitting photosynthetic carbon dioxide response curves for C3 leaves. Plant Cell Environ. 2007;30: 1035–1040. doi:10.1111/j.1365-3040.2007.01710.x

59. Guidi L, Degl'Innocenti E, Remorini D, Massai R, Tattini M. Interactions of water stress and solar irradiance on the physiology and biochemistry of Ligustrum vulgare. Tree Physiol. 2008;28: 873–883. doi:10.1093/treephys/28.6.873

60. Nakano Y, Asada K. Hydrogen Peroxide is Scavenged by Ascorbate-specific Peroxidase in Spinach Chloroplasts. Plant Cell Physiol. 1981;22: 867–880. doi:10.1093/oxfordjournals.pcp.a076232

61. Pinto MC de, Francis D, Gara LD. The redox state of the ascorbate-dehydroascorbate pair as a specific sensor of cell division in tobacco BY-2 cells. Protoplasma. 1999;209: 90–97. doi:10.1007/BF01415704

62. Ellman GL. Tissue sulfhydryl groups. Arch Biochem Biophys. 1959;82: 70–77. doi:10.1016/0003-9861(59)90090-6

63. Dezi S, Medlyn BE, Tonon G, Magnani F. The effect of nitrogen deposition on forest carbon sequestration: a model-based analysis. Glob Change Biol. 2010;16: 1470–1486. doi:10.1111/j.1365-2486.2009.02102.x

64. Amponsah IG, Lieffers VJ, Comeau PG, Brockley RP. Growth response and sapwood hydraulic properties of young lodgepole pine following repeated fertilization. Tree Physiol. 2004;24: 1099–1108. doi:10.1093/treephys/24.10.1099

65. Scholz FG, Bucci SJ, Goldstein G, Meinzer FC, Franco AC, Miralles-Wilhelm F; Removal of nutrient limitations by long-term fertilization decreases nocturnal water loss in savanna trees. [Internet]. 2007. Available: https://www.treesearch.fs.fed.us/pubs/29697

66. Wildt J, Kley D, Rockel A, Rockel P, Segschneider HJ. Emission of NO from several higher plant species. J Geophys Res Atmospheres. 1997;102: 5919–5927. doi:10.1029/96JD02968

67. Garcı´a-Mata C, Lamattina L. Nitric Oxide Induces Stomatal Closure and Enhances the Adaptive Plant Responses against Drought Stress. Plant Physiol. 2001;126: 1196–1204. doi:10.1104/pp.126.3.1196

68. Feng Y-L, Auge H, Ebeling SK. Invasive Buddleja davidii allocates more nitrogen to its photosynthetic machinery than five native woody species. Oecologia. 2007;153: 501–510. doi:10.1007/s00442-007-0759-2

69. Hikosaka K, Hirose T. Nitrogen uptake and use by competing individuals in a Xanthium canadense stand. Oecologia. 2001;126: 174–181. doi:10.1007/s004420000517

70. Aranda I, Pardo F, Gil L, Pardos JA. Anatomical basis of the change in leaf mass per area and nitrogen investment with relative irradiance within the canopy of eight temperate tree species. Acta Oecologica. 2004;25: 187–195. doi:10.1016/j.actao.2004.01.003

71. Riva EG de la, Olmo M, Poorter H, Ubera JL, Villar R. Leaf Mass per Area (LMA) and Its Relationship with Leaf Structure and Anatomy in 34 Mediterranean Woody Species along a Water Availability Gradient. PLOS ONE. 2016;11: e0148788. doi:10.1371/journal.pone.0148788

72. Bussotti F, Pollastrini M, Cascio C, Desotgiu R, Gerosa G, Marzuoli R, et al. Conclusive remarks. Reliability and comparability of chlorophyll fluorescence data from several field teams. Environ Exp Bot. 2011;73: 116–119. doi:10.1016/j.envexpbot.2010.10.023

73. Mittler R. Oxidative stress, antioxidants and stress tolerance. Trends Plant Sci. 2002;7: 405–410. doi:10.1016/S1360-1385(02)02312-9

74. Bassin S, Volk M, Fuhrer J. Species Composition of Subalpine Grassland is Sensitive to Nitrogen Deposition, but Not to Ozone, After Seven Years of Treatment. Ecosystems. 2013;16: 1105–1117. doi:10.1007/s10021-013-9670-3

75. Palmroth S, Bach LH, Nordin A, Palmqvist K. Nitrogen-addition effects on leaf traits and photosynthetic carbon gain of boreal forest understory shrubs. Oecologia. 2014;175: 457–470. doi:10.1007/s00442-014-2923-9

76. Strasser RJ, Tsimilli-Michael M, Qiang S, Goltsev V. Simultaneous in vivo recording of prompt and delayed fluorescence and 820-nm reflection changes during drying and after rehydration of the resurrection plant Haberlea rhodopensis. Biochim Biophys Acta BBA - Bioenerg. 2010;1797: 1313–1326. doi:10.1016/j.bbabio.2010.03.008

77. Yao X, Liu Q. Changes in morphological, photosynthetic and physiological responses of Mono Maple seedlings to enhanced UV-B and to nitrogen addition. Plant Growth Regul. 2006;50: 165. doi:10.1007/s10725-006-9116-4

78. Velikova V, Fares S, Loreto F. Isoprene and nitric oxide reduce damages in leaves exposed to oxidative stress. Plant Cell Environ. 2008;31: 1882–1894. doi:10.1111/j.1365-3040.2008.01893.x

79. Neill SJ, Desikan R, Hancock JT. Nitric oxide signalling in plants. New Phytol. 2003;159: 11–35. doi:10.1046/j.1469-8137.2003.00804.x

80. Beligni MV, Lamattina L. Nitric oxide counteracts cytotoxic processes mediated by reactive oxygen species in plant tissues. Planta. 1999;208: 337–344. doi:10.1007/s004250050567

81. Fares S, Loreto F, Kleist E, Wildt J. Stomatal uptake and stomatal deposition of ozone in isoprene and monoterpene emitting plants. Plant Biol. 2008;10: 44–54. doi:10.1055/s-2007-965257

82. Loreto F, Pinelli P, Manes F, Kollist H. Impact of ozone on monoterpene emissions and evidence for an isoprene-like antioxidant action of monoterpenes emitted by Quercus ilex leaves. Tree Physiol. 2004;24: 361–367. doi:10.1093/treephys/24.4.361

Conclusion

It is often argued that since biomarker effects are measured in living organisms, the information generated is particularly useful for the management and conservation of natural ecosystems.

The monitoring of biological effects has recently become an integral component of environmental monitoring programs as a supplement to the commonly used contaminant monitoring. Over the years, many biomarkers have been developed that are claimed to be efficient at providing an early warning of deleterious effects on biological systems and for estimating biological effects due to contaminants.

By the mid 1980s a wide range of biomarkers had been developed and suggested for use in monitoring programs. Yet, there was little agreement between researchers on which were the best or most appropriate techniques. The national and international monitoring programs take many years to arrive at an agreed program, yet biomarker research does not stop. On the contrary continuously new methods are being developed that are claimed to be “more sensitive” than previous methods, or “more reliable” or can detect new effects that had not been observed before. Notwithstanding, there is a need to examine the overall advantages (benefits) and disadvantages (limitations) of biomarker-based monitoring programs.

The wide range of biomarkers used in these studies responded differently in relation to the species they were tested on and the type of stress.

In my research, several biological responses have been studied in relation to three types of stress. In particular, the biomarkers tested were: the activity of antioxidant enzymes in relation to heavy metal stress, heat stress and ozone stress; ultrastructural damage, thiol peptide content, expression levels of protein and DNA damage in relation to heavy metal stress. All these biological responses have been studied in relation to other analyzes to improve understanding of the effects of different stresses on plants.

If we consider the activity of the antioxidant enzymes in the two higher plants in relation of heavy metals, they did not respond coherently to external perturbations but rather, the activity of the enzymes is inhibited by the toxicity of the metals. But if we consider the activity of these enzymes on bioindicator organisms, as the bryophyte used to evaluate the effects of heavy metals both in the field and in vitro or *Mentha* × *piperita* e *Mentha arvensis*

L. used to evaluate the effects of heat stress and *Fraxinus ornus* L. and *Quercus ilex* L. as a spice tolerant to ozone stress the responses are different. In fact, these biomarkers are suitable for environmental assessment only if used on certain tolerant species. On the other hand, the antioxidant activity can be considered a good biomarker for all three stresses studied. In fact, in heat stress and in ozone stress, the activity of enzymes is not inhibited by stress factors.

Differently the ultrastructural damage turns out to be a good biomarkers, as it coherently reflects the external alterations. In fact, the damages show a linear trend with the increase in the concentrations of heavy metals and / or the degree of environmental pollution. But if we consider the economic aspect and the practicality of the analysis the ultrastructural observations present too high costs and long times.

DNA damage could also be a valid response to evaluate environmental variations even if in some cases the Comet Assay was not able to highlight damage in samples exposed under extreme environmental conditions.

HSP70s induction have been a reliable biomarker tool in responses to oxidative stress induced by heavy metals, both in *in vitro* and *in vivo* experiments.

The content of phytochelatin is good biomarker, but it is specific for the response to metal stress.

In conclusion, I propose that is not possible consider a single biological response but you must consider the set of multiple responses in order to have a clearer and more precise analysis of environmental variations. To summarize, the biomarker approach permits acquisition of information can be utilized in the assessment and prediction of ecological damage. The biomarker approach is already viewed by some as the solution to many of the problems of environmental management. Others have argued that biomarkers offer few advantages over conventional approaches.

The new technology is rapidly reducing the difficulty of measuring biomarkers at all levels of the biological organization. As for costs, most of the measurements are much cheaper than others. Furthermore, some biomarkers offer limited specificity compared to others but their value lies in providing an integrated view of all the stress factors that affect organisms when they are measured simultaneously.

Different biomarkers are capable of indicating rapid responses to toxicant exposure or of providing an early warning of long-term effects due to pollutant toxicity.

With regard to ecological risk assessment, biomarkers allow exposure to pollutants to be detected and populations especially at risk to be identified.

The data obtained can be used with a biomarker database compiled from field and "*in vitro*" studies. Finally, biomarkers may permit progress associated with bioremediation efforts to be assessed.